Characterisation of a putative N-terminal GLUT4 kinase

Harper, Darren

Award date:
2002

Awarding institution:
University of Bath

Characterisation of a putative N-terminal GLUT4 kinase

Submitted by Darren Harper

For the degree of Doctor of Philosophy
of the University of Bath
2002

D Harper

ProQuest LLC
789 East Eisenhower Parkway
P.O. Box 1346
Ann Arbor, MI 48106-1346

ABSTRACT 1

ACKNOWLEDGEMENTS 3

ABBREVIATIONS 4

1 INTRODUCTION 7

1.1 INSULIN REGULATION OF GLUCOSE METABOLISM 7
1.2 FACILITATIVE GLUCOSE TRANSPORTERS 8
1.2.1 THE GLUCOSE TRANSPORTER FAMILY 9
1.2.2 GLUT4: THE INSULIN-REGULATABLE GLUCOSE TRANSPORTER 11
1.3 INSULIN SIGNALLING PATHWAYS 12
1.3.1 THE INSULIN RECEPTOR, STRUCTURE, LOCATION AND ACTIVATION 12
1.3.2 INSULIN RECEPTOR SUBSTRATES (IRSS) AND PHOSPHATIDYLINOSITOL 3-KINASE (PI3K). 13
1.3.2.1 Phosphatidylinositol 3-kinase (PI3K) 14
1.3.2.2 Specific insulin-dependent targeting of PI3K to an intracellular location through IRS mediation. 18
1.3.3 ASSOCIATION OF COMPONENTS OF THE INSULIN SIGNALLING PATHWAY WITH THE CYTOSKELETON. 20
1.3.4 PI3K INDEPENDENT INSULIN SIGNALLING PATHWAYS: AN INTRODUCTION TO LIPID RAFT AND CAVEOLAE INVOLVEMENT. 26
1.3.4.1 The Cbl/CAP pathway 27
1.4 LIPID RAFTS AND CAVEOLAE 31
1.4.1 LIPID RAFT CONCEPTUALISATION 31
1.4.2 LIPID RAFT ISOLATION: DISCOVERY OF THE INCLUSION AND EXCLUSION OF PROTEINS TO LIPID RAFT STRUCTURES. 32
1.4.3 CAVEOLAE: A DISTINCT SUBCLASS OF LIPID RAFTS. 36
1.4.4 ALTERNATIVE METHODS FOR LIPID RAFT / CAVEOLAE ANALYSIS 39
1.4.5 RESOLUTION OF MACRODOMAINS BY LIPID RAFT CLUSTERING; IMPLICATIONS IN CELL SIGNALLING AND CELLULAR SORTING. 42
1.4.6 INVOLVEMENT OF LIPID RAFTS IN INSULIN SIGNALLING, GLUT4 TRAFFICKING AND CELLULAR SORTING MECHANISMS. 45
1.4.6.1 Lipid rafts and insulin signalling 45
1.4.6.2 Lipid raft involvement in vesicle docking and fusion 48
1.4.6.3 Lipid rafts potential involvement in cellular sorting mechanisms 49

1.5 INTRACELLULAR TRAFFICKING OF GLUT4 49
1.5.1 THE INTRACELLULAR GLUT4 COMPARTMENT 49
1.5.1.1 Generation of the GLUT4 storage compartment 54
1.5.1.2 Insulin stimulated signalling regulates mobilisation of GLUT4 from different compartments. 59
1.5.2 INTRACELLULAR SORTING SIGNAL MOTIFS IN GLUT4 61
1.5.2.1 The Amino Terminus of GLUT4: studied in non-insulin responsive cells. 63
1.5.2.2 The Carboxyl Terminus of GLUT4: studied in non-insulin responsive cells. 65
1.5.2.3 The Amino and Carboxyl Termini: studied in insulin responsive cells. 66
1.5.2.4 Interaction of GLUT4 carboxyl domains with potential trafficking proteins: Cytoskeletal involvement in insulin induced GLUT4 translocation. 68
1.5.2.5 Intracellular trafficking modulation by phosphorylation state of GLUT4 motifs 69
1.5.3 COATED VESICLE FORMATION: THE ROLE OF ADAPTERS 71
1.5.3.1 Clathrin 71
1.5.3.2 Adapter Proteins 71
1.5.3.3 Binding of expanded receptor tail motifs 74
1.5.3.4 Regulation of Adapter Recruitment 76
1.5.3.4.1 ARF mediation of GTPγS and Brefeldin A action on Adapter Protein recruitment 78
1.5.3.4.2 Membrane lipid regulation of adapter protein complexes 79
1.5.4 ROLE OF THE CYTOSKELETON IN GLUT4 TRAFFICKING 80
1.5.4.1 Disruption studies 80
1.5.4.2 Visualisation studies 81
1.5.4.3 Actin and Microtubule Motors regulate movement of GSV's in response to insulin 82
1.5.5 MODULATION OF INTRACELLULAR pH INFLUENCES MEMBRANE TRAFFICKING EVENTS 84
1.5.5.1 Characteristics of v-ATPases 86
1.5.5.2 Inhibition of v-ATPases to investigate the role of these complexes in pH regulating trafficking processes 88

2 GENERAL MATERIALS & METHODS 91

2.1 MATERIALS 92
2.1.1 CHEMICAL REAGENTS 92
2.1.2 BUFFERS 93
2.1.3 ANTIBODIES 94

2.2 RAT ADIPOCYTE CELL PREPARATION 96
2.2.1 ISOLATION OF RAT ADIPOCYTES 96
2.2.2 SUBFRACTIONATION OF RAT ADIPOCYTES 96
2.3 PREPARATION OF SYNAPTOSOMES FROM RAT BRAIN 97
2.4 PROTEIN BIOCHEMISTRY TECHNIQUES 98
2.4.1 BCA PROTEIN ASSAY 98
2.4.2 SDS POLYACRYLAMIDE GEL ELECTROPHORESIS (SDS-PAGE) 99
2.4.3 ELECTROPHORETIC TRANSFER OF PROTEINS TO NITROCELLULOSE 100
2.4.4 WESTERN BLOTTING 101
2.5 ANTIBODY GENERATION 102
2.5.1 SYNTHESIS OF N TERMINAL PHOSPHORYLATED AND NON PHOSPHORYLATED GLUT4 PEPTIDES 102
2.5.2 PEPTIDE FREE SULPHYDRYL CONTENT DETERMINATION 102
2.5.3 PREPARATION OF PEPTIDE CONJUGATES 103
2.5.4 INJECTION PROTOCOL 105
2.5.5 ELISA PLATE ASSAY 106
2.5.6 ANTIBODY AFFINITY PURIFICATION 107
2.5.6.1 Generation of affinity purification column 107
2.5.6.2 Affinity purification of serum 108

3 SEARCHING FOR A GLUT4 N TERMINAL KINASE. 110

3.1 INTRODUCTION 110
3.2 EXPERIMENTAL BACKGROUND AND AIMS 114
3.3 EXPERIMENTAL METHODS 116
3.3.1 PEPTIDE CONJUGATION PROCEDURE 116
3.3.1.1 GLUT4 N-Terminus peptide conjugation 116
3.3.1.2 GLUT4 C-Terminus conjugation 118
3.3.2 "IN GEL" KINASE ASSAY PROTOCOL 119
3.4 RESULTS AND DISCUSSION FOR THE DEVELOPMENT OF THE "IN GEL" KINASE ASSAY. 121
3.4.1 IMMOBILISING PEPTIDES WITHIN THE SDS-PAGE GELS 121
3.4.2 ENHANCEMENT OF KINASE AUTOPHOSPHORYLATION BY POLY LYSINE 123
3.4.3 ENHANCEMENT OF SPECIFIC, PEPTIDE DIRECTED, KINASE PHOSPHORYLATION BY POLY-$_L$-LYSINE 125
3.4.4 IDENTIFICATION OF OPTIMAL PHOSPHORYLATION BUFFER 128
3.4.5 DETERMINATION OF THE RELATIONSHIP BETWEEN THE ~90 KDA KINASE DOUBLET AND CKII. 130

3.4.6 IDENTIFICATION OF SPECIFIC KINASE PHOSPHORYLATION OF THE GLUT4 N TERMINAL PEPTIDE 134
3.4.6.1 Investigating the possibility of enhanced phosphorylation of the 90 kDa doublet with increasing G4NTP conjugate concentration 134
3.4.6.2 Investigating the possibility of enhanced phosphorylation of the 90 kDa doublet with increasing G4NTP ratio within the conjugate. 137
3.4.6.3 Evidence of G4NTP phosphorylation by the 90 kDa kinase doublet. 140
3.5 CONCLUSIONS FROM CHAPTER 1 144

4 FURTHER CHARACTERISATION OF THE PUTATIVE N-TERMINAL GLUT4 KINASE. 145

4.1 INTRODUCTION AND EXPERIMENTAL AIMS 145
4.2 EXPERIMENTAL METHODS 146
4.2.1 MEMBRANE FRACTION TREATMENTS 146
4.2.1.1 Plasma Membrane treatments 146
4.2.1.2 LDM / HSP treatments 147
4.2.2 PROTEIN PRECIPITATION TECHNIQUES 148
4.2.2.1 Chloroform/methanol precipitation 148
4.2.2.2 Acetone precipitation 148
4.2.3 ISOLATION OF LIPID RAFTS USING A SUCROSE GRADIENT 149
4.2.4 IMMUNOCYTOCHEMISTRY ON MALE WISTER RATS ADIPOCYTES 150
4.3 RESULTS AND DISCUSSION 151
4.3.1 DETERMINATION OF THE MEMBRANE ASSOCIATION PROPERTIES OF THE G4NTP DIRECTED KINASE IN THE LDM 151
4.3.2 DETERMINATION OF THE MEMBRANE ASSOCIATION PROPERTIES OF THE G4NTP DIRECTED KINASE IN THE PM 157
4.3.2.1 Further investigation of G4NTP directed kinase association with lipid rafts: Initial sucrose density gradient analysis. 162
4.3.2.2 Further investigation of G4NTP directed kinase association with lipid rafts: Complete sucrose density gradient analysis. 165
4.4 ANALYSIS OF ANTIBODIES GENERATED AGAINST G4NTP AND G4PHOSPHONTP 169
4.4.1 BOILING OF ADIPOCYTE FRACTIONS DRAMATICALLY DIMINISHES GLUT4 DETECTION BY WESTERN BLOTTING 174
4.4.2 AFFINITY PURIFICATION OF N TERMINAL DIRECTED GLUT4 ANTIBODIES AND FURTHER ANALYSIS 175
4.4.3 IMMUNOCYTOCHEMISTRY RESULTS ON ISOLATED RAT ADIPOCYTES USING AFFINITY PURIFIED GLUT4 ANTIBODIES 182

4.4.4 CONCLUSIONS FROM CHAPTER 2 184

5 ATTEMPTS TO ISOLATE THE G4NTP DIRECTED KINASE AND DETERMINE ITS IDENTITY. 185

5.1 INTRODUCTION AND EXPERIMENTAL AIMS 185

5.2 EXPERIMENTAL METHODS 186

5.2.1 PHAGE DISPLAY 186

5.2.1.1 Generation of adipocyte cDNA library in T7-Select 10-3 phage 186

5.2.1.2 Phage Display selection procedure (Bio-panning) 188

5.2.1.3 Deriving sequence data from selected phage plaques 189

5.2.2 2-DIMENSIONAL ELECTROPHORESIS 190

5.2.2.1 PM solubilisation using Na Cholate 190

5.2.2.2 2-Dimensional Electrophoresis general procedure 191

5.2.2.3 Silver Stain visualisation of 2-Dimensional electrophoresis gels 193

5.2.3 ALTERNATIVE 2-DIMENSIONAL ELECTROPHORESIS: COMBINING IEF AND THE CONVENTIONAL "IN GEL" KINASE ASSAY 194

5.2.3.1 Sample preparation 194

5.2.3.2 Isoelectric focussing (IEF) general procedure 194

5.2.3.3 Transferring 1st dimensionally focussed proteins onto the "In Gel" kinase assay for 2nd dimensional separation. 195

5.3 RESULTS AND DISCUSSION 196

5.3.1 PHAGE DISPLAY RESULTS: A BRIEF SUMMARY 196

5.3.2 2-DIMENSIONAL ELECTROPHORESIS RESULTS 199

5.3.3 ALTERNATIVE 2-DIMENSIONAL ELECTROPHORESIS RESULTS 204

5.3.3.1 Development of IEF gel loading and sample transfer to the "In Gel" kinase assay 204

5.3.3.2 Characterisation of proteins in the treated LDM samples to determine functionality of the Alternative 2-Dimensional Electrophoresis system. 210

5.3.3.2.1 IEF characterisation 210

5.3.3.2.2 Second Dimensional focussing / "In Gel" kinase assay characterisation 212

5.3.4 CONCLUSIONS FROM CHAPTER 3 215

6 OVERALL CONCLUSIONS 218

7 REFERENCES 222

Abstract

In resting adipocytes a large proportion of the insulin regulated glucose transporter (GLUT4) is localised in an intracellular storage compartment. In response to insulin stimulation, GLUT4 appears to be rapidly mobilised from this storage area to the plasma membrane. The manner by which GLUT4 is internally sequestered into this specialised and critical compartment is dependent on motifs contained in the cytoplasmic termini of GLUT4. One of these motifs, FQQI, has a potential downstream phosphorylation site $GS^{10}EDGE$ that has high sequence identity with a domain of the α-subunit of GAD65, which is multiply phosphorylated by an unknown membrane associated kinase in synaptic vesicles.

Antibodies were raised against phosphorylated and non-phosphorylated $GS^{10}EDGE$ containing synthetic peptides and were subsequently affinity purified. Studies using the phosphorylated S^{10} specific antibody suggested that a population of GLUT4 existed in this phosphorylated state and appeared to be predominantly located in intracellular membrane fractions. Studies using the non-phosphorylated GLUT4 antibody showed typical insulin-stimulated redistribution of GLUT4 to the plasma membrane. However the population of phosphorylated GLUT4 appeared to stay confined within the intracellular location.

An "in gel" kinase assay technique was developed to identify the kinase that acted upon the postulated phosphorylation site within GLUT4. The technique involved the immobilisation of the $GS^{10}EDGE$ containing synthetic peptide within a gel matrix. This served as a substrate for the potential kinase. These studies identified a putative 90 kDa kinase, which specifically phosphorylated the N-terminal peptide. This protein was not related to Casein kinase II, which is known to phosphorylate serines in the context of acidic residues. The conjugation of the peptide to poly-$_L$-lysine appeared to enhance the activity of the kinase and this was further augmented through the utilisation of $MnCl_2$ in the phosphorylation buffer.
Further characterisation of the detected kinase suggested a predominant ionic association with intracellular membranous compartments. In addition a

population of the kinase appeared to partition into lipid raft fractions of adipocytes. The lipid rafts may provide a stable microenvironment, like that encountered in the "in gel" kinase assay, in which kinase activity is enhanced.

Attempts were made to isolate the kinase using the principles of 2-dimensional electrophoresis and phage display. These studies highlighted that the kinase was pH sensitive and that pH sensitivity prevented use of this technique for kinase isolation. These partial purification studies provide a platform for future isolation attempts that will be required to establish the *in vivo* significance of the GLUT4 N-terminal kinase.

Acknowledgements

First and foremost I would like to thank my girlfriend Amy for all her patience, love, and advice over the last three years. When times were hard she kept my spirits high and I am forever indebted to her.

I would also like to thank my family and friends for their understanding, as I haven't been the easiest person to know while writing up the thesis. I am very fortunate to have people who care enough to put up with me and I will always be grateful for that.

I would like to thank my supervisor Professor Geoff Holman for his advice, patience and critical reading of the thesis. I am also grateful to Dr. Graham Bloomberg (University of Bristol) for peptide synthesis and technical expertise.

A big thank you to all the people in laboratory 1.37, past and present, for making my time at the university of Bath an enjoyable experience. I will take away a lot of fond memories from my time there.

I would like to thank all the people at Abcam Ltd for their support, especially Dr Jonathan Milner who afforded me the opportunity to launch myself into the working environment.

I would also like to thank Gemma and Louise for all the cooked meals while I have been cooped in my room, staring at my computer screen, awaiting inspiration.

Finally I would like to thank my sponsors the Medical Research Council for their financial support.

Abbreviations

Ab	Antibody
AC	Acidic Cluster
ADP	Adenosine Di-phosphate
AEBSF	[4-(2-Aminoethyl)benzenesulfonylflouride, HCl]
ARF	ADP Ribosylation Factor
AP	Adapter Protein
APS	Ammonium Persulphate
ATB-BMPA	2-N-4-(1-azi-2,2,2-trifluroethyl)benzoyl-1,3-bis(D-mannos-4-yloxy-propylamine
ATP	Adenosine Trisphosphate
BSA	Bovine Serum Albumin
CAP	Cbl Associated Protein
CHO	Chinese Hamster Ovary Cells
Ci	Curies
CKII	Casein Kinase II
CLMs	Caveolin-rich Light Membranes
Da	Daltons
DAB	Diaminobenzidine
DIGs	Detergent-Insoluble Glycolipid-enriched membranes
DNAse	Deoxyribonuclease
DMF	Dimethylformamide
DRMs	Detergent Resistant Membranes
DTT	$_{DL}$-Dithiothreitol
DV-GSC	Disperse Vesicular GLUT4 Storage Compartment
ECL	Enhanced Chemiluminescence
EDTA	Diaminoethanetetra-acetic acid disodium salt
EEA1	Early Endosome Antigen 1
EGTA	Ethylene glycol-bis(β-aminoethyl ether)N,N,N',N'-tetraacetic acid
G4NTP	GLUT4 N-Terminal Peptide
GAD65	Glutamic Acid Decarboxylase 65
GEMs	Glycolipid-Enriched Membranes
GGA	Golgi-localised, γ ear containing ARF-binding proteins
GLUT	Glucose Transporter
GLUT1	Erythrocyte Glucose Transporter
GLUT4	Insulin-Regulated Glucose Transporter
GPI	Glycosylphosphatidylinositol

GSVs	GLUT4 Storage Vesicles
G_{max}	maximum gravity
HDM	High Density Microsomes
HEPES	(N-[2-Hydroxyethyl]piperazine-N'-[2-ethenesulfonic acid])
HES	HEPES-EGTA-Sucrose
HRP	Horseradish peroxidase
HSP	High Speed Pellet
IDDM	Insulin Dependent Diabetes Mellitus
IR	Insulin Receptor
IRAP	Insulin Regulated Aminopeptidase
IRS 1/2/3/4	Insulin Receptor Substrate-1/2/3/4
KRH	Krebs-Ringer-HEPES
LDM	Low density microsomes
M6PR	Mannose 6-phosphate Protein Receptor
NHE1	Na^+/H^+ Exchanger 1
NIDDM	Non-Insulin Dependent Diabetes Mellitus
PACS-1	Phosphofurin Acidic Cluster Sorting protein-1
PBS	Phosphate Buffered Saline
PCR	Polymerase Chain Reaction
PDGF	Platelet-derived Growth Factor
PH	Pleckstrin Homology Domain
PI	Phosphatidylinositol
PI 3-K	Phosphoinositide 3-kinase
PI 3-P	Phosphatidylinositol 3-phosphate
PI 4-P	Phosphatidylinositol 4-phosphate
PI 3,4-P_2	Phosphatidylinositol 3,4-bisphosphate
PI 4,5-P_2	Phosphatidylinositol 4,5-bisphosphate
PIP_3	Phosphatidylinositol 3,4,5-trisphosphate
PKA	Protein Kinase A
PKB/Akt	Protein Kinase B
PKC	Protein Kinase C
PLC	Phospholipase C
PLD	Phospholipase D
PM	Plasma Membrane
PMA	Phorbol 12-myristatae 13-acetate
PP2A	Protein Phosphatase 2A
PR-GSC	Perinuclear Reticular GLUT4 Storage Compartment
PTB	Phosphotyrosine-Binding Domain
PTK	Protein Tyrosine Kinase

Rpm	Revolutions per minute
SDS-PAGE	Sodium Dodecyl Sulphate-Polyacrylamide Gel Electrophoresis
SH2	Src Homology 2 Domain
SH3	Src Homology 3 Domain
SMCC	Succinimidyl 4-(N-maleimidomethyl) cyclohexane-1-carboxylate
SNAP	Soluble NSF Attachment Protein
SNARE	Soluble NSF Attachment Protein Receptor
TBS	Tris-buffered Saline
TBS-T	Tris-buffered Saline with Tween 20
TEMED	N,N,N', N'-tetramethylethylenediamine
TES	Tris-EDTA Sucrose
Tf	Transferrin
TfR	Transferrin Receptor
TGN	*trans*-Golgi Network
TGN38	*trans*-Golgi Network Marker 38
TGR	*trans*-Golgi Reticulum
TIFF	Triton-Insoluble Floating Fraction
Tris	Tris(hydroxymethyl)methylamine
t-SNARE	target SNAP receptor
Tween-20	Polyoxyethylene sorbitan monolaureate
TX100	Triton X-100
VAMP	Vesicle Attachment Membrane Protein
v-ATPase	vacuolar ATPase
v-SNARE	vesicle SNAP Receptor

1 Introduction

1.1 Insulin regulation of glucose metabolism

Glucose is the major fuel source of mammalian tissues and consequently regulation of glucose metabolism plays a pivotal role in metabolic homeostasis. In the fasting state glucose concentration in the blood normally lies between 3 – 5 mM, however after a meal glucose is absorbed into the bloodstream, elevating levels to around 7 mM. The increase in circulating blood glucose results in glucose uptake into many organs but also, more vitally, triggers the secretion of a hormone produced in the β cells of the pancreatic islets of Langerhans, known as insulin (DeFronzo *et al.*, 1992). The release of insulin results in a rapidly enhanced disposal of glucose from the circulation, by facilitative uptake into specific target tissues, muscle and adipose tissue. Skeletal muscle accounts for the bulk of insulin-stimulated glucose disposal *in vivo* (70-80%) (Bonadonna *et al.*, 1993); with adipose tissue playing a lesser, but still vital role. The enhanced uptake of glucose into these tissues can be attributed to the "translocation" of a pool of glucose transporters, from within the cell, to the plasma membrane cell surface. Under most conditions that prevail *in vivo*, glucose transport is rate limiting for glucose disposal. In fact the earliest abnormality that can be detected in sufferers of Non-Insulin Dependent Diabetes Mellitus (NIDDM) is a decreased insulin-stimulated glucose disposal in target tissues (Martin *et al.*, 1992). Insulin induced glucose transporter translocation is thought to result from a myriad of signalling cascades that alter trafficking of specific glucose transporters, from their basal routing, to allow their rapid recruitment to the cell surface. Although great strides have been made into the elucidation of these mechanisms there is still a great deal to learn. The following chapters will touch on many of the mechanisms thought to be involved in insulin stimulated glucose transporter trafficking and highlight areas that are pertinent to the data presented in the subsequent results chapters.

1.2 Facilitative Glucose Transporters

It is known that facilitative glucose uptake occurs through a family of highly related integral membrane proteins that share significant sequence similarity, termed glucose transporters (GLUT's). Sequence analysis of these GLUT's suggested they all comprise of twelve membrane-spanning helices, as initially postulated from hydropathy plots, with the amino terminus, carboxyl terminus, and a highly hydrophilic central domain of the protein all predicted to lie on the cytoplasmic face (Mueckler *et al.*, 1985). There are a number of conserved residues within all of these family members (see Fig 1.1). Amongst these several charged residues on the cytoplasmic surface of the protein have been implicated, through mutational analysis, to participate in substrate transport, via modulation of the proteins' conformation (Schurmann *et al.*, 1997). Other conserved residues of note are the tryptophan amino acids in helices 6 and 11, with tryptophan in helix 11 shown to be critical for transporter activity and ligand (cytochalasin B, forskolin) binding (Garcia *et al.*, 1992; Schurmann *et al.*, 1993).

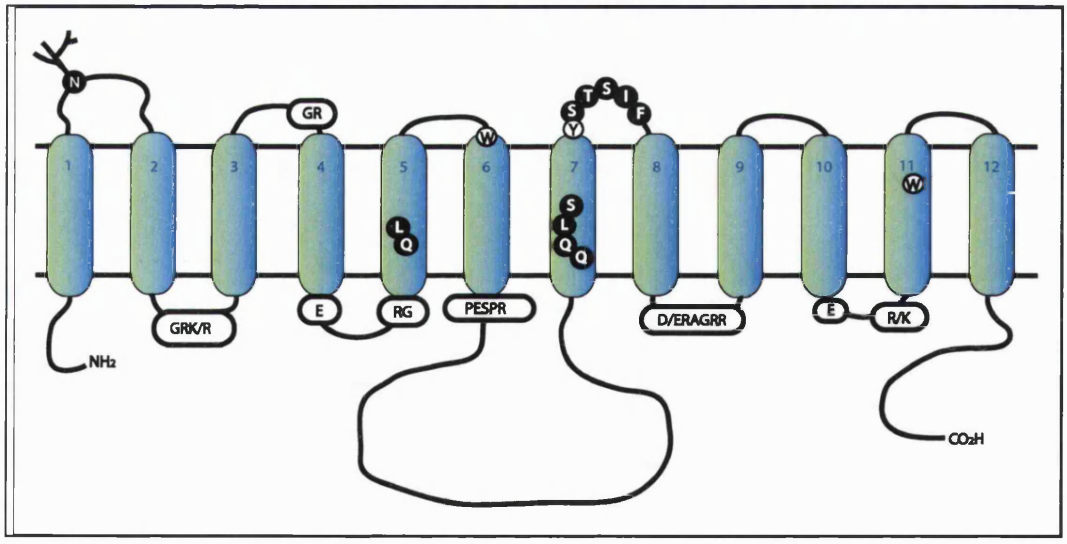

FIG 1.1: **Diagram depicting the structure of the GLUT proteins.** The GLUT proteins comprise 12 transmembrane helical domains. Residues highlighted on a white background are highly conserved in all GLUT proteins, whilst those highlighted in black are conserved in GLUT's 1-4. Adapted from (Joost and Thorens, 2001)

1.2.1 The Glucose Transporter Family

Evidence now exists that the number of proteins in the extended GLUT family, as defined by a minimal identity with GLUT1 (>28%), totals thirteen (Joost and Thorens, 2001). These proteins are divided into three subclasses, class I, II and III. Table 1.1 shows the tissue expression and categorisation of the GLUT isoforms.

CLASS / Description	Isoform	Alias	Tissue expression
CLASS I Classical glucose transporters.	**GLUT 1**	Erythrocyte-type glucose transporter	Placenta, brain, blood-tissue-barrier, adipose and muscle tissue
	GLUT 2	Liver-type glucose transporter	Liver, pancreatic β-cell, kidney proximal tubule and small intestine (basolateral membranes)
	GLUT 3	Brain-type glucose transporter	Brain and nerve cells in rodents. Brain, nerve; low levels in placenta, liver and heart (humans)
	GLUT 4	Insulin-regulatable glucose transporter	Muscle, adipose and heart tissue
CLASS II Fructose specific transporters and related proteins	**GLUT 5**		Intestine, testis, kidney
	GLUT 7		Unknown
	GLUT 9		Liver, kidney
	GLUT 11	GLUT 10	Heart, muscle
CLASS III Recently characterised GLUT's Shorter extracellular loop 1, that lacks glycosylation site.	**GLUT 6**	GLUT 9	Spleen, leukocytes, brain
	GLUT 8	GLUT X1	Testis, blastocyst, brain
	GLUT 10		Liver, pancreas
	GLUT 12	GLUT 8	Heart, prostate
	HMIT 1		Brain

Table 1.1: **Classification and tissue expression of GLUT isoforms in human and rodent tissues**. Taken from (Joost and Thorens, 2001) and (Gould and Seatter, 1997).

The term glucose transporter should be interpreted with some caution as the substrate specificity varies in certain GLUT members (e.g. GLUT5, fructose; HMIT1, myoinositol) and substrates have not been identified in many of the Class III proteins.

The most documented members of the GLUT family are the Class I isoforms, which appear to be specific for the D-isomer of glucose and are not coupled to any energy requiring components, such as ATP hydrolysis or a proton gradient. It has been postulated that glucose binds between transmembrane helices 7 and 10, allowing movement of glucose across the plasma membrane, down its chemical gradient, by a process of facilitative diffusion (Gould and Holman, 1993). Further research utilising mutational analysis has identified a number of residues and motifs that are conserved in all Class I GLUT's and may participate in glucose recognition and selection. These residues are highlighted in Fig 1.1 and include the $Q^{295}LS$ motif in helix 7, which has been suggested to interact with the incoming D-glucose at the C-1 position, (Seatter *et al.*, 1998) (see Fig 1.2).

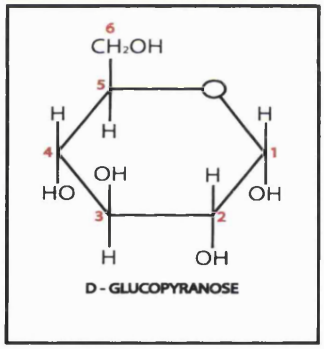

FIG 1.2: **D–Glucopyranose, the abundant form of D-Glucose found in biological systems.** Ring structure highlighting the six carbon positions.

Another motif identified, by site-directed mutagenesis, is the polar motif STS (STG in GLUT3). This resides in the exofacial loop between helices 7 and 8 and is thought to participate in a conformational change within the protein during the transport process (Doege *et al.*, 1998). Finally Glutamine 161 seems to form part of the exofacial substrate-binding site and is additionally postulated to be involved in modulating a conformational change within the protein, facilitating glucose uptake (Mueckler *et al.*, 1994).

1.2.2 GLUT4: The insulin-regulatable Glucose Transporter

In 1980 two groups, Suzuki and Kono (Suzuki and Kono, 1980) and Cushman and Wardzala (Cushman and Wardzala, 1980), reported that glucose transporter isoforms in non-stimulated rat adipose cells were located in a large intracellular pool and insulin stimulation caused their recruitment to the plasma membrane. Over subsequent years this phenomenon was mainly attributed to the presence of a specific isoform, that of GLUT4. Glucose transporter type 4 is set apart from the other glucose transporters because of its acute regulation by insulin. It has consequently been termed the insulin-regulatable Glucose Transporter.

In basal cells over 95% of GLUT4 is sequestered in intracellular compartments (Rea and James, 1997). Evidence from immunoelectron microscopy suggests that GLUT4 is localised to elements of the recycling pathway, including the *trans*-Golgi network (TGN), clathrin-coated vesicles and endosomes. However around 60% of the intracellular GLUT4 is found in tubulo-vesicular structures, clustered in the cytoplasm, in a perinuclear location (Gibbs *et al.*, 1988; Haney *et al.*, 1991; Slot *et al.*, 1991a). High-resolution studies have identified the tubules as saccular structures with fenestrated walls, which appear to be organised as a reticulum (Palacios *et al.*, 2001). The intracellular sequestration of GLUT4 in compartments, outside the recycling endosome pool used for GLUT1 and transferrin receptor (TfR) trafficking, may facilitate GLUT4s acute response to insulin (Holman *et al.*, 1994). Indeed photolabelling studies have identified an increase in the rate of GLUT4 exocytosis of around 9-fold, upon insulin stimulation (Yang and Holman, 1993), resulting in the 15-20-fold increase in glucose transport activity seen in the stimulated cells. This can be compared to an apparent 2-3-fold increase in GLUT1 exocytosis detected upon insulin stimulation. Interestingly in the continuous presence of insulin both GLUT4 and GLUT1 recycle at comparable rates leaving around 50% of the transporters in the plasma membrane at any one time (Smith *et al.*, 1991; Holman *et al.*, 1994). Once the insulin stimulus is removed and the cells return to a basal resting state, a large fraction of GLUT1 is still constitutively targeted to the cell surface (Rea and James, 1997). Conversely intracellular processing steps remove GLUT4 from the

endosome recycling pathway to the specialised compartment in the tubulo-vesicular system, culminating in a lower basal rate of GLUT4 exocytosis (Araki *et al.*, 1996) and the low population of GLUT4 observed at the cell surface.

1.3 Insulin Signalling Pathways

The altered intracellular sequestration and consequent redistribution of GLUT4, following insulin stimulation, may require regulation of multiple trafficking steps. These may be modulated by a myriad of signalling elements downstream of the insulin receptor. The critical components of this signalling pathway will be examined here and a picture of the complexity of this control process will begin to emerge.

1.3.1 The Insulin Receptor, structure, location and activation

The initial steps leading to insulin stimulated glucose transport are known to stem from activation of the insulin receptor (IR). The insulin receptor exists as a $\alpha 2\beta 2$ tetrameric complex, associated via three disulphide bridges. The α-subunits (135 kDa) are exclusively extracellular and contain the insulin-binding site. The β-subunits (95 kDa) are transmembrane peptides, possessing tyrosine kinase domains, which are located on the cytosolic portion of the β-chain.

Insulin binds to the α-subunits with a high affinity (Kd 0.1 nM). This high affinity is essential as the level of insulin in the blood is low (~0.1 nM). Following insulin binding, β-subunit autophosphorylation occurs at tyrosines 1146, 1150, 1151, 1316 and 1322 (Kasuga *et al.*, 1982; Gherzi *et al.*, 1987). Autophosphorylation increases the insulin receptor's capacity to phosphorylate other tyrosine residues on a family of soluble adapters or scaffolding molecules. These are known as insulin receptor substrates (IRS) which initiate the cellular signalling network.

1.3.2 Insulin receptor substrates (IRSs) and Phosphatidylinositol 3-kinase (PI3K).

Insulin receptor substrates (IRSs) are at the heart of the majority of insulin receptor downstream signalling events. There are currently 4 isoforms of IRS (IRS1-4) and they all contain a phosphotyrosine-binding domain (PTB) and an adjacent Pleckstrin homology (PH) domain at their amino terminus (White, 1998). The PTB domain spans 150 amino acids and binds directly to the $NPxY(p)^{960}$ motif in the juxtamembrane region of the IR. This interaction is thought to be enhanced by interactions of the PH and the PTB domains with membrane phospholipids and intracellular proteins (Takeuchi *et al.*, 1998; Yenush *et al.*, 1996; Burks *et al.*, 1998). Upon recruitment to the IR after insulin stimulation, IRS1 was known to be rapidly phosphorylated, with maximal phosphorylation achieved after 20-40s (Madoff *et al.*, 1988) at 22 potential tyrosine phosphorylation sites in their carboxyl termini. These phosphotyrosines serve as specific recognition sites for cellular substrates bearing Src homology 2 (SH2) domains (Sun *et al.*, 1991). Examples of proteins known to be recruited to IRSs through their SH2 domains are phosphatidylinositol 3-kinase (PI3K), the tyrosine kinase Fyn, the tyrosine-specific phosphatases SHPTP2 and Syp, and Grb2/SOS, which mediates loading of GTP onto $p21^{ras}$ (Backer *et al.*, 1993; Ogawa *et al.*, 1998; Kuhne *et al.*, 1993). The docking of these various proteins facilitates their activation leading to downstream protein complex activation and propagation of the insulin signal. An excellent example of this can be seen with the p85 regulatory subunit of PI3K. Phosphotyrosines 460, 608, 939 and 987 of IRS-1 are bound strongly by the SH2 domains of p85 and this binding has been shown to lead to a 3-5 fold stimulation in PI3K enzyme activity (Holman and Kasuga, 1997; Li *et al.*, 1999). The activation of PI3K is considered a key element in insulin stimulated GLUT4 translocation and glucose transport. Association of PI3K with IRSs not only facilitates its activation but also modulates its subcellular localisation and for this reason IRS and PI3K will be dealt with together in this chapter.

1.3.2.1 Phosphatidylinositol 3-kinase (PI3K)

Phosphatidylinositol 3-kinases (PI3K's) form a large family of evolutionary conserved enzymes that are involved in a vast array of biological events, such as intracellular vesicular transport, metabolism, growth, proliferation, differentiation and cytoskeletal rearrangements. All PI3Ks are characterised by their ability to phosphorylate the D3 position of the inositol ring in phosphatidyl (PtdIns) lipids. Three classes of PI3Ks are currently documented, defined by their structure and *in vitro* lipid substrate specificity (Shepherd *et al.*, 1998). See Fig 1.3 for domain structures of PI3K classes.

Class I PI3K's are heterodimers containing an adapter/ regulatory subunit and a tightly associated catalytic subunit. They show a broad lipid substrate specificity and can convert PtdIns, PtdIns(4)P and PtdIns(4,5)P_2 to PtdIns (3)P, PtdIns(3,4)P_2 and PtdIns(3,4,5)P_3 respectively (Staubs *et al.*, 1998; Whitman *et al.*, 1988). They appear to interact with the small GTP-binding protein Ras, however the function of this interaction is still under debate (Vanhaesebroeck *et al.*, 1999).

Class I_A PI3Ks comprise of a 110-120 kDa catalytic subunit (p110α, β and δ) associated with adapter proteins containing two SH2 domains and an N terminal Src-homology 3 (SH3) domain (p85α, p85β, p55γ and their splice variants). The SH2 domains interact with phosphotyrosine YxxM motifs present in a wide range of growth factor receptors and adapter proteins, linking this class of PI3Ks to tyrosine kinase signalling pathways.

Class I_B regulatory subunits are unrelated to those in Class I_A. The only subunit identified to date is termed p101, which forms a complex with a 120-kDa catalytic subunit p110γ. The p110γ subunit lacks a p85-binding site, which seems to have been replaced by a potential PH domain. It is postulated that the p101/p110γ complex is activated by binding of G$\beta\gamma$ subunits of heterotrimeric G proteins (Tang and Downes, 1997). *In vitro* experiments have indicated that all combinations of Gβ and Gγ isoforms are equally effective in activating p101/p110γ catalytic activity (Stephens *et al.*, 1994).

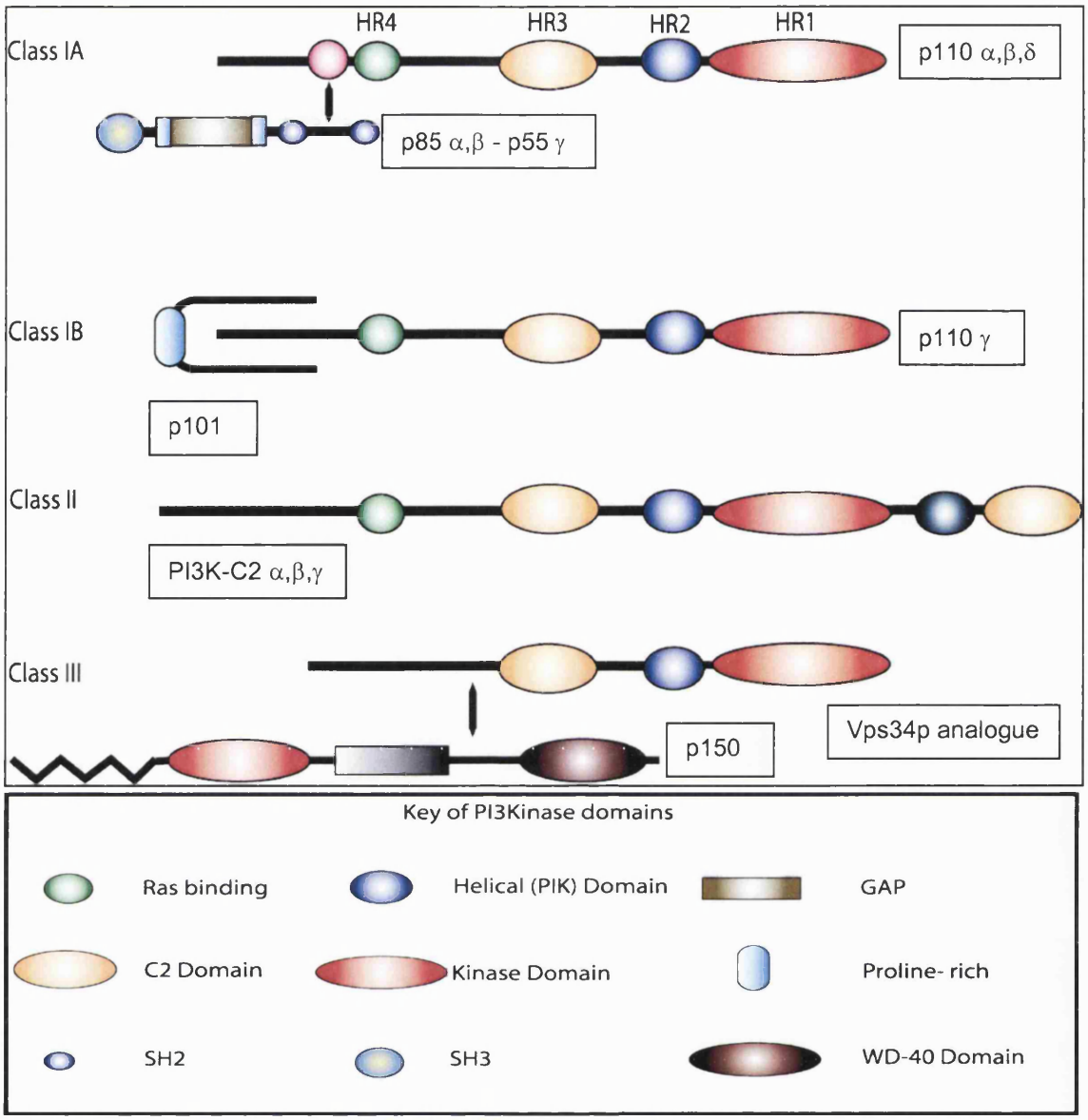

FIG 1.3: **Domain structures of PI3K's catalytic and adapter subunit isoforms.** Adapted from (Shepherd *et al.*, 1998) and (Vanhaesebroeck *et al.*, 2001). The kinase domain shown in p150 is that of a protein kinase domain rather than the lipid catalytic domain represented otherwise. The helical or PIK domain forms a structural spine, which may anchor the other domains in the correct position. In p110γ the helical domain may be involved in protein-protein interactions with p101 or Gβγ subunits.

Class II PI3K's are approximately 170 kDa comprising of three isoforms PI3K-C2α, β and γ. PI3K-C2α and β are ubiquitously expressed whereas PI3K-C2γ is mostly found in liver tissues. This class of PI3K lack adapter subunits and SH2 domains but are characterised by the presence of two tandem domains in the C terminal. The first is termed a PHOX homology domain, whose function remains unclear and the second is the C2 domain. The C2 domain can bind *in vitro* to phospholipids in a Ca^{2+} independent manner (Arcaro *et al.*, 1998). This independence from Ca^{2+} is consistent with the fact that the C2 domain of class II PI3K's lack the critical aspartate residues that are essential for Ca^{2+} co-ordination in Ca^{2+} dependent C2 domains. Class II PI3K utilise PtdIns and PtdIns(4)P as *in vitro* substrates with a strong preference for PtdIns (Vanhaesebroeck *et al.*, 1999), however *in vivo* substrates have not been confirmed. The manner of Class II PI3K activation is still to be confirmed but increased lipid kinase activity have been induced in Class II PI3K immunoprecipitates by epidermal growth factor, insulin, integrin ligation and the chemokine MCP-1 (Urso *et al.*, 1999; Brown *et al.*, 1999). Interestingly Class II PI3K's have been shown to be predominantly associated with phospholipid membranes in mammalian cells, which is in contrast to Class I PI3K's, which appear to be mainly cytosolic. PI3K-C2α has been co-purified with clathrin-coated vesicles (CCV's) (Domin *et al.*, 2000) and evidence exists that upon clathrin binding, to the amino terminal of PI3K-C2α, there is an increased *in vitro* lipid kinase activity towards phosphorylated inositide substrates (Gaidarov *et al.*, 2001). These findings raise the possibility that PI3K-C2α may be involved in clathrin-coated vesicle formation, utilising PtdIns(3)P, however further investigation will be required before any firm conclusions in this area can be made.

Class III PI3K's are specific for PtdIns only and are likely to be responsible for the generation of most of the PtdIns(3)P in cells. Despite extensive research only one member of this family has been characterised, the yeast vesicular-protein-sorting-protein (Vps34p) homologue, PtdIns 3-kinase (Herman *et al.*, 1991). This catalytic subunit is known to associate with a serine/threonine kinase, Vps15p in yeast and p150 in mammals. These adapter subunits can undergo N-terminal myristoylation that can target

them to membranes (Panaretou *et al.*, 1997). It is also known that Vps34p is involved in vesicular trafficking from the Golgi to the vacuole in yeast (Odorizzi *et al.*, 2000). This suggests that the PtdIns 3-kinase/p150 complex may function in intracellular trafficking within mammalian cells. However the extracellular stimuli that trigger Class III PI3K's and their specific function in cellular routing processes are yet to be determined.

The most widely accepted theory suggests that Class IA PI3K's are the principal enzymes of the PI3K's that mediate insulin's stimulation of GLUT4 translocation. Support for this stems from Class IA PI3K recruitment by IRS proteins and also the complete inhibition of insulin action on glucose transport by specific inhibitors of PI3K such as wortmannin and LY294002 (Clarke *et al.*, 1994; Cheatham *et al.*, 1994). Wortmannin and LY294002 are low-molecular-weight, cell permeable compounds that were commonly used in PI3K pathway elucidation due to their potency of inhibition with *in vitro* 50% inhibitory concentrations (IC_{50}) of ~5 nM and ~1 μM respectively for all PI3K's, with the exception of PI3K-C2α which is 10-fold less sensitive. However these conclusions became questionable for the following reasons. (1) Variance of wortmannin concentration will inactivate different PI3K's and so attribution of GLUT4 trafficking through insulin action on Class 1A PI3K could not be guaranteed. (2) It was discovered that LY294002 inhibits the widely expressed protein casein kinase-2 (CKII), (IC50 of 6.9 μM), which could adversely effect signalling pathways utilising this enzyme and give misrepresentative results in relation to PI3K (Davies *et al.*, 2000). Fortunately the initial postulation has been confirmed through studies utilising microinjection of dominant negative forms of the Class 1A adapter/regulatory subunits, (Kotani *et al.*, 1995) and antisense vectors to p85 (Yin *et al.*, 1998). These procedures resulted in the inhibition of GLUT4 translocation and glucose transport in insulin stimulated 3T3-L1 adipocytes and reaffirmed Class 1A PI3K involvement in GLUT4 translocation.

The involvement of other PI3K classes in GLUT4 insulin responsiveness cannot be ruled out, as the products of PI3K action may also play an important role in this process. A list of some of the downstream targets of the insulin-regulated PI3K lipid products include protein kinase C isoforms ζ and λ (Standaert *et al.*, 1999), regulatory proteins of the Akt/protein kinase

B system (Ueki *et al.*, 1998), the early endosome regulator EEA1, and ARF exchange factors GRP1, ARNO and cytohesin-1 (Olefsky, 1999). These targets may be linked to specific membrane trafficking components involved in GLUT4 translocation.

1.3.2.2 Specific insulin-dependent targeting of PI3K to an intracellular location through IRS mediation.

The observations that platelet-derived growth factor (PDGF) stimulates the total cellular PI3K but not glucose transport activity in 3T3-L1 cells led to the proposal that insulin stimulation causes a sub-compartmentalisation of PI3K to an intracellular site which cannot be influenced by PDGF. Indeed evidence now shows that insulin stimulates recruitment of Class 1A PI3K from the cytosol to the low-density microsome fraction in the cell, whereas PDGF stimulation results only in PI3K activity in the plasma membrane fraction (Yang *et al.*, 1996; Clark *et al.*, 1998; Ricort *et al.*, 1996). The specific targeting of PI3K in this system is still not completely understood but is thought to be mediated by an IRS or similar molecule.

Exactly which IRS proteins are involved in insulin stimulated GLUT4 translocation and glucose transport is still under debate. Early indications suggested that IRS1 was the major recruitment factor for PI3K, under insulin stimulation (Backer *et al.*, 1993). IRS1/PI3K association has since been shown to be necessary but not sufficient for GLUT4 translocation, induced by insulin stimulation. Microinjection or expression of dominant inhibitory PTB or SAIN domains of IRS1 block IRS1 interaction with the IR and reduce the interaction of IRS1 with PI3K. Using this approach in insulin-sensitive cultured adipocytes it was shown that, while being able to block mitogenic and membrane ruffling effects, these procedures did not affect GLUT4 translocation or glucose uptake in response to insulin (Sharma *et al.*, 1997). Also IRS1 knockout mice showed only a reduced maximal insulin stimulation of glucose transport activity (Araki *et al.*, 1994; Tamemoto *et al.*, 1994). IRS2 can also couple to p85α and this isoform may replace IRS1 in the knockout mice. This idea was given credibility with evidence that a lack of IRS1 associated PI3K, insulin stimulated activation in liver, muscle and

brown fat could be compensated for by IRS2 (Valverde *et al.*, 1999; Patti *et al.*, 1995). Interestingly it was discovered that in adipocyte cell lines derived from IRS2 knockout mice the lack of IRS2 associated function could not be compensated for by retrovirus-mediated over-expression of IRS1 but could be restored through re-expression of IRS2 (Fasshauer *et al.*, 2000). It was also observed that in these IRS2 knockout cell lines there was a ~50% decrease in insulin-stimulated glucose transport compared with wild type cells over the entire dosage range between 10 nM and 1 μM of insulin. This effect was shown to result from a decrease in insulin-stimulated GLUT4 translocation to the plasma membrane (Fasshauer *et al.*, 2000). These differences coupled with the poor conservation of the carboxyl-terminal regions of IRS1 and IRS2 (35% identity) suggest that these proteins are not merely interchangeable (White, 1998), but may reside in different subcellular compartments, which induce different cellular activities. This parallel pathway leading to PI3K activation may overlap and consequently if one pathway is blocked another may compensate. This situation may be further complicated by the possibility that other IRS/adapter proteins may be involved to achieve the full metabolic response of a muscle or adipose cell to insulin. IRS4 is undetectable in muscle or adipocytes and so is not involved in insulin stimulated GLUT4 translocation. The situation with IRS3 is less clear. IRS3 is predominantly found in the PM, contains an amino terminal PH and PTB domain and undergoes insulin stimulated tyrosine phosphorylation in adipocytes (Anai *et al.*, 1998). It was suggested that insulin action on glucose uptake in adipocytes from animals lacking IRS1 might involve IRS3 (Kaburagi *et al.*, 1997). However studies utilising IRS3 knockout mice showed no evidence of alterations in glucose tolerance compared with wild type mice (Liu *et al.*, 1999). It was reported that IRS3, phosphorylated mainly on the PM, may have a role in promoting cell proliferation and inhibiting adipocyte differentiation (Anai *et al.*, 1998), but it may be too early to dismiss IRS3's role in GLUT4 translocation.

Using the cytoplasmic domain of the Insulin receptor as bait, in a yeast two-hybrid screen, another interesting adapter protein containing a PH and SH2 domain (APS) was identified (Moodie *et al.*, 1999). APS belongs to a family of adapter proteins that include Src homology 2 (SH2-B) and the

lymphocyte specific adapter protein (Lnk). Further investigation revealed that APS was specifically detected in human skeletal muscle, heart, adipose tissue and differentiated 3T3-L1 adipocytes. It associates with phosphotyrosines situated within the activation loop of the IR, via its SH2 domain, and upon insulin stimulation is specifically tyrosine phosphorylated by the IR (Moodie *et al.*, 1999). Intriguingly in insulin stimulated 3T3-L1 adipocytes it was discovered that APS co-precipitated with the phosphorylated proto-oncogene c-Cbl (Ahmed *et al.*, 2000). It was already known that c-Cbl was a RING-type E2-dependent ubiquitin protein ligase (Joazeiro *et al.*, 1999). The associations of c-Cbl with tyrosine kinase receptors like epidermal growth factor (EGF), PDGF and CSF-1 lead to catalysis of their ubiquitination and their targeting for degradation or internalisation. A similar scenario appears to exist with the IR. In Chinese hamster ovary (CHO) cells over-expressing IR and APS, upon insulin stimulation, an APS/c-Cbl/IR complex formation was observed (Ahmed *et al.*, 2000). The ubiquitination of the IR by c-Cbl may be used to terminate the insulin signal or promote internalisation of the receptor. Indeed a strong correlation between insulin action, endocytosis of the activated IR and the promotion of IRS tyrosine phosphorylation has been shown (Kublaoui *et al.*, 1995). However other studies have produced conflicting results (Ceresa *et al.*, 1998). A compromise may be, that only a small amount of IR internalisation is required to propagate the insulin signal to IRS's. Further study will be required to clarify the involvement of APS and its potential activation of c-Cbl and IRS's, but it does present another interesting intricacy in this pathway.

1.3.3 Association of components of the insulin signalling pathway with the cytoskeleton.

The manner which insulin propagates signalling from the IR through IRS recruited PI3K is still under debate. As previously described PI3K is recruited from a cytosolic location to the LDM, or more precisely the high-speed pellet (HSP), upon insulin stimulation. This recruitment is primarily through protein interaction with IRS proteins, which in the basal state are

principally located in the HSP (60-80%) (Clark *et al.*, 2000). Initially subcellular fractionation studies suggested IRS1 was predominantly membrane associated, however treatment of HSP with non-ionic detergents, which liberated all membrane constituents, did not significantly solublise IRS1 or PI3K. In contrast to the detergent treatment both IRS1 and PI3K were readily soluble when the HSP fraction was maintained at a high ionic strength (Clark *et al.*, 1998). The treatment did not affect membrane integrity but would disturb protein-protein interactions and cytoskeletal elements. These studies led to two main proposals.

1. IRS1/2, PI3K and other signalling intermediates bind to form a large polypeptide complex possibly involving adapter protein 3 (AP3) in clathrin coated pits at the cell surface which associate with the IR upon insulin stimulation (VanRenterghem *et al.*, 1998).
2. IRS1/2, PI3K and other signalling intermediates form pre-assembled complexes that may be tethered to elements of the cytoskeleton that directly underlie the PM (Clark *et al.*, 1998).

The cytoskeletal theory is attractive as it provides an effective scaffold for recruitment of proteins, ensuring their correct juxtaposition with other enzymes, required for optimal signal propagation.

The cytoskeletal elements involved in the recruitment process remain uncertain, however numerous experimental observations have provided an insight into potential candidates. Olsen *et al.* provided evidence that both GLUT4 vesicles and IRS-1 bind specifically to microtubules in 3T3-L1 fibroblast homogenates (Olson *et al.*, 2001). Interestingly when the microtubule network was dissipated, using nocodazole treated cells, phosphorylation of IRS1 and activation of IRS1 associated PI3K were not inhibited, indicating that the microtubule network does not have a role in proximal insulin signalling (Olson *et al.*, 2001). Clark *et al.* identified bundles of filamentous networks in the HSP fraction from 3T3-L1 adipocytes using electron microscopy (Clark *et al.*, 1998). These filamentous networks could represent the F actin structures detected using rhodamine labelled phalloidin staining of differentiated 3T3L1 adipocytes (Kanzaki and Pessin, 2001) These structures appear to underlie and form contacts with the PM, generating a cortical scaffold, *i.e.* cortical actin. It appears that cortical actin is also found in isolated primary adipocytes and actually predominates over

stress fibres in these cells (Omata *et al.*, 2000). Cortical actin's involvement in a variety of functions in different cell types has been investigated. Suggestions that this form of actin acts as a barrier to vesicle docking have been based upon its transient depolymerisation during exocytosis and that secretion preferentially occurs at sites where the actin cortex is relatively thin (Vitale *et al.*, 1995; Norman *et al.*, 1996). The most interesting idea, in relation to insulin signalling, pertains to the idea that cortical actin acts as a scaffold. Using this idea it was proposed that IRS1/2 may move along the actin matrix and transiently interact with the membrane, through PH domain interactions, allowing IRS to associate with the IR (Whitehead *et al.*, 2000). There is also evidence that cortical F actin may not function in a static manner in morphologically differentiated adipocytes and primary rat adipocytes. It appears that in these cell types there is dynamic cortical actin re-modelling (polymerisation/de-polymerisation) upon insulin stimulation (Kanzaki and Pessin, 2001). Such processes could, in effect, act as molecular motors, rapidly conveying IRS1/IRS2 to specific target areas at or near the PM. Fig 1.4 represents a simplified model of potential targeting of IRS1/2 and PI3K, via the cytoskeleton.

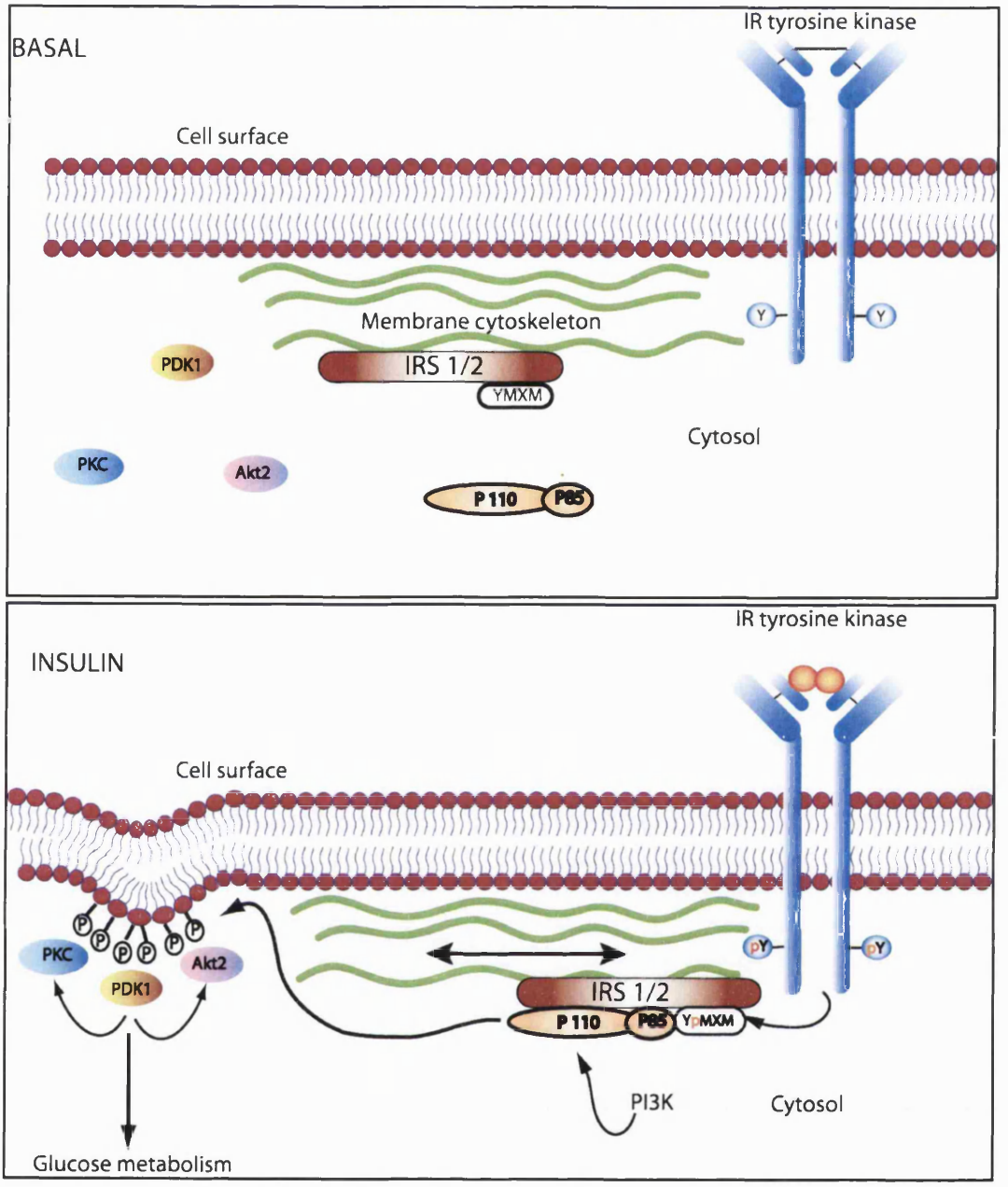

FIG 1.4: **Potential involvement of the cytoskeleton in cellular routing of elements of the insulin signalling cascade in response to insulin.** In the basal state IRS1/2 are attached to the cytoskeleton either by cortical actin, microtubule elements or both. Upon insulin stimulated IR autophosphorylation IRS1/2 are conveyed to the IR, either by sliding across the cytoskeletal scaffold, or by dynamic actin re-modelling. IRS1/2 undergoes tyrosine phosphorylation by the IR and PI3K is then recruited, forming an active complex, which is then targeted to specific sites within the PM. PIP3 generated at the PM then serves to recruit various downstream kinases like atypical PKC's, PDK1 and Akt2. These serve to propagate the insulin signal and co-ordinate glucose metabolism. Model adapted from (Whitehead *et al.*, 2000).

A stumbling point, with regards to an actin cytoskeleton conveying signalling components to the IR and specific PM locations, arises from studies where the microfilaments are disrupted. Cytochalasin D or latrunculin A treated 3T3-L1 adipocytes and primary rat adipocytes appeared to show no significant reduction in proximal insulin signalling, i.e. did not inhibit insulin activation of PI3K and Akt (Olson *et al.*, 2001; Omata *et al.*, 2000). These observations do not eliminate the credibility of the proposed model for the following reasons;

1. Cytochalasin D depolymerizes actin filaments by capping the growing barbed ends and consequently will be more effective at disrupting actively turning over filaments, such as stress fibres. The cortical actin filaments are potentially more resistant to this form of disruption and so may not be effectively dissipated.
2. Latrunculin A, like cytochalasin D, may preferentially disrupt actin structures other than the cortical actin framework. In 3T3-L1 adipocytes the abundance of stress fibres may obscure the effects of latrunculin A on cortical actin breakdown. As a consequence of this possible masking, there would be an apparent lack of inhibition of IRS1/2 modulation, in response to insulin, when using latrunculin A.
3. A unique feature of isolated primary rat adipocytes is the presence of a large lipid droplet inside the cell. This lipid droplet may shift the dose response curve for latrunculin A action to the right, due to the hydrophobic nature of the compound. This would again limit the functionality of latrunculin A and affect the outcome of the study.

If this model of a cytoskeletal scaffold is accepted it also provides an interesting platform for explanations into the termination of insulin signalling. Insulin treatment has been shown to progressively decrease levels of IRS1/2 found in the HSP of 3T3-L1 adipocytes, redistributing them to the cytosol (Heller-Harrison *et al.*, 1995; Clark *et al.*, 2000). Also, in basal cells, IRS1 is known to be phosphorylated on serine and threonine residues and insulin has been observed to acutely stimulate further increases in this phosphorylation (Li *et al.*, 1999). These two sets of observations have inevitably led to the proposal that insulin stimulated Ser/Thr phosphorylation causes conformational changes in IRS1/2 leading to their dissociation from the cytoskeleton and the IR (Clark *et al.*, 1998). This system would prevent

further IRS1/2 tyrosine phosphorylation, by the IR, and limit the subsequent activation of PI3K. The kinase responsible for this insulin stimulated Ser/Thr phosphorylation is still uncertain, however two candidates have been proposed from experimental observations. The first was identified in Xenopus, where a yeast two-hybrid screen, using xIRS1 PH-PTB domains, identified a xenopus homologue of Rho associated kinase (ROKα) as a potential xIRS1 binding protein (Farah *et al.*, 1998). ROKα was first identified as a Ser/Thr protein kinase of 160 kDa, which can also bind GTP-bound RhoA (Leung *et al.*, 1995). This has led to the proposal that ROKα may have a dual function in negative regulation of insulin signalling. ROKα may phosphorylate IRS1/2, causing its release from the IR, while also mediating RhoA induced cytoskeletal rearrangements that dissociate IRS1/2 from the cytoskeletal scaffold.

Another potential IRS1/2 Ser/Thr kinase is the atypical PKCζ. Overexpression of PKCζ in Fao cells accelerated the insulin stimulated breakdown of the IR/IRS1 complex, while wortmannin treatment had the opposite effect, abolishing complex breakdown and limiting increases in Ser/Thr phosphorylation of IRS1 (Liu *et al.*, 2001). This system provides a PI3K pathway, which activates PKCζ, resulting in the subsequent inhibition of IRS1/2.IR complex formation and further PI3K and PKCζ activation. This system is attractive as it provides a sensitive feedback control mechanism, preventing over-stimulation of the insulin-signalling pathway. However both the PKCζ and ROKα mechanisms require more research to ascertain if these processes are physiologically relevant in rat adipocyte tissues, and how this level of control relates to PI3K mediated GLUT4 translocation in response to insulin stimulation.

1.3.4 PI3K independent insulin signalling pathways: An introduction to lipid raft and caveolae involvement.

There is accumulating evidence that PIP3 generation by PI3K at the PM serves to recruit and activate the PH domain containing Ser/Thr phosphoinositide-dependent kinase (PDK1). PDK1 then activates further Ser/Thr downstream kinases, namely Akt 1/2 and the atypical PKC's (ζ/λ) (Vanhaesebroeck and Alessi, 2000). Studies involving manipulation of expression levels of these kinases or microinjection of kinase antibodies/ pseudo-substrate peptides have implicated Akt2 and the atypical PKC's in modulation of GLUT4 translocation (Hill *et al.*, 1999; Kohn *et al.*, 1996; Le Good *et al.*, 1998; Bandyopadhyay *et al.*, 1999; Etgen *et al.*, 1999). The precise involvement of both of these kinases in GLUT4 translocation and their downstream targets, linking them with GLUT4 vesicle trafficking, remain a point of speculation. Some of these potential targets are highlighted later in this introduction, but firstly we must go back to PI3K. PI3K is accepted as a critical component in the transmission of the insulin signal to mobilise GLUT4 to the PM. However it seems that PI3K alone is not sufficient to promote insulin-stimulated GLUT4 translocation and glucose uptake. There is increasing evidence that supplementary pathways may exist that account for the full physiological response of GLUT4 to insulin:

1. Cell permeable derivatives of PIP3 were unable to stimulate glucose transport in adipocytes, however they did restore insulin stimulated glucose transport in cells where PI3K was inhibited by wortmannin (Jiang *et al.*, 1998).
2. Growth factors such as PDGF, IL4, or β1-integrin clustering, stimulated IRS1 associated PI3K activity to a similar extent as that seen with insulin, however only minor effects were observed with regards to changes in glucose uptake (Isakoff *et al.*, 1995; Guilherme and Czech, 1998).
3. In skeletal muscle exercise, contraction and hypoxia induce GLUT4 translocation and glucose uptake independently of significant PI3K activation (Cushman *et al.*, 1998; Cortright and Dohm, 1997).

Considerable effort has been taken to identify other pathways that may be responsible for the full effect of insulin on GLUT4 translocation and glucose uptake. Studies on L6 myotubes where p38 mitogen-activated protein kinase (p38 MAPK) was inhibited by preincubation with SB203580 and SB202190 reduced insulin-stimulated glucose uptake by 40-60%, without altering GLUT4 translocation. These results suggested that insulin might activate GLUT4 via a p38 MAPK-dependent pathway that occurs after PI3K stimulated GLUT4 translocation (Somwar *et al.*, 2001). The involvement of p38 MAPK, in insulin stimulated glucose uptake, in physiologically relevant cells, such as primary adipocytes is yet to be firmly established, but provides an interesting alternative pathway.

A recent discovery, involving the previously characterised Cbl protein, has provided the most compelling evidence yet for a supplementary pathway, which is critical for insulin specific GLUT4 translocation and glucose uptake. (Chiang *et al.*, 2001)

1.3.4.1 The Cbl/CAP pathway

The role of Cbl is intriguing, it has been proposed to function in ligand dependent ubiquitination of a number of receptors, and also internalisation of the IR through interaction with APS. Another interesting feature of Cbl resides in its insulin stimulated phosphorylation, which appears to be specific for the differentiated adipocyte phenotype (Ribon and Saltiel, 1997). Cbl is present in other fibroblast cell lines but is not phosphorylated in response to insulin. These observations preclude the notion that Cbl phosphorylation is mediated through a direct interaction with the IR.

A yeast two-hybrid search for an adapter protein that might recruit Cbl to the IR, and account for the observed cell specificity, identified the Cbl-associated protein (CAP) (Ribon *et al.*, 1998). CAP was found to contain three carboxyl terminal SH3 domains, one of these associates with Cbl, and is predominantly expressed in insulin-sensitive tissues. In the basal state it seems that CAP recruits bound Cbl to the IR. Upon Cbl phosphorylation the CAP/Cbl complex is released from the IR and redistributes to a caveolin enriched, Triton-insoluble, plasma membrane domain, referred to as

caveolae/lipid rafts (Mastick and Saltiel, 1997). Yeast two-hybrid screens, using the amino-terminal region of CAP, identified a positive association with the caveolar protein flotillin (Baumann *et al.*, 2000; Bickel *et al.*, 1997). Flotillin may bind to the CAP/Cbl complex and direct its movement to the lipid raft. Indeed in 3T3-L1 adipocytes, expression of a CAP mutant containing its N-terminal domain, but lacking its SH3 domains, prevented Cbl localisation to lipid rafts and blocked insulin stimulated GLUT4 translocation and glucose uptake (Baumann *et al.*, 2001). It seems, from these studies, that localised subdomains within the Plasma Membrane (PM) may form a specialised signalling platform, from which the insulin signal is propagated. The observation that PI3K inhibitors had no effect on either the phosphorylation or translocation of Cbl (Baumann *et al.*, 2001), indicate that this axis comprises a distinct and parallel pathway to that of PI3K. Proteins recruited to this signalling platform, which help to explain the function of this proposed supplementary pathway, are now being identified. Studies in 3T3-L1 adipocytes identified that the insulin dependent phosphorylation of Cbl generates a specific docking site for the SH2 domains of endogenous c-CrkII tyrosine kinase (Ribon and Saltiel, 1997). CrkII had been previously shown to interact directly, through its SH3 domain, with the proline-rich domain of the guanine nucleotide exchange factor C3G (Knudsen *et al.*, 1994). Interestingly, in insulin stimulated 3T3-L1 adipocytes, both CrkII, C3G and Cbl appeared to migrate into Triton insoluble fractions over similar time courses, with maximal effects observed 3 minutes after insulin stimulation (Chiang *et al.*, 2001). It was postulated that the target of C3G could be a member of the rho family, G protein TC10 (Drivas *et al.*, 1990). TC10 is expressed in fat and muscle and is thought to reside in lipid raft domains within the PM. Experiments where C3G was over-expressed in 3T3-L1 adipocytes, in the absence of insulin, showed a quantitative conversion of TC10 to its active GTP bound state, indicative of C3G acting as a GEF for TC10 activation (Chiang *et al.*, 2001). A similar activation of TC10 in wild type cells was only witnessed after insulin stimulation, suggesting that insulin-stimulated recruitment and activation of C3G is required for subsequent activation of TC10. Studies where dominant interfering TC10 mutant (TC10/T31N) was microinjected or transfected in 3T3-L1 adipocytes showed a significant inhibition of insulin-stimulated

GLUT4 translocation (Chiang *et al.*, 2001). However it is worth noting that over-expression of C3G and activation of TC10, in the basal state, did not affect GLUT4 translocation per se but did cause a 4-5-fold leftward shift in the insulin dose response curve (Chiang *et al.*, 2001). These results suggest that TC10 alone is not sufficient to produce the full insulin response of GLUT4 but augments the action of PI3K. Indeed when C3G and active p110 where over-expressed in tandem the resulting GLUT4 translocation was observed to mimic, in full, that seen with insulin stimulation (Chiang *et al.*, 2001). Overall these studies indicate that the Cbl and PI3K pathways together may be sufficient to mediate the full effects of insulin on GLUT4 translocation and glucose transport. A model highlighting the dual roles of both of these pathways can be seen in Fig 1.5. The mechanism by which this TC10 pathway modulates GLUT4 response to insulin is uncertain but some proposals have been put forward. Expression of the TC10/T31N mutant, in fully differentiated adipocytes, completely disrupted cortical actin, and abolished insulin stimulated actin remodelling (Kanzaki and Pessin, 2001). Actin filament reorganisation has already been introduced as a means of spatially directing signalling complexes of the PI3K pathway, however it has also been hypothesised to have a more direct role in the trafficking of GLUT4, to the PM, in response to insulin (Omata *et al.*, 2000). It is therefore feasible that insulin activated TC10 might directly modulate cortical actin dynamics in adipocytes to facilitate exocytosis of GLUT4 to the PM.

Another potential function of TC10 is in the regulation of GLUT4 docking and fusion with the PM. This may involve the syntaxin 4 binding protein Synip. In the basal state Synip prevents association of VAMP2, in the GLUT4 vesicle, with the syntaxin 4/SNAP23 t-SNARE complex in the PM. Insulin stimulation is thought to result in the dissociation of Synip from syntaxin 4, allowing the aforementioned complex to form, resulting in GLUT4 vesicle docking and fusion (Min *et al.*, 1999). The insulin-stimulated dissociation of Synip is not blocked by wortmannin treatment, suggesting it is independent of the PI3K signalling pathway. This raises the possibility of Synip being under the control of the TC10 mediated pathway. Both the cytoskeletal remodelling and docking fusion theories are appealing and will be examined again in the course of this introduction.

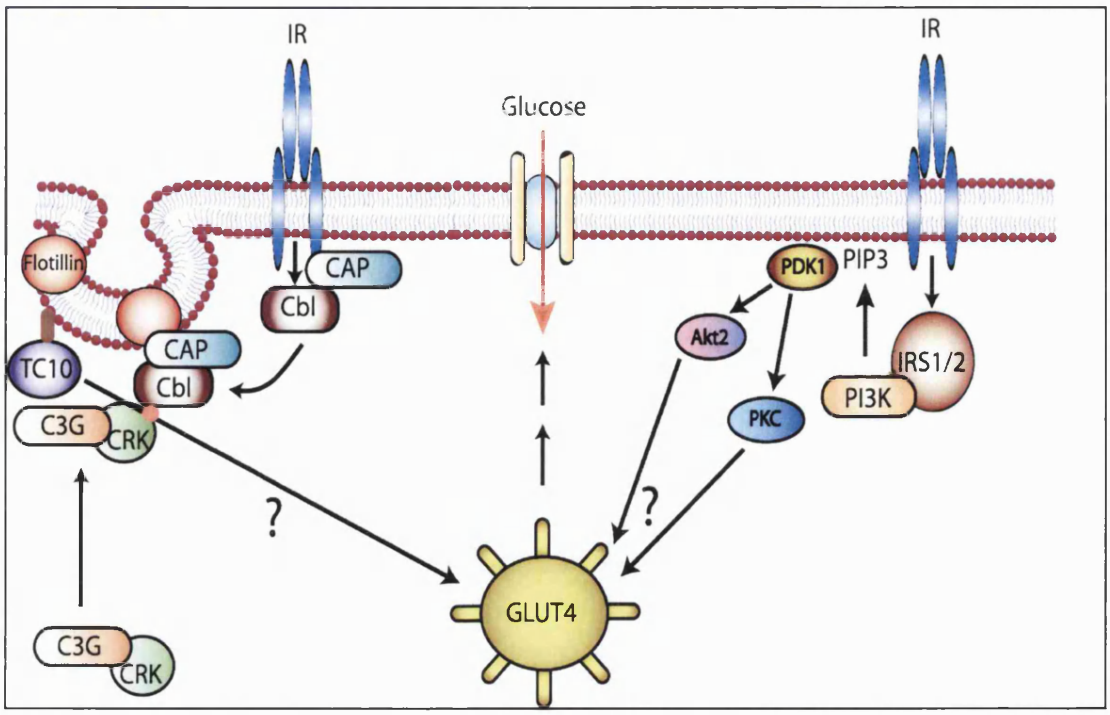

FIG 1.5: **Insulin stimulates two parallel signalling pathways that work in synergy to produce insulin stimulated GLUT4 translocation and glucose transport**. Insulin action results in the autophosphorylation of the IR, which activates IRS1/2 through tyrosine phosphorylation. IRS1/2 then recruit PI3K to the PM and its activation triggers a signalling cascade that initiates GLUT4 translocation. At the same time, insulin stimulates the phosphorylation of Cbl, which is associated with the IR through its interaction with CAP. This Cbl/CAP complex then dissociates from the IR and redistributes to specific PM microdomains (lipid rafts), through specific targeting of CAP to flotillin. The flotillin/CAP/Cbl complex forms a novel signalling platform that serves to recruit CrkII, and the GEF protein C3G. The recruitment of C3G to this microdomain places it in proximity to the small GTP binding protein TC10, which is a resident on the lipid raft. Consequently C3G catalyses the exchange of GTP for GDP on TC10, resulting in its activation. Activated TC10 augments the translocation of GLUT4 to the PM, possibly by modulating actin dynamics, or by regulating final docking and fusion events at the cell surface. Both pathways are independent of one another but are unable to promote GLUT4 translocation and glucose uptake individually. Diagram adapted from (Chiang *et al.*, 2001).

1.4 Lipid rafts and Caveolae

1.4.1 Lipid raft conceptualisation

The fluid mosaic model of Singer and Nicolson proposed that the lipid bilayer functions as a neutral two-dimensional solvent, in which proteins can freely diffuse through the "sea of lipids" of the plasma membrane (Singer and Nicolson, 1972). This model has been actively revised in recent years with the application of novel biophysical methods such as single particle tracking (Simson *et al.*, 1998). It is now accepted that lipids exist in several phases in model lipid bilayers, including gel, liquid-ordered and liquid-disordered states, in order of increasing fluidity. The liquid disordered state resembles that first described by Singer and Nicoloson, where the whole lipid bilayer is fluid. The gel-state represents the opposite extreme of the liquid disordered state, in which lipids could be described as being semi frozen within the bilayer. The liquid ordered state lies between the two extremes where phospholipids, with saturated hydrocarbon chains, pack tightly with cholesterol, but also retain the capacity to move within the plane of the membrane.

Although all the aforementioned models were biophysicaly sound there were great difficulties in proving the existence of such lipid states, within the complex environment of the cell. Observations based around lipid sorting in polarised epithelial cells (Madin-Darby canine kidney: MDCK cells) provided the first insights into how dynamic assemblies within the bilayer may occur (Van Meer and Simons, 1988). Simons and van Meer observed that apical and basolateral membrane domains of epithelial cell plasma membranes possess unique lipid compositions. They postulated that the high content of glycosphingolipids found in the apical membrane resulted from them being laterally segregated, in an intracellular compartment, and sorted into specialised apical carrier vesicles in the *trans* Golgi network (TGN). Sphingolipids contain long, saturated acyl chains, which can interact and pack together tightly. Glycerophospholipids which posses kinked unsaturated acyl chains are unable to undergo this type of clustering. It was proposed that the differential clustering ability of sphingolipids and

phospholipids could lead to a phase separation within the membrane, with sphingolipid-rich microdomains co-existing with phospholipid rich domains that are in the liquid disordered state (Brown and London, 2000). It was initially thought that these microdomains would resemble the gel state of model membranes, however it appears that cholesterol is also an essential component in this phase separation and leads to the microdomains existing in a state similar to the proposed liquid order phase. Cholesterol is present in high concentrations in the plasma membrane and other membranes and it appears to be intercalated with sphingolipids in the exoplasmic leaflet of the bilayer. Cholesterol appears to stabilise the saturated acyl chain lipids in the liquid ordered phase allowing them to form extended, tightly packed structures similar to the gel-like state but with a high degree of lateral mobility (Smaby *et al.*, 1996). Indeed studies using reconstituted liposomes suggested that the plasma membrane of eukaryotic cells contained enough sphingolipids to form ordered domains in the presence of cholesterol but not enough to form gel phase domains in the absence of cholesterol (Schroeder *et al.*, 1998). The notion of dynamic, gel like, microdomains moving through the "sea of lipids" led to the beginning of the characterisation of, what have been popularly termed, lipid rafts.

1.4.2 Lipid raft isolation: discovery of the inclusion and exclusion of proteins to lipid raft structures.

The importance of lipid rafts was only realised when methods for their isolation were developed. It was known that the clustering of sphingolipids led to them attaining a considerably higher melting temperature (T_M) than that observed for membrane phospholipids (Simons and Ikonen, 1997). This difference in T_M was postulated to correlate with an increase in detergent inextractability. Early studies to test this hypothesis utilised liposomes rich in cholesterol and sphingolipid. These liposomes were incompletely solubilised by the non-ionic detergent Triton X-100 (TX100) showing that in tightly packed conformations, similar to those postulated to exist in lipid rafts, lipid-lipid interactions can be more stable than lipid-detergent interactions (Schroeder *et al.*, 1994). Utilising the characteristic

detergent insolubility of complexed sphingolipids and cholesterol, Brown and Rose treated epithelial cell lysates with TX100. The resulting lipid raft complexes were observed to have a low buoyant density and were consequently isolated from solubilised membrane lipids and proteins by equilibrium gradient centrifugation (Brown and Rose, 1992). The fractions obtained from this isolation procedure were said to contain detergent-resistant membrane (DRM) fragments, which are in the liquid ordered state. When these DRM fragments were analysed an extraordinary discovery was made. It appeared that certain protein elements were enriched within DRM's, the most noticeable of which were glycosylphosphatidylinositol (GPI)-anchored proteins. Many GPI-anchored proteins contain saturated fatty acyl chains and it was proposed that these proteins partition preferentially into liquid ordered domains, which are also rich in saturated chains, and that detergent insolubility results from this association (Schroeder *et al.*, 1994). It was further determined that GPI-anchored proteins do not specifically associate with cholesterol as the protein was also found to be insoluble in cholesterol-free liposomes containing lipid in an ordered phase (Schroeder *et al.*, 1998). This strengthened the hypothesis that the recruitment of GPI-anchored proteins into DRM's was due to the generation of the liquid ordered phase of the lipid raft, within the PM, rather than physical association with components within the raft. This is a very important consideration when trying to understand the dynamic nature of these microdomains in the context of this introduction.

The isolation of lipid rafts from a wide variety of cell types, using the DRM methodology, has snowballed in recent years, with multiple definitions given to the isolated fractions. DRM's can alternatively be known as; caveolin-rich light membranes (CLMs), detergent-insoluble glycolipid-enriched membranes (DIGs), glycolipid-enriched membranes (GEMs) and triton-insoluble floating fraction (TIFF) (Cinek and Horejsi, 1992; Sargiacomo *et al.*, 1993; Shenoy-Scaria *et al.*, 1993; Chang *et al.*, 1994; Sevinsky *et al.*, 1996). As a result of this broad range research it became clear GPI-anchored proteins were only one of many proteins that partition into lipid rafts. Proteins found to have raft affinity include doubly acylated proteins, such as Src-family kinases or the α-subunits of heterotrimeric G proteins

(Resh, 1999). The fact that these proteins are modified with saturated acyl chains which pack well into an ordered lipid environment lends well to their association with lipid rafts. Surprisingly, cholesterol-linked and palmitoylated proteins such as Hedgehog (Rietveld *et al.*, 1999), and certain transmembrane proteins, particularly palmitoylated ones (Brown and London, 1998) were also found to be enriched in DRMs. It was thought that transmembrane proteins and prenyl groups would not favour a liquid-ordered lipid environment due to their bulky and branched nature. This apparent disparity created somewhat of an enigma as it was shown that palmitoylation may increase a proteins affinity for rafts (Melkonian *et al.*, 1999), although not all palmitoylated transmembrane proteins are in DRMs and not all transmembrane DRM proteins are palmitoylated. Studies initially suggested that sequences in the transmembrane domains near the exoplasmic leaflet were involved in protein lipid interactions, that may facilitate their DRM localisation (Perschl *et al.*, 1995; Scheiffele *et al.*, 1997). Although these studies gave some answers the issue was further complicated by the observations that mutations in the cytoplasmic domains of certain transmembrane proteins, which were unlikely to interact with lipids, could also modulate DRM association (Puertollano and Alonso, 1998; Bruckner *et al.*, 1999; Machleidt *et al.*, 2000). An explanation for these observations has not been clearly identified but may be due to differential kinetics or partition coefficients of these proteins within lipid rafts. It is possible that certain proteins could flux in and out of dynamic lipid raft environments. Under certain conditions their residency may increase, i.e. through interactions of these proteins with other proteins that are more stable in liquid ordered lipid domains.

A model of the possible organisation of a basic microdomain can be found in Fig 1.6.

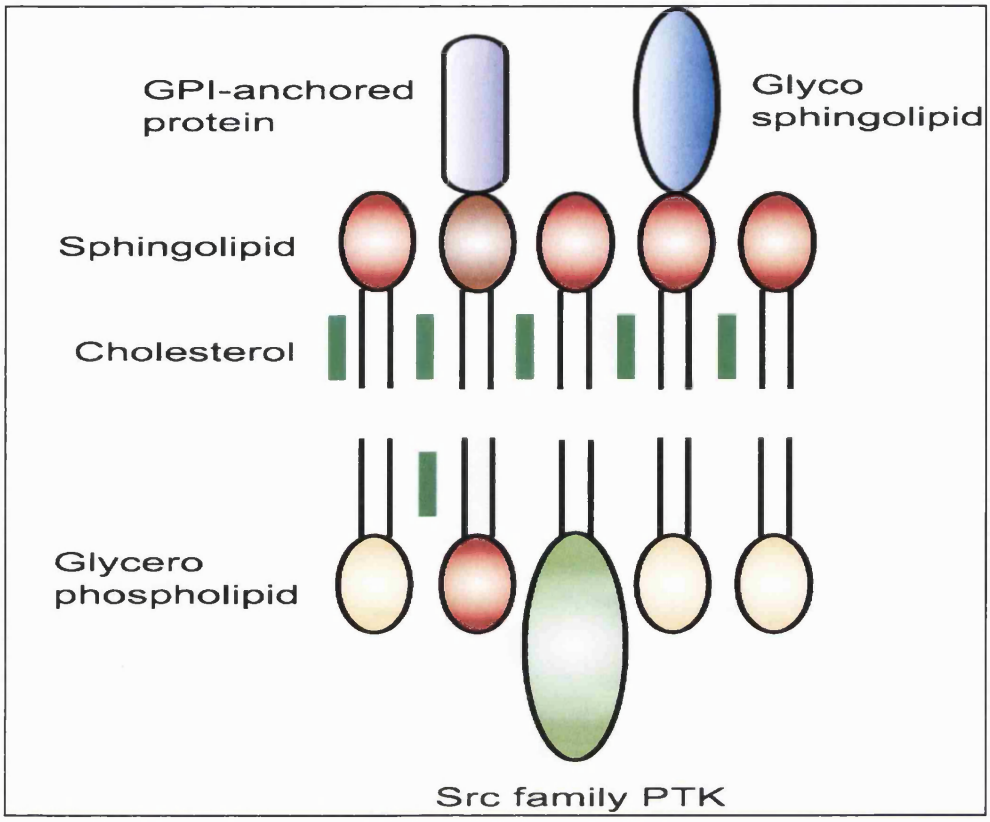

FIG 1.6: **Potential organisation of a basic microdomain "lipid raft".** Sphingolipids saturated acyl chains pack together, under the influence of cholesterol, to form liquid ordered phases within the plane of the plasma membrane. GPI-anchored proteins and glycosphingolipids are incorporated into the exoplasmic leaflet of the microdomain as their saturated acyl chains are preferentially more stable in this liquid ordered environment. Doubly acylated Src family protein tyrosine kinases (PTKs) or α subunits of heterotrimeric G proteins associate with the inner leaflet of the bilayer which is postulated to be rich in glycerophospholipids with saturated fatty acids and cholesterol. It is presumed that raft structure is initiated in the exoplasmic leaflet. The long saturated acyl chains of raft sphingolipids then interdigitate with the inner leaflet lipids, resulting in the corresponding organisation of the inner cytoplasmic leaflet into a liquid ordered state. Adapted from (Hoessli *et al.*, 2000).

1.4.3 Caveolae: A distinct subclass of lipid rafts.

Caveolae are distinguished as flask-shaped invaginations of the PM which were first identified in the 1950's (Yamada E, 1955; Palade G.E., 1953). They have been implicated in a form of endocytosis termed Transcytosis. This process is thought to involve the transport of macromolecules across the cell through a process of endocytosis of the macromolecule at one side of a monolayer and exocytosis at the other side (Schnitzer *et al.*, 1994). It was observed that filipin; a sterol binding agent, abolished this function of caveolae and suggested that cholesterol was an essential component in the maintenance of these structures. Increasing interest into potential alternative roles for Caveolae stemmed from the identification of a 22kDa phospho-protein originally detected in v-Src-transformed fibroblast cells (Glenney, Jr., 1989). This protein was shown to reside in caveolae and was subsequently found to be identical to another protein, vesicular integral membrane protein of 21kDa (VIP21) (Glenney, Jr., 1992). VIP21 had been shown to reside in non-coated vesicles, on the PM, and in *trans*-Golgi-derived transport vesicles, which resisted TX100 extraction (Kurzchalia *et al.*, 1992). Due to its discovery in caveolae the protein was termed caveolin-1 with molecular cloning identifying another two caveolins, caveolin 2 and caveolin 3 (Schlegel and Lisanti, 2001). Caveolin 1 and 2 are primarily expressed in adipocytes, endothelial cells, and fibroblastic cell types, whereas caveolin 3 is muscle-specific. Caveolins were shown to tightly associate with cholesterol and sphingolipids (Murata *et al.*, 1995). This association was shown to result in the polymerisation of caveolins, facilitating the formation of detergent resistant caveolae. The strong interaction of caveolin with cholesterol also led to the proposal that caveolae and caveolins are involved in the regulation of the cellular influx and efflux of cholesterol, something which was later proved to be correct (Babitt *et al.*, 1997; Fielding and Fielding, 2001a; Fielding and Fielding, 2001b; Uittenbogaard and Smart, 2000; Uittenbogaard *et al.*, 1998). Extensive research into caveolin1 membrane topology and polymerisation has accumulated since this discovery, which is beyond the scope of this introduction. For references see the following: (Dietzen *et al.*, 1995; Dupree

et al., 1993; Kurzchalia *et al.*, 1992; Li *et al.*, 1996a; Li *et al.*, 1996b; Li *et al.*, 1996c; Li *et al.*, 1996d; Luetterforst *et al.*, 1999; Murata *et al.*, 1995; Sargiacomo *et al.*, 1995; Schlegel and Lisanti, 2000). A model showing the insertion of caveolin 1 into the membrane and its various lipid and protein interactions has been compiled from these studies and is shown in Fig 1.7.

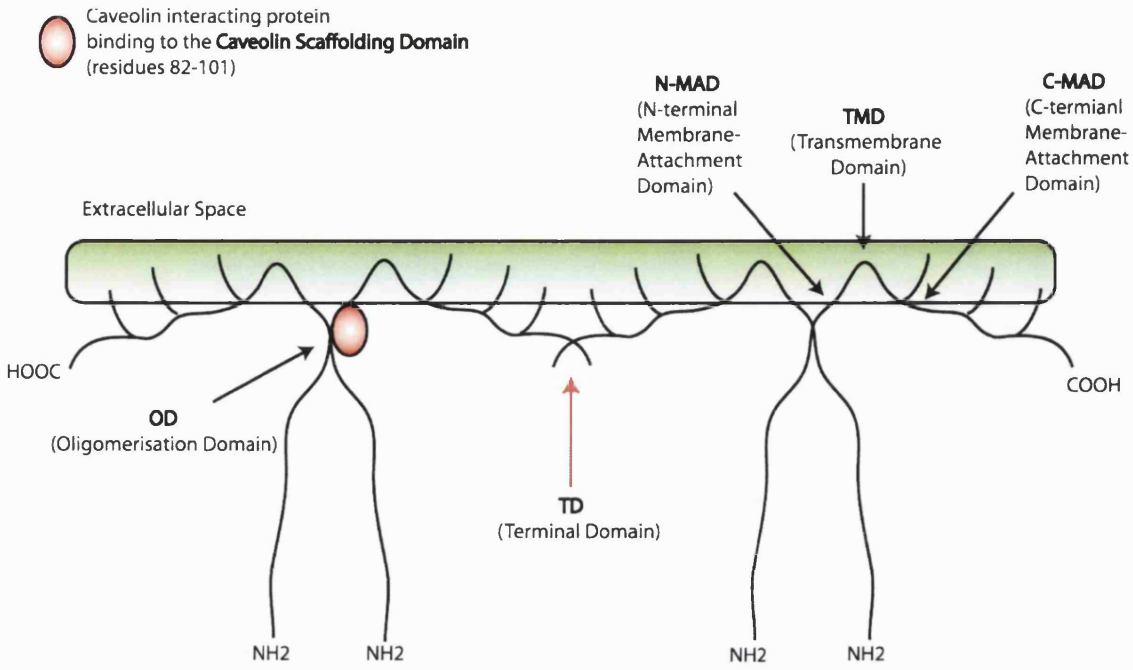

FIG 1.7: **Caveolin-1 membrane topology model.** Model shows 4 caveolin proteins inserted into the cytoplasmic side of the membrane. A central hydrophobic transmembrane domain (TMD) is thought to insert into the membrane. Caveolin is then retained to the membrane cytoplasmic surface through tight association of the N and C-terminal membrane attachment domains (NMAD and CMAD) with additional anchorage mediated by palmitic acid modifications, shown as upward hatches. Homo-oligomerization is thought to occur through interaction of adjacent Oligomerization domains (OD) found in the free amino terminal domains of caveolin-1. It appears that these oligomers can form a complex interlocking network of caveolins through interaction of adjacent Terminal domains (TD) found in the free carboxyl terminal domains of caveolin-1. In addition it appears that an area corresponding to residues 82-101 in caveolin-1, termed the caveolin scaffolding domain, can bind a range of caveolin-interacting proteins, including G-protein α subunits, Ha-Ras, Src family tyrosine kinases, endothelial NOS, EGF-R and related receptor tyrosine kinases, and protein kinase C isoforms (Okamoto *et al.*, 1998). Model adapted from (Schlegel and Lisanti, 2001).

The model shown in Fig 1.7 gives a simplistic representation of homo-oligomerisation of caveolin-1. Indeed complex oligomers containing as many as 14-16 individual molecules, form spherical structures which have been observed by electron microscopy (Sargiacomo *et al.*, 1995). Sargiacomo made the appealing analogy of these caveolin homo-oligomers functioning as "fishing lures" with multiple "hooks" or attachment sites for caveolin-interacting molecules. With the discovery of the caveolin scaffolding domain this idea opened up the intriguing possibility that caveolae may regulate specific signal transduction pathways. Recruiting, caveolin interacting, proteins into caveolae structures would rearrange their spatial localisation, placing them in close approximation, thereby facilitating signal propagation. Phage display has revealed that the caveolin scaffolding domain will bind to the following motifs; ΦXΦXXXXΦ, ΦXXXXΦXXΦ and ΦXΦXXXXΦXXΦ, where Φ is a phenylalanine, tyrosine, or tryptophan residue and X is any aminoacyl residue (Couet *et al.*, 1997). These motifs appear to be present in a plethora of signalling proteins including Gα subunits and the kinase domains of several tyrosine and serine/threonine protein kinases (Src family kinases, PKCα, MAP kinase, EGF-R, insulin receptor, and PDGF receptor), see (Okamoto *et al.*, 1998) for review. Upon binding of these proteins it was observed that caveolin-1 inactivates many of its binding partners (Razani *et al.*, 2000), sequestering them in the absence of activating signals, and thereby facilitating the formation of primed signalling complexes which are held in the inactive state until a stimulus is presented.

1.4.4 Alternative methods for lipid raft / caveolae analysis

With increasing study and advanced immunohistochemical visualisation technology the basic methodology for DRM and caveolae isolation through TX100 detergent inextractability and differential centrifugation has been thrown into question. It appears that there may be multiple subclasses of lipid rafts, defined by their protein and lipid components, that differentially partition between detergent-soluble and DRMs dependent on the detergent

used (Madore *et al.*, 1999; Roper *et al.*, 2000). It is also worth noting that cell lysates are chilled during detergent extraction and subsequent isolation. This has the effect of stabilising the liquid ordered phase of the lipid raft but could also result in the false incorporation of non-raft proteins, as the phase behaviour of the surrounding lipid bilayer may alter. This point has been hotly debated, with researchers showing that detergents do not induce the formation of liquid ordered domains, artifactually, in reconstituted liposomes containing comparable levels of phospholipids, sphingolipids and cholesterol as found in the PM (Schroeder *et al.*, 1998). Also the observation that GPI-anchored proteins are enriched in DRM's suggests that they are not merely sequestered at random into these complexes but must be in the microdomain bilayers before solubilisation (Cinek and Horejsi, 1992). However lipid raft associated proteins may not be detected by the DRM method if they are only weakly associated or if they are attached to cytoskeletal elements, which would preclude their floatation in the centrifugation process.

Various alternative methodologies have been developed to clarify the lipid raft association of various proteins. One such technique involves DRM isolation procedures coupled with modulation of cholesterol and or sphingolipid levels to dissociate proteins from lipid rafts. Using sterol binding/depletion drugs, or feeding cells with polyunsaturated fatty acids (Nichols *et al.*, 2001; Cerneus *et al.*, 1993; Hodel *et al.*, 2001; Webb *et al.*, 2000) it was shown that lipid raft associated proteins could be solubilised by TX100. However these studies have their own intrinsic problems as modulation of cholesterol and sphingolipid levels will affect not only the lipid rafts but also the surrounding membrane integrity leading to uncertain bilayer phase partitioning and potentially confusing results.

An adaptation of a table from (Simons and Toomre, 2000) detailing other techniques used to identify lipid rafts is shown in table 1.2

Technique	Identification	Live cells	Comments	References
Antibody patching and immunofluorescence microscopy	Identifies potential raft association	No	• Simple procedure • Commonly used • Better than flotation analysis for detection of weak raft associations • Cell-cell variability makes quantification difficult	(Harder *et al.*, 1998) (Janes *et al.*, 1999)
Immunoelectron microscopy	Identifies raft component localisation	No	• Encouraging results • High level of technical expertise required	(Wilson *et al.*, 2000) (Kurzchalia and Parton, 1999)
Chemical crosslinking	Identifies native raft protein structures	Yes	• Simple • Requires prior knowledge of raft components to determine appropriate conditions and reagents	(Friedrichson and Kurzchalia, 1998)
Single fluorophore tracking microscopy	Tracks the diffusion and dynamics of single raft proteins and lipids	Yes	• Expensive requiring state-of the art technology and expertise	(Schutz *et al.*, 2000)
Photonic force microscopy	Identifies microdomain size, diffusion and kinetic parameters	Yes	• Generates high levels of data • Expensive requiring state-of-the-art technology and expertise • Laborious data collection and analysis	(Pralle *et al.*, 2000)
Fluorescence resonance energy transfer (FRET)	Identifies spatial proximity of two raft components	Yes	• Highly specific approach • Requires informed selection of donor and acceptor probes	(Varma and Mayor, 1998) (Kenworthy *et al.*, 2000)

Table 1.2: **Table of alternative approaches to lipid raft characterisation.** Adapted from (Simons and Toomre, 2000)

1.4.5 Resolution of macrodomains by lipid raft clustering; implications in cell signalling and cellular sorting.

A caveat to the *in vivo* existence of lipid rafts was the apparent uniformity of putative raft markers, such as GPI-anchored proteins, over the cell surface, as detected by standard light microscopy. These observations could mean that lipid rafts might be so small that their resolution against the surrounding non-raft component of these lipid markers is impossible using basic microscopy techniques, Fig 1.8.

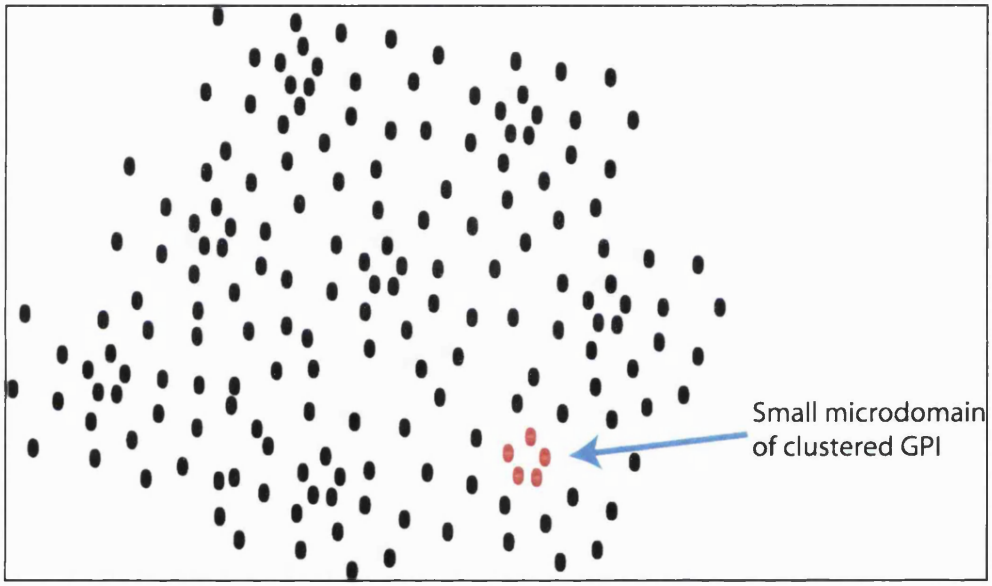

FIG 1.8: **Resolution of small lipid rafts by standard light microscopy.** Small microdomains would contain only a few marker proteins clustered together. When these are compared with the surrounding non-raft associated marker protein they may be difficult to distinguish. Antibodies or crosslinking agents may cause association of multiple small lipid rafts to form visible lipid raft patches, see below.

Indeed a high resolution technique, in which the motion of a single bead bound to a raft protein is monitored through measuring its local diffusion

(Photonic force microscopy), identified that raft proteins reside in confinement zones of roughly 50 nm (Pralle *et al.*, 2000). Also fluorescence resonance energy transfer (FRET) identified that the GPI-anchored folate receptor could be detected clustering in cholesterol-dependent domains of <70 nm, which were too small to be seen by conventional microscopy (Varma and Mayor, 1998). However, a contradictory study has shown that FRET analysis could not identify any significant clustering of GPI-anchored proteins, with the conclusion that in the plasma membrane, "lipid rafts either exist only as transiently stabilised structures or, if stable, comprise at most a minor fraction of the cell surface" (Kenworthy *et al.*, 2000). It has already been mentioned that different lipid raft marker proteins may have varying partition coefficients. As a consequence, proteins with moderate affinities may not be highly enriched in certain lipid rafts with respect to the surrounding PM. Interestingly when some lipid raft markers, with apparent uniform distributions, are clustered using antibodies or crosslinking agents their distribution dramatically alters, with the emergence of membrane patches. On its own this would not be indicative of native lipid raft existence, however studies have shown the clustering of one marker also causes redistribution of other proposed lipid raft proteins (Harder *et al.*, 1998; Janes *et al.*, 1999; Viola *et al.*, 1999). The fact that these secondary proteins are not thought to be associated directly with the marker proteins suggests that these are both resident in a stable microdomain. The resulting clustering of the marker proteins from separate microdomains subsequently form macrodomains in which the secondary proteins also appear to be in a clustered configuration.

If we consider multiple lipid raft sub-classes, including caveolae, containing differential protein compositions, then the potential homo or hetero clustering of lipid rafts creates a myriad of possibilities. Different stimuli could generate unique platforms, which serve to stabilise weakly associated lipid raft proteins and create dynamic highly sensitive signalling complexes. The possible ways in which lipid raft protein clustering may activate signalling complexes is shown in Fig 1.9.

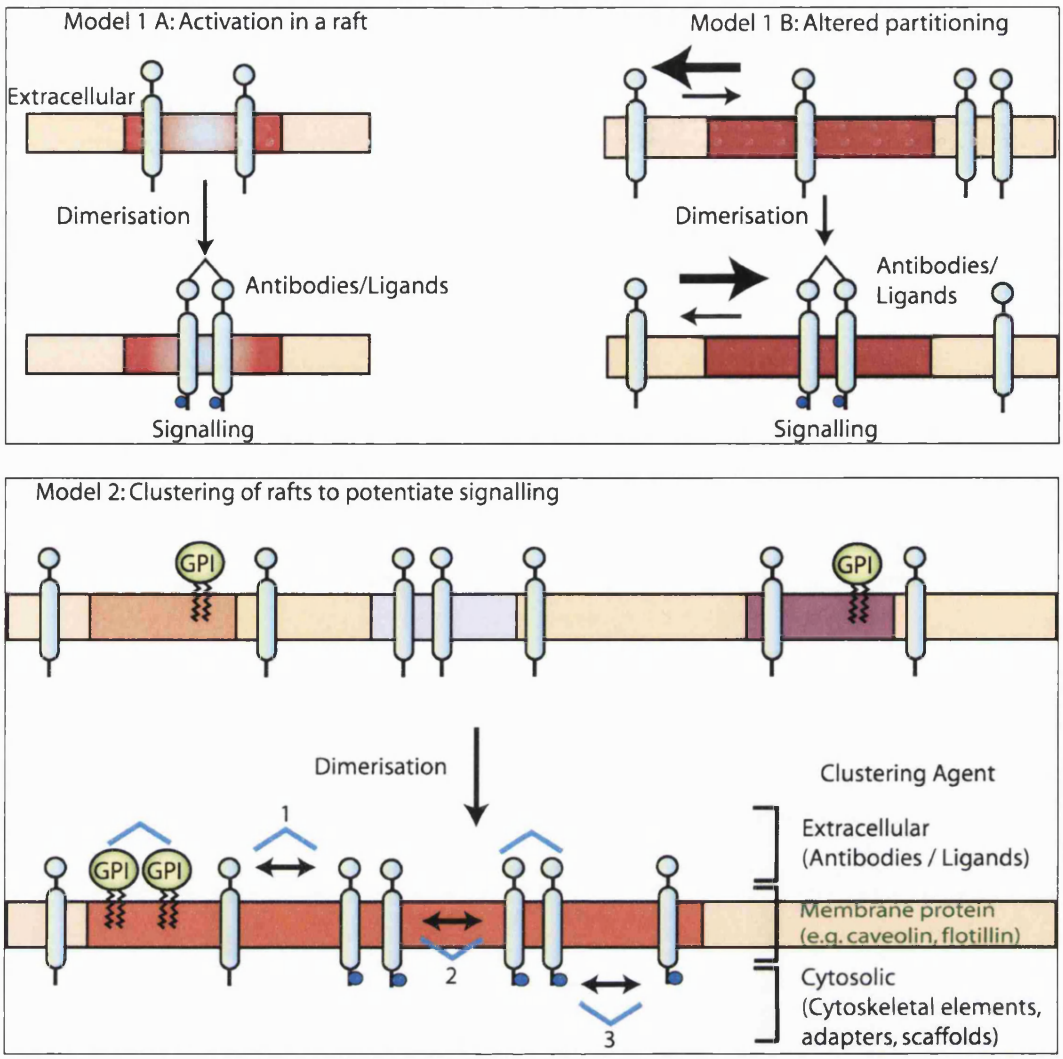

FIG 1.9: **Clustering of lipid raft proteins may initiate signalling complex formation**. Ligand binding or antibody crosslinking causes protein receptor dimerisation with resultant protein phosphorylation and signalling activation. The receptor proteins may be stable within the lipid raft or may be low residency lipid raft proteins whose phase distribution alters upon dimerisation and are subsequently stabilised within the lipid raft (Model 1A and 1B respectively). It is also possible that multiple subclasses of lipid rafts may form macro rafts, which contain unique protein compositions that become tightly associated and form signalling platforms. The clustering of these macro rafts may be induced through ligand binding (1), within the membrane by protein recruitment through caveolin or flottilin (2), or through cytoskeletal rearrangements and adapter complexes (3), (Model 2). The macro rafts would also function to retain weakly associated lipid raft proteins within the stable liquid ordered phase, without the requirement of being directly crosslinked to other proteins. Adapted from (Simons and Toomre, 2000).

The models proposed in Fig 1.9 are slowly being realised, with the creation of stable lipid raft environments being shown to produce optimal conditions for kinase activity and protein-protein interactions in a number of cellular signalling processes. A list of such lipid raft mediated signalling includes immunoglobulin E (IgE) signalling, during the allergic immuno response. It has been demonstrated that antigen mediated crosslinking of FcεRI receptor increases the proteins residency in lipid rafts leading to its activation and downstream signal propagation (Field *et al.*, 1995; Baird *et al.*, 1999; Holowka and Baird, 2001). Also T-cell antigen receptor signalling can be modulated through crosslinking of GPI-anchored proteins in microdomains of the T-cell surface, with lipid rafts increasingly thought to be integral in the formation of the immunological synapse (Janes *et al.*, 2000; Langlet *et al.*, 2000; Hoessli *et al.*, 2000). Signalling through the small GTPase H-ras is also thought to involve lipid rafts, with the palmitoylation of H-ras favouring its partitioning into caveolae. Disruption of caveolae structure, by cholesterol depletion with methyl-β-cyclodextran, or through expression of a dominant negative caveolin mutant, severely disrupted H-ras mediated activation of the serine/threonine Raf kinase protein family (Roy *et al.*, 1999). Many other systems are also thought to require lipid rafts but are beyond the scope of this introduction they can be found in Table 3 of (Simons and Toomre, 2000).

1.4.6 Involvement of lipid rafts in insulin signalling, GLUT4 trafficking and cellular sorting mechanisms.

1.4.6.1 Lipid rafts and insulin signalling

The role of lipid rafts in insulin regulated GLUT4 trafficking have already been proposed with the Cbl/CAP pathway detailed earlier. This pathway is thought to rely on recruitment of CAP/Cbl to a caveolae resident protein flotillin. It is believed that caveolae represent a considerable component of

lipid raft structures in the plasma membrane. Interestingly caveolin 1 and 2 are highly expressed in adipocytes with caveolin 1 expression increasing upon adipocyte differentiation (Scherer *et al.*, 1994; Scherer *et al.*, 1996). Caveolae are thought to be formed from lipid raft clustering through caveolin mediation (Simons and Ikonen, 1997; Schlegel *et al.*, 1998; Li *et al.*, 1998). Whether lipid rafts and caveolae in the PM form macro rafts with each other, upon the presentation of stimuli, remains uncertain but some evidence of GPI-anchored protein recruitment to caveolae through antibody crosslinking experiments suggests that this could occur (Maxfield and Mayor, 1997).

Caveolae have been implicated in providing a link between the IR and IRS1/2. Immunogold electron microscopy and immunofluorescence microscopy have identified a significant amount of the IR localised to caveolae (Gustavsson *et al.*, 1999). Interestingly the IR has also been found to contain one of the consensus binding sites for the caveolin scaffolding domain (Couet *et al.*, 1997) and was found to co-immunoprecipitate with caveolin, even when caveolae structures were dissipated through cholesterol depletion using β-cyclodextrin (Parpal *et al.*, 2001). Although the IR is apparently enriched in, detergent free, sucrose density gradient preparations of caveolin enriched fractions it is selectively lost in detergent isolated caveolae preparations (Gustavsson *et al.*, 1999). These observations may be accounted for if the IR is only weakly associated with caveolae. Indeed it has been previously shown that EGFR and the folate receptor are also selectively lost when detergent based caveolae preparations are used but are found highly enriched in the detergent-free caveolae isolation procedure (Smart *et al.*, 1995). In liver-derived cells lacking caveolae it has been shown that the IR becomes recruited to DRMs upon ligand binding (Vainio *et al.*, 2002). However ligand binding did not appear to alter IR localisation to caveolae in 3T3-L1 adipocytes (Gustavsson *et al.*, 1999). Cholesterol / caveolae depletion was shown not to effect insulin binding to the IR or its subsequent activation through autophosphorylation, however the tyrosine-specific phosphorylation of IRS1 in response to insulin was inhibited by 71 ± 6% (Parpal *et al.*, 2001). The

reason for this is unclear but recent evidence may shed light on the involvement of caveolae on IR downstream signal propagation. It has been demonstrated that, upon insulin binding, the IR phosphorylates caveolin through the downstream activation of caveolin bound Src family kinase Fyn (Mastick and Saltiel, 1997). The effects of caveolin phosphorylation are poorly understood but it has been shown that insulin stimulated phosphorylation of caveolin 1 at tyrosine residue 14 facilitates the binding of the SH2 domain of the adapter molecule Grb7 to caveolin 1 (Lee *et al.*, 2000). Grb14 belongs to the Grb 7 family and was shown to bind to the regulatory kinase loop of the IR through a novel domain termed the phosphorylated insulin receptor-interacting region (PIR) as early as 1 minute after insulin stimulation (Bereziat *et al.*, 2002). This coincides with the apparent insulin stimulated phosphorylation of caveolin 1 (Lee *et al.*, 2000). The Grb14 protein was shown to protect the IR from tyrosine phosphatase action, maintaining it in a phosphorylated state. However whilst serving a protective function, Grb14 has also been shown to induce an early delay in the activation of Akt and ERK 1/2 in CHO-IR cells through inhibition of IR's catalytic activity (Bereziat *et al.*, 2002). It is possible that phosphorylated caveolin 1 could modulate Grb14 interaction with the IR, removing Grb14 mediated IR inhibition, allowing IRS1 substrate phosphorylation. Caveolae disruption would reduce the level of caveolae associated Fyn kinase and would limit caveolin 1 phosphorylation and subsequent Grb14 association, leading to increased Grb14 retention on the IR and reduced catalytic activity towards IRS1. Another possibility is that Grb14 may serve to increases the recruitment of accessory proteins to caveolae upon insulin stimulation. Indeed Grb14 is known to contain a PTB domain that could link Grb14 to other tyrosine-phosphorylated proteins. This increased scaffold may facilitate interaction of the IR with IRS1 in some manner, which may depend on macro raft induced membrane curvature (Ikonen, 2001), or modulation of cytoskeletal elements to bring IRS1 within proximity of the IR. The involvement of the APS/Cbl/IR complex in IR stimulated IRS1 activation, through potential IR internalisation, (section 1.3.2.2) in relation to this proposed mechanism has not been investigated. The two mechanisms may work synergistically so that upon IR activation

the inhibition of its catalytic activity is removed with concomitant internalisation of the activated IR to interact with IRS1. These two mechanisms would facilitate a high level of control of downstream signal propagation, with the potential for feedback mechanisms to control not only the level of IR catalytic inhibition but also its proximity to IRS1. These mechanisms are by no means cast in stone and significantly more investigation is required before the involvement of caveolae in IR function is firmly established.

1.4.6.2 Lipid raft involvement in vesicle docking and fusion

Another role of lipid rafts, which will be touched upon briefly here, is their potential involvement in the concentration of SNARE proteins in the PM, facilitating membrane docking and fusion events. SNARE proteins syntaxin 1A and synaptosomal-associated protein (SNAP-25) were discovered to be highly enriched in lipid rafts (≈25 fold) (Chamberlain *et al.*, 2001). Chamberlain *et al.* also isolated the vesicle-associated membrane protein (VAMP2) in a distinct Lubrol WX resistant lipid raft, which was solubilised in conventional TX100 extraction procedures. However Lang and colleagues found that the same SNAREs were solubilised in both detergents (Lang *et al.*, 2001). Interestingly they did identify that these SNARE proteins clustered in a cholesterol-dependent manner through immuno-gold electron microscopy, with cholesterol depletion abolishing syntaxin clusters and reducing the rate of vesicle exocytosis. Although the exact nature of these SNARE clusters has not been fully established the concentration of SNAREs as defined through a macro raft hypothesis is appealing. It is believed that multiple trans-SNARE complexes are required for efficient fusion between membranes. Indeed reconstituted proteoliposomes only seem to fuse with appreciable rates and efficiency when abnormally high concentrations of SNARE proteins are used (Weber *et al.*, 1998).

1.4.6.3 Lipid rafts' potential involvement in cellular sorting mechanisms

It is thought that cholesterol-sphingolipid rafts are initially assembled in the Golgi (Brown and London, 1998) and may act as sorting platforms for inclusion of protein cargo destined for delivery to the PM (Simons and Ikonen, 1997). Once these lipid rafts are at the PM surface they are continuously endocytosed and recycled back to the PM either through classical clathrin-coated vesicles or, in the case of caveolae, the rafts may be internalised through a distinct mechanism leading to caveosome structures, (see (Pfeffer, 2001) for review). Caveosomes appear to be distinct from other endocytic machinery and have been postulated to be similar to lipid droplets, but their exact function is yet to be firmly established. Interestingly it seems that lipids are not distributed randomly throughout all endosomal membranes. Cholesterol and sphingomyelin are enriched in recycling endosomes but are found in relatively low levels in late endosomes for certain cell types (Kobayashi *et al.*, 1998a; Kobayashi *et al.*, 1998b). This raises the possibility that lipid rafts are differentially sorted within the endocytic pathway. There are a growing number of advocates for the proposal that lipid rafts may be an integral component for protein sorting mechanisms in the endocytic pathway (Tooze *et al.*, 2001; Gruenberg, 2001; Nichols *et al.*, 2001; Gagescu *et al.*, 2000).

1.5 Intracellular trafficking of GLUT4

1.5.1 The intracellular GLUT4 compartment

Numerous integral membrane proteins traffic to and from the PM through an endosomal recycling membrane system. As previously mentioned, (section 1.2.2) GLUT4 is localised to several elements of the recycling pathway

including the *trans*-Golgi network (TGN), clathrin coated vesicles and endosomes. Interestingly a large proportion of GLUT4 has been identified in tubular and vesicular structures, clustered in the cytoplasm, in a perinuclear location (Haney *et al.*, 1991; Malide *et al.*, 2000; Martin *et al.*, 2000). In resting cells over 95% of GLUT4 is sequestered in intracellular compartments (Rea and James, 1997). This is explained by kinetic studies using bis-mannose photolabelled GLUT4 and GLUT1 which showed that while GLUT4 has a similar rate of endocytosis to GLUT1 and TfR, in the basal state, its rate of exocytosis is around 3 times slower (Yang and Holman, 1993). These studies also demonstrated that insulin stimulates the targeted exocytosis of GLUT4 by 8-10 fold. In contrast GLUT1 and TfR exocytotic rates only increase 3 fold upon insulin stimulation. These observations may be explained by the proposal that a unique site of GLUT4 sequestration exists, away from the constitutive recycling endosomal system. This site may act to reduce the rate of GLUT4 exocytosis in the basal state and facilitate its rapid increase in response to insulin stimulation. This may be achieved by controlling a budding step from this compartment or modulating trafficking of GLUT4 vesicles to the cell surface and their subsequent docking and fusion (Slot *et al.*, 1991a).

There are several proteins, which are known to recycle between an intracellular pool and the PM through endosomal systems, such as the cation-dependent mannose 6-phosphate receptors (CD-MPRs), GLUT1, cellubrevin/VAMP3, and the transferrin receptor (TfR) (James and Piper, 1994). These proteins have been identified to co-distribute with GLUT4 to some degree and have consequently been used as markers to observe the differential sorting of GLUT4 within the cell. The recycling properties of TfR have been utilised in a technique termed endosome ablation, which have provided some of the most revealing observations in support of GLUT4 sequestration (Livingstone *et al.*, 1996). The technique involves transferrin, conjugated to horseradish peroxidase (HRP), being introduced and internalised by TfR into the endosomal system. Addition of 3,3'-diaminobenzidine (DAB) and H_2O_2 leads to HRP transferring electrons from DAB to H_2O_2 resulting in the crosslinking of the conjugate within its sequestered compartment. The crosslinking process results in the formation

of high molecular mass complexes within the compartment, which are rendered insoluble and are thus "ablated". In basal 3T3-L1 adipocytes this procedure resulted in the quantitative ablation of intracellular TfR, GLUT1, VAMP3, with around 90 % of TfR and VAMP3 being ablated after a 3 h incubation with Tf/HRP at 37°C (Martin *et al.*, 1996; Livingstone *et al.*, 1996). This ablation was determined to be specific for the recycling endosome system, as there was no significant ablation of TGN38 or lgp120, which are markers for the TGN and lysosomes respectively. Interestingly only 40 % of GLUT4 was ablated under these conditions. Insulin stimulation did not significantly alter the level of GLUT4 ablation, however the level of GLUT1 ablation significantly increased in insulin-stimulated cells. Indeed even after the recycling endosomal system is completely ablated insulin is still able to stimulate enhanced GLUT4 exocytosis to the PM, although the rate constant for this stimulation is reduced by half (Martin *et al.*, 1998). Two putative explanations for the ablation studies' findings were proposed. The first model involves the recycling of GLUT4 from the intracellular storage compartment to the PM via endosomes. The observed delay in GLUT4 recruitment to the cell surface, upon insulin stimulation, could thus be attributed to the reconstruction of the endosomal apparatus after ablation. The second model suggests that the insulin stimulated recruitment of GLUT4 from the intracellular storage compartment to the PM is direct. In this model the observed lag period would arise as a result of altered equilibrium dynamics as ablation of the endosomal system would perturb endocytosis of GLUT4 and effect the reloading of the intracellular storage compartment from the endosomal system. Increasing evidence tends to discredit the first model scheme and subsequently favour the second model scenario.

Studies using photolabelled GLUT4 identified that the initial rate of insulin stimulated GLUT4 exocytosis was significantly faster than the subsequent rates observed for GLUT4 recycling through the endosomes and secretory compartment, during the steady-state response to insulin (Holman *et al.*, 1994). If the first model holds true then it would be expected that both rates

should be the same, as GLUT4 would move through endosomes to the PM, both in the initial and continuous presence of insulin.

Immuno-EM on intracellular vesicles from adipocytes identified partial co-localisation of GLUT4 with VAMP3 which are now attributed to represent the endosomal pool of GLUT4 (Martin *et al.*, 1996). The same study discovered the v-SNARE VAMP2 co-localised identically with GLUT4, with 90 % of cellular VAMP2 unaffected by ablation procedures. These studies suggested that GLUT4 and VAMP2 are both sequestered in a distinct tubulo-vesicular, non-endosomal, compartment which has been termed the "perinuclear reticular GLUT4 storage compartment" (PR-GSC) (Holman and Sandoval, 2001). The nature of this GLUT4 storage compartment has since been more closely examined through exquisite analysis of cytoplasmic rims derived from rat adipose cells. Ramm *et al.* sandwiched adipose cells between an EM grid and a nitro-cellulose membrane and were able to isolate cytoplasmic rims away from the large lipid droplet, which is characteristic of adipose cells. The isolated rims' thickness (500 nm) allowed 3-Dimensional images of all the major organelles to be obtained, with highly efficient immuno-gold labelling of desired marker proteins (Ramm *et al.*, 2000). These studies revealed that, in basal cells, the majority of GLUT4 was distributed between tubules (PR-GSC) and small vesicles which Holman *et al.* defined as the "disperse vesicular GLUT4 storage compartment" (DV-GSC). Interestingly this procedure identified that the ratio of GLUT4:VAMP2 remained unaltered in VAMP2-positive vesicles after insulin stimulation. These observations preclude model 1 as it would be expected that the ratio of GLUT4:VAMP2 would be altered if the DV-GSC vesicles were re-mixed while passing through the endosomal compartments. Indeed the presence of VAMP2 in DV-GSC indicates that these vesicles may fuse directly with the PM upon insulin stimulation. The study also confirmed the previously detected specific association of the insulin-responsive aminopeptidase (IRAP) with DV-GSC vesicles (Elmendorf *et al.*, 1999; Garza and Birnbaum, 2000) and identified two major classes of GLUT4-positive vesicles in adipocytes. The presence or absence of the TGN to endosomal recycling protein CD-MPR defines these two classes of GLUT4 vesicles. In basal cells there is considerable overlap

(70%) in the intracellular distribution of CD-MPR and GLUT4 (Martin *et al.*, 1996; Hashiramoto and James, 2000; Klumperman *et al.*, 1993). However with the development of advanced whole mount immuno-EM techniques it became clear that, unlike GLUT4, the distribution of CD-MPR is relatively unaffected by insulin (Martin *et al.*, 2000). It appears that there are vesicles in which there is an apparently significant enrichment of GLUT4 with low levels of CD-MPR, for simplicities sake we will term these GLUT4(+)/CD-MPR(-) vesicles. The other GLUT4 containing vesicles appear to contain appreciable levels of CD-MPR and are thus termed GLUT4(+)/CD-MPR(+) vesicles. Upon insulin stimulation it appears that there is a specific loss of GLUT4 (+)/CD-MPR (-) vesicles (around 30%) (Martin *et al.*, 2000) whereas the observed total number of GLUT4(+)/CD-MPR(+) vesicles appeared to stay the same. Interestingly although the level of GLUT4 (+)/CD-MPR (+) vesicles did not alter, the concentration of GLUT4 within this class of vesicles did diminish upon insulin stimulation (around 30%) (Ramm *et al.*, 2000). These observations when placed into the context of the PR-GSC and DV-GSC hypothesis can be explained by the selective generation of a finite number of DV-GSC GLUT4(+)/CD-MPR(-) vesicles along with GLUT4(+)/CD-MPR(+) vesicles from the PR-GSC, in the basal state. Upon insulin stimulation these vesicles are rapidly recruited to the cell surface. At the same time the PR-GSC will need to generate new GLUT4(+)/CD-MPR(-) vesicles to maintain their specific recruitment to the cell surface. There may be re-sorting of GLUT4 out of the GLUT4(+)/CD-MPR(+) vesicles through there recycling back to the PR-GSC from the DV-GSC to accommodate this process. Prolonged insulin exposure would ultimately require reloading of the PR-GSC which might occur through sequestration of GLUT4 from the recycling endosomes and/or the TGN. A caveat to this model stems from the observation by Ramm that the amount of GLUT4 in tubules, which may correspond to the PR-GSC, did not appear to alter significantly upon insulin stimulation (Ramm *et al.*, 2000). Studies where GLUT4, tagged with green fluorescent protein (GFP), was monitored, in living 3T3-L1 adipocytes, by time-lapse confocal microscopy may offer an explanation to this problem (Fletcher *et al.*, 2000). This study identified two predominant subsets of GLUT4-GFP vesicles, the first was highly motile

while the other remains almost static. Upon insulin stimulation the motile vesicles were potentially recruited to the cell surface while the static vesicle population exhibited a gradual decrease in their fluorescence intensity which paralleled the observed increase in fluorescence detection at the PM. These observations could represent the replenishment of DV-GSC GLUT4(+)/CD-MPR(-) vesicles by the PR-GSC after the initial burst of GLUT4 vesicles to the PM. The time scale of this replenishment may be so rapid that the generation of new DV-GSC vesicles from the PR-GSC is not observed between the time frames of the confocal analysis. A dynamic equilibrium between the PR-GSC and the recycling endosomes/TGN would mean that any losses of GLUT4 from these compartments are mostly obscured by its rapid replenishment. Indeed in contrast to the results of Ramm et al., two papers did identify a slight decrease in labelling of TGN derived elements upon insulin stimulation (Martin *et al.*, 2000; Malide *et al.*, 2000).

1.5.1.1 Generation of the GLUT4 storage compartment

The generation of the GLUT4 storage compartment remains an area of much debate with many models proposed to account for the observed sequestration of GLUT4 in resting cells (Rea and James, 1997). Important observations into the generation of the storage compartment came from studies where cell morphology and GLUT4 expression were studied over 3T3-L1 fibroblasts differentiation to 3T3-L1 adipocytes (el Jack *et al.*, 1999; Ziehm *et al.*, 1993; Yang *et al.*, 1992). It appears that as 3T3-L1 fibroblasts differentiate to adipocytes, the development of a reservoir compartment precedes the emergence of GLUT4. Interestingly, unlike GLUT4, IRAP is present in fibroblasts and is sequestered in an insulin responsive compartment in the early stages of differentiation, again before the appearance of GLUT4 within the cell (Ross *et al.*, 1998). These studies suggest that GLUT4 is not the driving force in the generation of the GLUT4 storage compartment but that GLUT4 is directed to a pre-existing storage compartment in mature adipocytes.

Morphological studies have implied that the GLUT4 storage compartment is formed from specialised endosomes derived from the PM (Wei *et al.*, 1998) in a manner similar to that observed for synaptic vesicle biogenesis (Desnos *et al.*, 1995). Indeed EM studies have revealed GLUT4 positive clusters in tubulo-vesicular elements adjacent to sorting endosomes (Slot *et al.*, 1991b). Opposing theories suggest that the GLUT4 storage compartment is derived from the TGN, with initial studies suggesting that glucose storage vesicles budded directly from the TGN. Studies in atrial cardiomyocytes demonstrated that a significant amount of GLUT4 (50-60%) enters atrial natriuretic factor (ANF) secretory granules at the level of the TGN (Slot *et al.*, 1997). Slot proposed that the entry of GLUT4 into the TGN derived from the recycling pathway and not a biosynthetic route, as protein synthesis inhibition through cycloheximide treatment does not affect the accumulation of GLUT4 in the TGN. Problems with this theory arise from the apparent lack of co-localisation of the TGN marker TGN38 with glucose storage vesicles (GSV's) (Martin *et al.*, 1994). Also it appears that although IRAP and GLUT4 co-localise in tubulo-vesicular elements of atrial cardiomyocytes, IRAP does not feature significantly in the ANF secretory granules or the TGN of these cells. A possible explanation for these observations is that there may be a protein-sorting event at the level of the TGN that directs subsets of proteins to a post-TGN compartment. This compartment, referred to as the PR-GSC for the purpose of this introduction, may represent the functional equivalent of a pre-secretory compartment (Dittie *et al.*, 1997; Tooze, 1998). Interestingly analysis of the endogenous pro-protein convertase protein, furin, in BHK21 cells revealed that the processing of a biosynthetic substrate for furin occurs in a post-TGN processing compartment, which is in communication with early endocytic elements (Sariola *et al.*, 1995). It now appears that the PR-GSC could emanate from both the endosomes and the TGN. Indeed experiments with Brefeldin A (BFA) have indicated fusion of TGN-derived membranes with early endosomes, suggesting the existence of a recycling pathway between these two compartments (Lippincott-Schwartz *et al.*, 1991). The manner by which GLUT4 is sequestered into the PR-GSC remains unclear but may involve GLUT4 enrichment through interaction with a range of

adapter complexes at the level of the PR-GSC. Evidence to support this comes from observations using immunoelectron microscopy, which identified GLUT-4 localised to intracellular vesicles containing the Golgi-derived γ-adaptin subunit of AP-1 (Marsh *et al.*, 1998). Further to this immunoisolated GLUT4 vesicles have been shown to associate with significant levels of AP1 adapter subunits, which are TGN localised (Gillingham *et al.*, 1999). AP-1 could be involved in efficient budding of GLUT4 containing vesicles from the TGN to the PR-GSC or the PR-GSC to the DV-GSC that may consequently reflux back and forth between these compartments. However this may not be the only means for GLUT4 sequestration as novel adapter proteins have been discovered which might interact with GLUT4 in conjunction with AP1 and modulate its compartmental localisation. The TGN localisation of furin is thought to be achieved through its retrieval from the post-TGN endosomal compartment by binding of the novel cytosolic sorting protein phosphofurin acidic cluster sorting protein1 (PACS-1) (Wan *et al.*, 1998). The action of AP1 and PACS-1 together generates a situation where furin is in a cycling loop between the TGN and the post-TGN endosomal compartment. Modulation of furin's interaction with one or the other of these adapter proteins ultimately confers the localisation of the protein. This scenario seems to be mirrored at the level of the PM. Furin molecules internalised from the cell surface are also apparently retained in a local cycling loop between early endosomes and the plasma membrane (Molloy *et al.*, 1998), in a process that requires PACS-1, and AP2. Unfortunately a role for PACS-1 in GLUT4 trafficking cannot be established as it does not appear to be detected in adipocytes to date. However the bi-cycling theory is still a possibility if we consider the involvement of other adapter proteins in the retrieval process. Indeed AP3 has also been found to associate with isolated GLUT4 vesicles (Gillingham *et al.*, 1999) and this adapter has been implicated in endosomal sorting processes (Faundez *et al.*, 1998). Trafficking of GLUT4 at the level of the TGN/PR-GSC may also be mediated by the Golgi-localised, γ ear-containing, ARF-binding proteins (GGA's) which are monomeric proteins with adapter related domains (Robinson and Bonifacino, 2001). The various

binding specificities for the host of adapter proteins, coupled with the proposed bi-cycling nature of their interaction with trafficking proteins, may help to explain the dynamic relationship between the multiple compartments involved in GLUT4 sequestration and its specific insulin response. However considerable research is required to address which adapters influence GLUT4 localisation and how their interactions may be modulated. Some proposals for this modulation are given later in this introduction. A putative model for the trafficking of GLUT4 through multiple compartments and its relation to other trafficking proteins is shown in Fig 2.0.

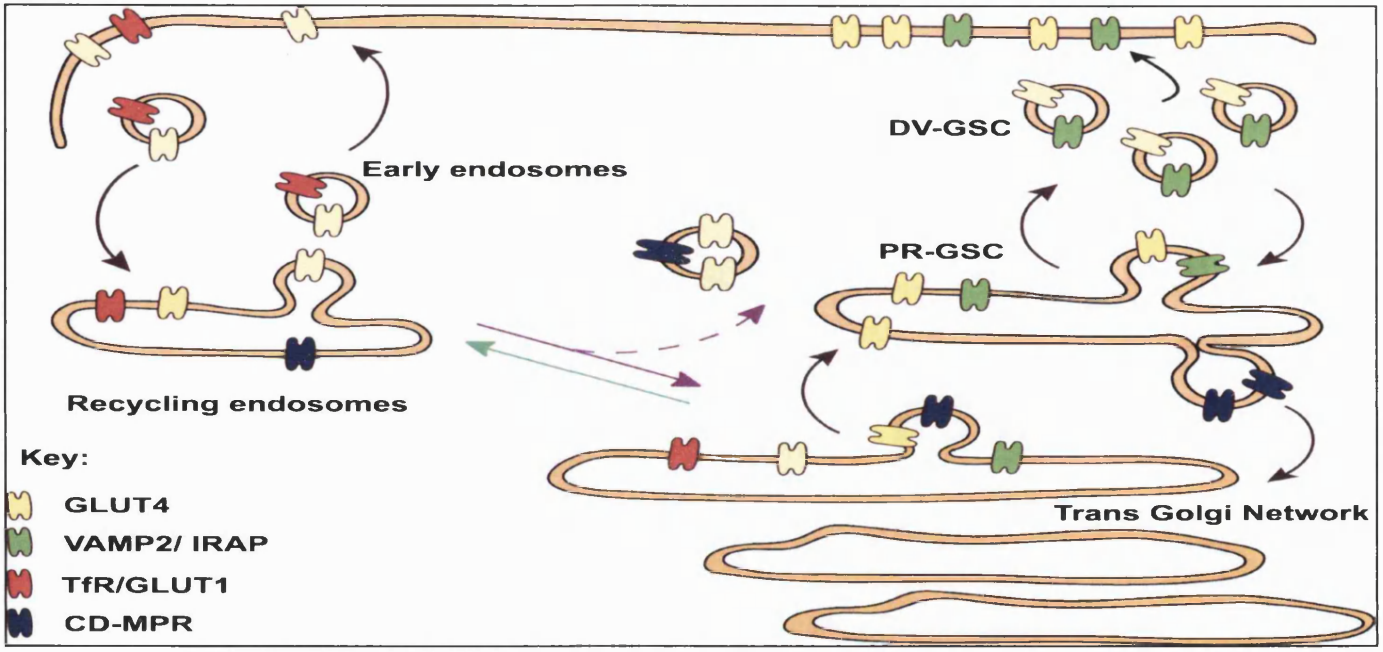

FIG 2.0: **Potential compartmental trafficking events of GLUT4 in relation to other trafficking proteins.** In resting cells GLUT4 is removed from the plasma membrane, mainly through internalisation and packaging into clathrin-coated vesicles. This procedure delivers GLUT4 to the endosome system, which is also occupied by TfR and GLUT1. Around 40% of GLUT4 remains accessible to this system, however the rate of GLUT4 recycling to the PM through the recycling endosome system is considerably slower than that observed for the constitutively recycling TfR and GLUT1 proteins. This slowed rate is thought to result from GLUT4 sorting and sequestration into the perinuclear reticular GLUT4 storage compartment (PR-GSC). This compartment may be derived from the TGN and may resemble a pre-secretory compartment, with a restricted protein population, which is enriched in VAMP2 and IRAP. GLUT4 may be sorted away from TfR and GLUT1 in the endosomes before entry into the recycling system, within the recycling system itself or even through sorting within the TGN. The PR-GSC is in equilibrium with a dispersed vesicular GLUT4 storage compartment, which generates highly enriched GLUT4 vesicles that are distinct from GLUT4 vesicles containing CD-MPR. Upon insulin stimulation GLUT4 is recruited to the PM through the recycling endosome pathway in the same manner as that seen for GLUT1 and TfR. However the major source of mobilised GLUT4 seen at the cell surface stems from the GLUT4 enriched DV-GSC vesicles which rapidly move to the PM. The diminished GLUT4 enriched DV-GSC vesicles could be supplemented by dynamic resorting of the GLUT4/CD-MPR vesicles, within the PR-GSC, to generate fresh GLUT4 enriched vesicles. The PR-GSC is itself supplemented with GLUT4 through its dynamic association with the recycling endosomal pool of GLUT4 and through potential GLUT4 recruitment directly from the TGN.

1.5.1.2 Insulin stimulated signalling regulates mobilisation of GLUT4 from different compartments.

The model shown in Fig 2.0 identifies how GLUT4 may respond to insulin through regulation of multiple compartmental trafficking processes. Increasing evidence suggests that different signalling pathways may modulate the regulation of individual compartments and are differentially activated in response to insulin, and other stimuli, that cause GLUT4 recruitment to the cell surface. It appears that the endosomal pool containing GLUT4 and GLUT1 can be regulated by insulin, phorbol esters and by the protein phosphatase inhibitor okadaic acid.

Phorbol esters are thought to stimulate PKC and stimulation of rat adipocytes with phorbol 12-myristate 13-acetate (PMA) appears to induce a four-fold increase in translocation of GLUT4 and GLUT1 to the cell surface (Gibbs *et al.*, 1991; Holman *et al.*, 1990). This effect is considerably less than that observed through insulin stimulation. Interestingly down-regulation of PKC by phorbol 12,13-dibutyrate pre-treatment inhibits PMA-stimulated GLUT4 translocation but does not have any discernible effect on insulin stimulated GLUT4 translocation (Todaka *et al.*, 1996). It is postulated that phorbol esters mobilise a distinct endosomal pool containing GLUT4 and GLUT1. Indeed wortmannin inhibition of PI3K prevents insulin stimulated GLUT4 translocation but appears to have little effect on PMA action (Todaka *et al.*, 1996), further confirming the different modular action of these two sets of stimuli.

Okadaic acid has also been demonstrated to stimulate a four-fold increase in GLUT4 translocation to the cell surface. Okadaic acid has been proposed to affect serine phosphorylation of IRS1 leading to a potential feedback inhibition effect like that proposed in section 1.3.3 (Tanti *et al.*, 1994). However okadaic acid has also been observed to increase phosphorylation of Serine 488 in the carboxyl terminal of GLUT4 by as much as three fold (Lawrence, Jr. *et al.*, 1990a). This enhanced phosphorylation was not observed through insulin stimulation alone and although okadaic acid stimulated GLUT4 translocation it was also observed to partially inhibit the actions of insulin on GLUT4 translocation and glucose transport. If okadaic

acid action is considered in relation to the bi-cycling model, proposed earlier, then modification of GLUT4 by phosphorylation might promote its translocation from the endosomal cycling loop to the cell surface. Dephosphorylation of this region by protein phosphatases would then shift GLUT4's equilibrium in this loop favouring internalisation. Okadaic acid functions to inhibit the action of protein phosphatase I and IIa, allowing increased accumulation of phosphorylated C-terminal GLUT4, and consequent translocation of GLUT4 to the cell surface. The partial inhibition in GLUT4 translocation, observed following insulin stimulation of okadaic acid-treated cells, may stem from altered equilibrium dynamics. Reloading of the PR-GSC from the endosomal pool of GLUT4 may be hindered by the previous alteration of the recycling loop dynamic by okadaic acid and this may consequently reduce the level of GLUT4 translocated from the DV-GSC in response to insulin. This idea is in opposition to Lawrence's postulation that phosphorylation of the C-terminal of GLUT4 promotes its internalisation. This theory was based on the apparent lack of an insulin stimulated increase in C-terminal GLUT4 phosphorylation. However, under insulin stimulation, the net level of phosphorylated GLUT4 may appear to be kept at a constant as a result of GLUT4's dynamic trafficking, through multiple compartments, in which rapid phosphorylation and dephosphorylation events may occur to control its dynamics in multiple cycling loops.

In addition to signalling control of the endosomal pool of GLUT4, studies have implied a specific role for protein kinase B (Akt) in the regulation GLUT4 trafficking from the PR-GSC/DV-GSC to the PM (Foran *et al.*, 1999). Evidence for this proposal stemmed from expression of a constitutively active Akt protein (Akt-DD) that was shown to induce GLUT4, but not GLUT1 or TfR, translocation to the cell surface. Additionally *Clostridium botulinum* toxins B or E that cleave VAMP2 and SNAP23, preventing efficient fusion of vesicles containing VAMP2 with the PM, were found to totally inhibit Akt-DD induce GLUT4 translocation. Use of the toxins in insulin stimulated cells inhibited GLUT4 translocation by 65%. The GLUT4 that translocated to the PM under toxin exposed conditions was considered to come from GLUT4 vesicles which do not contain VAMP2 and stem from the recycling endosomal pool of GLUT4 like GLUT1 and TfR,

whose insulin induced translocation to the PM were unaffected by toxin exposure. The regulation of PR-GSC/DV-GSC by Akt is further supported by the observation that agonists such as exercise and GTPγS, which are independent of Akt, seem to mobilise GLUT4 from an endosomal location and not from the PR-GSC (Millar *et al.*, 1999a; Ploug *et al.*, 1998).

1.5.2 Intracellular sorting signal motifs in GLUT4

GLUT1 and GLUT4 share high sequence similarity and predicted secondary structure but have very different trafficking properties within resting cells. Interestingly the differential distribution of these two proteins is not restricted to insulin responsive cells. Studies where GLUT4 and GLUT1 are expressed in non-insulin responsive cells such as HepG2 or 3T3-L1 fibroblasts via DNA-mediated gene transfer suggest that GLUT4 and GLUT1 partition into different locations in much the same fashion as seen in insulin responsive cells (Haney *et al.*, 1991). However GLUT4 expressed in 3T3-L1 fibroblasts is not responsive to insulin, suggesting that non-insulin responsive cells posses the correct components to effectively sequester GLUT4, away from GLUT1, but additional mechanisms dictate GLUT4's trafficking, out of the intracellular storage compartment, upon insulin stimulation. It has been the goal of many laboratories to define the molecular features of GLUT4, which dictate its intracellular sequestration and unique targeting. Initial studies focussed on the regulation of GLUT4 internalisation through the recognition of motifs, within the cytoplasmic tails of GLUT4, by subcellular trafficking binding proteins. A model highlighting potential binding motifs within the GLUT4 cytoplasmic tails is shown in Fig 2.1. The possible roles of these motifs will be detailed in the course of this introduction.

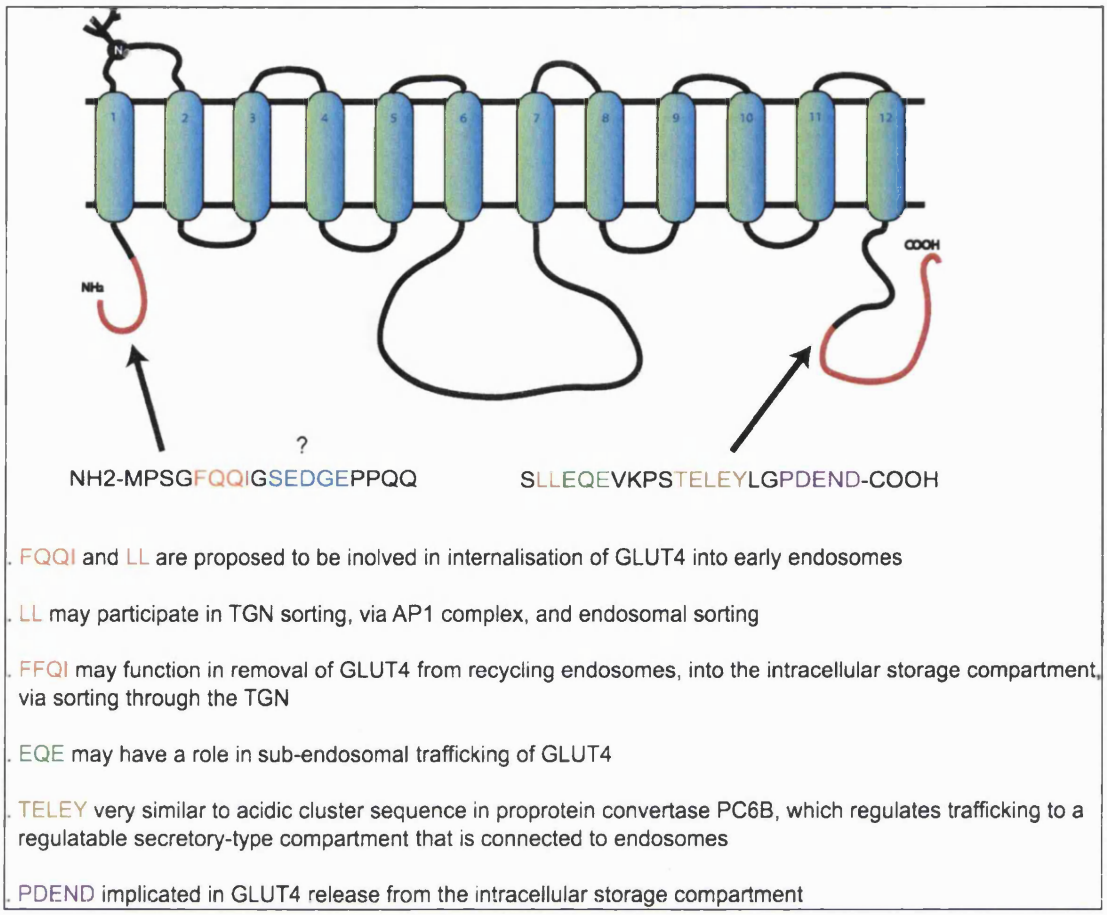

FIG 2.1: **Schematic illustration of GLUT4, identifying motifs within the cytoplasmic domains of GLUT4 that may be involved in its unique trafficking properties.** Individual motifs may directly interact with adapter binding proteins but the strength of this interaction may be facilitated by other surrounding motifs.

The exact motifs involved in GLUT4's unique trafficking remain a point of contention between the leading research groups in the field, with the relative significance of two particular amino acid motifs at the centre of the argument. One of the motifs in question is found in the N-terminal cytosolic domain of GLUT4 $F^{5}QQI^{8}$ while the other is situated in the C-terminal cytosolic domain $L^{489}L^{490}$.

1.5.2.1 The Amino Terminus of GLUT4: studied in non-insulin responsive cells.

In 1992 Piper and colleagues generated chimeras of GLUT1 and GLUT4 which they transiently expressed in CHO cells. They showed that a substitution of the amino terminal region of GLUT4, with that of GLUT1, abolished its intracellular sequestration. If the amino terminal region of GLUT1 was substituted for that of GLUT4 this protein was sequestered into a compartment similar to that observed in adipocytes (Piper *et al.*, 1992). Similar substitutions in the carboxyl terminal region of GLUT1 and GLUT4 resulted in no observable change in sequestration of these proteins from the wild type controls. Consequently Piper suggested that the amino terminus was both "necessary and sufficient" for the intracellular sequestration of GLUT4. Additional studies revealed that the first 13 amino acids of GLUT4, in the cytosolic tail of the protein, were responsible for GLUT4 segregation. Deletion of this region, or substitution of phenylalanine-5 for alanine within this sequence, resulted in a significant increase in the observed levels of GLUT4 seen at the cell surface (Piper *et al.*, 1993a). Further to this, these modifications also abolished the co-localisation of GLUT4 with clathrin lattices at the PM, suggesting that this domain area may be involved in facilitating GLUT4 incorporation into clathrin coated pits in an endocytic process. The FQQI motif found in the N-terminal of GLUT4 seems to bear a close resemblance to tyrosine containing internalisation motifs found in the cytoplasmic tails of the recycling receptors TfR and CD-MPR (Collawn *et al.*, 1990). Many more proteins also contain a similar motif with a consensus definition of YxxΦ (Y is tyrosine or potentially phenylalanine, x is any amino acid and Φ is any hydrophobic amino acid)

which forms a β-turn in solution (Trowbridge *et al.*, 1993; Pytowski *et al.*, 1995). This motif is recognised by a range of adapter proteins, chiefly AP2 at the PM, which are thought to facilitate the recruitment of proteins into clathrin coated pits for efficient endocytosis (Pearse and Robinson, 1990). Fascinatingly when the first 23 amino acids of GLUT4 were grafted onto the H1 subunit of the asialoglycoprotein receptor its level of internalisation compared to the wild type receptor was significantly increased. Also the chimera protein was found to localise to a perinuclear region, which was also seen to be occupied by expressed wild type GLUT4 (Piper *et al.*, 1993a). These observations indicated that the N terminal cytosolic domain of GLUT4 was not only involved in GLUT4 internalisation but also in its subsequent recruitment to the intracellular storage compartment.

Unfortunately these initial observations were not the end of the story. Trafficking kinetic studies using GLUT4:TfR chimeras, in which the N-terminal of TfR was substituted for that of GLUT4, suggested that the N-terminal did not facilitate intracellular sequestration (Garippa *et al.*, 1994). The GLUT4:TfR chimera appeared to recycle back to the PM at the same rate as that observed for the wild type TfR, suggesting that the addition of the N-terminal region of GLUT4 was not re-routing the TfR. These studies did show a 50% reduction in the internalisation rate of the chimera protein, which was reduced a further twofold by substitution of phenylalanine for alanine in the FQQI region of the chimera. This was in agreement with trafficking studies of ATB-BMPA-tagged GLUT4, F5 mutants, in CHO cells, which showed a 40% reduction in internalisation rates compared with wild type labelled GLUT4 (Araki *et al.*, 1996). Overall these studies suggested that the FQQI motif functions as a relatively weak endocytic determinant. Indeed when F5 was replaced with a tyrosine residue, forming the classical consensus internalisation motif, the rate of internalisation of the mutated GLUT4:TfR chimera increased to that observed for the wild type TfR (Garippa *et al.*, 1994). The reduced rate of endocytosis incurred using the FQQI motif, compared with that of the classical YxxΦ, may be important in the differentiation of GLUT4 away from other trafficking proteins and requires further study.

1.5.2.2 The Carboxyl Terminus of GLUT4: studied in non-insulin responsive cells.

In 1993 a series of publications questioned the proposal that the amino terminal was "necessary and sufficient" for the intracellular sequestration of GLUT4. Indeed many went so far to say that it was the carboxyl-terminal region which was integral for such a process (Czech *et al.*, 1993; Verhey *et al.*, 1993). Both studies generated GLUT1:GLUT4 chimeras substituting the C-terminal regions of these proteins with each other. Additionally an epitope tag within the GLUT4 was added to these chimeras which could be recognised by antibodies and differentiate these proteins from endogenous GLUT1 and GLUT4. The chimeras where expressed in COS-7 cells (Czech *et al.,* 1993) or NIH 3T3 and PC12 cells (Verhey *et al.,* 1993) and both showed that substitution of GLUT4 C-terminal domain for that of GLUT1 resulted in the GLUT4 chimera displaying GLUT1 trafficking characteristics. Conversely the substitution of the C-terminal domain of GLUT1 with that of GLUT4 led to the GLUT1 chimera being effectively sequestered into an intracellular compartment in much the same fashion as observed for the native GLUT4 protein. Verhey and colleagues did find a partial role for the N-terminal GLUT4 domain in GLUT4 intracellular sequestration but concluded that the C-terminal region of GLUT4 was of primary significance in the unique cellular routing of the protein.

Further investigation into the specific determinants, within the C-terminal of GLUT4, that influenced its sequestration revealed that the $L^{489}L^{490}$ motif was crucial for this process. GLUT1 chimeras in which the LL was mutated to alanine and serine, within the substituted GLUT4 C-terminal domain, resulted in the re-localisation of the chimera, away from the perinuclear storage compartment, towards the cell surface (Verhey and Birnbaum, 1994). Again ATB-BMPA-tagged mutant GLUT4 trafficking studies in CHO cells supported this observation. Mutation of LL to AA in these studies did not alter the endocytic rate but did increase the recycling rate which may be expected if the mutation diverted GLUT4 away from an intracellular storage pool leaving it in the recycling endosome pool (Araki *et al.*, 1996).

1.5.2.3 The Amino and Carboxyl Termini: studied in insulin responsive cells.

Initial studies to identify the significance of the N and C-terminal domains involvement in GLUT4's unique trafficking provided conflicting data with regard to defining which domain was necessary for intracellular sequestration. These studies all involved the expression of chimeric/mutant GLUT4 species in non-insulin responsive cells, which may not posses the cell specific factors which mediate insulin-stimulated trafficking of GLUT4 in bona-fide insulin-responsive cells. Indeed 3T3-L1 fibroblast differentiation studies show that although a intracellular storage compartment is present in 3T3-L1 fibroblasts this compartment is unresponsive to insulin (section 1.5.2). It is a possibility that GLUT4 trafficking into the storage compartment seen in non-insulin responsive cells, is mediated by different signals to those required for its sequestration into the insulin-responsive intracellular storage compartment present in insulin-responsive cells such as 3T3-L1 adipocytes and L6 myoblasts. Another problem in interpreting the aforementioned trafficking data is that the high levels of protein expression induced by some of the above procedures (Piper *et al.*, 1992) may saturate the sorting machinery leading to a default routing to the cell surface. Support for this stems from studies involving transgenic mice overexpressing GLUT4 (Liu *et al.*, 1993). These mice showed highly elevated PM levels of GLUT4, in the basal state, which was suggested to result from saturation of either the storage compartment or the trafficking machinery responsible for normal basal sorting of GLUT4 away from the rapidly recycling endosomal pool.

Clarification of the involvement of GLUT4 signals in insulin-responsive cells came from a series of studies in 1995. Marsh and colleagues showed that both the amino and carboxyl terminal motifs function in distinct targeting of GLUT4 in 3T3-L1 adipocytes (Marsh *et al.*, 1995). This conclusion was supported by Birnbaum and colleagues who went further to suggest that the carboxyl terminal is essential for sorting GLUT4 to an insulin-responsive compartment and implicated the amino terminal as an important component in GLUT4 internalisation in mouse 3T3-L1 adipocytes (Verhey *et al.*, 1995). Interestingly these studies and those performed in L6 myoblasts suggested

that the LL motif in the C-terminal of GLUT4 was necessary but not sufficient for the intracellular sequestration of GLUT4, implicating other residues within this region to influence this process (Haney *et al.*, 1995).

Some of the most elegant characterisation studies were performed by Gould and James, who further expanded the role of the FQQI and LL motifs (Melvin *et al.*, 1999). They created a series of constructs that were expressed at near endogenous levels in 3T3-L1 adipocytes. The TAG construct related to epitope-tagged wild type GLUT4, FAG related to epitope-tagged N-terminal $F^5 \rightarrow A$ mutant GLUT4 and LAG related to epitope –tagged C-terminal $L^{489}L^{490} \rightarrow AA$ mutant GLUT4. The intracellular location of the mutant GLUT4's was then determined by analysing their subsequent levels of ablation after TfR/DAB/H2O2 treatment (Section 1.5.1). These studies found that the FAG mutant localised to the recycling endosomal pathway and was ablated to a far greater extent than the LAG mutant which escaped ablation even more effectively than wild type TAG GLUT4. The observation that the LAG mutant co-fractionated with IRAP in sucrose density gradient fractions suggests that the reduced ablation of this mutant may stem from its increased retention in the intracellular storage compartment. It was concluded that the FQQI and LL motifs may both be involved in internalisation of GLUT4 into early endosomes and that FQQI may additionally be involved in the removal of GLUT4 from the endosomal pool into a non-ablated compartment, via sorting into the TGN. This was further substantiated through observations made by Sandoval and colleagues who also concluded that the FQQI motif was essential in GLUT4 trafficking to the perinuclear storage compartment (Palacios *et al.*, 2001). James and Gould also proposed an additional function for the LL motif in sorting GLUT4 back out of the TGN into the recycling endosomal system. The LAG mutant would act to functionally prevent LAG GLUT4 re-entering the recycling endosomes and consequently reduce the level of its ablation.

If these results are considered in relation to the proposed PR-GSC/DV-GSC model (Section 1.5.1.2) then FQQI and LL may form a bi-cycling loop, with FQQI mediating GLUT4 entry into the PR-GSC from recycling endosomes or the TGN, and LL mediating GLUT4 trafficking out of the PR-GSC to the recycling endosomes or the TGN. The signals involved in the highly selective sorting of GLUT4 from the PR-GSC to the DV-GSC are not

obvious from these studies. It may be that, like the scenario found for the apparent duality of FQQI and LL motifs involved in GLUT4 internalisation, the lack of one motif can be compensated by the presence of the other (Holman and Sandoval, 2001). Studies are increasingly implicating other motifs, found in the N and C terminal domains, in GLUT4 sorting (Shewan *et al.*, 2000; Cope *et al.*, 2000; Martinez-Arca *et al.*, 2000) (See Fig 2.1 for brief synopsis). The plethora of signal determinants that may modulate GLUT4 trafficking, add credence to the redundancy theory, as abrogation in one motif may be safeguarded by the existence of multiple failsafe mechanisms. Indeed rapid internalisation of IRAP has been shown to require any two of three distinct motifs $M^{15,16}$, DED^{64-66} and $L^{76}L^{77}$ (Johnson *et al.*, 2001).

1.5.2.4 Interaction of GLUT4 carboxyl domains with potential trafficking proteins: Cytoskeletal involvement in insulin induced GLUT4 translocation.

Injection of a synthetic peptide corresponding to the C-terminal cytoplasmic domain of GLUT4 was found to induce insulin-like GLUT4 recruitment to the cell surface and glucose transport stimulation in rat adipocytes (Lee and Jung, 1997). The authors suggested that cellular proteins might interact with carboxyl domains, either as adapters whose interaction is required for GLUT4 trafficking, or as enzymes that prime GLUT4 for trafficking by modification. Although adapter proteins like AP1 have been implicated in this process (Melvin *et al.*, 1999) no definite physiological protein interactions have been found with the C-terminal of GLUT4. Yeast two-hybrid assays have identified C-terminal GLUT4 interacting proteins such as YP10, a 1-3-hydroxyacyl-CoA dehyrogenase (HAD) isoform (Shi *et al.*, 1999) and more interestingly C109, a myosin II related protein (Lee *et al.*, 1997). Incorporation of C109 into rat adipocytes was found to greatly reduce GLUT4 PM levels and glucose flux capacity. GST- C109 avidly bound to the GLUT4-vesicles isolated from basal rat adipocytes, but not those isolated from insulin treated adipocytes, suggesting that myosin or a myosin-like protein may be involved in insulin-regulated movement of

GLUT4 to a functionally specialised area in the PM. GST-C-terminal GLUT4 fusion protein has also been identified to specifically associate with 1,6-bisphosphate aldolase (Kao *et al.*, 1999). Aldolase was also shown to interact with F-actin and disruption of this interaction through microinjection of aldolase-specific antibodies or introduction of 2-deoxy-D-glucose inhibited insulin-stimulated GLUT4 exocytosis. There was no observable alteration in the level of endocytosis invoking the possibility that dynamic actin rearrangements thought to be involved in insulin signal transmission (Section 1.3.3) may also play a more direct role in trafficking of GLUT4 from the DV-GSC to the PM.

1.5.2.5 Intracellular trafficking modulation by phosphorylation state of GLUT4 motifs

As previously mentioned in section 1.5.1.2, Ser^{488} in the SLLE area of the C-terminal domain of GLUT4 is capable of being phosphorylated. This phosphorylation is thought to be mediated by cAMP-dependent protein kinase (Lawrence, Jr. *et al.*, 1990b). It has been shown that isoproterenol (a β-adrenergic agonist) inhibits insulin stimulated glucose transport without decreasing the number of plasma membrane transporters (Joost *et al.*, 1987). It may be that the action of isoproterenol via a cAMP-dependent pathway results in phosphorylation of Ser^{488} or an associated regulatory protein and this in some way alters the intrinsic activity of glucose flux by GLUT4 (Schurmann *et al.*, 1992).

Furin endoprotease bi cycling as detailed in section 1.5.1.1 involves differential interaction of furin with PACS-1 and a host of adapter proteins. Studies have identified an acidic cluster (AC) motif in the cytoplasmic tail of furin which together with a pair of serine residues forms a casein kinase II (CKII) phosphorylation site. Indeed phosphorylation of furin by CKII is thought to mediate its interaction with PACS-1 and the balance between AC dephosphorylation by PP2A and its phosphorylation by CKII determines the predominance of furin's localisation within multiple endpoints (Jones *et al.*, 1995; Molloy *et al.*, 1998). There is evidence that CKII phosphorylation of the cytoplasmic tails of CD-MPR, and other proteins such as PC6B,

generates PACS-1 binding sites and modulates their cellular routing (Meresse and Hoflack, 1993; Crump *et al.*, 2001). It is interesting to note that the LL motif found in the C terminal of GLUT4 is juxtaposed by a proximal acidic cluster motif (TELEYLGP). When this region was mutated there was increased TfR-HRP mediated ablation of the mutant GLUT4 suggesting that this region was involved in GLUT4's sorting into the PR-GSC/DV-GSC (Shewan *et al.*, 2000). The N terminal targeting domain of GAD65, the membrane-associated form of the enzyme glutamic acid decarboxylase that is responsible for GABA synthesis in neurons (Namchuk *et al.*, 1997), contains eight out of eleven amino acids that are sequence identical to the N terminal of GLUT4, see Fig 2.2.

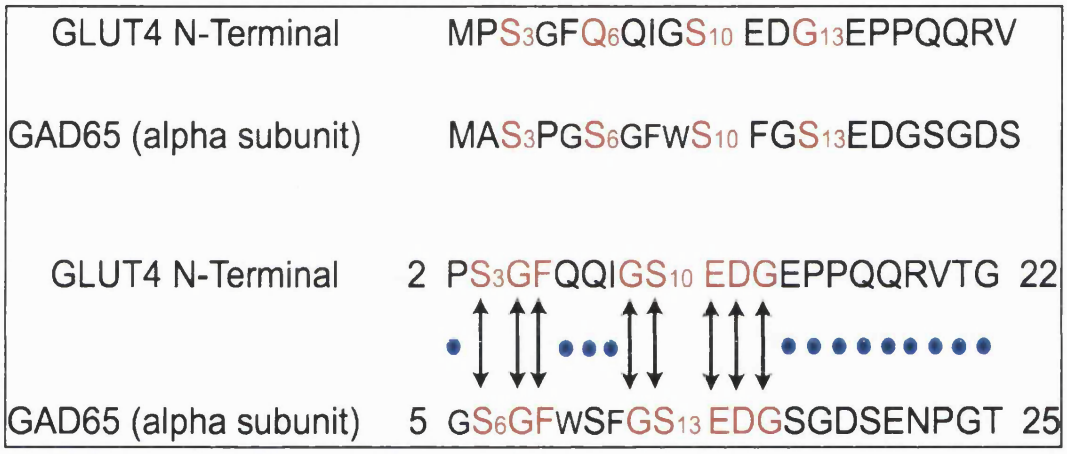

FIG 2.2: **Sequence identity between GAD65α and the N-terminal of GLUT4.** The sequences of GLUT4 and GAD65α were retrieved from the Kyoto Encyclopaedia of Genes and Genomes (KEGG) and aligned using the BESTFIT algorithm of Smith and Waterman (1998).

Within the area of homology, between GLUT4 and GAD65α, lies a potential CKII acidic cluster phosphorylation site S^{10}EDGE which could modulate the interaction of proteins with the upstream FQQI motif or with this site itself. Indeed GAD65α has been shown to by multiply phosphorylated by an unidentified membrane associated kinase, which is thought to regulate specific aspects of GAD65 function in the synaptic vesicle membrane (Namchuk *et al.*, 1997).

1.5.3 Coated vesicle formation: The role of adapters

1.5.3.1 Clathrin

The formation of vesicles composed of distinct subsets of proteins is thought to result through their concentration, via coat proteins, and subsequent vesiculation of the donor membrane. Coated vesicles were first effectively visualised using negative staining microscopy (Kadota and Kaneseki, 1969) and appeared to consist of a spectacular lattice of polyhedral structures, which were later purified and termed clathrin (Pearse, 1976). The basic clathrin assembly unit, the triskelion, is a trimeric structure containing three 175-kDa heavy chains (HC) and an equivalent number of 30-40-kDa light chains, LC_a and LC_b, which are randomly distributed (Hirst and Robinson, 1998). These clathrin triskelions polymerise into a lattice along the cytosolic face of a region of membrane, which causes the inward deformation of the membrane, resulting in the clathrin-coated pit configuration. Studies where low – density lipoprotein (LDL) endocytosis were monitored, through electron microscopy, showed that LDL was concentrated in clathrin-coated pits. Interestingly, by incubating samples at 37°C before fixing, these coated pits could be observed pinching off the membrane to form coated vesicles which were later uncoated (Anderson *et al.*, 1977). In addition to LDL it is now evident that a host of proteins are internalised in a clathrin-coated pit mediated process including GLUT4, TfR and epidermal growth factor receptor (EGFR) (Rea and James, 1997; Hirst and Robinson, 1998).

1.5.3.2 Adapter Proteins

Receptors competing to be transported by the coated pit system are analogous to skiers joining a cable-car network. Only skiers with the appropriate ski pass will be allowed entry, and although different groups of skiers may be present in any one cable car, they are all taken to the same

station. Certain skiers may posses passes that allow them to venture all over the slope where as others may have restricted access to specific areas (Pearse *et al.*, 2000). Adapter proteins (AP's) can be regarded as the ski pass screeners of this process, ensuring that only the skiers with the correct pass are allowed onto the cable car. Adapter proteins at both the PM and TGN recognise specific integral membrane proteins, through their cytosolic domains, binding them and polymerising clathrin to drive clathrin coated vesicle formation (Vigers *et al.*, 1986; Kirchhausen, 1999).

There are currently four known AP's, that form heterotetrameric complexes with similar structures that can be envisaged as resembling a Mickey Mouse head. They consist of two 100 kDa adaptins (γ and β1-(AP1), α and β2 (AP2), δ and β3 (AP3), ε and β4 (AP4)), a medium ~45 kDa μ chain (μ1, μ2, μ3 and μ4 respectively), and a small ~20 kDa σ chain (σ1, σ2, σ3 and σ4). These subunits are also thought to exist in two or more distinct isoforms, encoded by different genes, allowing multiple configurations within each adapter subtype. The variance within each adapter may be required to fine tune their localisation and trafficking properties (Ball *et al.*, 1995; Takatsu *et al.*, 1998; Lewin *et al.*, 1998; Folsch *et al.*, 2001). A model of the four known adapter complexes, showing the presumed interactions of the aforementioned subunits, is shown in Fig 2.3.

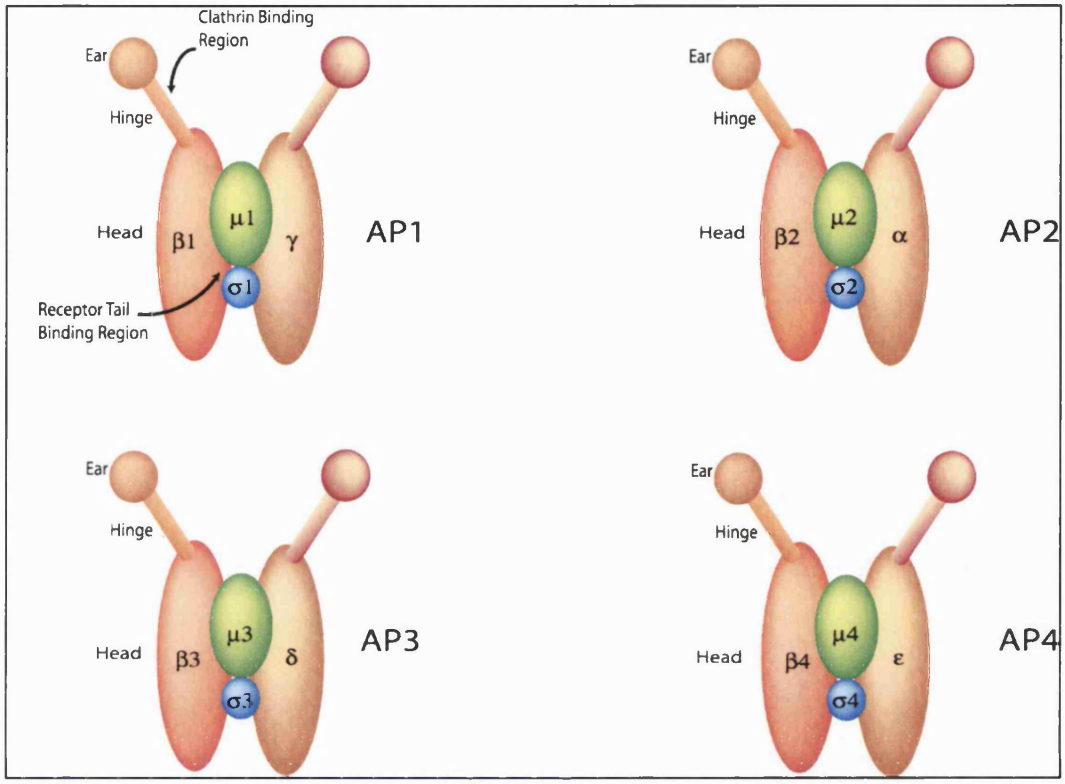

FIG 2.3: **Structure and composition of the Adapter Proteins.** All four complexes comprise two large subunits: a β subunit and a more divergent subunit. The carboxy-terminal domains of the two large subunits project as "ears", connected to the "head " of the complex by flexible hinges. Yeast two-hybrid data suggests that the γ/α/δ/ε subunits interact with the σ subunits, the β subunits interact with the μ subunits and the two large subunits interact with each other. Adapted from (Robinson and Bonifacino, 2001).

Characterisation of the adapter complexes has indicated that the β-subunits are critical for clathrin binding. The site of interaction is thought to reside in the hinge domain, although an involvement of the β ears and hinge domains of the γ and α subunits, in the stable binding of clathrin, have also been proposed (Shih *et al.*, 1995; Dell'Angelica *et al.*, 1998; Owen *et al.*, 2000; Morgan *et al.*, 2000). Most experimental data suggest that the Yxxθ motif of several trafficking proteins interacts with the μ subunits of both AP1 and AP2 (Ohno *et al.*, 1996; Owen *et al.*, 1999), with this also likely to be the case for AP3 and AP4. Interestingly the β subunit may also function in the selection of cargo, with Far-Western blots identifiying an interaction between purified asialoglcoprotein and the β2 subunit (Beltzer and Spiess, 1991). Crosslinking studies using protein derived peptides also revealed that the β1 subunit recognised a series of peptides (including a C-terminal peptide of GLUT4) that contained the LL motif (Rapoport *et al.*, 1998). However the recognition of LL motifs may not be mutually exclusive to the β subunit as the μ subunit has also been shown to interact with this region (Hofmann *et al.*, 1999). A role for the σ subunits in cargo selection has also been proposed, with yeast two-hybrid studies identifying that σ3A-subunit associates with non-tyrosine phosphorylated IRS1 (VanRenterghem *et al.*, 1998) (See Section 1.3.3). The α, β and γ ears of these complexes are thought to recruit a myriad of accessory proteins which aid in coat assembly, membrane fission and may be involved in the co-ordinated effects of endocytosis associated with changes in actin cytoskeleton and lipid metabolism. One of these accessory proteins includes Dynamin, which is associated with microtubules that may mediate its function in pinching off clathrin coated pits to form clathrin coated vesicles. A detailed review of Dynamin and other accessory proteins can be found in Takei and Haucke, (2001).

1.5.3.3 Binding of expanded receptor tail motifs

Binding of AP μ subunits to the classical Yxxθ and LL binding motifs was considered to be intolerant of substitution of either the tyrosine or the bulky

hydrophobic side chain θ. Crystallography studies using the μ2 binding domain of AP2 complexed with signalling motif peptides derived from TGN38 and EGFR peptides helped to explain this specificity (Owen and Evans, 1998). The μ2 binding domain appeared to comprise of 16 β-strands arranged into a further two subdomains which constituted binding pockets for the aromatic and hydrophobic amino acids found in the Yxxθ motifs of the peptides. These interactions were described as a "two pinned plug into a socket", by Owen and Evans, who also found that this socket excluded LL sequences. Interestingly the Yxxθ motif bound to μ2 in an extended conformation and not in the biochemical predicted β-turn configuration. The apparent transition of a cytoplasmic tail domain from a closed to open conformation to facilitate binding to adapter μ subunits may afford another level of selectivity for a range of trafficking proteins that contain Yxxθ motifs. Recently the two-pinned plug model has been revised with the addition of a third determinant site on the μ2 binding subunit (Owen *et al.*, 2001). It now appears that some sequences can function as a "three pinned plug". The best characterised of these is the cell adhesion protein P selectin, whose Yxxθ-like motif is tolerant to substitutions of the Y and θ residues. Crystallography studies have shown that P selectin binds to the μ2 subunit in the same manner as classically envisaged, however a leucine residue in the Y-3 position is accommodated in a third hydrophobic pocket, previously uncharacterised (Owen *et al.*, 2001). The three-pinned plug model expands the range of sequence recognition sites for potential AP interacting proteins, as the sorting machinery may interact over a larger motif area than just the Yxxθ motif. Indeed it is possible that regions between Y+4 to Y+7 may interact with a different subunit of the AP complex, incurring an extra level of protein selectivity. The combined use of a quantitative two-hybrid assay and an *in vitro* competition assay highlighted that mutation of some residues affected interactions with μ1 and μ2 to the same extent, whereas other mutations had differential effects (Ohno *et al.*, 1996). These observations further support the notion that broad sequence determinants control the differential binding affinity of the range of adapter proteins and ultimately control the cellular routing of that protein. The interaction of various adapter proteins with specific proteins could be further refined through

phosphorylation events within the recognition area (Section 1.5.2.5). Indeed phosphorylation of a site four residues upstream of the LL motif in the CD-MPR enhances its sorting into a post-Golgi compartment (Mauxion *et al.*, 1996).

1.5.3.4 Regulation of Adapter Recruitment

Different adapter proteins are involved in clathrin-coated vesicle formation at specific sites within the cell. AP1 and AP4 bind to the TGN and TGN-related compartments, AP2 is found mainly at the PM, while AP3 binds to peripheral and endosomal membranes (Hirst and Robinson, 1998). The manner by which AP's are recruited to these locations is still not completely clear but increasing evidence points towards the involvement of the ADP-ribosylation factors (ARFs) in the recruitment of AP1, AP3 and AP4. See Fig 2.4 for a basic model for the initial steps involved in clathrin coated vesicle generation.

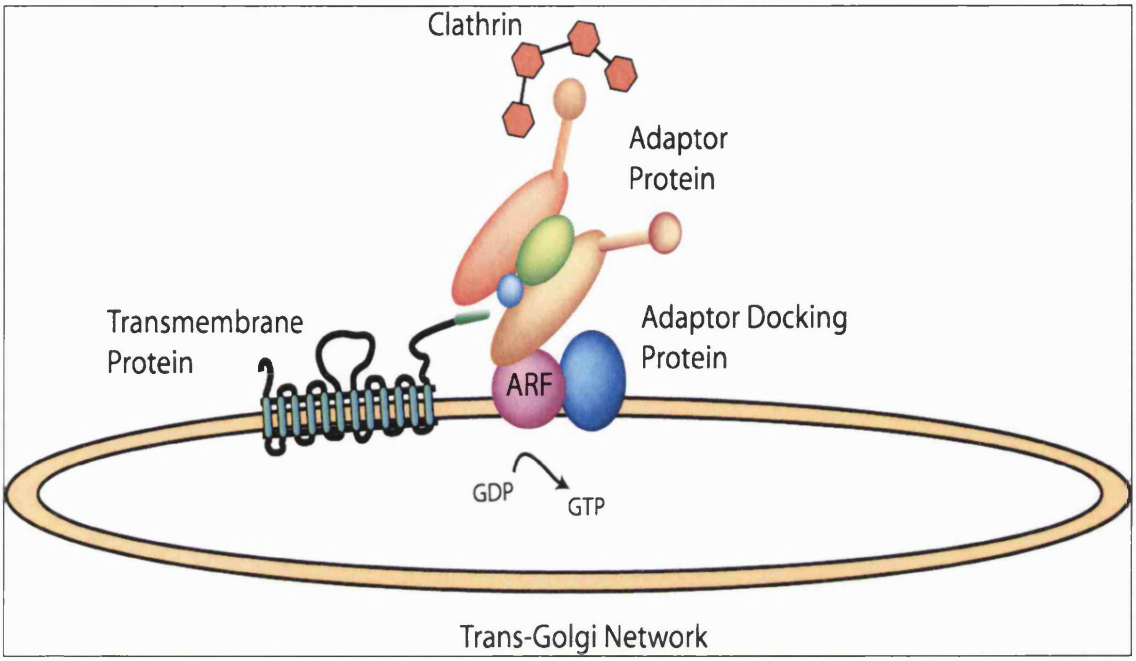

FIG 2.4 **Early steps in AP1, AP3 and AP4 mediated clathrin coated vesicle formation.** GTP-bound ARF1 binds to the membrane, and facilitates the recruitment of the aforementioned adapter proteins that in turn recruit polymerising clathrin triskelions. The binding of transmembrane cytoplasmic tails to AP complexes potentially strengthens AP binding to the membrane. A series of adapter proteins may recruit further adapters to the membrane and consequently lead to the concentration of clathrin within a region of the membrane, which facilitates its formation into a clathrin-coated pit. The adapter proteins such as Dynamin may also function in the scission of these coated pits by pinching them off to form clathrin-coated vesicles. Adapted from the Alison Gillingham model (Thesis publication available for University of Bath library)

1.5.3.4.1 ARF mediation of GTPγS and Brefeldin A action on Adapter Protein recruitment

The association of AP1 with membranes can be triggered by incubation with GTPγS and inhibited by the fungal metabolite, Brefeldin A (BFA) (Robinson and Kreis, 1992; Wong and Brodsky, 1992). The mechanisms involved in these processes are thought to mediated by the 20-kDa nucleotide binding ARF proteins that are members of the Ras GTPase superfamily. These proteins are divided into 3 classes; ARFs 1,2 and 3 are in class I, ARFs 4 and 5 are in class II and ARF6 is in class III (Hosaka *et al.*, 1996). ARF proteins cycle between active GTP-bound and inactive GDP-bound forms, which are modulated through interactions with ARF Guanine nucleotide exchange factors (GEFs) and ARF-GTPase activating proteins (GAPs), for a review see (Roth, 1999). BFA stabilises inactive abortive complexes between ARF1 and ARF-GEFs thereby impairing the recruitment of ARF1 and subsequently AP1 to membranes (Jackson and Casanova, 2000). GTPγS treatment, which maintains ARF in its active state, was found to reconstitute AP1 recruitment to Golgi membranes using only an adapter-enriched fraction from cytosol, purified myristoylated ARF1, and Golgi membranes (Traub *et al.*, 1993).

ARF1 is thought to mediate not only the recruitment of AP1 but also AP3, AP4 and the recently discovered families of monomeric adapter-related proteins Golgi-localised, γ ear-containing, ARF- binding proteins (GGAs) (Robinson and Bonifacino, 2001). However the role of ARFs in recruiting AP2 complexes to the PM is not clear, as BFA treatment does not affect this process. Interestingly GTPγS treatment has been shown to aberrantly target AP2 to endosomal membranes in a process thought to involve ARF1 (West *et al.*, 1997). This theory was substantiated by the observation that ARF-depleted cytosol perturbed the effects of GTPγS on AP2 endosomal recruitment, but this activity could be restored upon addition or recombinant myristoylated ARF1. ARF proteins are known to activate phospholipase D (PLD) (Roth, 1999) and addition of exogenous PLD was found to mimic the actions of GTPγS in recruiting AP2 to endosomes (West *et al.*, 1997).

Inhibition of PLD by neomycin was found to abolish recruitment of AP2 to both endosomes and the PM, however PLD inhibition had no significant effect on the recruitment of AP1 to the TGN. These results suggested AP2 recruitment to the PM is mediated by an ARF1 independent step but is dependent on PLD activity. The manner by which AP2 is recruited to the PM is still being elucidated and may involve BFA resistant ARF6 which is resident in the PM and therefore may act as a membrane docking protein (Millar *et al.*, 1999b). The idea of a resident membrane docking protein being implicated in AP2 recruitment has also been observed in synaptic vesicle endocytosis from squid giant synapse pre-terminals (Fukuda *et al.*, 1995). The protein involved in this process is synaptotagmin, which contains an AP2 binding site in its C-terminal cytoplasmic domain. Microinjection of antibodies raised to this domain was found to reduce the generation of synaptic vesicles by 90% as observed by electron microscopy. Synaptotagmin appears to be expressed ubiquitously, and is increasingly implicated as a necessary component in the endocytosis process in most cell types (Haucke and De Camilli, 1999). It appears that synaptotagmin interacts with AP2 through both the α and μ2 subunits (Haucke *et al.*, 2000) and that this interaction is strengthened by the interaction of tyrosine-based cargo proteins interacting with AP2, possibly by inducing a conformational change within the AP2 complex that facilitates a stronger interaction with synaptotagmin.

1.5.3.4.2 Membrane lipid regulation of adapter protein complexes

Adapter proteins have also been shown to interact with membrane lipids, especially phosphoinositides. This interaction is thought to occur within residues 21-80 of the α-adaptin with a high degree of preference for phosphatidylinositol (4,5)-bisphosphate (PtdIns (4,5) P2) and PtdIns (3,4,5) P3 at physiological concentrations (Beck and Keen, 1991). Experiments in which PtdIns (4,5) P2 has been modified by addition of neomycin, which binds to PtdIns (4,5) P2, inhibits AP2 recruitment to membranes (section 1.5.3.4.1) (West *et al.*, 1997). The action of PtdIns (4,5) P2 has also been proposed to be involved in a co-operative interaction between

synaptotagmin which enhances the binding of AP2 to the membrane and may also modulate its interaction with tyrosine-based motifs of cargo proteins (Rapoport *et al.*, 1997). Further to this it has been discovered that PtdIns (3,4,5) P3 interaction with AP1 inhibits the binding of LL motif containing proteins (Rapoport *et al.*, 1998). The modulation of phosphoinositides may consequently play a role in controlling the dynamic recruitment and sorting of proteins containing LL and Yxxθ like motifs by different adapter proteins and ultimately control their trafficking characteristics. Indeed Class II PI3K's have been shown to be predominantly associated with phospholipid membranes in mammalian cells. PI3K-C2α has been co-purified with clathrin-coated vesicles (CCV's) (Domin *et al.*, 2000), and evidence exists that upon clathrin binding, to the amino terminal of PI3K-C2α, there is an increased *in vitro* lipid kinase activity towards phosphorylated inositide substrates (Gaidarov *et al.*, 2001) (Section 1.3.2.1).

1.5.4 Role of the Cytoskeleton in GLUT4 trafficking

As previously mentioned (Section 1.5.2.4) proteins have been identified that interact with various regions of GLUT4 and infer a role for cytoskeletal-mediated trafficking of GLUT4 to the cell surface. Indeed it appears that both the microtubule and actin-based cytoskeletal networks play an important role in insulin stimulated GLUT4 vesicle trafficking from the DV-GSC to the cell surface (Olson *et al.*, 2001; Fletcher *et al.*, 2000; Omata *et al.*, 2000).

1.5.4.1 Disruption studies

The role for both actin and microtubule networks in insulin stimulated GLUT4 trafficking stems from studies in which these networks are disrupted. Latrunculin A and B are known to disrupt F actin by sequestering actin monomers and shifting the equilibrium to the disassembled state, whereas nocodazole, colchicine and vinblastin depolymerise microtubules.

Disruption of the microtubule network in 3T3-L1 adipocytes was shown to inhibit insulin stimulated GLUT4 translocation to the PM by around 40%, whereas there was no observable inhibition in insulin stimulated TfR recruitment to the cell surface (Fletcher *et al.*, 2000). From these observations it was proposed that the microtubule network is required for trafficking of GLUT4 from the insulin-responsive compartment but not for GLUT4 translocation from the endosomal pool. Interestingly pre-treatment of isolated rat primary adipocytes with Latrunculin A has been shown to markedly inhibit subsequent insulin-stimulated GLUT4 translocation (Omata *et al.*, 2000). This effect of latrunculin A was reversed upon its removal and did not prevent insulin activation of PI3K and Akt, suggesting that the effects of latrunculin A were not mediated by non-specific damage to the cell and that the cytoskeletal elements involved in GLUT4 translocation may be different to those that mediate insulin signalling (Section 1.3.3). Studies in which both nocodazole and latrunculin B were incubated with 3T3-L1 adipocytes for 60 minutes completely abolished insulin stimulated GLUT4 translocation to the PM, further supporting the idea of a combined involvement for the two cytoskeletal networks (Emoto *et al.*, 2001).

1.5.4.2 Visualisation studies

The development of "Ultra fast" microscopy techniques means that effective analysis of four-dimensional images (3-D over time) is now possible. Studies using this technique revealed that GLUT4-eGFP (enhanced green fluorescent protein) expressed in 3T3-L1 adipocytes is enriched in vesicles which rapidly travel from the juxtanuclear region to the PM in response to insulin with a half time of 5-7 minutes at 37 °C (Patki *et al.*, 2001). Interestingly it appeared that streams of tubulo-vesicular structures were emanating from the juxtanuclear region and this was abolished in response to nocodazole treatment leading to a relatively homogeneous dispersion of GLUT4-eGFP throughout the cytoplasm, which be could reversed 5 minutes after the removal of nocodazole. The distance over which GLUT-GFP vesicles move has also been shown to correlate with the integrity of the microtubule cytoskeleton. Fibroblasts consist of long microtubules and

extended GLUT4-GFP movements are seen in these cells whereas adipocytes posses shorter, more fragmented, microtubules and have correspondingly shorter GLUT4-GFP movements as observed by time lapse confocal microscopy (Fletcher *et al.*, 2000). The proposal that emanated from these studies is that insulin stimulates the interaction of GLUT4 enriched vesicles with microtubule networks and actin is required both for this interaction and also for targeting of GLUT4 to specific sites at the PM (Patki *et al.*, 2001).

1.5.4.3 Actin and Microtubule Motors regulate movement of GSV's in response to insulin

In non-polarised cells the –ve ends of microtubules are located at the cell centre near centrosomes while the +ve ends extend project out towards the cell periphery. Simultaneously actin microfilaments are localised as cortical actin patches at the cell surface and as actin cables within the cell (Kamal and Goldstein, 2000). The configuration of these networks can be considered to resemble tracks along which GSV's may travel. The manner by which they travel is still unclear but is thought to be mediated by an array of microtubule and actin based motors. Indeed Czech and colleagues have proposed a model in which insulin promotes movement of GLUT4 containing vesicles towards the cell surface through the action of kinesin motors (Emoto *et al.*, 2001). They also proposed that the effects of nocodazole are to remove dynein motor directed movement of GSV's in the –ve end direction of the microtubules and consequently promote the outward mobility of the vesicles by default. For a review of microtubule based motors see (Hirokawa *et al.*, 1998). Although highly speculative it is postulated that actin motors could co-ordinate the interaction of GSV's with microtubules (Patki *et al.*, 2001). The disruption of actin microfilaments was observed to render the GSV's relatively immobile and this was considered to be due to the prevention of their "piggy backing" onto microtubules. The proposed actin/microtubule duality in vesicular trafficking has been shown in relation to melanosome (pigment granules) transport (Rogers and Gelfand, 2000). In this system, pigment granules move bi-directionally along

microtubules under the control of dynein and kinesin II motors and also along actin filaments under the control of myosin V. The means by which proteins are switched between actin and microtubule track is unclear but yeast two-hybrid studies have shown a direct interaction between Myosin V and kinesin (Huang *et al.*, 1999), indicating the existence of multifunctional motor complexes, which can traffic vesicles along both cytoskeletal tracks. It is also speculated that molecular mechanisms possibly utilising non-conventional myosin, the cytoplasmic linker protein CLIP-170 and dynein, operate to switch vesicles between opposing tracks (Wu *et al.*, 2000). The alternate binding of actin and microtubule based motors may also play a role in vesicle track switching. It appears that motor proteins are potential targets for phosphorylation (Sato-Yoshitake *et al.*, 1992) and may be novel targets for insulin-stimulated transduction pathways.

A physiological role for motor proteins directing GSV's to the PM has not been established in that the GSV proteins involved in the interaction with these motors have not been identified. Treatment of 3T3-L1 cell preparations with 1% TX100 were found to abolish binding of GLUT4 and IRAP to polymerised tubulin indicating that these proteins do not interact directly with microtubules and another protein, present in GSV's, must be responsible for this action (Olson *et al.*, 2001). These data suggest that insulin stimulated recruitment of GLUT4 enriched vesicles from the DV-GSC may not be mediated by GLUT4 at all. In this scenario the specificity for insulin stimulated recruitment of GLUT4 to the PM is determined not in its selection by motor proteins but by the segregation of GLUT4 into vesicles containing specific motor interacting proteins, at the level of the TGN or PR-GSC.

Rab5 GTPase has been identified as a regulatory protein involved in directing vesicle transport and endosomal fusion in the early endocytic pathway (Bucci *et al.*, 1995). Olefsky and colleagues found that Rab5 physically associated with dynein in immunoprecipitants and that this association was constant in basal, insulin stimulated and insulin withdrawn cells (Huang *et al.*, 2001). They also identified that Rab5 is in its GTP bound active state in basal cells and insulin acts to inhibit Rab5 activity and release dynein from microtubules, in a PI3K dependent manner. The injection of Rab5 and α dynein heavy chain antibodies were found to

increase the amount of GLUT4 at the cell surface in basal cells but had no effect on insulin-stimulated GLUT4 translocation. Interestingly after insulin was removed from these cells the level of GLUT4 internalisation was significantly reduced. The following model was proposed to account for all of these observations.

Rab5, associated with the motor protein dynein, is inactivated upon insulin stimulation in a PI3K dependent process. This results in the dissociation of dynein from microtubules, preventing GLUT4 vesicles being trafficked back towards the PR-GSC in a –ve end directed microtubule process. In conjunction with the reduction in GSV internalisation, the release of GSV's from microtubules facilitates their exocytosis to the cell surface, possibly mediated by myosin driven locomotion along actin filaments underlying the PM.

1.5.5 Modulation of intracellular pH influences membrane trafficking events

In 1893 Elie Metchnikoff realised that material taken up by protozoa, through what is now known as the process of endocytosis, was degraded after encountering an acidic internal environment. Since this early discovery the role of intracellular pH has been addressed in depth and a functional significance has been attached to pH in facilitating processes in the biosynthetic and endocytic pathways (Mellman, 1992). It appears that molecules internalised from the PM encounter increasingly acidic environments as they progress through endosomes towards lysosomes, a phenomenon that is mirrored in the exocytotic route of synthesised proteins trafficked from the ER to secretory vesicles. The varying levels of acidity found in certain intracellular compartments is thought to facilitate vital functions within these compartments. For example in late endosomes and lysosomes there is a pH of around 5 which is thought to enhance the activation of enzymatic hydrolases which function to degrade molecules present in this compartment (Mellman, 1992). Another well established function of low endosomal pH is to dissociate lysosomally destined ligands from membrane-associated receptors (Mellman *et al.*, 1986) usually at the

level of early endosomes with the formation of endosome carrier vesicles (ECVs) which traffic proteins destined for degradation towards late endosomes. It has also been documented that the acidic interior of the TGN, immature and mature secretory granules is obligatory for peptide precursor processing (Orci *et al.*, 1987). A cytochemical probe, which accumulates in acidic compartments and can be detected by immunocytochemistry. revealed that maturation of clathrin-coated secretory vesicles is accompanied by a progressive acidification of the vesicular milieu. This acidification may promote the physical interaction between processing enzymes and their substrate by inducing conformational changes in the precursor molecules that lead to exposure of cleavage sites. In this regard it is possible that the acidic environment may induce conformational changes in proteins found in secretory like compartments, such as GLUT4 and IRAP, altering their binding specificities towards adapter proteins or cytoskeletal tethering proteins. The acidity in all of the organelles mentioned is maintained by vacuolar ATP-dependent pumps (v-ATPases) and by ion-exchangers including the Na^+/H^+ exchanger (NHE1). For the purpose of this introduction only the v-ATPases will be examined. A review of Na^+/H^+ exchangers can be found in Wakabayashi *et al.*, (1997). One point of interest with regard to these exchangers is their inhibition by isoproterenol. Isoproterenol inhibits Na^+/H^+ exchange via a β2-adrenergic receptor activation, which occurs through adenylate cyclase stimulation and a cAMP-dependent mechanism (Arsenis, 1995). Interestingly the action of isoproterenol leads to an observed decrease in insulin stimulated glucose transport (Vannucci *et al.*, 1992). Interestingly although western blot analysis of adipocyte PM fractions indicates the total level of GLUT4 is not altered by isoproterenol the accessibility of GLUT4 to photolabelling reagents is significantly impaired (Yang *et al.*, 2002). It is hypothesised that a two-phase fusion reaction exists in which GLUT4 is translocated to the PM and held initially in an occluded PM location. Insulin stimulation rapidly re-targets GLUT4 to an accessible region in the PM, where GLUT4 can actively transport glucose. The Na^+/H^+ exchanger creating a slightly more alkaline environment may modulate this rapid re-targeting. Its inhibition by isoproterenol maintains cytosol acidification levels perturbing the re-

targeting process, resulting in GLUT4 residing in the occluded region of the PM.

1.5.5.1 Characteristics of v-ATPases

The v-ATPases are composed of two complex functional domains, the V_1 domain and the V_0 domain. The V_1 domain is a 570-kDa protein composed of multiple subunits (A – H) with the A and B subunits being shown to participate in the formation of the nucleotide-binding site. The V_0 domain is a 260-kDa integral complex comprising of subunits (a, d, c, c' and c"). The structure and interaction of all of these subunits has been determined for v-ATPase from clathrin-coated vesicles and is shown is Fig 2.5. It appears that v-ATPase is targeted to the membrane through the V_0 domain which also mediates subsequent proton translocation across the membrane surface. The method by which proton translocation is achieved is still not fully understood but is thought to resemble the rotary mechanism proposed for the F_0-ATPase of mitochondria (Vik and Antonio, 1994). This model suggests that the hydrolysis of ATP induces the rotation of the central subunits, generating a pore, which allows proton translocation across the membrane.

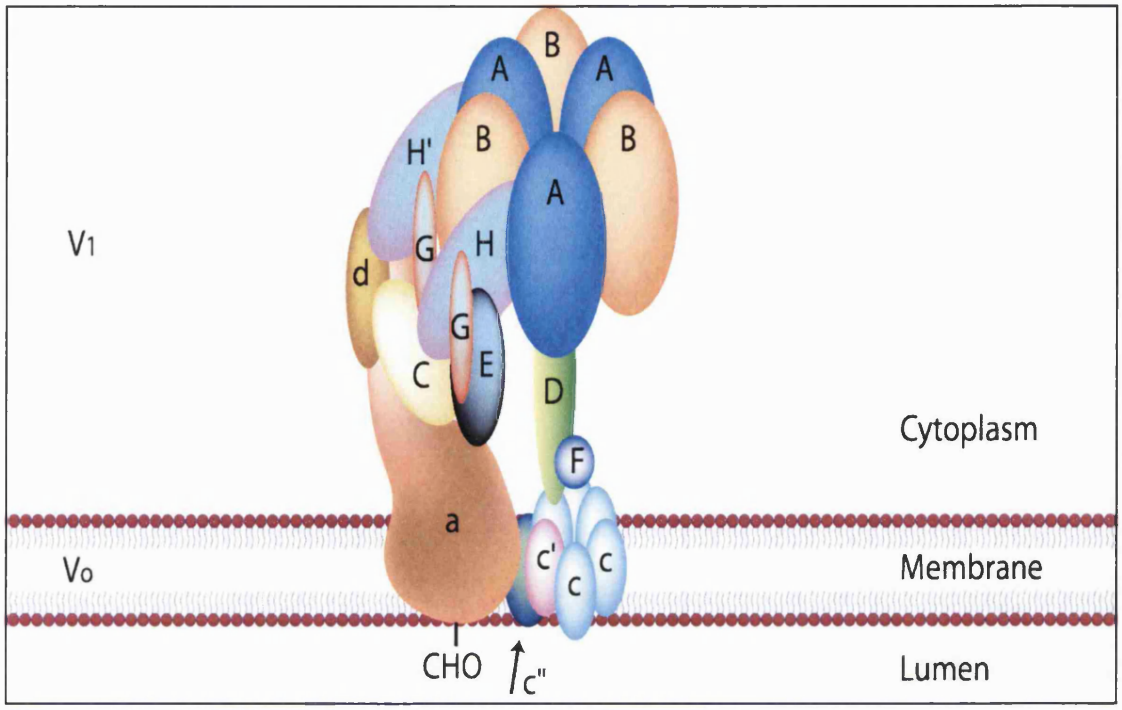

FIG 2.5: **Structural model of the coated vesicle v-ATPase.** Subunits of the V_1 domain are shown (A-H) while V_0 domain subunits are shown (a, d, c, c' and c"). A central stalk region is composed of subunits D and F, while a peripheral stalk region is composed of subunits C, E, G and H. ATP is thought to bind to the A/B subunits in the V_1 domain and hydrolysis of ATP is thought to drive the rotation of subunits in the V_0 domain resulting in proton translocation across the membrane. Model adapted from (Xu *et al.*, 1999).

1.5.5.2 Inhibition of v-ATPases to investigate the role of these complexes in pH regulating trafficking processes

In 1984 naturally occurring bafilomycins, including bafilomycin A_1 were isolated from the mycelium of *Streptomyces griseus* (Werner *et al.*, 1984). Bafilomycin A_1 selectively inhibits v-ATPase but not F_1F_0 or E_1E_0 ATPases (Keeling *et al.*, 1997). This specificity is considered to result from the binding of this macrolide antibiotic to one of the subunits in the V_0 domain (Mattsson and Keeling, 1996) with the macrolactone ring of bafilomycin A_1 contributing to the inhibition of v-ATPase proton translocation (Drose *et al.*, 1993). The specific inhibition of v-ATPases by bafilomycin A_1 has made it a useful tool for studying the role of v-ATPases in regulating intravesicular acidity in membrane trafficking events. Bafilomycin A_1 inhibits lysosomal acidification and degradation of endocytosed EGF, however the internalisation of EGF and its transport to lysosomes is unaltered, suggesting a control of hydrolases by specific pH's within these organelles (Yoshimori *et al.*, 1991). The modulation of enzyme activity by v-ATPase inhibition through bafilomycin A_1 action has also been shown for the proposed GAD65 kinase found in synaptic vesicles (Section 1.5.2.5) (Hsu *et al.*, 1999). It appears that in resting synaptic vesicle GAD65 forms a complex with HSC70, which further associates with the linker cysteine string protein (CSP) that tethers GAD65 to the synaptic vesicle membrane. GAD65 is activated by the membrane-associated kinase only when the proton gradient within the vesicle has been restored by v-ATPase. Bafilomycin A_1 abolishes the activation of GAD65 preventing GABA synthesis which is usually transported into the synaptic vesicle by the resident GABA transporter, see Fig 2.6.

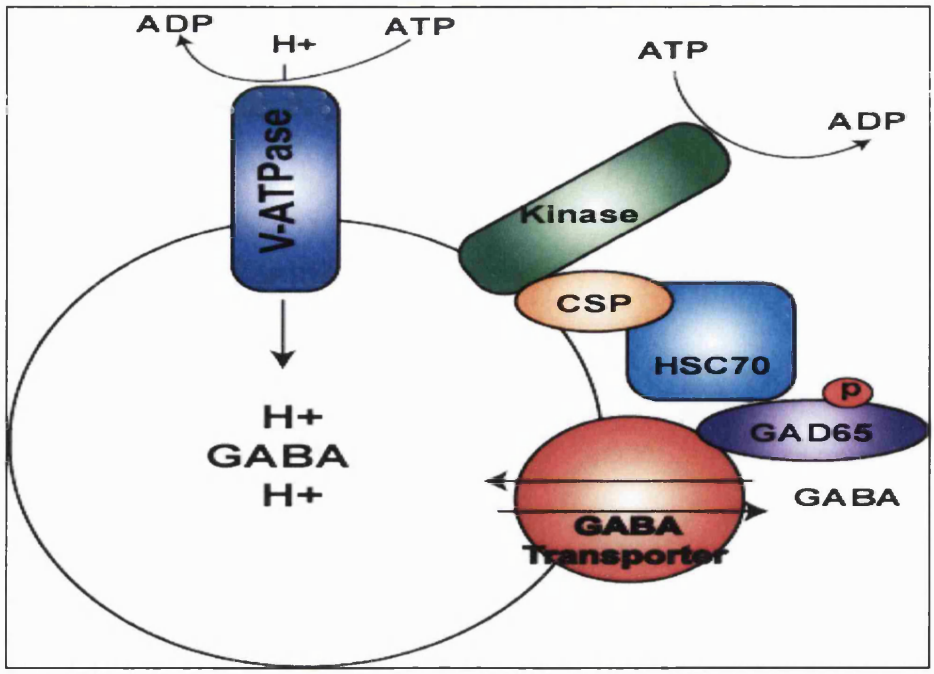

FIG 2.6: **Proposed model of the role of v-ATPase regulation of GABA synthesis in synaptic vesicles.** Adapted from (Hsu *et al.*, 1999)

The effects of bafilomycin A1 treatment on the recycling endosome system are unclear and appear to differ between cell types studies. TfR trafficking in CHO cells treated with bafilomycin A_1 showed an increase in endosomal pH approaching neutral with a concomitant reduction in TfR exocytosis by 50 % without any noticeable change in its internalisation (Johnson *et al.*, 1993). However alternative studies in bafilomycin A_1 treated CHO and 3T3-L1 adipocytes showed that elevated endosomal pH had little effect on the recycling pathway dynamics and did not significantly alter the amount of TfR found associated with intracellular membranes or the PM (van Weert *et al.*, 1995; Chinni and Shisheva, 1999). It is interesting to note that although recycling of endocytosed Tf to the plasma membrane continued in the presence of bafilomycin A_1, recycled Tf did not dissociate from its receptor, at neutral endosomal pH (van Weert *et al.*, 1995).

It appears that vesicular acidification is also important in the regulation of protein binding. Indeed ARF GTPases have been shown to be recruited to TGN membranes in response to a decrease in pH which is thought to be mediated by v-ATPase (Zeuzem *et al.*, 1992). Studies have also shown that

self-condensation of regulated secretory proteins in the TGN/immature granules is regulated by v-ATPase mediated microenvironment acidification, with bafilomycin A_1 treatment seen to interfere with this process in *Xenopus* intermediate pituitary cells (Schoonderwoert *et al.*, 2000).

Bafilomycin A_1 also effects GLUT4 recycling by stimulating GLUT4 translocation from the intracellular pool to the PM in 3T3-L1 adipocytes (Chinni and Shisheva, 1999). This stimulation was considered to be independent of the recycling endosome pathway utilised by TfR and IR autophosphorylation. Interestingly the addition of wortmannin to bafilomycin A_1 treated cells did not alter the observed level of GLUT4 translocation. It appears that v-ATPases may be regulated by signalling molecules such as PKC (Merzendorfer *et al.*, 1997; Saltis *et al.*, 1991; Standaert *et al.*, 1997) suggesting that insulin may modulate v-ATPase activity in specific compartments. Indeed insulin has been shown to increase the intracellular pH within skeletal muscle (Klip *et al.*, 1986). It is therefore possible that insulin responsive cells in the basal state maintain GLUT4 in a largely intracellular pool by the action of adapter proteins. The recognition of various motifs, within GLUT4's cytoplasmic tails, may be modulated by the acidic environment within these intracellular compartments, which is controlled by v-ATPases. Insulin stimulation leads to a signalling cascade that may inactivate certain v-ATPases, resulting in the alkalisation of certain intracellular compartments. This may allow recognition of motifs, present in the GSV's, by cytoskeletal motor proteins, which then rapidly recruit these vesicles to the PM. The action of Na^+H^+ exchangers at the PM maintains the alkaline pH and facilitates the rapid re-targeting of GLUT4 from occluded PM locations to the cell surface, allowing facilitative glucose transport to occur

1.6 The Experimental Aims of the Work Described in this Thesis

The aim of this study was to discover if an N terminal GLUT4 kinase existed and to try and assess the identity of such a putative kinase i.e. is the kinase CKII related? The identification of specific kinases for GLUT4 required a considerably more sensitive and specific approach than that achieved through whole cell "*in vitro*" phosphorylation studies.

A technique termed the "In Gel" kinase assay was considered to meet the requirements for this study and its development and optimisation was paramount to successful identification of a putative N terminal GLUT4 kinase.

Development of kinase isolation techniques including phage display, two-dimensional electrophoresis and Isoelectric focussing were run in parallel with studies attempting to identify the putative kinase and its potential physiological significance.

In association with the aforementioned techniques, antibodies were generated against the N terminal region of GLUT4 and a corresponding region in which Ser^{10} was phosphorylated. It was hoped that these antibodies would provide evidence for the *in vivo* phosphorylation of the N terminal of GLUT4 and also identify any differential localisation of the phosphorylated N terminal GLUT4 from its non-phosphorylated counterpart, which would help to predict functionality of the kinase.

2 General Materials & Methods

2.1 Materials

Unless otherwise stated, all general laboratory chemicals were of analytical grade and purchased from either Sigma – Aldrich Chemical Company (Poole, Dorset, UK), Fisons Scientific UK Ltd. (Loughborough, UK), BDH Laboratory Supplies (Merck Ltd., Poole, Dorset, UK) or Amersham International (Little Chalfont, UK).

2.1.1 Chemical Reagents

- Collagenase type 1 from *Clostridium histolyticum* was purchased from Worthington Biochemical Corporation (Freehold, NJ).
- Dr. G. Danielson (Novo Nordisk) kindly supplied Monocomponent porcine insulin. 1 mg was initially dissolved in 1 ml of 30 mM HCl and was subsequently diluted to 3 ml in ddH_2O. 1 ml of this stock solution was then diluted to 50 ml in 1% (w/v) BSA/KRH buffer with the resulting 1 μM solution aliquoted and stored at -20°C.
- Bovine Serum Albumin (BSA) (Bovine Cohn Fraction V was purchased from Intergen Company (Newark, NJ). 10% (w/v) BSA stock solutions were prepared and pH adjusted with 10 M NaOH to pH 7.4. This solution was then filtered through Millipore type A (mixed cellulose esters) membrane filters (0.8 μm pore size), aliquoted and stored at -20°C.
- Protease inhibitors were added to certain buffers.[4-(2-Aminoethyl)benzenesulfonylflouride, HCl] (AEBSF) was used at a final concentration of 0.1 mM. Antipan, aprotinin, pepstatin A and leupeptin protease inhibitors (Sigma) were used at a final concentration of 1 μg/ml.
- Radioactive [γ^{32}P] ATP and GTP (3000 Ci/mole) and enhanced chemiluminescence (ECL) reagents were obtained from Amersham International.

2.1.2 Buffers

The following buffers were commonly used throughout the studies described.

- *Krebs-Ringer-HEPES (KRH)*: 140 mM NaCl, 4.7 mM KCl, 2.5 mM $CaCl_2$, 1.25 mM $MgSO_4$, 2.5 mM Na H_2PO_4, 10 mM HEPES, (pH 7.4).

- *Krebs Solution (For synaptosomes):* 145 mM NaCl, 5.0 mM KCl, 1.2 mM $CaCl_2$ (600 μl 1M stock in 500 ml total buffer volume, added just before use), 1.3 mM $MgCl_2.6H_2O$, 1.2 mM NaH2PO4, 10 mM Glucose, 20 mM HEPES, (pH 7.5).

- *Phosphate Buffered Saline (PBS)*: 154 mM NaCl, 12.5 mM $Na_2HPO_4.12H_2O$, (pH 7.2).

- *TBS-Tween 20 (TBS-T):* 10 mM Tris, (pH 7.4), 154 mM NaCl, 0.1% (v/v) Tween-20.

- *HEPES-EGTA-Sucrose (HES):* 20 mM HEPES, (pH 7.0), 0.5 mM EGTA, 250 mM Sucrose.

- *Digestion Buffer*: 3.5% (w/v) BSA in KRH buffer supplemented with 5 mM glucose and 700 μg/ml collagenase.

- *Sample Buffer*: Protein samples were solubilised in 10% SDS (w/v), 0.5 M Tris HCl (pH 6.8), 5% of 0.05% bromophenol blue (w/v), 10% glycerol (v/v). The reducing agent was 10% (v/v) 2- mercaptoethanol unless otherwise stated.

- *Resolving Gel Buffer*: 1.5 M Tris HCl, 0.4% (w/v) SDS, (pH 8.8).

- *Stacking Gel Buffer*: 0.5 M Tris HCl, 0.4% (w/v) SDS, (pH 6.1).

- *Electrophoresis running Buffer*: 25 mM Tris HCl, (pH 6.3), 0.1% (w/v) SDS, 0.2 M glycine.

- *Transfer Buffer*: 39 mM glycine, 48 mM Tris, 0.0375% SDS (w/v), 20% methanol (v/v), (pH 8.8).

- *ELISA Plate Coating Buffer*: 15 mM Na_2CO_3, 35 mM $NaHCO_3$, 0.01% (v/v) Na Azide, (pH 9.6).

- *ELISA Plate Blocking Buffer*: PBS, 0.1% (v/v) Tween-20, 1% (w/v) Casein, add casein and dissolve with mixing overnight at 4°C.

- *ELISA Sodium Acetate/citrate Buffer* : 1.66 M Sodium Acetate, 33 mM Citric acid, (pH6.0).

2.1.3 Antibodies

The sources of the primary and secondary antibodies, complete with the dilutions used in Western blotting are detailed in table 2.1.

Antibody	Polyclonal/ Monoclonal	Source	Working dilution for Western blot
Rabbit α GLUT4 C-terminal	Polyclonal Serum	In House production	1:4000
Rabbit α GLUT4 C-terminal	Polyclonal Affinity Purified	In House production	1:4000
Rabbit α GLUT4 N-terminal	Polyclonal Serum	In House production	1:1000
Rabbit α GLUT4 N-terminal	Polyclonal Affinity Purified	In House production	1:1000
Rabbit α GLUT4 Phosphorylated N-terminal	Polyclonal Serum	In House production	1:1000
Rabbit α GLUT4 Phosphorylated N-terminal	Polyclonal Affinity Purified	In House production	1:1000

Rabbit α Phosphotyrosine	Polyclonal Affinity Purified	Calbiochem, Darmstadt, Germany	1:1000
Rabbit α IRS-1	Polyclonal Affinity Purified	Upstate Biotechnology, Buckingham, England	1 μg/ml 1:1000
Mouse α (p85) PI3K	Monoclonal, Clone 4	BD Transduction Labs, Lexington, KY, USA	1:4000
Rabbit α IR (β subunit)	Polyclonal Affinity Purified	Santa Cruz Biotechnology, Inc.	1:1000
Sheep α Akt 2 (PKB β)	Polyclonal Affinity Purified	Upstate Biotechnology's, Buckingham, England	2 μg/ml 1:500
Rabbit α Syntaxin 4	Polyclonal Affinity Purified	In House production	1:5000
Mouse α VAMP2	Monoclonal	Clone 69.1, gift from R. Jahn, Germany	1:1000
Mouse α TfR	Monoclonal	Clone H68.4 Zymed Laboratories Inc	1:1000
Mouse α Caveolin	Monoclonal	Dr. Jorgen Vinten, Copenhagen	1:500
Goat α rabbit IgG peroxidase conjugate	NA	Sigma ImmunoChemicals, St Louis, USA.	1:4000
Goat α mouse IgG peroxidase conjugate	NA	Sigma ImmunoChemicals, St Louis, USA.	1:1000
Rabbit α sheep IgG peroxidase conjugate	NA	Upstate Biotechnology's, Buckingham, England	1:1000

Table 2.1: Primary and Secondary antibodies usage.

2.2 Rat Adipocyte cell preparation

2.2.1 Isolation of Rat Adipocytes

Epididymal fat pads from male Wister rats (180-200 g) were used as the source of adipose cells. This was washed briefly in 1% (w/v) BSA/KRH buffer at 37°C. The fat pads were then finely diced with scissors in digestion buffer (see Buffers 2.1.2) at a ratio of 4 fat pads per 5 ml digestion buffer in 25 ml Sterilin clear-polystyrene tubes. The tissue was then digested over a period of 40-50 min with vigorous shaking at 37°C until a fine tissue suspension was achieved. Any undigested material was then removed via filtration through 250 μm nylon mesh (Lockertex) into individual 23 ml polystyrene flat-bottomed tubes (Sarstedt). Adipocyte cells were washed 4-5 times with 1% (w/v) BSA/KRH buffer at 37°C, allowing the fat cells to float to the top of the buffer and settle before the buffer infranatant was removed using a 13 gauge x 10 cm needle attached to a 50 ml syringe. The resulting cell suspension was whitish in appearance and the buffer clear. At this point the cells were pooled and buffer levels adjusted to obtain a 40% cytocrit. Often at this juncture the cells were divided equally into two samples and one was subjected to 20 nM insulin treatment for 20 min at 37°C.

2.2.2 Subfractionation of Rat Adipocytes

Insulin treated and non-treated cells were washed twice in HES buffer containing protease inhibitors (see Buffers 2.1.2) at 18°C then re-suspended to a final volume of 1.5 ml (cells in HES buffer). The cells were homogenised with 10 strokes in a 55 ml Potter-Elvehjem homogeniser with a defined 150 μm clearance (Thomas Scientific). The resulting homogenate was spun at 1000 rpm in a Beckman SS34 rotor for 1 min at 4°C to give a fat layer and infranatant layer, the latter of which was removed with a 21 gauge needle and appropriate syringe. The infranatant was subjected to

sequential centrifugation using a Beckman TL-100 benchtop ultracentrifuge at 4°C, with a TLA-100.3 fixed angle rotor. Centrifugation of samples at 17500 g_{max} for 20 min resulted in a crude plasma membrane (PM) pellet with a microsomal/cytosol supernatant. The supernatant was spun at 49000 g_{max} for 9 min with the resulting pellet termed the high-density microsomes (HDM) fraction. The post HDM supernatant was centrifuged at 541000 g_{max} for 17 min to obtain the pellet containing the low-density microsomes (LDM). The crude PM pellet was re-suspended in 300 µl of HES buffer (plus protease inhibitors) and dispensed carefully onto a 600 µl 38% sucrose cushion (1.12 M sucrose, 10 mM Tris-HCl, (pH 7.2), 10 mM EDTA). This was spun at 105000 g_{max} for 20 min using the TLS-5S swinging bucket rotor. The PM's were then carefully removed from the cushion interface and re-suspended in a total of 3 ml HES buffer (plus protease inhibitors). This was then centrifuged at 74000 g_{max} for 9 min and the supernatant was removed and retained as cytosol. The pellet was washed once more with the final supernatant being discarded and the pellet containing purified PM retained. The PM, LDM and HDM pellets were re-suspended in HES buffer (plus protease inhibitors), aliquoted, then snap frozen in liquid nitrogen and stored at -70°C.

2.3 Preparation of Synaptosomes from rat brain

The procedure detailed was adapted from (Phelan and Gordan-Weeks, 1997). Male Wister rats (200-250 g) were sacrificed by decapitation and their brains removed and placed in an ice cold sucrose solution (0.32 M sucrose, 5 mM HEPES (pH 7.4)). The cerebellum region was removed and the tissue then chopped into small pieces using a scalpel. The tissue was then weighed and made up to a final tissue to medium ratio of 10% (w/v) in 0.32 M sucrose solution (plus protease inhibitors). The tissue was then homogenised with 15 strokes in a 55 ml Potter-Elvehjem homogeniser with a defined 150 µm clearance (Thomas Scientific). The homogenate was then poured into centrifuge tubes and spun at 3000 rpm in a Beckman SS34 rotor for 10 min at 4°C to prepare the post-nuclear supernatant fraction. The

supernatant was then transferred to a clean centrifuge tube using a 10 ml pipette and spun at 20000 g_{max} in a Beckman centrifuge using a SS34 rotor at 4°C for 30 min. While this centrifugation step was taking place 12 ml of ice cold 1.2 M sucrose solution containing 5 mM HEPES (pH 7.4) was dispensed into an SW27 ultracentrifuge tube. A 0.8 M ice cold sucrose solution was then carefully layered on top of the 1.2 M sucrose solution by pipetting the solution down the side of the tube. Once the centrifugation process was completed the resulting supernatant was discarded leaving a pellet containing the crude mitochondrial and synaptosome fraction. This pellet was re-suspended in 10 ml of ice cold 0.32 M sucrose solution and was then carefully layered onto the 0.8 M sucrose solution in the same manner as previously detailed. The tube was then filled to the level with 0.32 M ice cold sucrose solution to prevent the tube collapsing while spinning. The tube was spun at 100000 g_{max} for 90 min in a Beckman ultracentrifuge at 4°C. A band was clearly visible at the interface between the 0.32 M and 0.8 M sucrose solutions and this was carefully removed and re-suspended to a total volume of 15 ml in Krebs solution (plus protease inhibitors) (Section 2.1.2). This was then spun twice at 12000 g_{max} for 20 min at 4°C with the supernatant discarded between spins and the pellet re-suspended in 10 ml of the same buffer. The final pellet was re-suspended in a total volume of 3 ml Krebs solution plus protease inhibitors, aliquoted into eppendorf tubes, snap frozen in liquid nitrogen and stored at -70°C.

2.4 Protein Biochemistry Techniques

2.4.1 BCA Protein Assay

Protein concentration was determined using the Pierce bicinchoninic acid (BCA) protein assay. A protein standard curve was constructed using a 1 mg/ml BSA stock aliquoted in volumes of 0, 2, 4, 6, 8, 10 µl and made up to a final volume of 10 µl with 0.1 M NaOH. Protein samples were either used neat or at a 1:10 dilution in a volume of 10 µl made up in 0.1 M NaOH

(protein samples were usually analysed in triplicate). 200 µl of BCA working reagent was added to all the 10 µl samples and colour development, due to Cu_2+ and BCA complex formation, was monitored after 30 min incubation at 37°C by reading their absorbence at 562 nm in a microplate spectrophotometer.

2.4.2 SDS Polyacrylamide Gel electrophoresis (SDS-PAGE)

Protein samples were first solubilised in sample buffer (see Buffers 2.1.2) and heated at 95°C for 5 min, unless otherwise stated. The samples were then pulse spun down in a benchtop microfuge for 30 sec and loaded onto either the PROTEAN II xi slab cell system (Bio-Rad) (large slab gels) or the Atto Dual Mini Vertical PAGE cell system (Genetic Research Instrumentation Ltd), (mini gels). All the gels were 1.5 mm in thickness. The gels were made from Acrylamide/Bis-acrylamide stock (30.8% T, 2.6% C (Protogel National Diagnostics)) with appropriate gel buffers (see Buffers 2.1.2). The gels were polymerised by the addition of ammonium persulphate (Bio-Rad), which was made as a fresh 100 mg/ml stock in ddH_2O, and TEMED. The volumes used to create different percentage gels can be found in table 2.2.

Stock Solutions	Resolving Gel			Stacking Gel
Percentage Gel (Crosslinking)	8%	10%	12%	
Resolving gel buffer (ml)	25	25	25	-
Stacking gel buffer (ml)	-	-	-	3.4
Acrylamide stock (ml)	20	25	30	5.0
ddH_2O (ml)	30	25	20	7.5
Ammonium persulphate (ml)	0.5	0.5	0.5	0.1
TEMED (µl)	40	40	40	20

Table 2.2: **Varying compositions of gel components to achieve differential levels of crosslinking within polyacrylamide gels.** The volumes shown here are enough to make up two large slab gels and four mini gels.

The protein loaded gels also had broad range molecular weight markers (New England Biolabs) added. The gel chambers of the required electrophoresis systems were filled with Electrophoresis running buffer (see Buffers 2.1.2) and an electric current established. Mini gels were run at a constant 200 V while large slab gels were run at a constant current of 25 mA through the stacking gel and then the current was increased to a steady 35 mA through the resolving gel. The electric current was halted for both systems once the dye front had eluted away from the bottom of the gel. The gels were extracted from their respective systems and then proteins were either transferred onto nitrocellulose (see Methods 2.4.3), or rotated gently in stain solution (0.2% (w/v) coomassie blue R-250, 30% (v/v) methanol, 10% (v/v) glacial acetic acid) for 30 min, and then de-stained in de-stain solution (30% (v/v) methanol, 10% (v/v) glacial acetic acid) for an appreciable period to visualise protein bands clearly.

2.4.3 Electrophoretic Transfer of Proteins to Nitrocellulose

Following SDS-PAGE, gels were soaked in transfer buffer (see Buffers 2.1.2) for 5 min. Each gel was then inserted into a sandwich that consisted of nine sheets of electrode paper, followed by a layer of nitrocellulose (BioTrace, 0.45 μm pore size, Gelman Sciences), then the gel and finally another nine sheets of electrode paper. All of the sheets and the anode and cathode plates were pre-wetted in transfer buffer, with air bubbles removed between layers. The transfer was carried out in a Pharmacia Multiphor II NovaBlot unit at a field strength of 0.8 mA/cm^2 gel area for 110 min. After the transfer procedure was complete the membrane was washed in ddH_2O and stained briefly with 0.1% (w/v) Ponceau S in 3% (v/v) trichloroacetic acid to visualise protein bands and identify molecular weight markers.

2.4.4 Western Blotting

The nitrocellulose membrane was briefly washed in transfer buffer and then TBS-T (see Buffers 2.1.2), to remove the Ponceau staining. The membrane was then blocked for 30 min using 5% (w/v) Marvel dried skimmed milk in TBS-T. The membrane was then washed in TBS-T and incubated for 90 min in 1% (w/v) BSA/TBS-T containing the relevant primary antibody concentration (see Antibodies 2.1.3). After primary antibody incubation the membrane was washed six times for 10 min in TBS-T and then incubated in 5% (w/v) Marvel/TBS-T containing the relevant secondary antibody (see Antibodies 2.1.3) for 30 min. The TBS-T washes were repeated as before and the membrane was finally incubated in ECL detection reagent (see Chemical Reagents 2.1.1) for 1 min. The ECL treated membrane was then exposed to ECL Hyperfilm, until a chemiluminescent signal could be clearly visualised upon development. N.B. Later ECL treated membranes were visualised and quantified using the EpiChem II Darkroom machine and its associated software (UVP imaging system, UK).

2.5 Antibody generation

2.5.1 Synthesis of N terminal phosphorylated and non phosphorylated GLUT4 peptides

30 mg of the following peptides were synthesised at the University of Bristol peptide synthesis laboratory.

N Terminal GLUT4 $_{NH2}$-I-G-S-E-D-G-E-P-P-Q-Q-C-$_{COOH}$
MW 1259.3 Da

N Terminal GLUT4 $_{(EXTENDED)}$ $_{NH2}$-P-S-G-F-Q-Q-I-G-S-E-D-G-E-P-P-Q-C-$_{COOH}$
MW 1774.9 Da

Phosphorylated $_{NH2}$-I-G-S(P)-E-D-G-E-P-P-Q-Q-C-$_{COOH}$
N Terminal GLUT4 MW 1339.5 Da

All peptides were synthesised from the carboxyl terminal cysteine residue, which was incorporated into the peptides to facilitate conjugation to other proteins. The peptides were > 95% purity and came in a lyophilised form which was stored at -20°C until required.

2.5.2 Peptide free sulphydryl content determination

For effective conjugation of the peptides to the carrier protein KLH (see Methods 2.5.3) the cysteine residue should be in a reduced state. A useful way to determine this is to analyse the amount of free sulphydryl content within the peptide. 5,5'-Dithiobis (2-nitrobenzoic acid) or Ellman's reagent (BDH) was used to determine the free sulphydryl content of the peptides and calculate the level of reduced peptide.

8 mg Ellman's reagent was dissolved in 1 ml ethanol to make a stock solution. A 1 mg/ml stock solution of $_{L}$cysteine in 0.1 M Na Phosphate buffer

(pH 8.0) was prepared along with 1 mg/ml stock solutions of the peptides in the same buffer. A dilution series of cysteine and peptide solutions was prepared and dispensed, in duplicate, as 40 μl total volume aliquots into 96 well microtitre plates (Nunc). A 20-fold dilution of the Ellman's reagent stock was prepared in 0.1 M Na Phosphate buffer (pH 8.0) and 200 μl of this solution was added per well. An appreciable colour was allowed to develop in the cysteine control samples and the plates were then read at 412 nm in a spectrophotometer. A negative control containing Ellman's reagent and buffer only was used to eliminate background levels from the sample readings and a standard plot of the serial cysteine readings was produced. The relative free sulphydryl content of the peptides could be determined by comparing the O.D. readings against this standard plot and the level of reduced peptide could subsequently be calculated.

2.5.3 Preparation of peptide conjugates

In order for an immune response to be developed towards the N terminal GLUT4 and phosphorylated N terminal GLUT4 peptides they first needed to be conjugated to the carrier protein Keyhole Limpet Haemocyanin (KLH, Sigma). KLH was in a lyophilised form and was reconstituted in 2 ml ddH_2O to give a 10 mg/ml buffered solution containing 31 mM $NaPO_4$, 0.46 M NaCl and 41 mM sucrose. 3 mg of sulpho-succinimidyl 4-(N-maleimidomethyl) cyclohexane-1-carboxylate (sulpho-SMCC) (Pierce) was dissolved in 1.5 ml 20 mM $NaHCO_3$ (pH 8.2), for each conjugation, and this was mixed with 1 ml of the KLH suspension. The mixtures were then rotated at room temperature for 30 min to allow amide bond formation by the NHS ester reaction scheme shown.

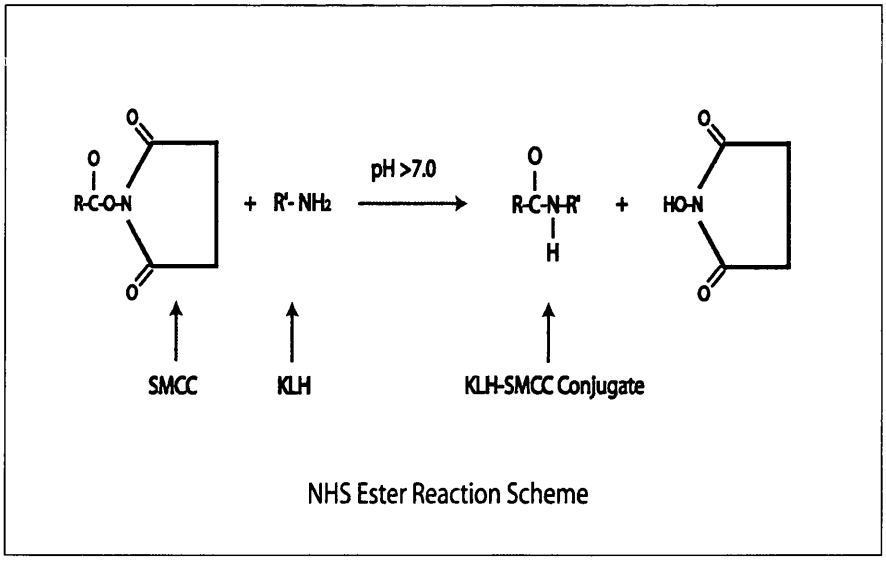

NHS Ester Reaction Scheme

While the reaction was proceeding two PD10 columns (Sephadex G-25 M Amersham Pharmacia Biotech) were pre-equilibrated with 25 ml of equilibration buffer (50 mM Sodium phosphate buffer, (pH 7.0)). The conjugate mixtures were loaded onto the pre-equilibrated columns and allowed too run in fully. The KLH-SMCC conjugates were then eluted in 3.5 ml equilibration buffer with the unbound sulpho-SMCC retained within the column. 5 mg of N-terminal GLUT4 peptide and phosphorylated N-terminal GLUT4 peptide were accurately weighed out and dissolved in 0.5 ml of equilibration buffer. The dissolved peptides were mixed with the eluted KLH-SMCC conjugates and rotated at room temperature overnight. The maleimide group of SMCC forms a thioether bond with the free sulfhydyls in the cysteine residues of the peptides by the Maleimide reaction scheme shown.

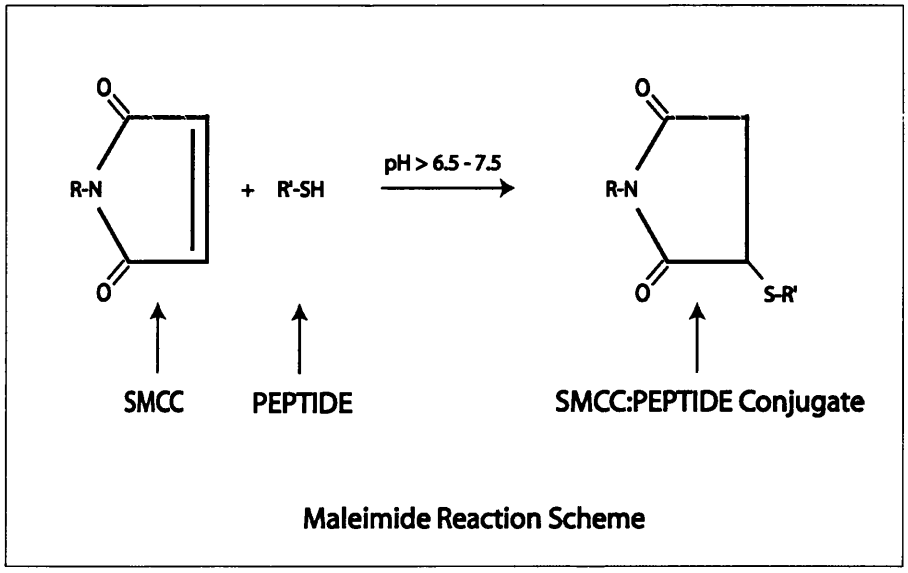

Maleimide Reaction Scheme

The conjugate concentration was determined by BCA protein assay (see Methods 2.4.1) and the conjugated samples aliquoted into 0.4 mg samples and stored at -20°C.

2.5.4 Injection protocol

Two 0.4 mg aliquots of the appropriate peptide/KLH conjugate were defrosted and made up to a total volume of 1 ml with 50 mM sodium phosphate, (pH 7.2). 1 ml of Titermax Gold adjuvant (Sigma) was warmed to room temperature and vortexed for 30 s to give an even emulsion. A luer lock syringe (Sigma) was loaded with the emulsion and another syringe was loaded with 0.5 ml of peptide/KLH solution (antigen solution). The two syringes were connected via a 3-way disposable plastic luer lock and the antigen pushed into the Titermax solution, then mixed back and froth for 2 min until a meringue-like-water-in-oil emulsion was formed. A fresh syringe was loaded with the remaining 0.5 ml of the antigen solution and the process repeated. Finally the emulsion was transferred into one syringe and injected into two New Zealand White rabbits with 4 subcutaneous injections of 0.25 ml per rabbit. Booster injections were performed every four weeks and test bleeds obtained every two weeks after injections. The bleeds were taken from the ear veins of anaesthetised rabbits and placed in glass test

tubes which were allowed to clot overnight at 4°C. The serum was extracted using glass pipettes and any cell debris removed by centrifugation at 2000 rpm in a benchtop centrifuge. The serum were divided into smaller samples of around 200 µl and stored at -20°C. Some of these samples were later analysed via Western blot and ELISA protocols to determine optimum antibody titres (see Methods 2.4.4 and 2.5.5). Rabbits were bleed out after 4 months giving around 100 ml serum per rabbit.

2.5.5 ELISA plate assay

A 50% glycerol stock was made in Coating Buffer (see Buffers 2.1.2). 2 ml of this glycerol stock was added to 2 mg of N-terminal GLUT4 peptide, Phosphorylated N-terminal GLUT4 peptide and KLH carrier protein. 100 µl of these solutions was then further diluted in 10 ml coating buffer giving a final concentration of 10 µg/ml. The remaining peptide glycerol stocks were stored at –20°C until further required. Individual C8 Maxisorp plates (Nunc) were coated with 100 µl of the 10 µg/ml peptide solution per well, covered and incubated overnight at 4°C. The plates were then washed three times in PBS 0.1% Tween-20 (PBS-T) with rigorous expulsion of liquids out of the wells. The wells were subsequently filled with Blocking Buffer (see Buffers 2.1.2) and incubated with gentle shaking for 1 h at room temperature. The plates were washed twice with PBS-T as before. A 1/100 dilution of obtained antibody serum (see Methods 2.5.3) was made in PBS-T. 200 µl of this dilution was placed in the first well of the washed plate and 100 µl withdrawn and placed into the second well containing 100 µl PBS-T. This serial dilution was performed up to 15 times to give a serum concentration of 1:3276800 in well 16. The plates were then covered and incubated with gentle shaking for 2 h at room temperature. The plates were then washed three times with PBS-T with vigorous expulsion of the liquids from the wells. 100 µl of Anti rabbit IgG HRP linked antibody conjugate (1:4000 dilution in PBS-T) was added to each well and the plates covered and incubated for a further 2 h at room temperature. The plates were then washed three times with PBS-T and then twice in PBS.

The Sodium Acetate/citrate buffer (see Buffers 2.1.2) was diluted 1:20 in ddH_2O and the pH checked (pH 6.0). 49.5 ml of this solution was then added to 0.5 ml of Tetramethyl Benzidine (TMB) (10 mg/ml in DMSO), plus 10 µl of 30% (v/v) H_2O_2. 100 µl of this substrate solution was then added to each of the washed wells. The plates were incubated at room temperature for 5-15 min until a good blue colour had developed over the range of serum dilutions. The reaction was then stopped with the addition of 50 µl of 1.84 M H_2SO_4 per well. The plates were then read in a microplate spectrophotometer with filter 1 measuring O.D. at 450 nm and filter 2 measuring O.D. at 700 nm (This filter is used to normalise the readings and eliminate background values). Results were plotted at O.D. 450 nm up to 3.0 against dilution factor.

2.5.6 Antibody Affinity purification

Serum identified from the ELISA plate assays to have the highest affinity for their respective peptides were affinity purified against the peptide antigen coupled to a SulphoLink® Coupling Gel column (Pierce and Warriner Chem. Co., Rockford, IL). The SulphoLink® matrix contains a 12 atom spacer arm with iodoacetyl moieties for efficient conjugation to the peptide's cysteine residue.

2.5.6.1 Generation of affinity purification column

2 ml of SulphoLink Coupling gel per column was brought to room temperature and then packed into empty PD10 columns. The columns were equilibrated with six column volumes of coupling buffer (50 mM Tris, 5 mM EDTA, (pH 8.5). The column was then capped at the bottom and 2 ml of 1 mg/ml peptide in coupling buffer was added. The top of the column was then capped and the mixture incubated at room temperature for 30 min without mixing. The bottom and top caps were removed and the column allowed draining. The column was then washed with three column volumes of coupling buffer and the bottom cap replaced. 2 ml of 50 mM Cysteine

solution in coupling buffer was added to the column and the top cap replaced. The column was gently rotated for 15 min at room temperature and then for a further 30 min without mixing. The cysteine solution acts to block unbound iodoacetyl moieties on the SulphoLink gel. The column was then drained as before and then washed with 16 column volumes of 1 M NaCl followed by 16 column volumes of degassed 0.05% sodium azide solution. The bottom cap was replaced and 2 ml of 0.05% sodium azide solution added. The top cap was then replaced and the column stored in an upright position at 4°C until required.

2.5.6.2 Affinity purification of serum

The prepared column was brought to room temperature and the bottom and top caps removed, allowing the column to be drained. The column was then equilibrated with four column volumes of PBS (see Buffers 2.1.2). 3 ml of the corresponding serum was added to the column, followed by 2 ml of PBS. The caps were replaced and the column was slowly rotated for 90 min at room temperature. The caps were then removed and the flow through collected and retained. The column was washed with two column volumes of 1 M NaCl, to remove weakly associated proteins, followed by six column volumes of PBS. The column was eluted by applying 8 ml Glycine buffer (100 mM Glycine (pH 2.75)) with 1 ml fractions collected and neutralised with 50 µl of 1 M Tris (pH 9.5). The fractions protein levels were analysed using the BCA protein assay (see Methods 2.4.1) with the subsequent pooling of fractions with the highest protein concentrations. The pooled sample was placed in a 5 ml Slidealyzer dialysis cassette (Pierce) and dialysed against PBS overnight at 4°C. The solution was then concentrated down to an appreciable volume by covering the dialysis cassette in PEG 20000 (Merck), which acts to remove water out of the solution. The protein content was measured using a modified BCA protein assay in which the BSA standard curve was replaced by an IgG protein standard so that the resulting protein concentration was expressed as mg/ml IgG. The affinity purified antibody solution was made upto a 40% glycerol stock, with the protein concentration adjusted accordingly, and then stored at -20°C until

required. The column was washed with 10 column volumes of PBS followed by 16 column volumes of degassed 0.05% sodium azide. The bottom cap was replaced and 2 ml of 0.05% sodium azide was added to the column. The top cap was then replaced and the column stored upright at 4°C until further required.

3 Searching for a GLUT4 N terminal kinase.

3.1 Introduction

Previous attempts to identify potential phosphorylation sites within GLUT4 have relied on '*in vitro*' phosphorylation studies in which rat adipocytes preparations were pre-incubated with a source of [^{32}P] (James *et al.*, 1989; Lawrence, Jr. *et al.*, 1990b; Joost *et al.*, 1987; Schurmann *et al.*, 1992). An initial study, into glucose transporter phosphorylation, pre-labelled adipocyte cells with sodium [^{32}P] phosphate 0.1 mCi/ml for 80 min and then exposed the cells to a host of agents (Joost *et al.*, 1987). The study concluded that no detectable phosphate was incorporated into PM glucose transporters from basal, insulin or isoproterenol treated cells. However incubation of [^{32}P] pre-labelled adipose cells with phorbol 12-myristate 13-acetate (PMA) stimulated a significant phosphorylation event within the glucose transporter. Intriguingly this phosphorylation had no effect on glucose transporter intrinsic activity or its translocation with no detectable [^{32}P] phosphate incorporation observed with any of the agents, in LDM derived glucose transporters. This study was complicated by the later discovery of multiple glucose transporters, which needed to be addressed separately.

The discovery of the insulin regulatable glucose transporter (GLUT4 or IRGT) triggered further "*in vitro*" phosphorylation studies to ascertain if the phosphorylation of GLUT4 had a more direct effect on its activity or cellular trafficking than that observed for GLUT1. Studies in which adipose cells were pre-labelled with [$^{32}P_i$], for two hrs, revealed a basal labelling of at least 0.2 moles of phosphate per mole of GLUT4 (James *et al.*, 1989). Insulin stimulation again produced no observable increase in the relative levels of phosphorylated GLUT4. However James and colleagues could not rule out the possibility that small subsets of GLUT4 could have been phosphorylated, in response to insulin, but could not be effectively detected due to their insulin induced re-distribution. Interestingly this study revealed a significant (two-fold) stimulation in, both LDM and PM derived GLUT4 phosphorylation when adipose cells were initially exposed to insulin

followed by 5min exposure to the β-adrenergic receptor agonist isoproterenol. In addition to its observed stimulatory role isoproterenol action was also shown to inhibit insulin stimulated glucose transport activity by 40% without altering insulin stimulated distribution of GLUT4.

Many of the effects of β-adrenergic agonists such as isoproterenol are mediated by raised intracellular levels of cyclic AMP (cAMP) and it was shown that cAMP derivatives 8-bromo-cAMP and dibutyryl-cAMP produced the same increased level of phosphorylation of GLUT4 as seen for isoproterenol (James *et al.*, 1989). The cAMP-dependent protein kinase (PKA) modulates many of the actions of intracellular cAMP and was therefore considered a potential candidate linking GLUT4 phosphorylation to some form of signalling pathway. Indeed incubation of GLUT4 enriched LDM fractions with the catalytic subunit of PKA catalysed the phosphorylation of GLUT4 (James *et al.*, 1989). This observation was supported by later studies (Schurmann *et al.*, 1992; Nishimura *et al.*, 1991; Lawrence, Jr. *et al.*, 1990b), which also suggested the involvement of PKA action in GLUT4 phosphorylation. PKA mediated phosphorylation of GLUT4 was initially proposed to modulate its intrinsic glucose transport activity (James *et al.*, 1989). However this idea was re-assessed after a later study identified that PKA phosphorylation was largely restricted to intracellular membrane (LDM) GLUT4, with a much lower level of PKA mediated phosphorylation of PM GLUT4 that had no discernible effect on its glucose transport activity (Schurmann *et al.*, 1992). Piper and colleagues generated a range of GLUT1/GLUT4 chimeras in CHO cells and their results suggested that the actions of isoproterenol and dibutyryl-cAMP on glucose transport activity were distinct from the phosphorylation of GLUT4 (Piper *et al.*, 1993b). They proposed that these agents caused direct binding of a nucleotide to carboxyl terminal region of GLUT4 and it was this binding that modulated GLUT4's intrinsic glucose transport activity. Some studies still infer a role for GLUT4 phosphorylation in mediating glucose transport activity, through the actions of fluctuating cytosolic calcium levels (Begum *et al.*, 1993; Reusch *et al.*, 1993; Reusch *et al.*, 1991). These studies suggested that increased calcium levels affected insulin's ability to trigger de-phosphorylation of GLUT4 by phosphoserine phosphatase 1 (PSPase

1). Further study is required to establish if the observed decreases in glucose transport activity are as a direct result of increased GLUT4 phosphorylation or are mediated by another mechanism that is invoked through elevated cytosolic calcium levels.

A potential role for PKA, and the documented PKC (Schurmann *et al.*, 1992), phosphorylation of GLUT4 was first highlighted in a study using the type I and IIa protein phosphatase inhibitor okadaic acid (Lawrence, Jr. *et al.*, 1990a). Okadaic acid triggered a 4 fold increase in GLUT4 translocation to the PM and a 3-fold increase in the level of phosphorylated PM GLUT4 relative to the intracellular pool of GLUT4 in control cells. Interestingly, when okadaic acid was used in conjunction with insulin, okadaic acid partially inhibited the ability of insulin to enhance GLUT4 translocation to the PM. Explanations for these observations have been previously discussed (See Main Introduction 1.5.1.2). It appears that phosphorylation of GLUT4 may be involved in its cellular routing through multiple bi-cycling loops. It is possible that a range of kinases (including PKA and PKC) and phosphatases may be employed to modulate the phosphorylation of GLUT4 in specific cellular locations. Consequently the overall phosphorylation of GLUT4 may be misleading, as localised increases in GLUT4 phosphorylation in one of the cycling loops may be compensated by dephosphorylation events occurring simultaneously in another loop. It is worth considering that small differences in phosphorylation between localised populations of GLUT4 would not be detected using the techniques utilised in these studies and a more delicate, highly specific procedure is needed to verify the roles each kinase/phosphatase plays in GLUT4 phosphorylation status.

Attention with regards to the potential sites of phosphorylation within GLUT4 has centred on the carboxyl terminal of GLUT4 after a study published by Lawrence and colleagues (Lawrence, Jr. *et al.*, 1990b). This study immunoprecipitated pre-labelled GLUT4 from rat adipocytes, as in the previously mentioned studies, and then set about digesting GLUT4 through the action of cyanogen bromide (CnBr). CnBr cleaved methionine residues within GLUT4 resulting in eleven smaller GLUT4 fragments which were further analysed to ascertain which areas within GLUT4 were phosphorylated. These studies suggested that phosphorylation was

restricted to sites in one of the amino or carboxyl terminal fragments of GLUT4 as detected by autoradiography of the peptide fragments in SDS-PAGE gels. At the time of this study the sequence of the amino terminal region of GLUT4 had not been firmly established and no antibody was available for its detection, there was a GLUT4 carboxyl terminal directed antibody which confirmed that the phosphorylated fragment corresponded to the carboxyl terminal region of GLUT4. Further tryptic digestion of this fragment identified that the principle region of GLUT4 phosphorylation resided in Ser^{488}, although other sites of phosphorylation within the carboxyl terminal fragment, such as Ser^{480}, could be detected. Phosphorylation of the amino terminal fragment was considered not to take place and has wholly been neglected since this study. The study conducted by Lawrence and colleagues is by no means indicative that all phosphorylation events take place within the carboxyl terminal of GLUT4. Firstly the band detected by the C-Terminal GLUT4 antibody may have also contained N-Terminal GLUT4 fragments which could not be detected as there was no antibody for this procedure. Also if the level of N-terminal GLUT4 phosphorylation is restricted to a small population of cellular GLUT4 at any one time point then the inherent losses associated with the process of immunoprecipitating pre-labelled GLUT4, coupled with extracting this GLUT4 out of an SDS-PAGE gel for CnBr digestion and subsequent re-running of the fragment on another SDS-PAGE gel could mean that the amount of phosphorylated N terminal GLUT4 was simply too low to be detected.

The lack of investigation into the potential phosphorylation of the amino terminal of GLUT4 is surprising as the N terminal region of GLUT4, downstream of the FQQI motif, bears a close sequence identity to a known multiple phosphorylation site within the GAD65α subunit (see Introduction 1.5.2.5), which is phosphorylated by a currently unidentified kinase. Interestingly, the GAD65α phosphorylation site contains an acidic cluster region that is similar to regions found in CD-MPR and furin. The acidic cluster regions within these proteins are thought to direct their interaction with Casein kinase II (CKII), which phosphorylates these proteins, modulating their interaction with proteins that define their trafficking status (see Introduction 1.5.2.5).

Covalent modification of the N terminal region of GLUT4, through Serine^{10} phosphorylation, by a closely related kinase to that employed for GAD65α phosphorylation is proposed from these observations. The phosphorylation of this region may be involved in modulating GLUT4 cellular routing, sorting from the cell surface, or possibly removal of GLUT4 from the recycling endosomal pool into the TGN and/or the specialised intracellular insulin responsive compartment.

3.2 Experimental Background and Aims

The aim of this study is to discover if an N terminal GLUT4 kinase exists and to try and assess the identity of such a putative kinase i.e. is the kinase CKII related? As previously mentioned the identification of specific kinases for GLUT4 requires a considerably more sensitive and specific approach than that achieved through whole cell "*in vitro*" phosphorylation studies. A technique termed the "In Gel" kinase assay was considered to meet the requirements for this study. In its infancy the "In Gel" assay was a procedure used to identify protein kinase activity in purified protein samples, following their electrophoresis on SDS-PAGE gels (Geahlen *et al.*, 1986). The principle behind this technique was that the protein substrate for the purified protein kinase of interest was polymerised within the SDS-PAGE gel. The purified protein kinase was then run onto the gel and subsequently re-natured within the gel. The gel was then incubated with [γ-^{32}P] ATP and phosphorylation of either the substrate, including in the gel or the kinase itself could be visualised through autoradiography of the gel. The beauty of this system was that the kinase of interest could be easily identified by its apparent molecular weight on the gel and also the system was highly sensitive with as little as 0.01 μg of cAMP-dependent protein kinase producing sufficient enzyme activity when incubated with gels containing 1 mg/ml casein (Geahlen *et al.*, 1986). Indeed the detection limits of this assay system have proved so sensitive that a variety of kinases have been detected in crude tissue lysates (Geahlen *et al.*, 1986; Kameshita and Fujisawa, 1989; Hutchcroft *et al.*, 1991; Bischoff *et al.*, 1998).

The need for relatively large amounts of purified protein substrates, to polymerise within the gel, hampered the popularisation of this technique for many years. Indeed this technique could not be applied to study the postulated variety of kinases for GLUT4, as large amounts of this protein are currently impossible to generate and readily purify. However the study of GLUT4 kinases may be possible from adaptation of a study which demonstrated that detection of protein kinase activities towards oligopeptides in SDS-PAGE gels was possible (Kameshita and Fujisawa, 1996). Kameshita and colleagues generated oligopeptides corresponding to areas of proteins that were suspected to be targets for phosphorylation by particular kinases. They found that these peptides could be effectively retained within the gel matrix if they were crosslinked to amino acid polymers, such as poly-$_L$-lysine, and served as effective substrates for kinases contained within crude tissue lysates. This technique displays enhanced sensitivity over its predecessor with as little as 2.5 ρg of the catalytic subunit of cAMP-dependent protein kinase producing detectable kinase activity when 4.5 μM of the synthetic peptide (cAMPtide) conjugated to poly (Lys) was used as the substrate (Kameshita and Fujisawa, 1996). Also the significant advantage of this technique over the use of purified protein "In gel" substrates is that single kinase activities can be detected for pre-determined regions within the protein, rather than highlighting all the kinases that may phosphorylate multiple sites within the whole protein.

With this specificity in mind, peptides were synthesised that corresponded to the area of interest (namely the area with high sequence identity to GAD65) in the N-Terminus of the GLUT4 molecule (see methods 2.5.1). The means of retaining this peptide within the gel matrix, optimising the conditions of its usage to detect a putative kinase for the N-Terminus of GLUT4 and the findings of these studies are detailed in the rest of this chapter.

3.3 Experimental Methods

3.3.1 Peptide conjugation procedure

3.3.1.1 GLUT4 N-Terminus peptide conjugation

Many conjugation protocols were utilised throughout the course of study. The optimal method is shown below and various modifications will be discussed in accordance with results shown later.

2 mg of Poly-L-Lysine (MW 70,000 – 150,000 Da) (Sigma) was dissolved in 1.25 ml of 20 mM $NaHCO_3$ buffer, (pH 8.2). This solution was then mixed with succinimidyl 4–(N–maleimidomethyl) cyclohexane-1-carboxylate (SMCC) (Pierce) which was dissolved in 140 µl of Dimethylformamide (DMF). The mixture was rotated for 30 min at room temperature to allow amide bond formation by the NHS ester reaction scheme shown below.

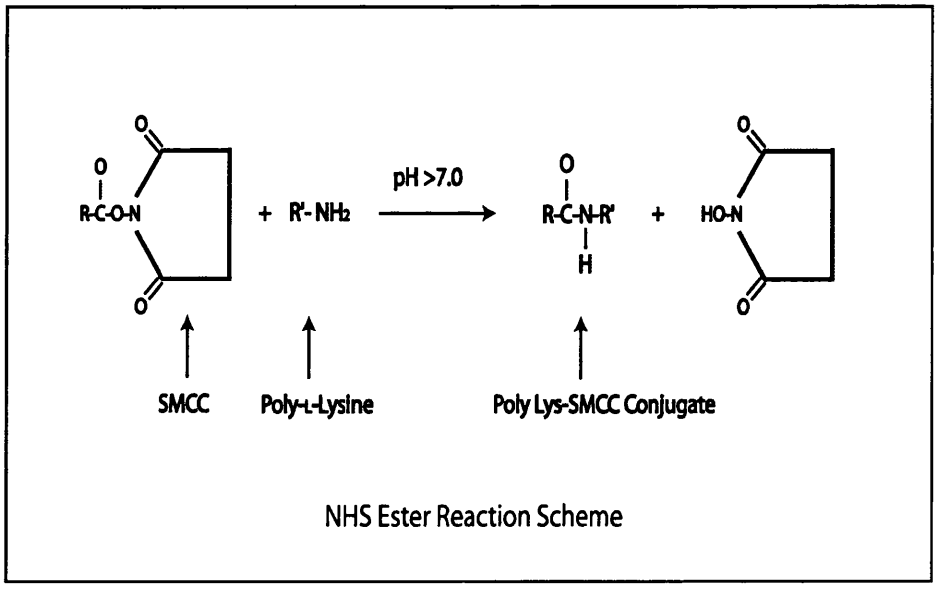

NHS Ester Reaction Scheme

While the reaction was proceeding a PD10 column (Sephadex G-25 M Amersham Pharmacia Biotech) was pre-equilibrated with 25 ml of 50 mM $NaPO_4$ buffer (pH 7.0). The mixture was made up to a total volume of 2.5 ml in the equilibration buffer and loaded onto the pre-equilibrated PD10

column. Once the mixture had completely run into the column the column was eluted with 3.5 ml of equilibration buffer, with unbound SMCC retained within the column. 2 mg (unless otherwise stated) of GLUT4 N terminal peptide (G4NTP) was added to the eluate and this mixture was gently rotated for 3 h at room temperature. The maleimide group of SMCC forms a thioether bond with the free sulfhydryls in the cysteine residue of the peptide by the maleimide reaction scheme shown below.

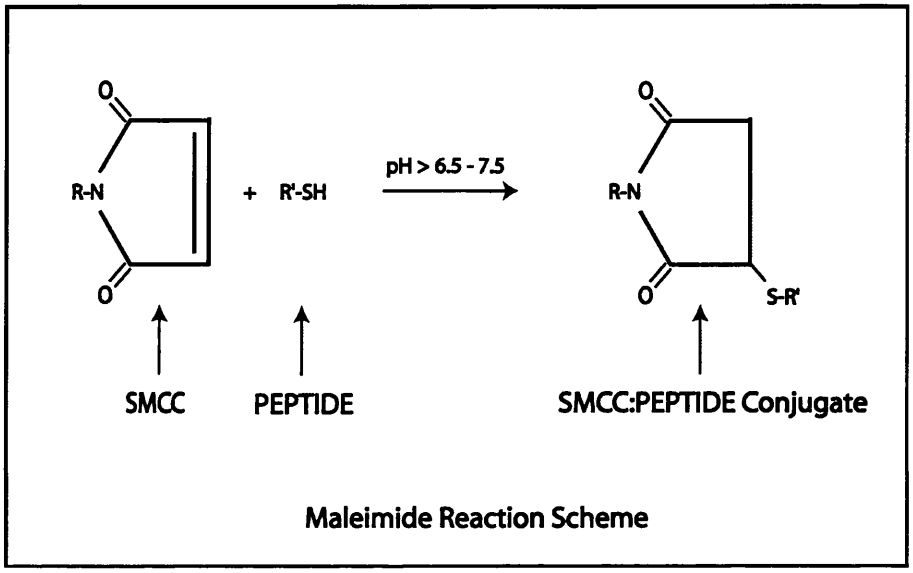

The reaction was stopped by the addition of 5 mM DTT and the conjugate aliquoted to the appropriate volume, depending upon the concentration requirements, and stored at -20°C until required.

3.3.1.2 GLUT4 C-Terminus conjugation

The peptide used in this procedure corresponds to the carboxyl cytosolic region of GLUT4 and was synthesised in house. The sequence of this peptide is shown below.

NH_2-T-P-S^{488}-L-L-E-Q-E-COOH

5 mg of the GLUT4 C-Terminus peptide was re-suspended in 1350 µl of 20 mM $NaHCO_3$ (pH 8.2) and 7.5 mg of the crosslinker (SPA) 2-PEG (MW 3400 Da) (Shearwater Polymers Inc.) was re-suspended in 140 µl of DMF. The two solutions were mixed together giving a total volume of 1.5 ml with a DMF concentration of 10%. The mixture was rotated gently for 1 h at room temperature to allow binding of the primary amine group on the amino terminal of the peptide to bind to the crosslinker.

5 mg of Poly-$_L$-Lysine (MW 70,000-150,000 Da) was re-suspended in 500 µl of 20 mM $NaHCO_3$ (pH 8.2) and then added to the mixture. The mixture was then transferred into a Bijou and rotated gently for a further 1 h at room temperature to facilitate binding of the crosslinker to the amino groups of Poly-$_L$-Lysine.

7 mg of acetic acid NHS (Sigma) in 140 µl of DMF was then added to this mixture to block amino groups on the Poly-$_L$-Lysine that had not bound crosslinker. The mixture was again rotated for one hour at room temperature after which 5 mM DTT total volume was added to stop any further reactions.

A PD10 column was pre-equilibrated with 25 ml of 20 mM $NaHCO_3$ buffer (pH 8.2). The mixture was made up to a final volume of 2.5 ml with equilibration buffer and then loaded onto the column and allowed to run in fully. The column was then eluted with 3.5 ml of equilibration buffer leaving unbound acetic acid NHS and (SPA) 2-PEG in the bed volume. Assuming that a 10% loss of the conjugate had occurred in this purification step the conjugate was aliquoted into appropriate volumes for assay requirements and stored at -20°C until required.

3.3.2 "In Gel" Kinase assay protocol

The protocol given here is that of the optimised assay, deviations from this methodology will be discussed in accordance with results shown later.

An appropriate amount of peptide conjugate was added into a 10% resolving gel mixture before the addition of ammonium persulphate and TEMED (see Methods 2.4.2). The gel solution should be mixed gently to avoid generation of bubbles and then polymerised as previously detailed. Appropriate samples were prepared, loaded and run into the gel as detailed in Methods 2.4.2.

Upon satisfactory running of the samples the gels are taken from the running apparatus and subjected to two 1h washes in 20% isopropanol in 50 mM HEPES buffer (pH 8.0). The Isopropanol used acts to remove SDS from the gels, which aids in subsequent renaturation of the proteins within the gel matrix. The gels are then washed for 1h at room temperature in Buffer A (50 mM HEPES (pH 8.0), 5 mM 2-mercaptoethanol). The gels are then treated twice with 100 ml washes of guanidine HCl (Sigma) in Buffer A, for 1h at room temperature. The effect of guanidine HCl is to denature the proteins, within the gel matrix, into random coils that can be renatured more effectively. Before renaturation can take place the denaturant needs to be effectively removed and this is achieved by four 250 ml washes of renaturation buffer (Buffer A containing 0.04% (v/v) Tween 20) for 15 min at room temperature. The gels are then incubated overnight in renaturation buffer at 4°C to facilitate the recovery of the proteins native structure within the gel matrix.

Upon effective renaturation of the proteins the gels are quickly rinsed in ddH_2O and then incubated in 100 ml of phosphorylation buffer (25 mM HEPES (pH 7.4), 10 mM $MnCl_2$, 100 μCi [$\gamma^{32}P$] ATP), for 3 h, at room temperature. The gels are then washed four times with ddH_2O, for 15 min, at room temperature. Any further reactions are stopped by six 500 ml washes of Stopping Buffer (5% (w/v) Trichloroacetic acid (TCA), 1% (w/v) Sodium Pyrophosphate). In addition to preventing further phosphorylation events the stopping buffer also acts to remove unused radio-labelled ATP, resulting in a cleaner background in the gels subsequent analysis.

To visualise the proteins within the gel and the protein markers the gels are stained and fixed according to Methods 2.4.2. The gels are then dried onto 3MM blotting paper using the Labconco gel dryer and Heto master jet vacuum pump at 60°C for 90 min. The gels are then exposed to autoradiograph film (Kodak) for an appreciable time and proteins, which had incorporated labelled [γ^{32}P], are then visualised and assessed.

For quantification purposes the autoradiograph images were scanned using the CanoScan N6760 reflective scanner (Canon, UK). Please note that quantification, using reflective scanning of autoradiographs, has been called into question. Ghost images may alter the actual densitromic readings performed on the scanned image. Consequently only images scanned using a transmitence scanner can be effectively quantified.

3.4 Results and Discussion for the development of the "In Gel" kinase assay.

3.4.1 Immobilising peptides within the SDS-PAGE gels

The synthesised peptide $_{NH2}$-I-G-S-E-D-G-E-P-P-Q-Q-C-$_{COOH,}$ corresponding to the hypothesised area of recognition by a putative kinase, was initially incorporated into the polymerised gel. A control gel containing no incorporated peptide was processed in conjunction with the peptide containing gel to act as a negative control. The results from these preliminary experiments did not identify any possible protein targets, as there were no significant differences between the control gel and the peptide containing gel (data not shown). An observation made by Kameshita and colleagues offered a possible explanation towards the lack of positive protein targets from these preliminary studies. They suggested that around 80% of peptides composed of 18 amino acids, or less, are eluted from SDS-PAGE gels under electrophoresis (Kameshita and Fujisawa, 1996). This may mean that the level of the 12 amino acid peptide retained within the gel matrix may have been so low that any enhancement of peptide or kinase phosphorylation may have been undetectable over the levels of protein kinase autophosphorylation observed in the control gels. The remedy for this problem was to conjugate the peptide to Poly-$_{L}$-Lysine as detailed in 3.1. The methodology for the conjugation process has been previously described (see Experimental Methods 3.3.1.1). The "In Gel" kinase assay shown in Fig 3.1 was performed essentially as detailed in Experimental Methods 3.3.2, with the exception of the method for removal of unbound radiolabelled ATP. This was removed by incubation of the gels in two changes of 40 mM HEPES buffer (pH 7.4) into which 15 g of Dowex anion exchange resin (Sigma), in dialysis tubing, was placed. The Dowex resin acts to bind any free ATP and a period of 2 h was used for this process. Following this treatment the gels were further incubated in 300 ml of 40 mM HEPES buffer (pH 7.4) containing 1% (w/v) sodium pyrophosphate for 3 h at room temperature with gentle rotation. After this

the gels were fixed, stained and processed in the same manner as detailed in Experimental Methods 3.3.2. The results of one of the early "In Gel" kinase assays utilising the peptide conjugation scheme can be seen in Fig 3.1.

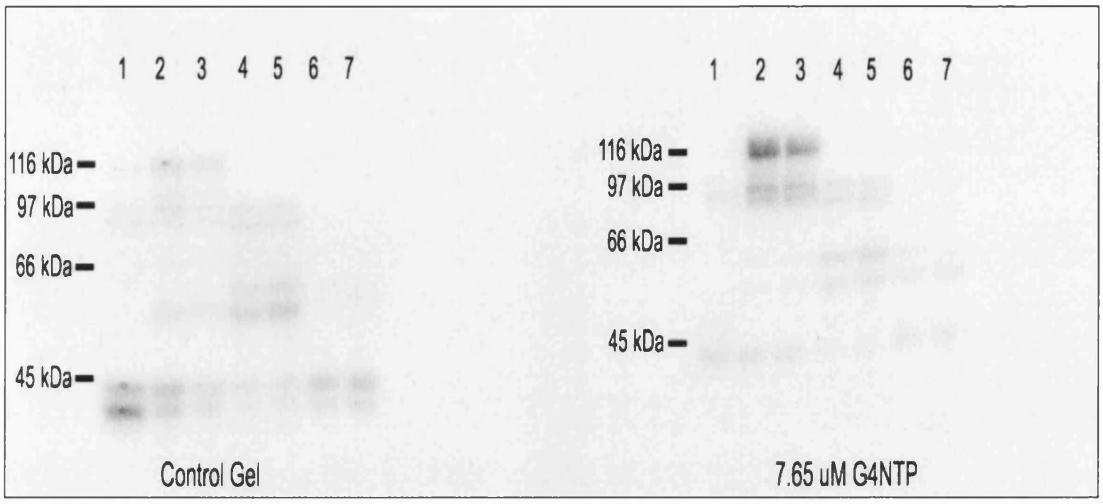

FIG 3.1: **Detection of a putative kinase that appears to phosphorylate the GLUT4 N-Terminus peptide conjugate.** 40 μg of protein was loaded per lane onto a 10% SDS-PAGE control gel and another gel containing 7.65 μM G4NTP, conjugated to Poly-$_L$-Lysine, which was polymerised within the gel matrix. Lane 1: Crude synaptosome preparation; Lane 2: Basal LDM; Lane 3: Insulin LDM; Lane 4: Basal PM; Lane 5: Insulin PM; Lane 6: Basal Cytosol; Lane 7: Insulin Cytosol. The gels were processed as previously described (see 3.4.2), using 100 μCi [γ^{32}P] ATP in the phosphorylation buffer. The image shown was scanned from a 1hr-autoradiograph development of the treated gels. The gels are placed together to show that they are from the same autoradiograph and have been subjected to the same exposure. The results shown here are representative of two studies.

The autoradiograph developments from these studies showed that autophosphorylation of kinases within the "In gel" assay was occurring, as bands could be easily detected on the control gels that had no substrate incorporated into them. Early studies suggested that the presence of the G4NTP conjugate, within the gel, appeared to reduce the level of autophosphorylation within certain kinases, as observed with protein bands corresponding to molecular weights of around 40 kDa. The reason for this was unclear, as were the identities of the protein kinases in question, however it could be that the presence of the G4NTP conjugate interfered with the renaturation of these particular kinases and consequently their activity was reduced.

There appeared to be a doublet of around 90 kDa and a band of around 110 kDa that displayed a clear enhancement of $\gamma^{32}P$ incorporation, which was not reproduced in the control gels and this may be a result of the enhanced catalytic activity of the kinases in these regions. An interesting early observation from these studies was that the kinases highlighted seemed to reside in membranous protein fractions, with detection in the PM and to a greater extent in the LDM fractions, and no observable detection in the cytosolic samples. With regard to the synaptosomal fractions, the increase in the 90 kDa doublet or the 110 kDa band was not evident in this preparation, however the synaptosome preparation itself was very crude and latter studies will show the usefulness of this fraction with regards to the kinases of interest.

3.4.2 Enhancement of kinase autophosphorylation by poly Lysine

Preliminary studies, using the "In gel" assay, provided potential protein targets for kinases that may phosphorylate N-terminal GLUT4. However a critical question regarding these results was, what effect did the conjugation material have upon the level of phosphorylation seen by the various protein kinases detected? To resolve this issue the experiments were repeated, however the control gels were polymerised with the conjugation polymer poly-$_L$-Lysine at the same concentration as would be present in the G4NTP

conjugated gels. These studies would account for any effects, whether stimulatory or inhibitory, that poly-$_L$-Lysine may have on the "In Gel" kinase assay development. The result of one of these studies can be seen in Fig 3.2.

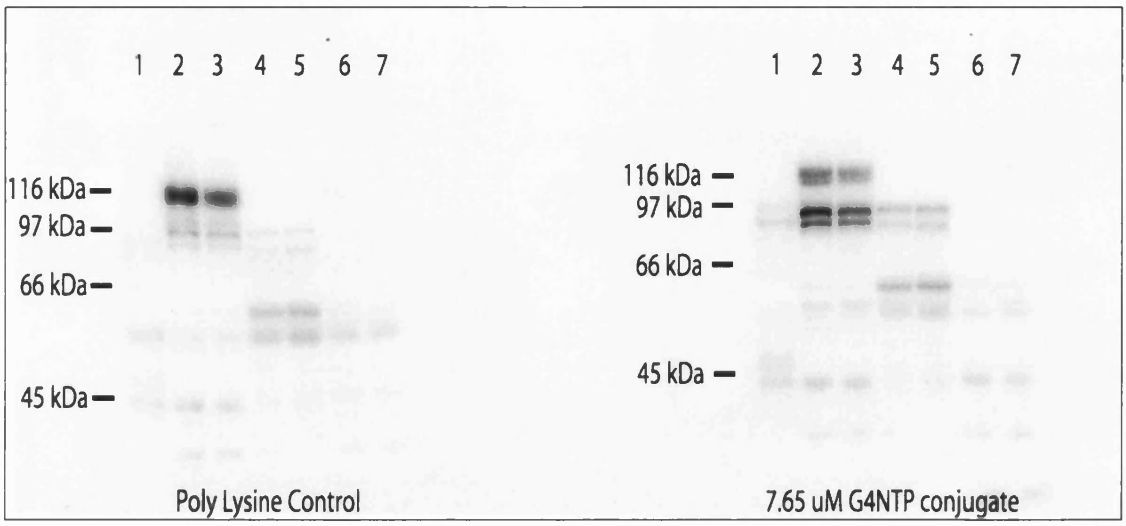

FIG 3.2: **Poly-$_L$-Lysine does not stimulate the catalytic activity of the kinase doublet.** 40 μg of protein was loaded per lane onto a 10% SDS-PAGE control gel containing Poly-$_L$-Lysine polymerised within the gel and another gel containing 7.65 μM G4NTP, conjugated to poly-$_L$-Lysine, which was also polymerised within the gel matrix. Lane 1: Crude synaptosome preparation; Lane 2: Basal LDM; Lane 3: Insulin LDM; Lane 4: Basal PM; Lane 5: Insulin PM; Lane 6: Basal Cytosol; Lane 7: Insulin Cytosol. The gels were processed as previously described (see 3.4.2), using 100 μCi [γ32P] ATP in the phosphorylation buffer. The image shown was scanned from a 30 min-autoradiograph development of the treated gels. The gels are placed together to show that they are from the same autoradiograph and have been subjected to the same exposure. The results shown here are representative of three studies.

The results from these studies were encouraging and appeared to give a much clearer distinction between kinases that may be specifically stimulated by the G4NTP conjugate. There seemed to be near equivalence of most of the band densities observed between the control gel and the G4NTP conjugate gel. Most notably the bands in the region of 45 kDa, which were noticeably different when the control gel had no poly-$_L$-Lysine incorporated, were not significantly different between the two gels. The use of poly-$_L$-Lysine in the control gel matrix was consequently used in all future studies, as it seemed to effectively mimic the level of protein kinase renaturation, within the gel, induced with the G4NTP conjugate. Using this procedure, background levels of autophosphorylation obtained by renatured protein kinases should be effectively regulated between the two gels, with only specific interactions with G4NTP producing differences in band density. Indeed there were significant differences in band density in the regions of the 90-kDa protein doublet, again in the membrane-associated fractions. The bands around 110 kDa were not enhanced in the G4NTP conjugate gels, and using the modified control gel this protein kinase did not appear to be enhanced by the G4NTP in later experiments. This meant that the focus for a potential GLUT4 N-terminal kinase was placed on the 90-kDa protein doublet, for the context of this study.

3.4.3 Enhancement of specific, peptide directed, kinase phosphorylation by poly-$_L$-Lysine

The previous findings suggested that poly-$_L$-Lysine alone did not stimulate γ^{32}P incorporation into the region of the 90 kDa kinase doublet. These observations are in agreement with the studies of Kameshita and colleagues who also observed no significant protein kinase activity in gels containing poly-$_L$-Lysine only (Kameshita and Fujisawa, 1996). Interestingly the studies of Kameshita's group did show that poly-$_L$-Lysine conjugated to specific peptides, did significantly increase specific protein kinase activities, however the reasons for this were not fully understood. It was considered imperative to establish if poly-$_L$-Lysine, conjugated to G4NTP, contributed to

the observed kinase activity increase seen for the 95 kDa kinase doublet and also why this happened.

A study of the literature surrounding the effects of poly-$_L$-Lysine in *in vitro* assays revealed the following:

- A study conducted by Avruch and colleagues, using MAP Kinase II, showed that poly-$_L$-Lysine directly interacted and modified the catalytic function of the enzyme, but this was strongly influenced by the identity of the specific peptide substrate used. It was suggested that poly-$_L$-Lysine may mimic a basic domain within a potential substrate, distant from the phosphorylation site, which might bind to a non-catalytic domain of the kinase and promote its interaction with the substrate (Kyriakis and Avruch, 1990).
- Pinna and colleagues observed that polybasic effectors specifically interact with Casein kinase II (CKII), potentially altering the structure of its peptide binding site. They also demonstrated that *in vitro* phosphorylation of several substrates is enhanced by poly-$_L$-Lysine concentrations comparable to those of the enzyme (Meggio *et al.*, 1992).
- Benitez and colleagues performed a surface-plasma-resonance analysis of poly-$_L$-Lysine interactions with a peptide substrate of protein kinase CKII. They proposed that stimulation of enzyme activity followed poly-$_L$-Lysine binding to the peptide rather than the enzyme (Benitez *et al.*, 1997).

This information led to the idea that maybe the charged amino groups on the long poly-$_L$-Lysine chain enhanced the interaction of specific kinases with the immobilised peptide substrate in the "In Gel" kinase assay. This idea was explored by specifically "blocking" the charged residues through their acylation. The acylation of Lysine residues was performed on G4NTP poly-$_L$-Lysine conjugates that were generated as detailed in Experimental Methods 3.3.1.1. However before DTT was added to the conjugate they were equilibrated in 20 mM $NaHCO_3$ (pH 8.2) and then reacted overnight at room temperature with 5 mg of acetic acid NHS (Sigma), in 280 µl DMF, by end to end rotation. The NHS binds to the amino groups of the poly-$_L$-Lysine and they are then effectively acylated.

The modified "blocked" G4NTP poly-$_L$-Lysine conjugate was then compared to the "unblocked" conjugate in the "In Gel" kinase assay as detailed in Experimental Methods 3.3.2. Equivalent levels of peptide conjugate were loaded so that the effect of eliminating the basic charge on the poly-$_L$-Lysine with respect to $\gamma^{32}P$ incorporation into the 90 kDa doublet bands could be effectively observed. The results of one of these studies can be seen in Fig 3.3.

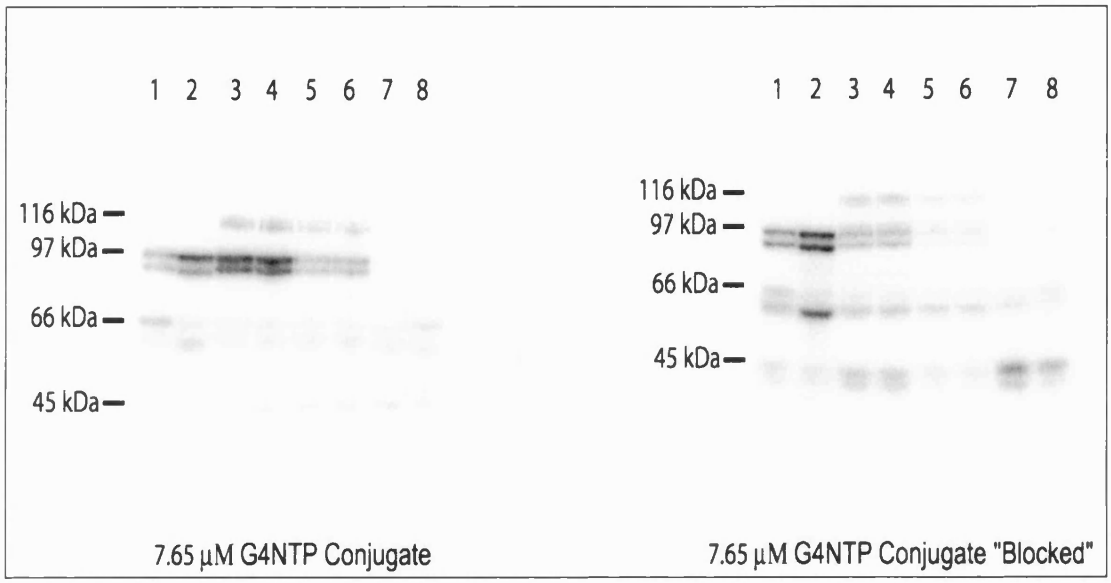

FIG 3.3: **Comparison of charge effects of poly-$_L$-Lysine on γ32P incorporation into the 90-kDa kinase doublet.** 40 µg of protein was loaded per lane onto a 10% SDS-PAGE gel containing 7.65 µM G4NTP conjugated to poly-$_L$-Lysine, and also a gel containing 7.65 µM G4NTP conjugated to poly-$_L$-Lysine which had its amino groups acylated "blocked". Lane 1: Basal PM; Lane 2: Insulin PM; Lane 3 and 4: Basal LDM; Lane 5 and 6: Insulin LDM; Lane 7: Basal Cytosol; Lane 8: Insulin Cytosol. The gels were processed as previously described (see 3.4.2), using 100 µCi [$\gamma^{32}P$] ATP in the phosphorylation buffer. The image shown was scanned from a 1h-autoradiograph development of the treated gels. The gels are placed together to show that they are from the same autoradiograph and have been subjected to the same exposure.

The results of this study suggested that the charge on poly-$_L$-Lysine does seem to enhance $\gamma^{32}P$ incorporation into the 90-kDa kinase doublet. Overall the band intensities in the blocked conjugate gel are visibly lower than those seen in the standard unblocked conjugate gel. Again no observable detection of the kinase doublet was found in the cytosolic samples, further supporting the notion that the kinase of interest was membrane associated. A questionable result in the diagram shown regarded the Insulin PM fractions in the blocked conjugate gel. It appeared that there was an increased protein loading in this gel, compared with the corresponding unblocked conjugate gel. This could be due to retention of some of the protein in the pipette tip when the protein lysates were loaded onto the two gels, or possibly uneven mixing of the protein fractions when they were aliquoted out. The duplicate lanes in the LDM samples indicated that equal loading had occurred elsewhere on the gel and this was an isolated incident. To safeguard for any further irregularities, future studies ensured that the mixing of the samples before loading was more rigorous and a more accurate dispensing pipette was used, to be sure that equal sample volumes were dispensed between the two gels.

3.4.4 Identification of optimal phosphorylation buffer

The standard phosphorylation buffer used for the "In Gel" kinase assay contained $MnCl_2$, opposed to $MgCl_2$ that is commonly utilised for conventional *in vitro* kinase assays. The foundation for the preferential use of $MnCl_2$ stemmed from observations made by Hutchcroft and colleagues. They found that, at the low ATP concentrations used for their "In Gel" kinase assays, Mn^{2+} was considerably more effective than Mg^{2+} in supporting an "In Gel" kinase reaction (Hutchcroft *et al.*, 1991). However it was considered wise to determine if the use of $MnCl_2$ in the study of the kinase doublet was appropriate. Consequently two identical gels containing 7.65 μM G4NTP conjugate were made and processed as detailed in Experimental Methods 3.3.2, except that one of the gels was reacted in a phosphorylation buffer in which 10 mM $MgCl_2$ was substituted for 10 mM $MnCl_2$. The results from one of these studies can be seen in Fig 3.4.

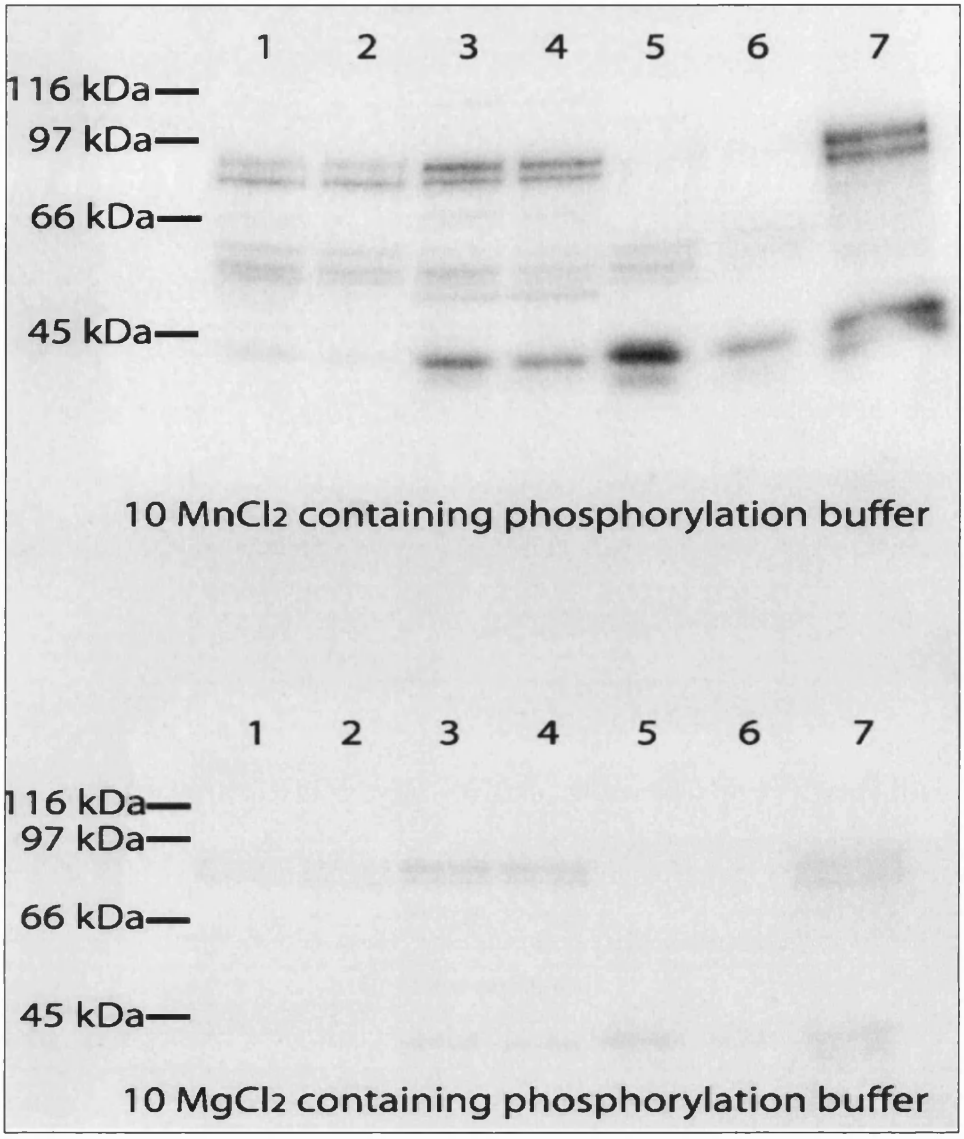

FIG 3.4: **Kinase activity is significantly enhanced (~4 fold) in 10 mM $MnCl_2$ containing phosphorylation buffer compared with the level of activity observed with 10 mM $MgCl_2$ containing phosphorylation buffer.** 20 μg of protein was loaded per lane onto identical 10% SDS-PAGE gel containing 7.65 μM G4NTP conjugated to poly-$_L$-Lysine. Lane 1: Basal PM; Lane 2: Insulin PM; Lane 3: Basal LDM; Lane 4: Insulin LDM; Lane 5: Basal Cytosol; Lane 6: Insulin Cytosol; Lane 7: Synaptosome preparation. The gels were processed as previously described (see 3.4.2), using 25 μCi [γ^{32}P] ATP in each phosphorylation buffer. The image shown was scanned from a 3h-autoradiograph development of the treated gels and is representative of two studies. The gels are placed together to show that they are from the same autoradiograph and have been subjected to the same exposure.

The results obtained confirmed that $MnCl_2$ was preferable to $MgCl_2$ for future use in the phosphorylation buffer composition for the "In Gel" kinase assay. Using a shareware densitometry package (Beta 3b Scion Image) an average enhancement of around 4 fold in kinase activity was observed when 10 mM $MnCl_2$ was used instead of 10 mM $MgCl_2$. Interestingly Geahlen and colleagues observed that Mn^{2+} proved to be more effective than Mg^{2+} in supporting phosphorylation, with CKII and the cAMP-dependent protein kinase catalytic subunit enhanced by 5-fold and 40-fold respectively (Geahlen *et al.*, 1986). The means by which $MnCl_2$ significantly enhances the reaction mechanism for "In Gel" assays is not clear but seems to be linked to the lower levels of ATP used in these assays.

It was also interesting to observe a doublet band of approximately the same size as the 90 kDa doublet, found in adipocyte membrane fractions, in an improved synaptosomal preparation. The synaptosomal preparation was the same as detailed in General Methods 2.3, however this sample was far superior to previous preparations, both in terms of quality and recovered protein levels, as a result of increased technical experience and quicker processing times. The detection of the 90 kDa kinase doublet in the synaptosomal sample was very encouraging. The close sequence identity of the N terminal GLUT4 peptide with the region of GAD65α that is phosphorylated by an, as yet, unidentified synaptic vesicle membrane associated kinase adds some credibility to the possibility that the same kinase or a closely related kinase may act on both GLUT4 and GAD65α.

3.4.5 Determination of the relationship between the ~90 kDa kinase doublet and CKII.

The identification of a reactive ~90 kDa doublet which seems to be activated by interaction with the GLUT4 N terminal peptide does not concur with the kinase being CKII. The CKII holoenzyme is a heterotetramer of $\alpha_2\beta_2$ or $\alpha\alpha'\beta_2$. The α and α' subunits are catalytically active by themselves and have a M_r of 42-44 kDa (α) or 38 kDa (α'). The β subunit M_r 26 kDa is inactive by itself but has been shown to stimulate the catalytic activity of the

α subunit by 5-10 fold (Allende and Allende, 1995). No bands within this range appear to be enhanced in the G4NTP conjugate gels, however this does not exclude the possibility that the kinase detected is CKII related. For example several types of cell exhibit cell surface protein kinase (ecto-PK) activities that share certain characteristics with protein kinase CKII (Walter *et al.*, 1996).

A unique characteristic associated with CKII and CKII-like kinases is that they can use both ATP and GTP as phosphate donors, with a preference for GTP utilisation in the presence of $MnCl_2$ (Gatica, 1993). This phenomenon was utilised to determine if the 90 kDa kinase doublet detected in the "In Gel" kinase assays was CKII related. Two sets of identical gels were processed and subjected to phosphorylation in either [γ^{32P}] ATP or an equal concentration of [γ^{32P}] GTP containing phosphorylation buffers containing 10 mM $MnCl_2$. The results from one of the studies can be seen in Fig 3.5.

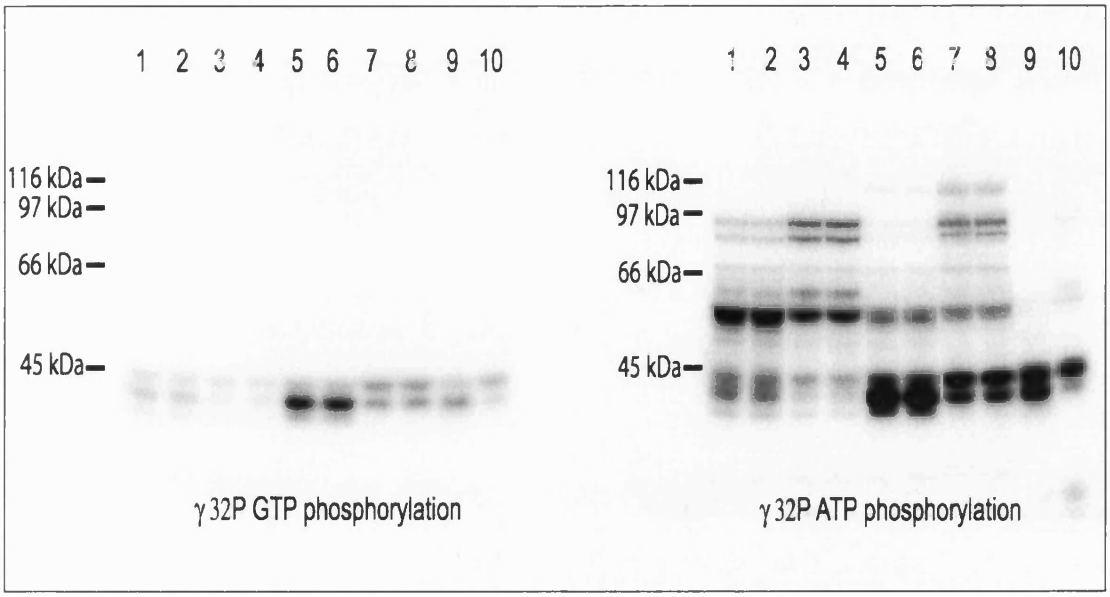

FIG 3.5: **Comparison of GTP and ATP phosphorylated "In Gel" assays shows the 90 kDa kinase doublet is not CKII related.** 40 μg of protein was loaded per lane onto identical 10% SDS-PAGE gel containing 7.65 μM G4NTP conjugated to poly Lysine. Lane 1 and 2: Basal PM; Lane 3 and 4: Insulin PM; Lane 5 and 6: Basal LDM; Lane 7 and 8: Insulin LDM; Lane 9: Basal Cytosol; Lane 10: Insulin Cytosol. The gels were processed as previously described (see 3.4.2), using 100 μCi [γ^{32}P] ATP or [γ^{32}P] GTP in each phosphorylation buffer. The image shown was scanned from a 2.5hr-autoradiograph development of the treated gels. The gels are placed together to show that they are from the same autoradiograph and have been subjected to the same exposure.

The [γ^{32}P] GTP treated gel identified bands in the 40-45 kDa range that correspond to the predicted size of the α and α' subunits of CKII. These subunits were also detected in an "In Gel" kinase assay in which Casein, the preferred *in vitro* substrate for CKII, was immobilised in the gel (data not shown). These results suggest that the bands seen in the 40 kDa region of the "In Gel" kinase assays are CKII. However the effectiveness of GTP as a phosphate donor, while specific for CKII, does not appear to be any better than that of ATP from these studies.

The most interesting observation from these studies was that no detection of the 90 kDa kinase doublet could be observed in the [γ^{32}P] GTP loaded "In Gel" kinase assay, suggesting that the kinase is not CKII related as it does not appear to use GTP as a phosphate donor.

Another conclusion drawn from these studies was that the radioactivity detected on the incubated gels was due to specific incorporation of radiolabelled phosphate and not non-specific association with protein bands in the gel. If there was any non-specific association then the GTP gel should have shown evidence of other radiolabelled protein bands and this was not the case. By inference we can conclude that this should also be the case for the ATP gels. Studies in which 100 μM ATP was added to the [γ^{32}P] ATP phosphorylation buffer further supported this conclusion, as the cold ATP completely removed any [γ^{32}P] incorporation into the processed gels (data not shown).

It was noticeable from the study shown in Fig 3.5 that there appeared to be an increase in the level either of the amounts of kinase or in the kinase activity in the insulin treated membrane fractions. The basal/insulin distribution of the 90 kDa kinase doublet varied between some experiments and so this increase is by no means representative of the distribution of the kinase of interest. The variance could be due to the differential distribution of the kinase between different adipocyte isolation and subfractionation procedures, or to different levels of phosphorylation of the kinases, at the point of loading onto the SDS-PAGE gels, which would naturally effect the level of [γ^{32}P] incorporation into the kinase upon its reaction in the "In Gel" assay.

3.4.6 Identification of specific kinase phosphorylation of the GLUT4 N Terminal Peptide

The next stage in the investigation involved ascertaining what was causing the enhancement of the 90 kDa kinase doublet in the G4NTP containing gels. Possible explanations are:

- Increased autophosphorylation of the kinase when it interacts with the G4NTP conjugate, possibly due to increased recovery of renatured kinase through this interaction.
- Phosphorylation of Ser_{10} within the G4NTP conjugate by the ~90 kDa kinase doublet.
- A combination of enhanced kinase autophosphorylation and specific peptide phosphorylation.

A series of experiments were designed to try and identify which of the proposed mechanisms were in operation for the kinase of interest.

The kinase doublet has sometimes been referred to here as a single kinase. The doublet may represent two different isoforms of a kinase catalytic subunit, like that of CKII, or two levels of post-translational modification of the same catalytic subunit. These possibilities are explored in Results Chapter 2.

3.4.6.1 Investigating the possibility of enhanced phosphorylation of the 90 kDa doublet with increasing G4NTP conjugate concentration

An investigation into the effects of increasing concentrations of the G4NTP conjugate within a series of gels was designed to identify if this had any effect on increased $\gamma^{32}P$ incorporation into the 90 kDa bands. 7.65 μM, 15.3 μM and 30.6 μM G4NTP conjugate concentrations were used and the control poly-$_L$-Lysine only gel was set at 30.6 μM to account for the maximum level of renaturation benefit offered by this level of protein in the gel matrix. The results from this study are given in Fig 3.6 and a quantified analysis of selected band enhancement, namely the PM samples, is shown

in Fig 3.7. Please note that the analysis is of the 90 kDa kinase doublet as a whole. The single bands could not be effectively quantified, due to resolution limitations of the software used in this procedure.

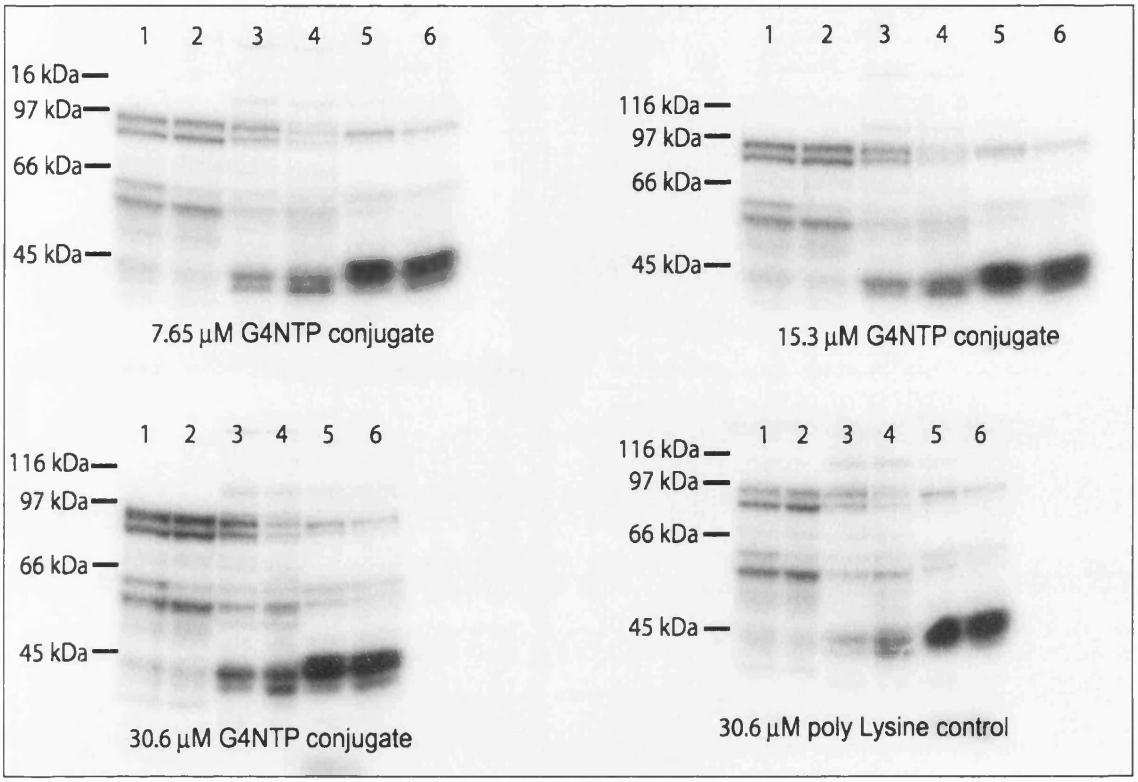

FIG 3.6: **Enhanced [γ32P] incorporation in the 90 kDa kinase doublet with increasing G4NTP conjugate concentration within the gel matrix.** 30 µg of protein was loaded per lane onto as series of 10% SDS-PAGE gels containing 7.65 µM, 15.3 µM and 30.6 µM G4NTP conjugated to poly Lysine, or 30.6 µM poly-$_L$-Lysine only. Lane 1: Basal PM; Lane 2: Insulin PM; Lane 3: Basal LDM; Lane 4: Insulin LDM; Lane 5: Basal Cytosol; Lane 6: Insulin Cytosol. The gels were processed as previously described (see 3.4.2), using 25 µCi [γ^{32}P] ATP per gel in each phosphorylation buffer. The image shown was scanned from a 1h-autoradiograph development of the treated gels. The gels are placed together to show that they are from the same autoradiograph and have been subjected to the same exposure.

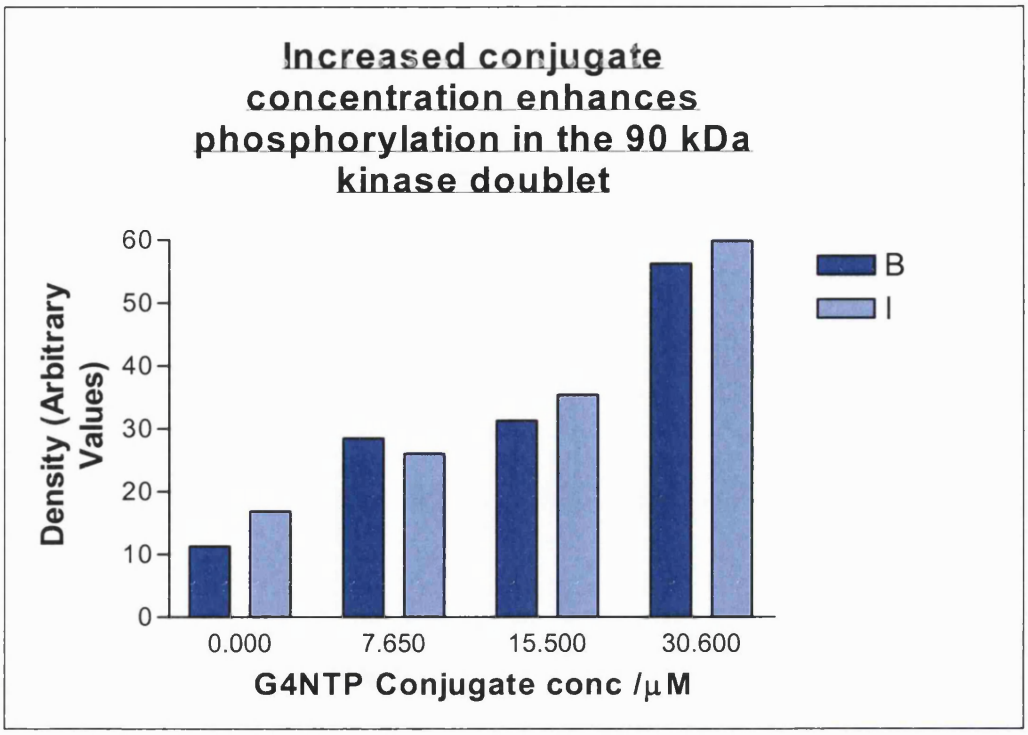

FIG 3.7: **Bar graph representing quantified densitromic values from the scanned autoradiographs shown in Fig 3.6.** The 90 kDa kinase doublets of basal and insulin stimulated PM fractions were scanned and their respective densities measured for the concentration series of "In Gel" G4NTP conjugate gels. The 30.6 μM poly Lysine only gel was used as the control and has been given the value of 0.0 for the purpose of this plot.

The results of this initial study suggested that the level of peptide present within the gel affected the level of [γ^{32}P] incorporation into the region of the 90 kDa kinase doublet and indicated that a reaction may occur between the peptide and the kinase in question. However these results did not identify if the reaction between the peptide and the kinase led to phosphorylation of Ser^{10}, within the G4NTP, or merely enhanced autophosphorylation of the kinase, in a peptide-conjugate dependent fashion. As a consequence of this realisation further repeats of this particular study were not undertaken and the results above are shown merely to show the progression of the experimental analysis.

3.4.6.2 Investigating the possibility of enhanced phosphorylation of the 90 kDa doublet with increasing G4NTP ratio within the conjugate.

In the previous study the level of poly-$_L$-Lysine increased to the same level as the peptide and it was previously shown that poly-$_L$-Lysine enhanced the reaction between specific peptide substrates and their respective kinases (Results 3.1.3). In view of this a modified study was required to assess the impact that increasing G4NTP concentration had upon the incorporation of γ^{32}P into the 90 kDa doublet bands and identify if peptide phosphorylation was involved in this process. The new methodology utilised a series of G4NTP-poly-$_L$-Lysine conjugates in which the G4NTP:poly-$_L$-Lysine ratio was altered. This series of conjugates were incorporated into 10% SDS-PAGE gels with the effect that while there was an increasing peptide concentration, over the series of gels, the level of poly-$_L$-Lysine remained unchanged. A 10 μM poly-$_L$-Lysine only control gel was also generated that was the same as the maximal concentration of G4NTP used in these studies. The control gel mimics the level of renaturation of the protein kinase aided by this concentration of protein, within the gel matrix, which then effects the level of kinase autophosphorylation. The results from one of the studies is shown in Fig 3.8 and a quantified analysis of the level of band enhancement, from two separate studies, is shown in Fig 3.9.

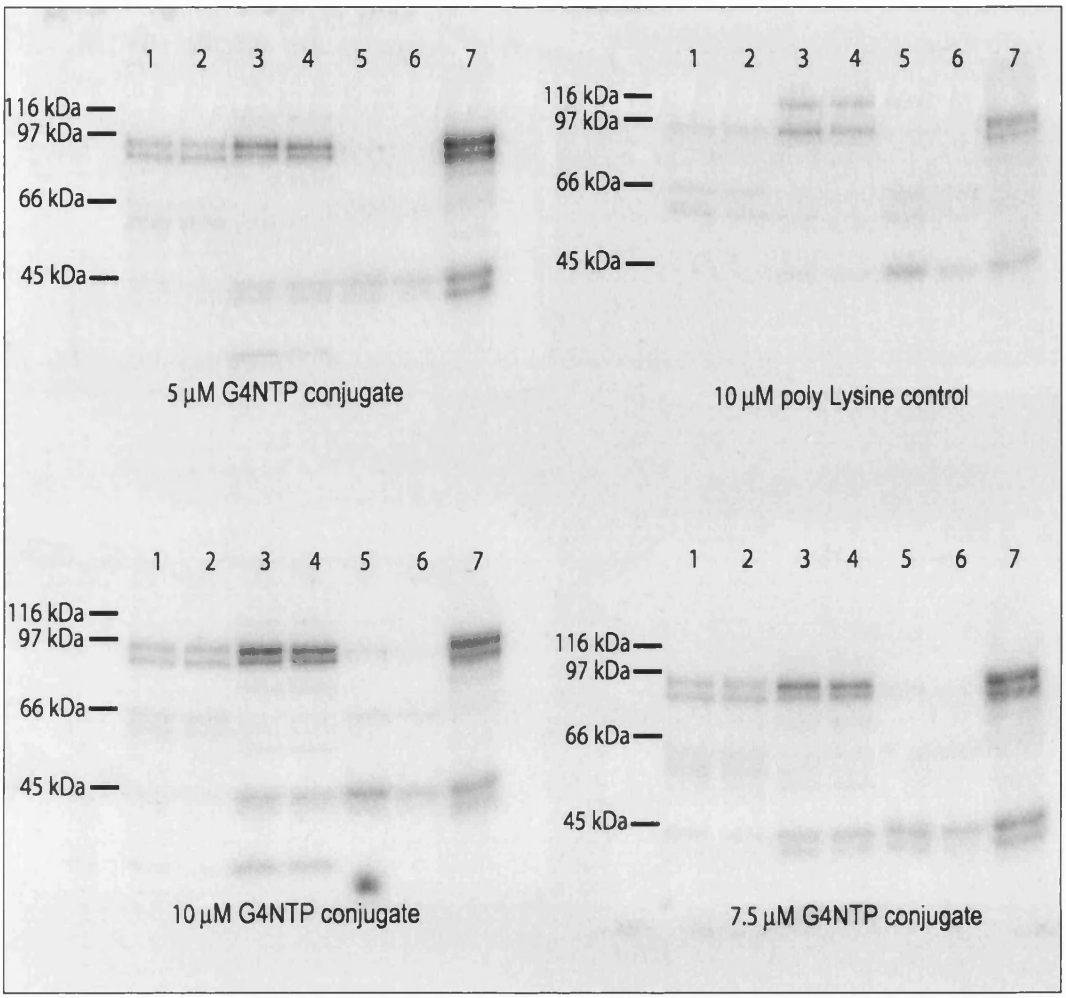

FIG 3.8: **Enhanced [γ32P] incorporation into the 90 kDa kinase doublet when increasing G4NTP:poly-$_L$-Lysine ratio generated conjugates are immobilised within the gel matrix.** 20 µg of protein was loaded per lane onto as series of 10% SDS-PAGE gels containing 5 µM, 7.5 µM and 10 µM G4NTP with a fixed amount of poly-$_L$-Lysine in each conjugate. A control gel containing 10 µM poly-$_L$-Lysine only was also prepared. Lane 1: Basal PM; Lane 2: Insulin PM; Lane 3: Basal LDM; Lane 4: Insulin LDM; Lane 5: Basal Cytosol; Lane 6: Insulin Cytosol; Lane 7: Synaptosome preparation. The gels were processed as previously described (see 3.4.2), using 25 µCi [γ^{32}P] ATP per gel in each phosphorylation buffer. The image shown was scanned from a 1h-autoradiograph development of the treated gels. The gels are placed together to show that they are from the same autoradiograph and have been subjected to the same exposure. The result shown is representative of two independent studies.

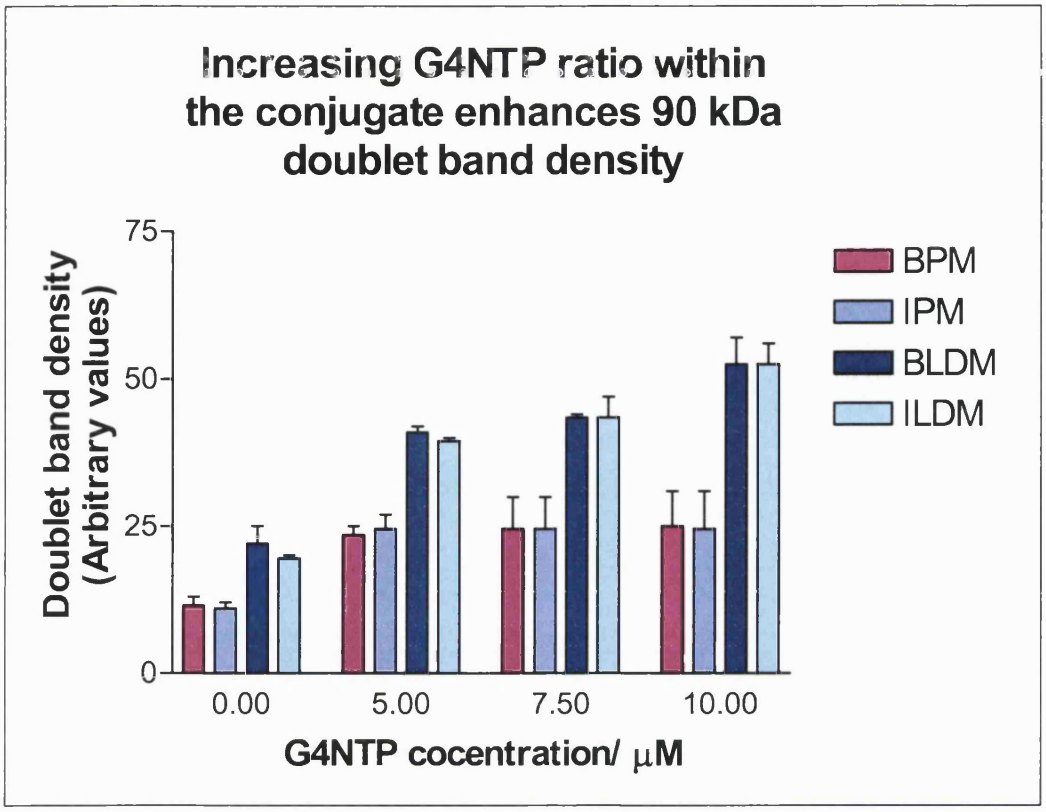

FIG 3.9: **Bar graph representing quantified densitromic values from the scanned autoradiographs shown in Fig 3.7 and one other study.** The 90 kDa kinase doublets of BPM, IPM, BLDM and ILDM fractions were scanned and their respective densities measured for the concentration series of "In Gel" G4NTP: fixed ratio poly-$_L$-Lysine conjugate gels. The 10 μM poly-$_L$-Lysine only gel was used as the control and has been given the value of 0.0 for the purpose of this plot. Results are shown from two independent studies with SEM values used to generate the associated error bars.

Increasing G4NTP concentration within the gel by altering the conjugate ratio of G4NTP:poly-$_L$-Lysine showed enhanced band development of the 90 kDa kinase, most notably in the LDM-containing fractions but also in the PM fractions. There was enhancement of the 90 kDa bands above that seen in the control gel for the synaptosomal samples, although it appears that increasing the concentration of G4NTP above 5 μM did not increase the band density any further. This may be due to the fact that the G4NTP is

not the exact substrate for the GAD65 kinase and there may be a finite level of association of the G4NTP with this kinase.

The results with the PM and LDM fractions established that increasing the peptide concentration, within the conjugate, elevated $\gamma^{32}P$ incorporation into the 90 kDa bands and this could not be attributed to enhanced poly-$_L$-Lysine action, as may have been the case for the studies shown in Fig 3.6 and Fig 3.7. The results suggested that the enhancement in $\gamma^{32}P$ incorporation observed could be due to direct phosphorylation of the peptide itself, however there was still the possibility that the enhancement was due to increasing levels of kinase autophosphorylation.

3.4.6.3 Evidence of G4NTP phosphorylation by the 90 kDa kinase doublet.

To validate the peptide specificity of the identified 90 kDa kinase, a peptide conjugate was prepared containing a synthetic peptide corresponding to an area of the carboxyl terminal of GLUT4 (G4CTP), (see experimental methods 3.3.1.2). This conjugate was then incorporated into a 10% SDS-PAGE gel at the same concentration as for the G4NTP conjugate. Another conjugate was also prepared to determine if the Ser^{10} within the G4NTP was phosphorylated by the 90 kDa kinase. This conjugate contained the Phosphorylated N term GLUT4 peptide (G4pNTP), (see general methods 2.5.1), which was also incorporated into a 10% SDS-PAGE gel at the same concentration as for the G4NTP conjugate. Theoretically any band enhancement between the G4NTP and G4pNTP conjugate containing gels should be attributable to the incorporation of $\gamma^{32}P$ into the G4NTP, as the level of kinase autophosphorylation should remain constant. The results of these studies are given in Fig 3.10 with a quantified analysis of band enhancement of selected bands for the Control G4NTP and G4pNTP conjugate gels shown in Fig 3.11.

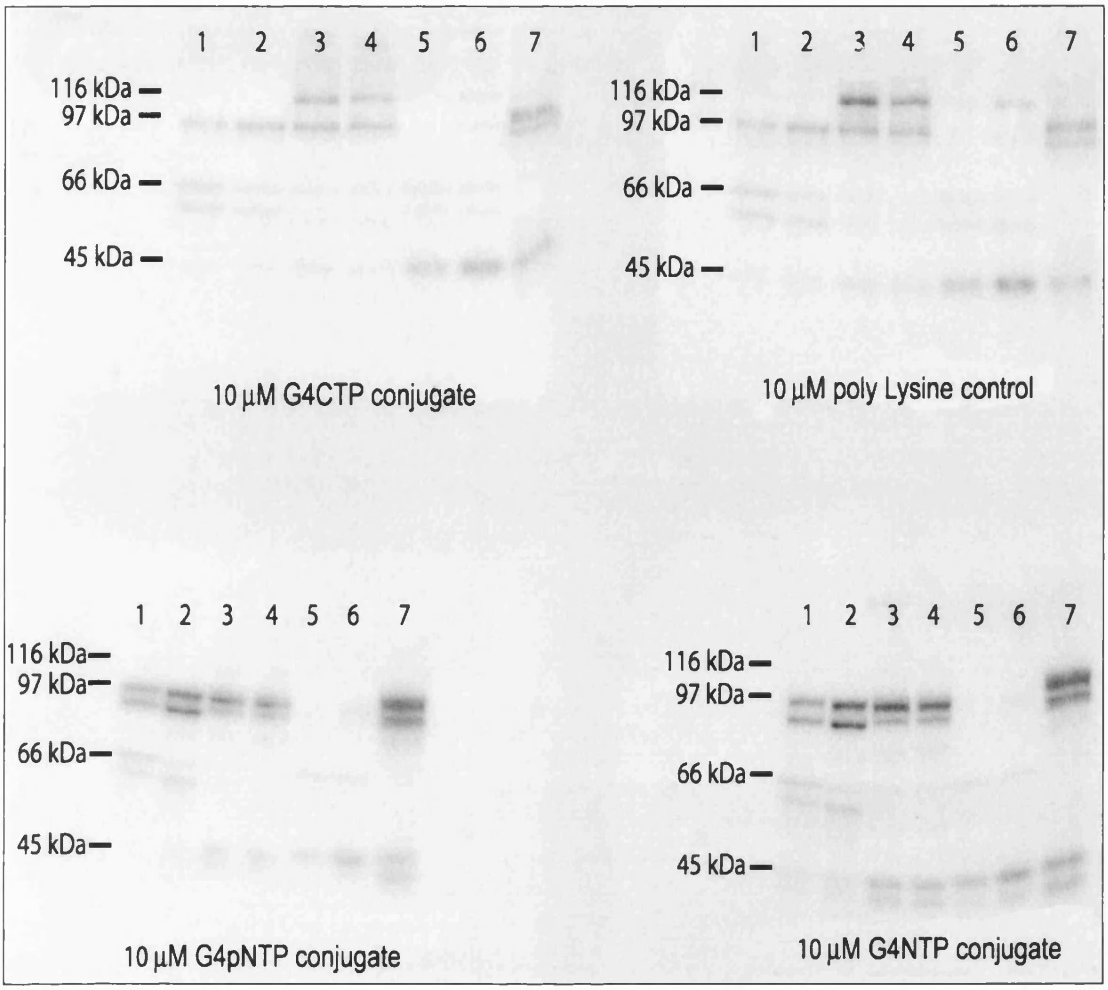

FIG 3.10: **Comparison of γ32P incorporation into the 90 kDa kinase doublet between G4NTP, G4CTP and G4pNTP conjugate containing "In Gel" assays suggests specific phosphorylation of the G4NTP by the kinase of interest.** 20 µg of protein was loaded per lane onto as series of 10% SDS-PAGE gels containing 10 µM G4NTP, G4CTP or G4pNTP conjugates. A control gel containing 10 µM poly-$_L$-Lysine only was also prepared. Lane 1: Basal PM; Lane 2: Insulin PM; Lane 3: Basal LDM; Lane 4: Insulin LDM; Lane 5: Basal Cytosol; Lane 6: Insulin Cytosol; Lane 7: Synaptosome preparation. The gels were processed as previously described (see 3.4.2), using 25 µCi [γ^{32}P] ATP per gel in each phosphorylation buffer. The image shown was scanned from a 1h-autoradiograph development of the treated gels. The gels are placed together to show that they are from the same autoradiograph and have been subjected to the same exposure. The G4CTP and control poly-$_L$-Lysine gels are representative of two independent studies.

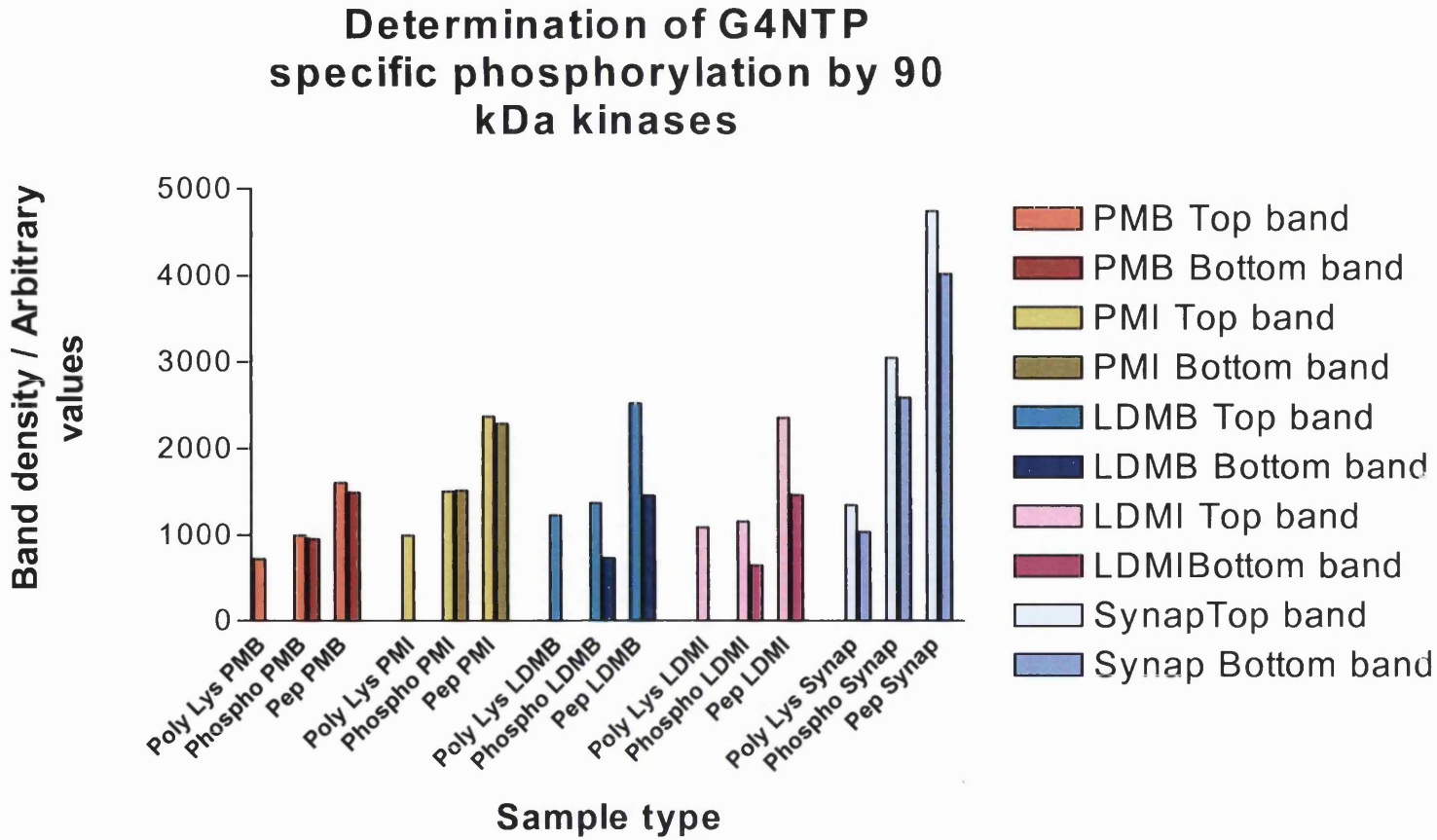

FIG 3.11: **Bar graph of densitromic values obtained from scans of the 90 kDa doublet bands from the studies shown in Fig 3.10 suggest specific phosphorylation of G4NTP by the kinase.** The densities of the top and bottom bands of the 90 kDa kinase bands were measured for all of the samples from the G4NTP conjugate, G4pNTP conjugate and poly Lysine control gels. The density values shown are arbitrary values obtained from the analysis program

There was no significant difference in the 90 kDa bands intensities between the poly-$_L$-Lysine control gel and the G4CTP conjugate. It was hoped there would be differential enhancement of bands that corresponded to the kinases thought to act on the G4CTP, like cAMP dependent kinase, using the G4CTP conjugated gel. The lack of any noticeable differences may be attributed to this kinase requiring different conditions for activation in the "In Gel" kinase assay, namely modified phosphorylation conditions requiring pre-incubation with cAMP and or $CaCl_2$, as found for detection of CaM-kinase II in MAP2 containing gels (Kameshita and Fujisawa, 1989). The results did highlight the specificity of the 90 kDa kinase for G4NTP and reduced the possibility that enhancements seen in relation to G4NTP conjugated gels were purely due to poly-$_L$-Lysine stimulation.

The densitromic scan results shown in Fig 3.11 indicated that there was increased incorporation of $\gamma^{32}P$ into the G4NTP conjugate containing gel compared with that observed in the G4pNTP conjugate containing gel. The observed increase in band density between the poly-$_L$-Lysine control gel and the G4pNTP conjugate containing gel should be attributed to enhanced autophosphorylation of the kinase by the presence of its specific peptide and not to phosphorylation of the peptide. However there was the possibility that some of the enhancement seen in the G4pNTP conjugate containing gels is due to Ser^{10} phosphorylation as a small proportion of the G4pNTP used for the conjugation may have contained non phosphorylated Ser^{10}. Also the conjugation process and subsequent treatments for the "In Gel" kinase assay may have removed a certain proportion of the phosphate from the G4pNTP, although this is unlikely as phosphorylated serine should be relatively resistant to dissociation.

3.5 Conclusions

The research conducted in this chapter identified a potential kinase that was stimulated in response to the presence of the GLUT4 N terminal peptide. The kinase appeared as a doublet of around 90 kDa, which was considered to represent two post-translational modified versions of the same kinase. The modification might be as a result of differing phosphorylation states of the protein, however further characterisation is required to confirm this. The kinase repeatedly displayed an increased $\gamma^{32}P$ incorporation in membrane associated adipocyte fractions and synaptosomes preparations when a G4NTP poly-$_L$-Lysine conjugate was immobilised in the running gel matrix. Poly-$_L$-Lysine appeared to specifically enhance the specific incorporation of $\gamma^{32}P$, possibly by providing a positively charged microenvironment that facilitated specific substrate recognition by the kinases. The kinase appeared to be unrelated to CKII, due to its inability to utilise GTP as a phosphate donor. The interaction between the kinase and the G4NTP appeared to be specific as no significant band enhancement was observed when other, non-related, peptide conjugates were used in the assay system. It also appeared that a proportion of the band enhancement might be attributed to phosphorylation of Ser^{10}, within the G4NTP, by the detected kinase.

The potential existence of a kinase that phosphorylates the N terminal of GLUT4 could provide an important link between signalling modulation and GLUT4 trafficking. Consequently identification of the kinase was of paramount importance to ascertain if it did indeed stimulate *in vivo* phosphorylation of GLUT4.

4 Further characterisation of the putative N-terminal GLUT4 kinase.

4.1 Introduction and experimental aims

The discovery of a 90-kDa kinase doublet, that appeared to phosphorylate the G4NTP, (G4NTP directed kinase) spurred future research into its identification and characterisation. Attempts to isolate the kinase were run in parallel with studies attempting to identify the localisation of the putative kinase and its potential physiological significance. The isolation studies and their outcomes are discussed in section 5 while this section will deal with the remaining characterisation and localisation studies.

James and colleagues had shown that a significant proportion of proteins found in the LDM fractions corresponded to cytoskeletal associated proteins or large protein complexes which spun down in these sample preparations (Clark *et al.*, 2000) (see Introduction 1.3.3). These complexes were distinguished from membrane proteins by their insolubility in the non- ionic detergent Triton X100 (TX100). However TX100 insolubility is also a characteristic of lipid rafts (see Introduction 1.4). Differentiation between lipid raft and cytoskeletal association of protein components within membrane fractions such as the PM and LDM can be achieved through a procedure called flotation analysis. The procedure works through the use of established density gradients, with cytoskeletal associated proteins pelleting at the bottom and lipid raft associated proteins equilibrating at a defined region within the density gradient.

These techniques were utilised in the study of the G4NTP directed kinase, to ascertain its association properties with the membrane fractions it was detected in. Potential problems associated with these techniques will also be discussed.

In association with the aforementioned techniques, antibodies were generated against the N terminal region of GLUT4 and a corresponding region in which Ser^{10} was phosphorylated, using the same peptides as used

for the identification of the 90 kDa kinase doublet. It was hoped that these antibodies would provide evidence for the *in vivo* phosphorylation of the N terminal of GLUT4 and also identify any differential localisation of the phosphorylated N terminal GLUT4 from its non-phosphorylated counterpart, which would help to predict functionality of the kinase.

4.2 Experimental methods

4.2.1 Membrane fraction treatments

The methods detailed here are an adaptation of a study performed by James and colleagues, (Clark *et al.*, 1998) to determine proteins' membrane association in PM fractions and also LDM fractions. Note that the centrifugal speeds used in the post treatment pelleting of LDM were higher than those used to obtain the LDM fractions and have been consequently designated as High Speed Pellets (HSP).

4.2.1.1 Plasma Membrane treatments

150 μg of basal and insulin treated PM fractions were resuspended ten times, using a 2 ml syringe with a 25 gauge needle, in one of the following solutions.

- 1 ml HESII buffer (see buffers 2.1.2), with Protease Inhibitors (PI) (see chemical reagents 2.1.1).
- 150 μl 60 mM Octylglucoside (OG) in HESII buffer with PI (Giving 1:1 protein:volume).
- 150 μl 1% (v/v) Triton X-100 (TX100) in HESII buffer with PI (giving 1:1 protein:volume).
- 1 ml 0.5 M NaCl in HESII buffer with PI
- 1 ml 1.0 M NaCl in HESII buffer with PI

Note that all the aforementioned solutions were prepared and chilled on ice for 30 min before their addition to the protein samples. The resuspended

samples were left on ice for a further hour. The OG and TX100 samples were topped up to 1 ml with the corresponding chilled before and then all samples were centrifuged at 37,000 rpm for 9 min at 4°C using a Beckman TL-100 benchtop ultracentrifuge at 4°C, with a TLA-100.3 fixed angle rotor. The supernatant was removed and either discarded or the protein precipitated for study by SDS-PAGE analysis (see 4.2.2). The pelleted material was resuspended in an appropriate volume of buffered solution or sample buffer for SDS-PAGE analysis.

4.2.1.2 LDM / HSP treatments

200 μg of basal and insulin-treated LDM fractions were resuspended ten times, using a 2 ml syringe with a 25 gauge needle, in one of the following solutions.

- 1 ml HESII buffer (see buffers 2.1.2), with Protease Inhibitors (PI) (see chemical reagents 2.1.1).
- 1 ml 60 mM Octylglucoside (OG) in HESII buffer with PI (Giving 1:1 protein:volume).
- 1 ml 1% (v/v) Triton X-100 (TX100) in HESII buffer with PI (giving 1:1 protein:volume).
- 1 ml 1.0 M NaCl in HESII buffer with PI

Note that all the aforementioned solutions were prepared and chilled on ice for 30 min before their addition to the protein samples. The resuspended samples were left on ice for a further hour. The samples were centrifuged at 70,000 rpm for 75 min at 4°C using a Beckman TL-100 benchtop ultracentrifuge at 4°C, with a TLA-100.3 fixed angle rotor. The supernatant was removed and either discarded or the protein precipitated for study by SDS-PAGE analysis (see 4.2.2). The pelleted material was resuspended in an appropriate volume of buffered solution or sample buffer for SDS-PAGE analysis.

4.2.2 Protein precipitation techniques

4.2.2.1 Chloroform/methanol precipitation

The description given here uses a fixed volume size but this was varied proportionally with different samples, depending on their total volumes. 150 µl of protein solution was placed in a 1.5 ml microfuge tube and to this 600 µl of methanol was added. The tube was then mixed by four inversions of the capped tube then centrifuged for 10 s in a bench top microcentrifuge at room temperature. 150 µl of chloroform was then added and the contents mixed thoroughly using a vortex mixer. The capped tube was then centrifuged for a further 10 s and then 450 µl of ddH_2O was added and the tube mixed well using the vortex mixer. The capped tube was then centrifuged for 10 s to separate the two liquid phases that formed upon addition of the water. The upper phase was carefully removed and discarded with a residual layer 1-3 mm deep left behind as most of the protein is to be found at the interface. 450 µl of methanol was added to the remaining solution and the solution mixed briefly by vortexing. The capped tube was then centrifuged for 4 min to allow pelleting of the precipitated protein that should appear as a visible white protein mass. The remaining solution was aspirated off and disposed as chlorinated solvent with the pellet then dried by incubation in a drying cupboard at 37°C for 20 min. The pellets were then dissolved in sample buffer for SDS-PAGE analysis or stated buffers for Isoelectric focussing (IEF) work (see Chapter 3).

4.2.2.2 Acetone precipitation

To one volume of protein sample five volumes of -20°C acetone was added and the mixture vortexed for 10 s. The mixture was then incubated at -20°C for 30 min. The samples were then centrifuged for 5 min at 10000g using a microcentrifuge-154. The supernatant was aspirated off and the pellet left to air dry at room temperature. The dried pellet was then dissolved in sample

buffer for SDS-PAGE analysis or stated buffers for Isoelectric focussing (IEF) work (see Chapter 3).

4.2.3 Isolation of lipid rafts using a sucrose gradient

The PM fractions were resuspended in 2 ml of Gradient Buffer (20 mM Tris, 150 mM NaCl, 1 mM EDTA (pH 7.4)), containing 1% Triton X 100, at 4°C. The samples were homogenised ten times using a syringe with a 23G needle and then incubated on ice for 30 min. While the samples were incubating a series of sucrose solutions were prepared in Gradient Buffer, 80%, 35% and 5% (w/v). The samples were mixed with 2 ml of ice cold 80% (w/v) sucrose solution to give a final sucrose concentration of 40% (w/v). Each solution was then dispensed into the bottom of a 12 ml tube for the SW41 rotor (Beckmann). This solution was overlaid with 4 ml of 35% (w/v) sucrose solution followed by 3.5 ml of a 5% (w/v) sucrose solution. The tubes were then balanced and centrifuged for 19 h at 38,000 rpm at 4°C using a Beckmann L-80 ultracentrifuge. The resulting gradients were examined in one of two ways.

1. The lipid raft fraction was recovered at the 35/5% sucrose density interface, and washed by centrifugation for 10 min at 15,000g, using the Beckman TL-100 benchtop ultracentrifuge, at 4°C with Gradient Buffer. The pellets were resuspended in an appropriate volume of Gradient buffer and protein concentrations determined by BCA protein assay (see Methods 2.4.1). The pellet at the bottom of the gradient was also resuspended and tested as described in later experimental results.
2. Twelve fractions of 1 ml were taken from the top to the bottom of the gradient with a thirteenth fraction generated from re-suspending the pellet at the bottom of the gradient in 1 ml of Gradient Buffer. Samples volumes were then taken from these fractions and analysed by western blot and "In Gel" kinase assay. In some instances the proteins were precipitated out of the samples (see 4.2.2) and resusupended in sample buffer for subsequent loading on to SDS-PAGE gels.

4.2.4 Immunocytochemistry on male Wister rats' adipocytes

Epididymal fat pads from male Wister rats (180-200 g) were used as the source of adipose cells. The procedure for adipocyte extraction and processing was the same as that detailed in Methods 2.2.1. The resulting suspension was whitish in appearance and the buffer clear. At this point the cells were pooled and buffer levels adjusted to obtain a 40% cytocrit. Half of the material was then stimulated with insulin as detailed in Methods 2.2.1. The basal and insulin treated suspensions were then fixed in 4% (v/v) formaldehyde, in PBS (pH 7.4), for 20 min at 37°C. The fixed cells were washed three times with PBS, then blocked and permeabilized in Blocking buffer (0.1% (w/v) saponin, 1% (w/v) BSA, and 3% (v/v) goat serum) for 45 min at room temperature. The cells were incubated with the appropriate antibody, diluted in a total volume of 500 μl of Blocking buffer, for 2 h at room temperature, with gentle rotation. The cells were washed four times in Washing buffer (PBS with 0.1% (w/v) saponin and 1% (w/v) BSA) to remove excess primary antibody. The cells were incubated in 250 μl total volume of Washing buffer containing 1:200 dilution of anti-rabbit FITC secondary antibody for 1 h at room temperature, with gentle rotation. The cells were washed four times with Washing buffer and then aliquoted onto glass slides. 50 μl of Vectashield mounting medium for fluorescence with DAPI was added to the cells and mixed gently. A coverslip was then placed over the mixture and sealed down to the glass slide using clear nail varnish. Detection of antibody localised fluorescence was visualised using the X63 oil lens of the Zeiss Axiovert LSM510 Laser Scanning Microscope.

4.3 Results and Discussion

4.3.1 Determination of the membrane association properties of the G4NTP directed kinase in the LDM

The studies presented in Chapter 1 highlighted that the G4NTP directed kinase appeared to be resident in both the PM and LDM membrane fractions, with no noticeable detection in cytosolic samples. The highest level of detection for the kinase appeared to be in the LDM samples and was consequently the first choice for further investigation. To further define the nature of the interaction of G4NTP directed kinase with the LDM the effects of high ionic strength and two different detergents, on the solubility of the protein, were examined (see Methods 4.2.1.2). TX100 is a non-ionic detergent that can solublise a range of integral membrane proteins. This detergent does not solublise cytoskeletal associated proteins, or most lipid raft structures, when used at 4°C. β-octylglucoside is also a non-ionic detergent, however it is known to solublise a range of caveolae and lipid raft associated proteins (Waheed *et al.*, 2001; Clark *et al.*, 1998; Brown and Rose, 1992). In contrast to both detergents the high ionic environment provided by 1 M NaCl should not affect lipid raft or integral membrane proteins but will dissociate cytoskeletal-associated proteins and proteins bound ionically to membrane fractions. The results shown in Fig 4.1 and Fig 4.2 show four proteins p85 (PI3K), IR β subunit, IRS1 and GLUT4, after the various treatments mentioned. Their solubility profiles were compared to those observed for the G4NTP directed kinase to identify any similarities in binding characteristics and form the foundation for directed future research.

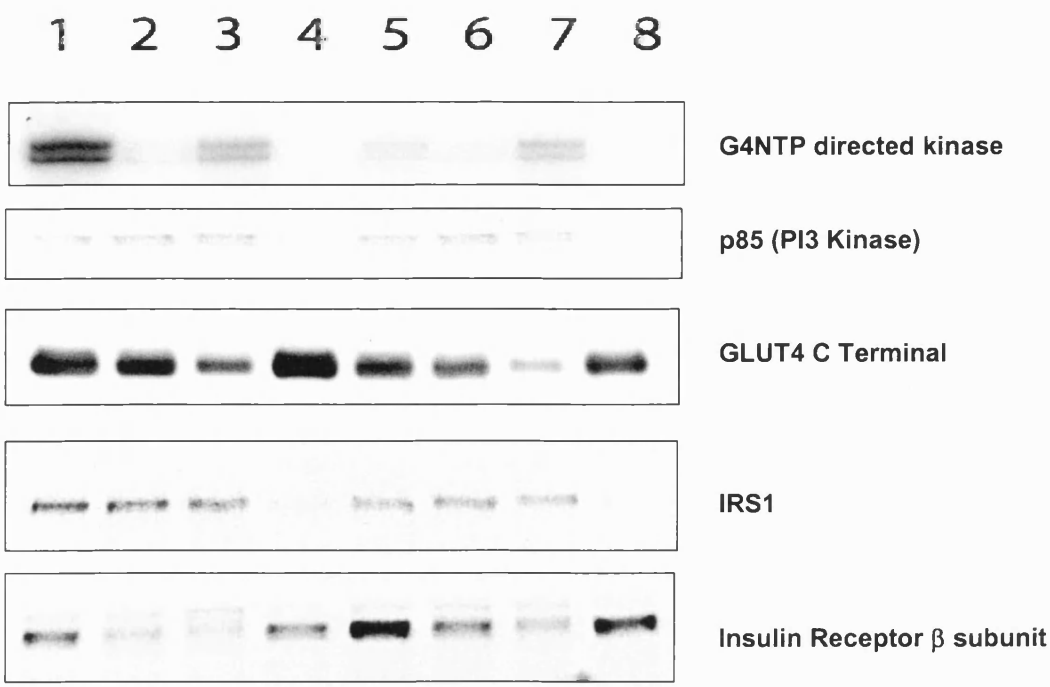

FIG 4.1: **Pre-treatment of LDM/HSP samples differentially modulates their recovery as analysed through western blot analysis and "In Gel" kinase assay**. 200 μg of BLDM and ILDM samples were used for each condition. Following sample treatments the resulting protein pellets were resuspended in 100 μl of sample buffer that was then divided into four 25 μl aliquots. Two aliquots were loaded onto two 10% SDS PAGE gels for western blotting. The remaining two aliquots were loaded onto a 10% SDS-PAGE control gel, containing poly lysine polymerised within the gel, and another gel containing 10 μM G4NTP, conjugated to poly Lysine, polymerised within the gel matrix. The "In Gel" kinase assay result shown was obtained from the G4NTP containing gel. All other results are from western blot analysis using antibodies against the proteins detailed. Lane 1: BHSP Control (37.5 μg loading); Lane 2: BHSP 60 mM OG treated protein pellet; Lane 3: BHSP 1% (v/v) TX100 treated protein pellet; Lane 4: BHSP 1M NaCl treated protein pellet; Lane 5:IHSP Control (37.5 μg loading); Lane 6: IHSP 60 mM OG treated protein pellet; Lane 7: IHSP 1% (v/v) TX100 treated protein pellet; Lane 8: IHSP 1M NaCl treated protein pellet. The results shown are representative of two separate studies.

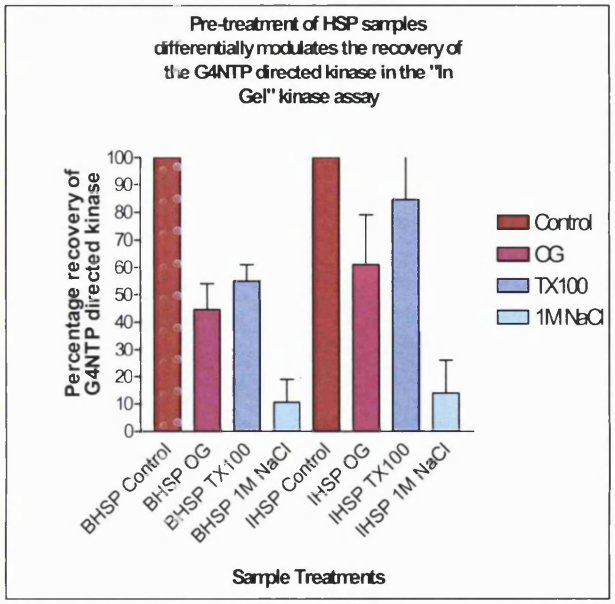

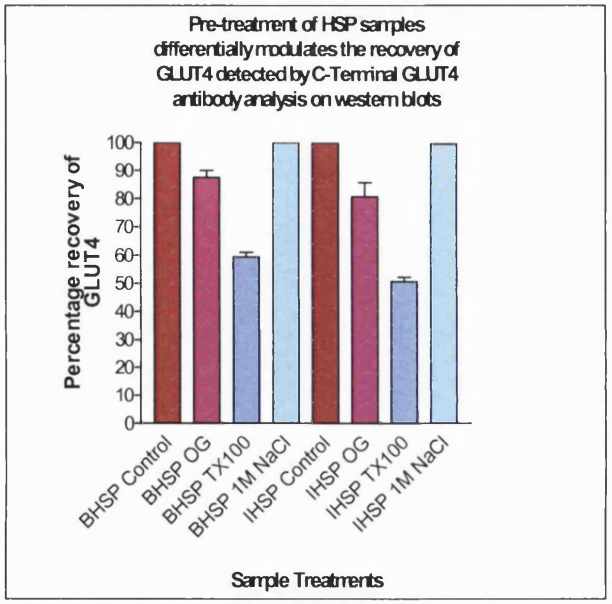

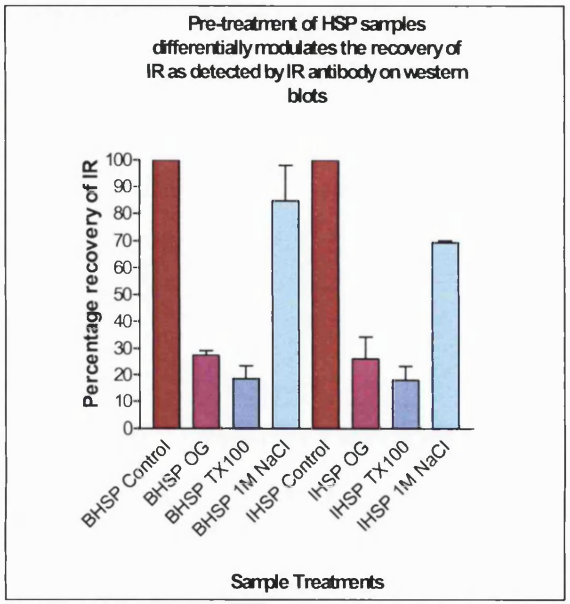

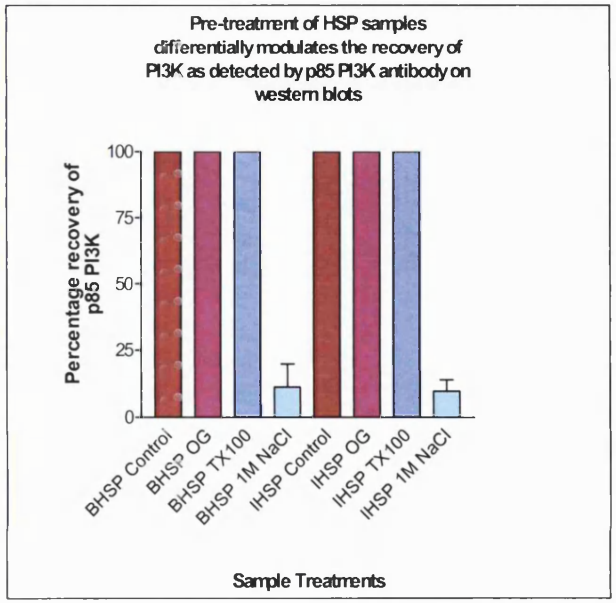

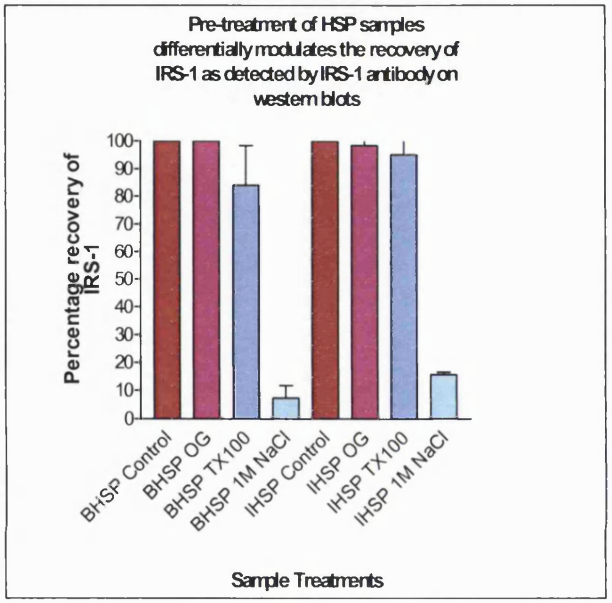

FIG 4.2: **Graphical representation of the western blot and "In Gel" kinase assays showing the differential recovery of HSP proteins following their pre-treatment with various agents**. Results shown are calculated from two separate experiments as a percentage recovery of the PM controls, which have been denoted as 100% recovery. All BHSP treatments are calculated from the BHSP control whilst all IHSP treatments are calculated from the IHSP control. Please note that these plots do not show the differential levels of protein detected between basal and insulin samples that are seen on the corresponding FIG 4.1.

Analysis of the results obtained from the solubilisation studies showed that both IRS-1 and p85 (PI3K) are only significantly solubilised when exposed to the high ionic environment of 1 M NaCl. These results are in agreement with those of James and colleagues (Clark *et al.*, 1998) who proposed that both of these proteins may be ionically associated with cytoskeletal elements, which co-ordinate their movement and functionality within the cell (see Introduction 1.3.3). In contrast the solubility of the IR was not significantly enhanced by exposure to 1 M NaCl in basal HSP samples. There was a more noticeable reduction in the recovery of IHSP IR with 1 M NaCl. The reasons for this are not instantly apparent, as the IR is an integral membrane protein and should not be influenced by an ionic environment. Further to this end the IR was highly solubilised by incubation with both non-ionic detergents, with between 70-80% decreases in the recovery of IR under these treatments. The results with the IR also showed an overall increase in the relative levels of IR in the HSP fraction after insulin stimulation. These results may support the concept of IR internalisation, upon insulin stimulation, to aid in the modulation of downstream signalling events (see Introduction 1.3.2.2), however further investigation would be required to confirm these findings.

The solubility of GLUT4 was not significantly affected by 1 M NaCl treatments, as would be expected for this transmembrane protein. Interestingly, unlike the IR, GLUT4 did not appear to be as extensively solubilised by Octylglucoside treatment. Indeed even the significant solubilisation of GLUT4 seen with TX100 treatment still resulted in the recovery of around 50% of the protein. This result may be a consequence of insufficient treatment incubation times or the possible protection of GLUT4, in the HSP fraction, through association with other protein components such as large cytoskeletal elements or lipid rafts resistant to both detergents. A possible future experiment to test the cytoskeletal theory would involve incubation with TX100 and 1 M NaCl in conjunction with each other to see if this significantly reduced the recovery of GLUT4.

The results obtained from the "In Gel" kinase assay for the G4NTP directed kinase were intriguing. The highest degree of solubilisation appeared to occur when the HSP samples were exposed to 1 M NaCl, with around an

80% decrease in recovery of the enzyme, as detected by the assay. Initially this would suggest that the G4NTP directed kinase behaves in a similar manner to the proteins IRS-1 and PI3K and may be associated to cytoskeletal elements, which may act as a scaffold from which GLUT4 may become juxtaposed to the kinase and potentially phosphorylated. However the kinase also appears to be solubilised significantly in both BHSP and IHSP fractions by β-octylglucoside, suggesting a secondary association with possible lipid raft structures. The effect of β-octylglucoside was diminished in IHSP samples suggesting that there may be an alteration in kinase binding specificity in the insulin stimulated state, with increased ionic interactions with intracellular structures or membranes.

Although compelling these results must be viewed with some caution as, unlike the western blot data, the results obtained for the G4NTP directed kinase are influenced by not only the recovery of the kinase protein but also the recovery of active kinase. Renaturation of the kinase in the gel is essential for the functionality of the "In Gel" kinase assay. Consequently any effect of the treatments upon the degree of renaturation of the kinase could alter the results significantly. This would seem unlikely for the detergent treatments as all the samples are exposed to SDS detergent in the sample buffer, before gel loading, which should compete off the other detergents. Also the effects of SDS on protein renaturation appear to be negligible from the studies discussed in Chapter 1. The 1 M NaCl treatment may modulate the complete renaturation of the kinase but this would also seem unlikely, as this environment is relatively mild and should not permanently alter charges on kinase protein residues that would adversely affect correct protein refolding. Consequently the high degree of G4NTP directed kinase solubilisation was considered to outweigh the potential reduction in active kinase recovery, with 1 M NaCl treatments utilised for further isolation procedures (See Chapter 3).

Further evidence that solubilisation of the G4NTP directed kinase was relatively resistant to TX100 treatment at 4°C and that detergent treatments did not adversely affect the renaturation of the kinase can be seen in Fig 4.3.

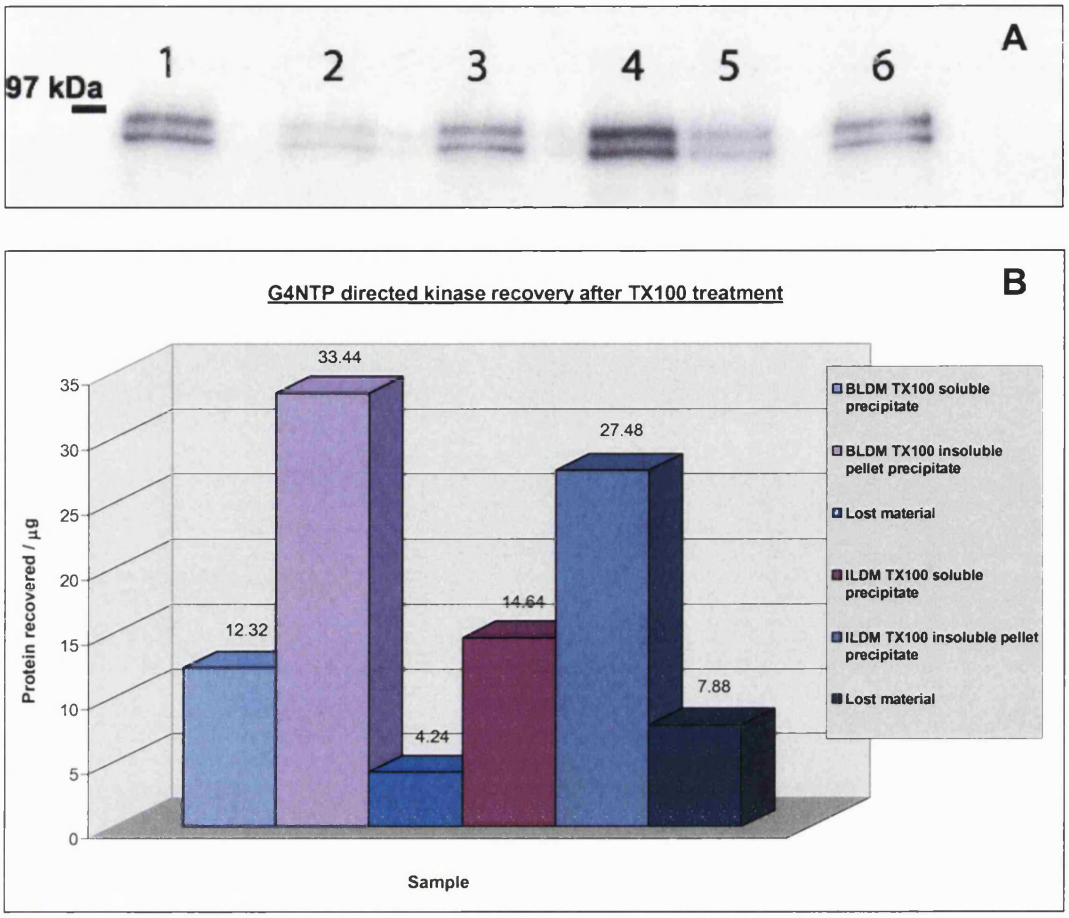

FIG 4.11: **LDM localised G4NTP directed kinase appears to predominantly partition in the TX100 insoluble pellet.** 100 µg BLDM and ILDM samples were treated with ice cold 1% TX100 for 30 min and then the insoluble protein pelleted. The soluble protein fractions were precipitated using the chloroform/methanol technique. The insoluble protein pellet and the precipitated soluble proteins were resuspended in sample buffer and loaded onto 10 µM G4NTP conjugate containing 10% SDS PAGE gels and a control gel that were then subjected to "In Gel" kinase assays. The G4NTP gel is shown in (A). Lane 1: 40 µg BLDM control; Lane 2: BLDM soluble precipitate; Lane 3: BLDM insoluble pellet; Lane 4: 40 µg ILDM control; Lane 5: ILDM soluble precipitate; Lane 6: ILDM insoluble pellet. The autoradiograph was densitromicaly scanned and the relative protein contents for each fraction calculated with respect to the respective LDM controls. The plot shown in (B) shows these calculated values and also highlights the relative amount of G4NTP directed kinase lost in the procedure.

The results shown in Fig 4.3 show that between 5-10% of the G4NTP directed kinase was lost in the solubilisation and subsequent chloroform/methanol extraction procedures (see methods 4.2.2.1). These results indicate that neither treatment significantly affected the ability to recover kinase activity, as the losses incurred were reasonable with regards to the losses expected with sample transfer using these techniques. Also the results showed that the majority of the kinase remained insoluble, with a ratio of roughly two parts insoluble to one part soluble G4NTP directed kinase detected in the BLDM sample.

4.3.2 Determination of the membrane association properties of the G4NTP directed kinase in the PM

Although the levels of the G4NTP directed kinase were not as high as detected in the LDM fractions there was still significant detection of the kinase in the PM fractions from both basal and insulin stimulated adipocytes. With this in mind a similar initial screening procedure was adopted to that used for analysis of the LDM/HSP fractions. Three proteins were used as solubility determinants for the PM tests, the IR β subunit, GLUT4 and Caveolin1. A suitable protein that would be removed from the PM under high ionic strength could not be studied in these tests, as a suitable antibody was not available.

The results of the solubilisation studies for the three reference proteins along with the findings for the PM associated G4NTP directed kinase are shown in Fig 4.4, with a graphical representation of these findings displayed in Fig 4.5.

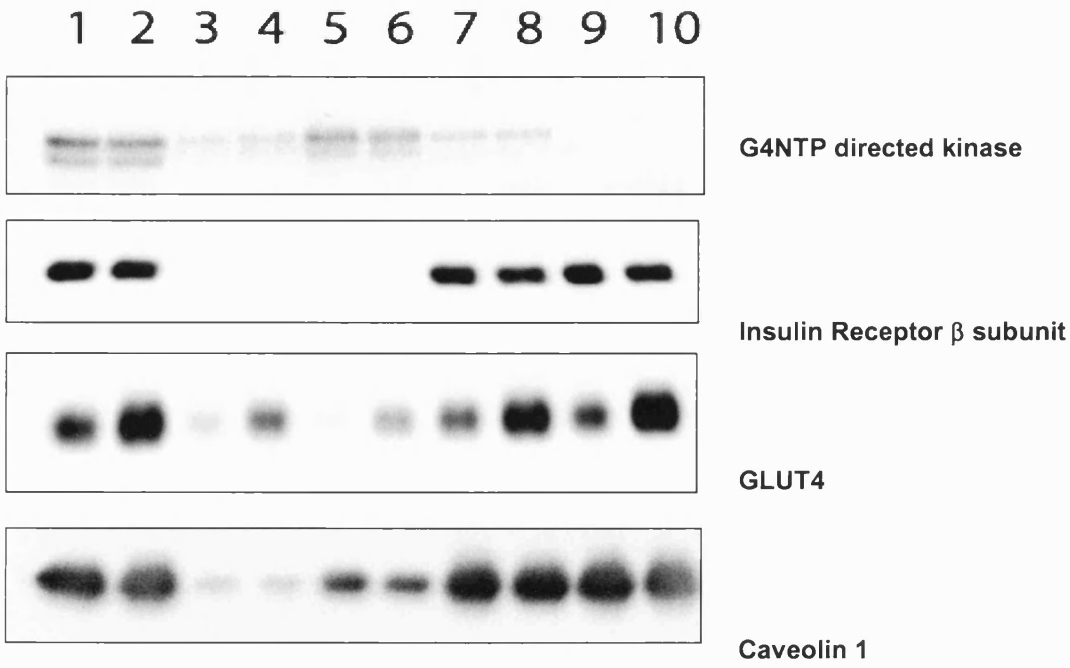

FIG 4.4: **Pre-treatment of PM samples differentially modulates their recovery as analysed through western blot analysis and "In Gel" kinase assay.** 150 μg of BPM and IPM samples was used for each condition. Following sample treatments the resulting protein pellets were resuspended in 100 μl of sample buffer that was then divided into four 25 μl aliquots. Two aliquots were loaded onto two 10% SDS PAGE gels for western blotting. The remaining two aliquots were loaded onto a 10% SDS-PAGE control gel, containing poly-$_L$-lysine polymerised within the gel, and another gel containing 10 μM G4NTP, conjugated to poly-$_L$-Lysine that was polymerised within the gel matrix. The "In Gel" kinase assay result shown was obtained from the G4NTP containing gel. All other results are from western blot analysis using antibodies against the proteins detailed. Lane 1: BPM Control (37.5 μg loading); Lane 2: IPM Control (37.5 μg loading); Lane 3: BPM 60 mM OG treated protein pellet; Lane 4: IPM 60 mM OG treated protein pellet; Lane 5: BPM 1% (v/v) TX100 treated protein pellet; Lane 6: IPM 1% (v/v) TX100 treated protein pellet; Lane 7: BPM 0.5 M NaCl treated protein pellet; Lane 8: IPM 0.5 M NaCl treated protein pellet; Lane 9: BPM 1 M NaCl treated protein pellet; Lane 10: IPM 1 M NaCl treated protein pellet. The results shown are representative of two separate studies.

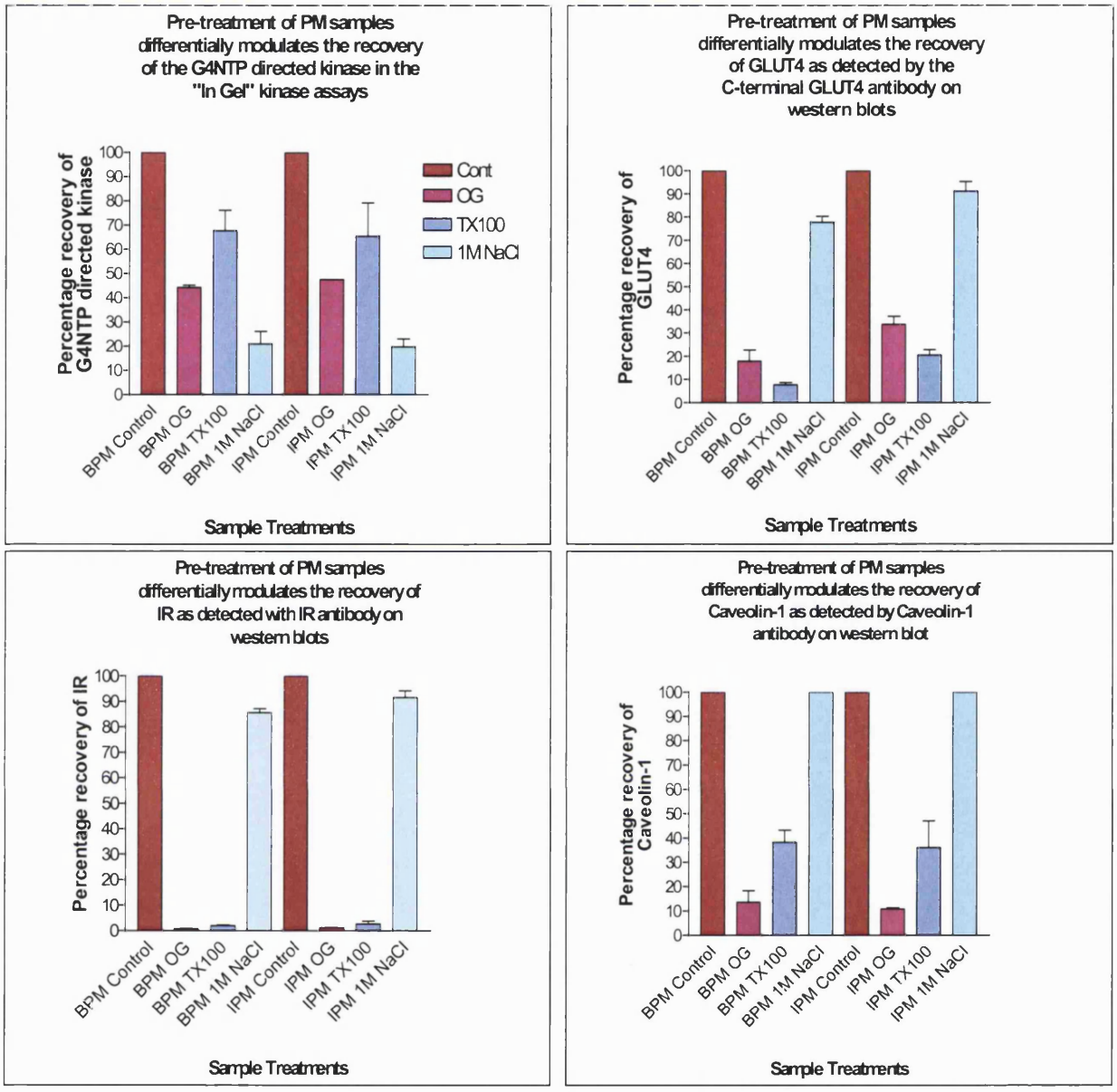

FIG 4.5: **Graphical representation of the western blot and "In Gel" kinase assays showing the differential recovery of PM proteins following their pre-treatment with various agents.** Results shown are calculated from two separate experiments as a percentage recovery of the PM controls, which have been denoted as 100% recovery. All BPM treatments are calculated from the BPM control whilst all IPM treatments are calculated from the IPM control. Please note that these plots do not show the differential levels of protein detected between basal and insulin samples that are seen on the corresponding FIG 4.4.

The effectiveness of the two non-ionic detergents in the solubilisation of the integral membrane proteins in the PM fractions were more clearly highlighted in this series of experiments than witnessed in the LDM/HSP assays. Indeed the western blot results from the detection of the β subunit of the IR showed almost complete solubilisation of the protein by both OG and TX100, with little effect under high ionic environment exposure.

Analysis of the GLUT4 solubility profile also showed that the majority of the protein was solubilised under OG treatment, and this was further improved under TX100 incubation at 4°C. Analysis of the results for GLUT4, after normalisation against control fractions (see Fig 4.5), highlighted that GLUT4 appeared to be around 10% more resistant to the effects of detergent solubilisation in the IPM fractions over that seen in the BPM. This could possibly represent protein association modulation in a small population of GLUT4 rendering them insoluble to OG and TX100, however further studies would be required to clarify this speculation.

The results for Caveolin 1 showed no effects of high ionic environment on protein solubilisation and around 60% solubilisation with TX100 at 4°C. Interestingly the level of Caveolin 1 solubility was 85-90% when the OG was used in the treatment procedure. These results concurred with accepted findings of a population of Caveolin-1, in lipid raft structures (Caveolin), that were resistant to TX100 but would solublise in OG (Brown and Rose, 1992; Schlegel and Lisanti, 2001) (see Introduction 1.4.3).

The results for the "In gel" assay detected solubilisation of the G4NTP directed kinase were similar to those observed in the HSP solubilisation studies. The kinase again appeared to be highly solubilised when exposed to a high ionic environment (approximately 80% solubilisation) suggesting a high degree of ionic association with the PM. Also the G4NTP directed kinase was preferentially solubilised by OG over TX100 with around 55-50% solubilisation using OG compared with the 30% solubilisation seen with TX100. Interestingly there appeared to be no significant differences in kinase solubility between basal and insulin stimulated PM fractions unlike that seen in the HSP fractions. These results could be interpreted by a model in which the G4NTP directed kinase is permanently associated either

directly, or through some form of underlying scaffold, to the PM that is juxtaposed to dynamic lipid raft structures. At any one time there may be a population of G4NTP directed kinase associated with raft structures that may serve as assembly platforms for activated signalling complexes. Under this model insulin would not increase the proportion of the G4NTP directed kinase associated with lipid rafts but may modulate the *in vivo* activity of the kinase towards GLUT4, controlling the degree of N terminal GLUT4 phosphorylation. Interestingly certain laboratories have shown that the raft/microdomain environment maintains the Src kinases Lck and Fyn in a higher state of activation (Hoessli *et al.*, 2000). The authors suggested that the raft membrane environment provides optimal conditions for the catalytic activity of kinases and their modular activity. Although purely speculation, maybe the structured matrix environment provided for the renatured kinase in the "In Gel" kinase assay system could, in part, mimic the stabilised environment produced by the lipid rafts. Also the close proximity of the G4NTP peptide to the kinase may be similar to the situation encountered with recruitment of proteins to their respective kinases in the lipid raft model. This may help to explain why the "In Gel" kinase assay detects the G4NTP directed kinase, whereas many conventional *in vitro* phosphorylation assays have failed to detect any significant phosphorylation of the N terminal of GLUT4. Interestingly it appears that the GAD65 directed kinase is permanently membrane associated and attains optimal functionality only when a stable protein complex has formed with cysteine string protein (CSP), heat shock complex (HSC70) and GAD65 (Hsu *et al.*, 2000). Further studies are required to confirm these ideas and the model is further complicated with later findings detailed in Chapter 3.

4.3.2.1 Further investigation of G4NTP directed kinase association with lipid rafts: Initial sucrose density gradient analysis.

Potential associations between the G4NTP directed kinase and lipid raft structures were investigated further through the utilisation of density gradient flotation analysis (see methods 4.2.3 for sucrose density gradients and 4.2.4 for Optiprep gradients). The first analysis of this type was based on the sucrose density gradient procedure with the 35/5% sucrose gradient interface taken to contain the TX100 insoluble lipid raft structures. For the "In Gel" kinase assay other samples were also taken from the completed separation including the insoluble pellet at the bottom of the gradient; a sample of the soluble layer directly above the pellet; and a soluble fraction from the top of the gradient. These samples were taken to give a rough idea of the distribution of the kinase, within the gradient, and were not for quantitative purposes. A general quantification of the lipid raft fraction was possible as this was pelleted and resuspended in a fixed volume, which was then divided into defined sample sizes. This allowed an approximation of protein equivalency to be established that could then be compared with the control samples to calculate a relative protein recovery estimation. The western blot analysis focussed on the lipid raft fractions only, with detection of GLUT4 and syntaxin 4 alongside a lipid raft/caveloae marker Caveolin-1. The results of the western blot and "In Gel" kinase assay analysis derived from the sucrose density gradient flotation procedure are shown in Fig 4.6 complete with a graphical representation of the calculations of relative protein recovery.

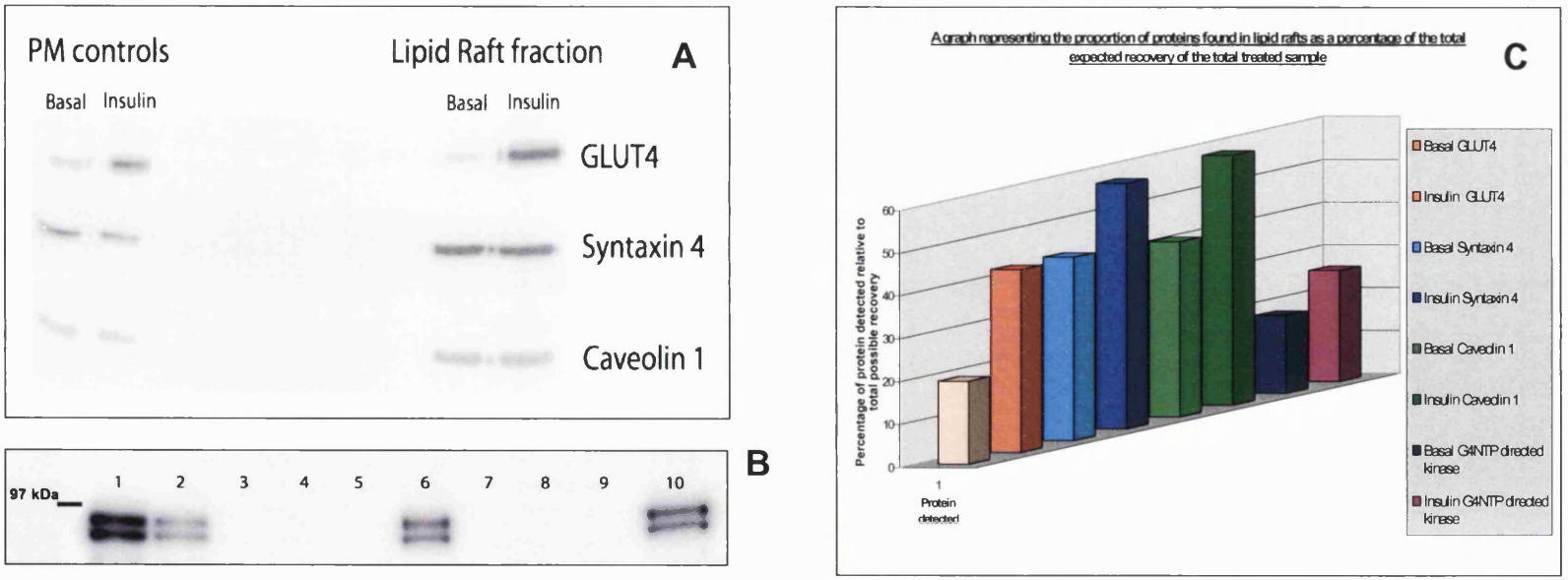

FIG 4.6: **Initial sucrose denisty gradient lipid raft flotation assays indicated that a significant proportion of the G4NTP directed kinase is localised to potential lipid raft structures**. BPM and IPM samples were subjected to sucrose density gradient lipid raft flotation procedures, with resultant TX100 insoluble fractions collected at the 35/5 % sucrose gradient interface and pelleted. The pellets were resuspended in sample buffer, with 48 μg total protein equivalents loaded for SDS PAGE and western blot analysis **(A)**. 10 μg BPM and IPM loading controls were used to calculate the amount of the various proteins detected by western blot, after densitronomy band analysis. The protein levels were then represented as a percentage of the total protein equivalent estimated for that fraction, with the results plotted **(C)**. In addition the following samples were loaded onto 10 μM G4NTP peptide conjugate containing SDS PAGE gels for "In Gel" kinase assay analysis **(B)**. Lane 1: 20 μg BPM control; Lane 2: 8 μg Na Cholate pooled sample test; Lane 3: BPM gradient bottom insoluble pellet 40μl; Lane 4: BPM soluble fraction bottom 40 μl; Lane 5 BPM soluble fraction top 40 μl. Lanes 6 Lipid raft derived fraction 60 μg protein equvalent; Lanes 7-10 are the same as for lanes 3-6 but with IPM derived gradient frations. The Western blot data is represenative of two separate studies.

The results provided some interesting initial conclusions regarding the lipid raft isolation technique. The graphical plot highlighted that the percentage of protein in the lipid raft fractions, calculated out of the total protein equivalent recovery, appeared to increase in the insulin stimulated PM fractions over that calculated for the Basal PM fractions, for all detected proteins. The amount of GLUT4 and Syntaxin 4, in the lipid rafts, appeared higher than expected highlighting that the percentages shown should only be viewed as an approximation. The relative increased detection of GLUT4 in the IPM suggested that these results purely reflected the increased levels of GLUT4, in the insulin stimulated plasma membrane. However Listanti and colleagues provided experimental data showing a significant increase in the amount of GLUT4 associated with caveolin-rich membrane domains, along with an increase in the amount of caveolin associated with the plasma membrane, in insulin stimulated 3T3 L1 adipocytes (Scherer *et al.*, 1994). These studies are not supported by Ramm and colleagues who used a cryo-sectioning technique in combination with quantitative immunoelectron microscopy to study GLUT4 compartments in isolated rat white adipose cells. They concluded that GLUT4 molecules were not randomly distributed on the plasma membrane, but neither were they enriched in caveolae (Malide *et al.*, 2000). Clearly there is some controversy surrounding this area and although the results presented sided with Lisanti and colleagues the fractions that were isolated may not have been 100% bona fide lipid rafts. Immunoelectron microscopy is currently the preferred method for validating protein localisation within lipid rafts, which was beyond the scope of this report, meaning that definitive conclusions can not be drawn from this study, however further investigation may be warranted.

The results from the "In Gel" kinase assay for the detection of the G4NTP directed kinase showed that a significant proportion of the kinase was found in the lipid raft fractions (18% in BPM and 26% in IPM). As discussed before these values were only an approximation and the actual values may be lower than those quoted.

The results did not identify any G4NTP directed kinase in any of the other fractions tested, even in the resuspended insoluble gradient pellet. This

meant that a large proportion of the kinase remained unaccounted for, using this methodology (around 80%). However the soluble samples taken for analysis were small (40 μl) compared to the total available volume throughout the entire gradient (12 ml). It is conceivable that if the G4NTP directed kinase equilibrated over a range of the gradient then the amount used may have been too small for detection of the kinase using the "In Gel" kinase assay.

Consequently although this initial test identified significant levels of the kinase in potential lipid raft structures only a complete analysis of the whole gradient would provide tangible results with respect to the distribution of the G4NTP directed kinase.

It is worth pointing out that the sample in lane 2 on Fig 4.6 (B) represents a Na Cholate solubilised sample of G4NTP directed kinase. This form of solubilisation will be dealt with further in Chapter 3 but for the purposes of this experiment it was used as a second loading control. The sample's protein level was determined by BCA protein assay to be 8 μg and this was then loaded onto the gel for subsequent analysis. By comparing the density of the G4NTP directed kinase bands, found for this sample, with the BPM loading control, the protein equivalent level was determined to be 8.38 μg. This validated the calculation methodology and increased confidence in the linearity of the assay detection range.

4.3.2.2 Further investigation of G4NTP directed kinase association with lipid rafts: Complete sucrose density gradient analysis.

The sucrose density flotation gradient method was repeated, but this time the entire final gradients were analysed, to give an overall representation of the varying distribution of the analysed proteins, which included the G4NTP directed kinase (see methods 4.2.3). The western blot analysis of GLUT4, IR β subunit, Syntaxin 4 and Caveolin-1 distribution along with the "In Gel" kinase assay results for the G4NTP directed kinase are shown in Fig 4.7 with a graphical representation of the analysis shown in Fig 4.8.

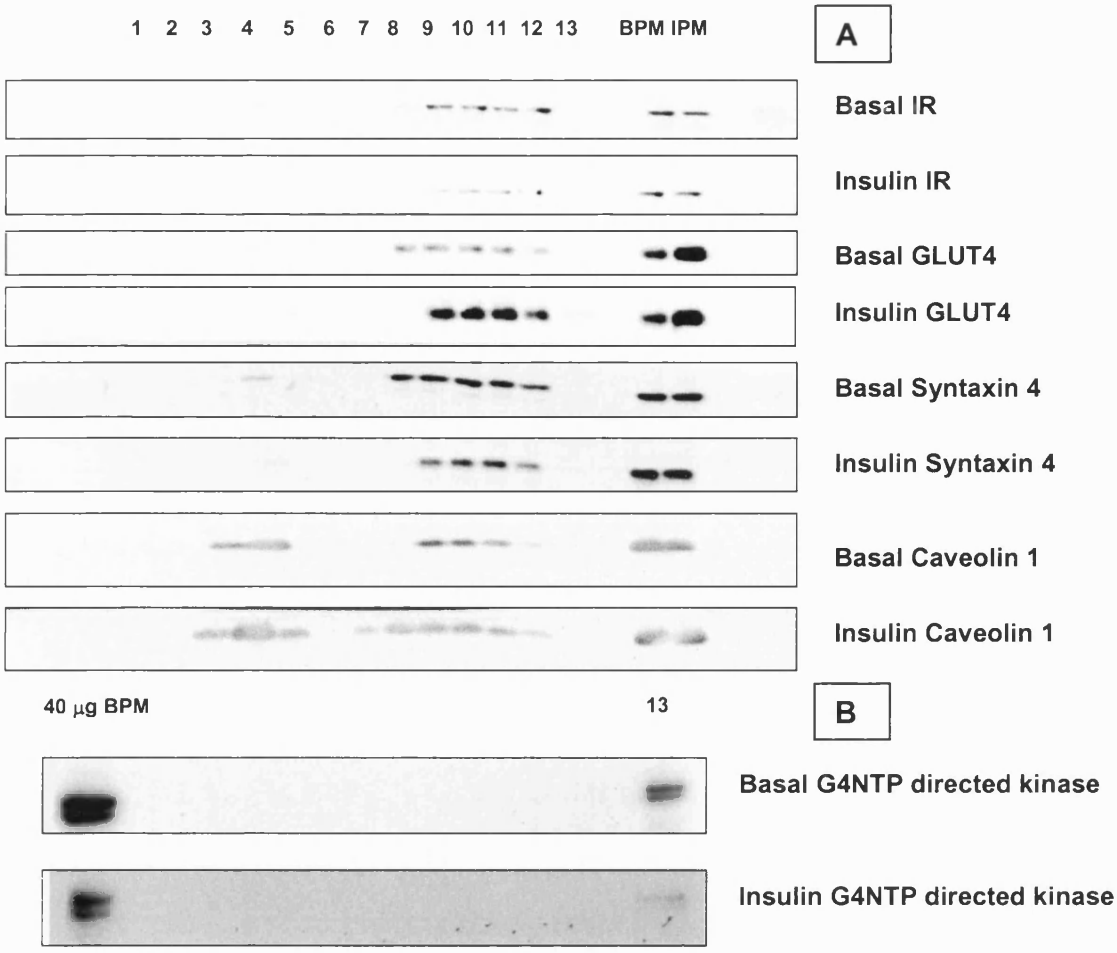

FIG 4.7: **PM proteins differentially disperse into two distinct phases, within the established sucrose density gradient, one corresponding to fully solubilised protein samples and the other representing a potential lipid raft phase, with higher buoyant density**. 300 μg BPM and IPM samples were subjected to sucrose density gradient separation, in the presence of 1% (v/v) TX100, for 19 hours at 38,000 rpm at 4°C using a Beckman L-80 ultracentrifuge. Fractions 1-12 represent the 1 ml fractions collected from the top of the column down to the bottom, that were subsequently subjected to acetone precipitation. The resultant pellets were resusupended in 150 μl of sample buffer + DTT. 50 μl aliquots (100 μg protein equivalent) were loaded per lane for SDS PAGE and western blot analysis (A). 20 μl samples (40 μg protein equivalent) were loaded per lane in gels containing 10 μM G4NTP, conjugated to poly-L-Lysine, for "In Gel" kinase assays, to detect the G4NTP directed kinase. 20 μg PM controls were used in A and 40 μg BPM control was used in B.

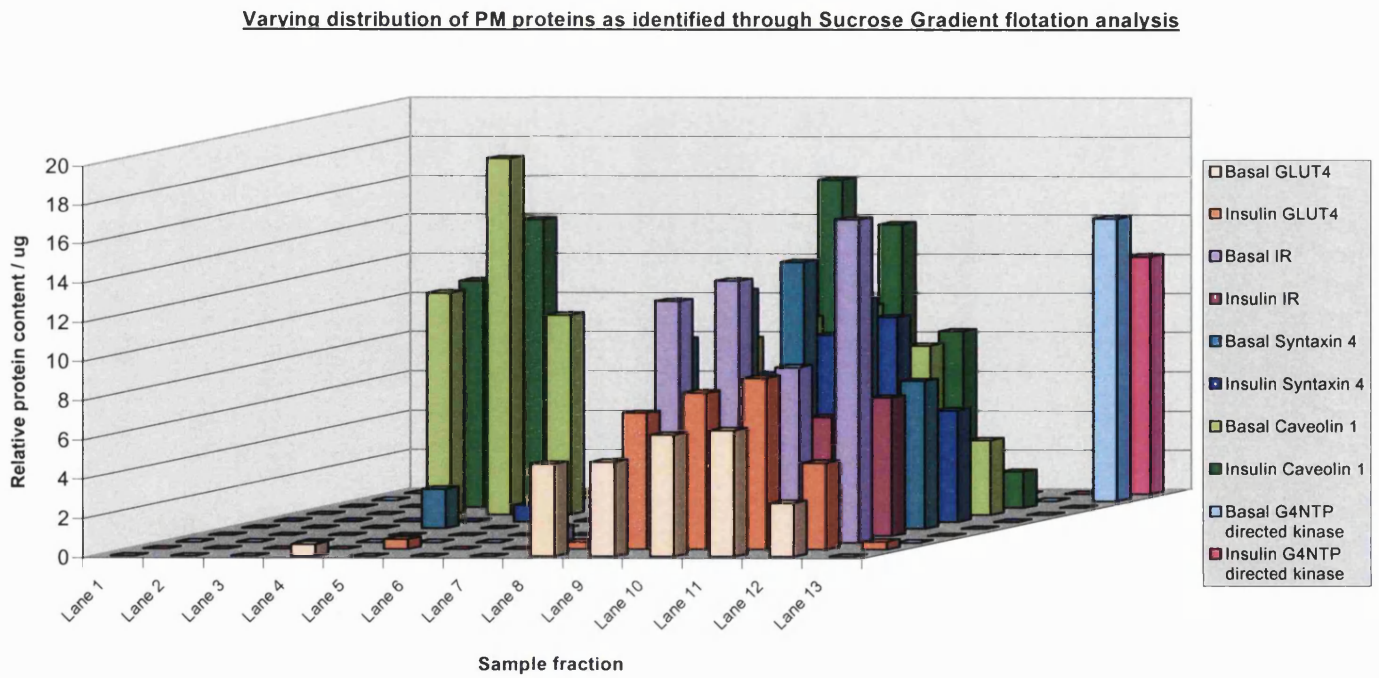

FIG 4.8: PM proteins differentially disperse into two distinct phases, within the established sucrose density gradient, one corresponding to fully solubilised protein samples and the other representing a potential lipid raft phase with higher buoyant density. The plot was produced from the data presented in Fig 4.7 with integrated optical densities converted into relative protein content values. These values were calculated in relation to the 20 μg BPM or IPM control samples run for each western blot with a potential 100 μg equivalence of protein distributed over all 13 fractions. The G4NTP directed kinase values were calculated in relation to the 40 μg BPM control used for the "In Gel" kinase assays with a potential 40 μg equivalence of protein distributed over all 13 fractions.

The results highlighted that proteins appeared to differentially disperse into two distinct phases within the established sucrose density gradient. One phase represented the TX100 solubilised proteins, which were located between fractions 8-12 near the bottom of the gradient. The other phase fell between fractions 3-5, corresponding to the 5/35% interface in the gradient, with the higher buoyant density of these proteins considered to result from their association with lipid raft components.

A significant population of Caveolin 1 appeared to equilibrate in the lipid raft phase of the gradient (~40%). These findings were also approximately the same as identified in the initial gradient study (see Fig 4.6 C) and in agreement with this protein being an integral component of certain lipid raft/caveolae microdomains (see introduction 1.4.3). Although a small population of GLUT4 and Syntaxin 4 were identified in the lipid raft phase this study did not support the initial findings shown in Fig 4.6 C and the significance of these proteins associating with lipid rafts could be called into question.

Intriguingly the G4NTP directed kinase was only detected in fraction 13, derived from the insoluble protein pellet at the bottom of the gradient. This result confirmed initial solubility findings for the PM derived kinase (see Fig 4.4 and 4.5) which suggested that a significant population of the kinase was ionically associated with the PM. However a population of the kinase was expected in the lipid raft phase and overall recovery of the relative protein levels were low (14-16%). A potential explanation may stem from the acetone precipitation used to isolate the protein samples from the gradient fractions. It may be possible that this technique adversely affected the stability of the kinase and subsequently decreased the ability of the kinase to completely re-nature within the gel and hence reduced the observed activity of the kinase.

Confirmation of these results was not possible as several attempts to reproduce the sucrose density gradient flotation procedure failed to produce a band at the 5/35% interface, indicative of a successful separation. The reasons for this were unclear, but may be attributable to problems encountered with the centrifuges over this period, with ineffective cooling, which is known to adversely effect TX100 solubilisation properties, considered to be the most likely explanation.

4.4 Analysis of antibodies generated against G4NTP and G4phosphoNTP

Antibodies to the G4NTP and GLUT4 phosphorlyated Ser^{10} peptide (G4phosphoNTP) were collected over a period of 3 months (see methods 2.5 for a full explanation of the antibody generation procedure). Two rabbits were immunised for each project and all bleeds were initially analysed, by ELISA, too ascertain if a specific response had been mounted to the peptide immunogens. Rabbit 255 showed an encouraging immunogenic response towards the G4NTP, with the ELISA results for all project bleeds shown in Fig 4.9. Rabbit 250 showed a promising immunogenic response towards the G4phosphoNTP, with the ELISA results for all project bleeds shown in Fig 4.10.

Selected bleeds from Rabbits 255 and 250 were then used as the primary antibodies for western blots against rat adipocyte PM and LDM fractions to ascertain if the ELISA data correlated with functional detection of the GLUT4 protein. The results from the western blot analysis of both antibodies, in conjunction with a control C terminal directed GLUT4 antibody are shown in Fig 4.11.

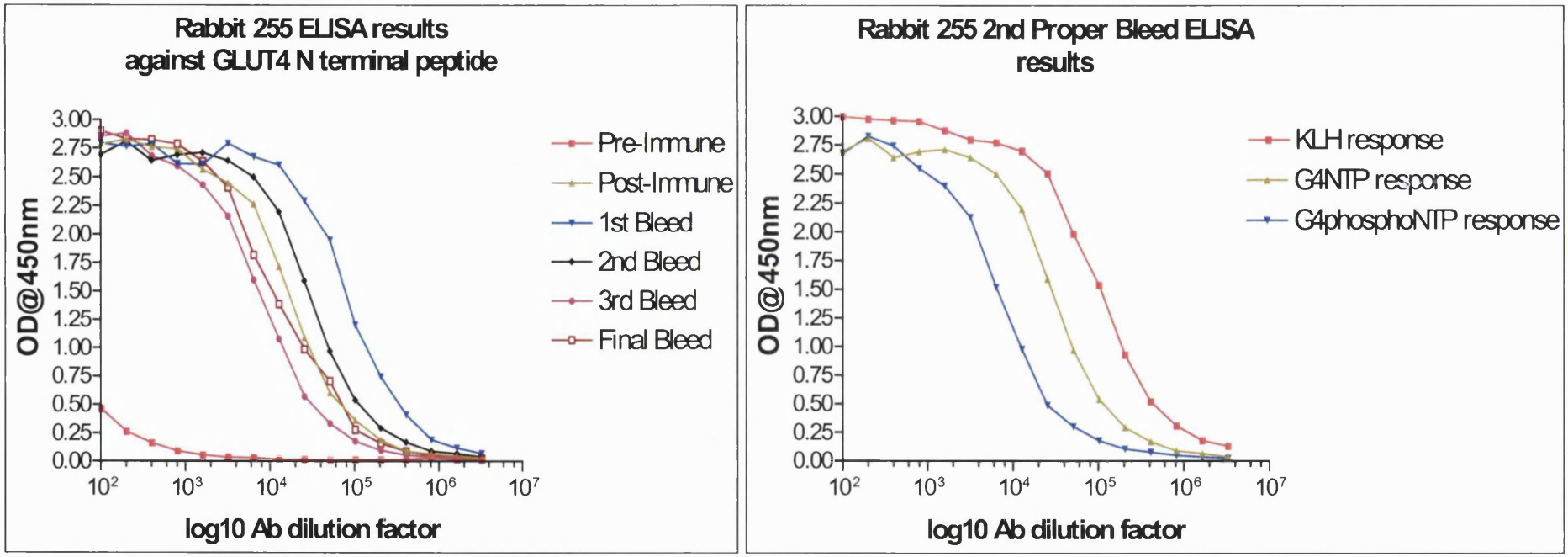

FIG 4.9: **ELISA analysis from Rabbit 255 bleeds shows specific immunogenic response to G4NTP.** All bleeds from rabbit 255 were subjected to ELISA analysis against plates coated with G4NTP. The pre immune serum was used as a negative control to show that the rabbit possessed no intrinsic immune response to the peptide antigen before immunisation. Titre values can be estimated by analysis of Optical density readings at the excitation wavelength of 450 nm over the logarithmic dilution range of the sera. Although the 1st Test bleed appeared to have the highest titre the second Test bleed was used as this was thought to contain more specific IgG. The ELISA data shown in the right hand diagram compares the 2nd Test bleed against the G4NTP immunogen, the KLH carrier protein and the G4phosphoNTP to ascertain the level of cross-reactivity of this antibody and consequently evaluate its functionality and specificity.

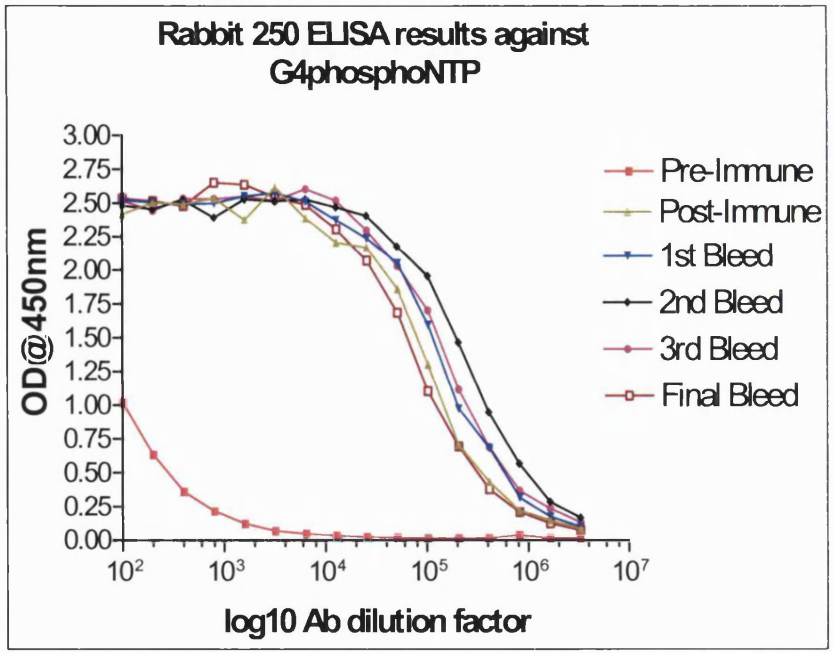

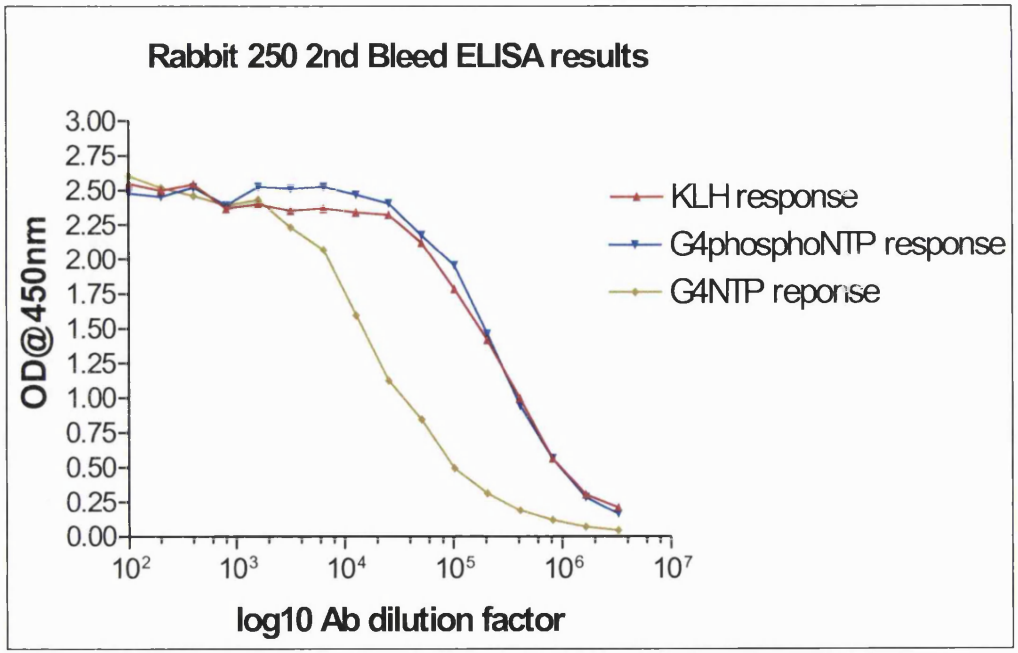

FIG 4.10: **ELISA analysis from Rabbit 250 bleeds shows specific immunogenic response to G4phosphoNTP.** All bleeds from rabbit 250 were subjected to ELISA analysis against plates coated with G4phosphoNTP. The pre immune serum was used as a negative control to show that the rabbit possessed no intrinsic immune response to the peptide antigen before immunisation. Titre values can be estimated by analysis of Optical density readings at the excitation wavelength of 450 nm over the logarithmic dilution range of the sera. The second test bleed showed the highest titre value from this analysis and was subsequently chosen for further evaluation. The ELISA data shown in the right hand diagram compares the 2nd Test bleed against the G4NTP immunogen, the KLH carrier protein and the G4phosphoNTP to ascertain the level of cross-reactivity of this antibody and consequently evaluate its functionality and specificity.

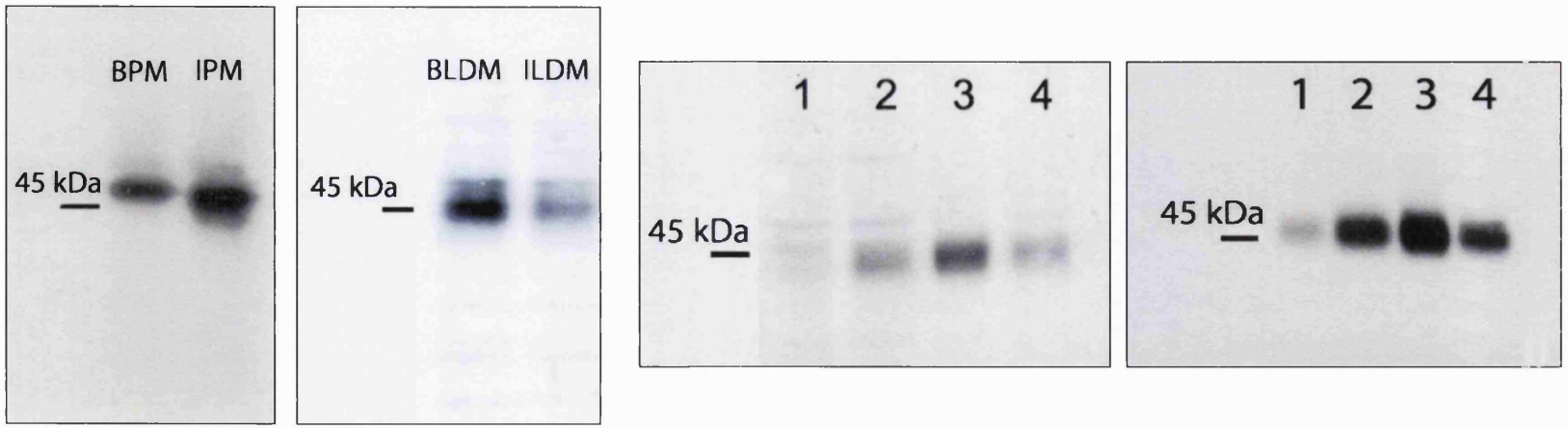

A: 255 Second Bleed G4NTP directed antibody

B: 250 Second Bleed G4phosphoNTP directed antibody

C: GLUT4 C terminal directed antibody

FIG 4.11: **Scanned images from ECL western blot developments using antibodies derived from optimal bleeds as determined from ELISA analysis.** SDS PAGE gels were loaded with 20 μg of BPM and IPM and 10 μg of BLDM and ILDM fractions and then transferred for western blot analysis. Rabbit 255, second bleed, against GLUT4 N terminal was used at a 1:1000 dilution of the serum for optimal detection (A). Rabbit 250, second bleed, against the GLUT4 phosphorylated N terminal of GLUT4 was used at a 1:1000 dilution of the serum for detection (B). The GLUT4 C terminal affinity purified antibody was used at a 1:4000 dilution as a positive control to assess the effectiveness of the other antibodies (C). Lane 1: BPM; Lane 2: IPM; Lane 3 BLDM; Lane 4 ILDM. The blots shown are representative of two separate studies.

The results for both antibodies were very encouraging, displaying specific detection against not only their respective peptide immunogens, in ELISA analysis, but also against the GLUT4 protein in western blot analysis.

The first test bleed antibody in rabbit 255 showed the highest titre value, however the second test bleed (8 weeks post immunisation) was used for further evaluation, as the resulting IgG would be more specific, reducing cross reactivity with the G4phosphoNTP and possibly any N terminal phosphorylated GLUT4. Indeed ELISA analysis of rabbit 255, second-bleed, did identify an increased titre value, for this antibody, against the G4NTP compared with the G4phosphoNTP (see right hand plot in Fig 4.9). The KLH titre shown in the ELISA plot serves as a guide for the effectiveness of the immune response. The KLH protein is used as a carrier for the peptides, due to its highly antigenic nature. The KLH protein consequently elicits an immune response that is often higher than that observed for the respective peptide. As the specificity of the peptide directed antibody increases the antibody response curve approaches that seen for the KLH protein, with responses at or above this level representing an effective immunisation programme.

The western blot analysis for the G4NTP directed antibody was very encouraging with detection of a protein band in the same region as that detected by the control affinity purified C terminal GLUT4 directed antibody. Although the strength of signal recorded for the G4NTP directed antibody was not as high as observed for the control, the classic basal/insulin differences in the PM and LDM fractions were clearly observable, suggesting that the antibody was detecting the N terminal of GLUT4.

The second test bleed antibody in rabbit 250 showed the highest titre value against the G4phosphoNTP and also showed a significant recognition specificity over the G4NTP (see right hand plot in Fig 4.10). The G4phosphoNTP directed response was very similar to that observed against the KLH carrier protein suggesting that the immunisation protocol was highly effective.

The western blot analysis for the G4phosphoNTP directed antibody showed the same distribution pattern for GLUT4 in basal and insulin stimulated PM and LDM fractions as witnessed for the C and N terminal GLUT4 antibodies. However the signal from the G4phosphoNTP directed antibody

was relatively weak, with background non-specific bands in higher abundance. It was conceivable that the similar distribution pattern seen for this antibody could be attributed to the smaller population ofG4NTP epitope directed antibody, present in the sera, as detected from ELISA analysis. It was evident from this initial analysis that it would be beneficial to affinity purify both antibodies to obtain a clearer indication of their functionality.

4.4.1 Boiling of adipocyte fractions dramatically diminishes GLUT4 detection by western blotting

The initial characterisation of the GLUT4 antibodies was hampered by the poor recovery of GLUT4 in the early western blots. The reason behind the apparent lack of GLUT4 detection was thoroughly investigated with the problems finally identified to stem from the preparation of the samples loaded on to the SDS PAGE gels. For a large proportion of lysates samples are often solubilised by heating in SDS containing sample buffer, with β-mercaptoethanol. An experiment was performed where total membrane samples, from rat adipocytes, were either boiled in sample buffer for 10 min or incubated in sample buffer for 30 min at room temperature in both 0.5 ml and 1.5 ml Starstedt eppendorfs. The results of this study are shown in Fig 4.12

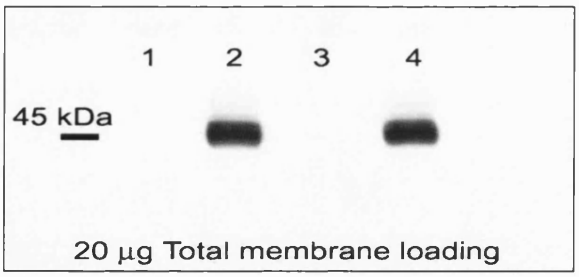

FIG 4.12: **Boiling rat adipocyte total membrane fractions dramatically decreases GLUT4 detection by the C terminal GLUT4 antibody.** Lane 1: Boiled TM sample in 0.5 ml eppendorf; Lane 2: RT TM sample in 0.5 ml eppendorf; Lane 3: Boiled TM sample in 1.5 ml eppendorf; Lane 4: RT sample in 1.5 ml eppendorf. The affinity purified C terminal GLUT4 antibody was used for subsequent GLUT4 detection at 1:4000 dilution.

The results from this experiment were very dramatic with hardly any recovery of the GLUT4 when the samples were boiled in SDS sample buffer containing β-mercaptoethanol. The reasoning behind this result remains unclear but may stem from the mass agglutination of GLUT4 if the protein is removed from its membranous environment too rapidly, as would occur with boiling of the sample in SDS sample buffer. Another possibility could be that the GLUT4 is retained on the eppendorf tube. Other tubes made of slightly different polymers could be used to overcome this problem, however for the course of all future studies on GLUT4 antibodies the samples were solubilised at room temperature for 30 min in sample buffer to optimise the recovery of GLUT4.

4.4.2 Affinity purification of N terminal directed GLUT4 antibodies and further analysis

The G4NTP directed antibody from the second bleed of rabbit 255 and the G4phosphoNTP directed antibody from the second bleed of rabbit 250 were affinity purified against their respective peptides, as detailed in Methods 2.5.6. The resultant affinity purified antibodies were then analysed by the ELISA procedure used for the initial characterisation of the sera, whereby the antibodies were tested against both peptides to ascertain the level of cross reactivity between the phosphorylated and non-phosphorylated directed N terminal GLUT4 antibodies. The results from the ELISA analysis are shown in Fig 4.13, with western blot analysis, on a range of rat adipocyte fractions, for both antibodies highlighted in Fig 4.14.

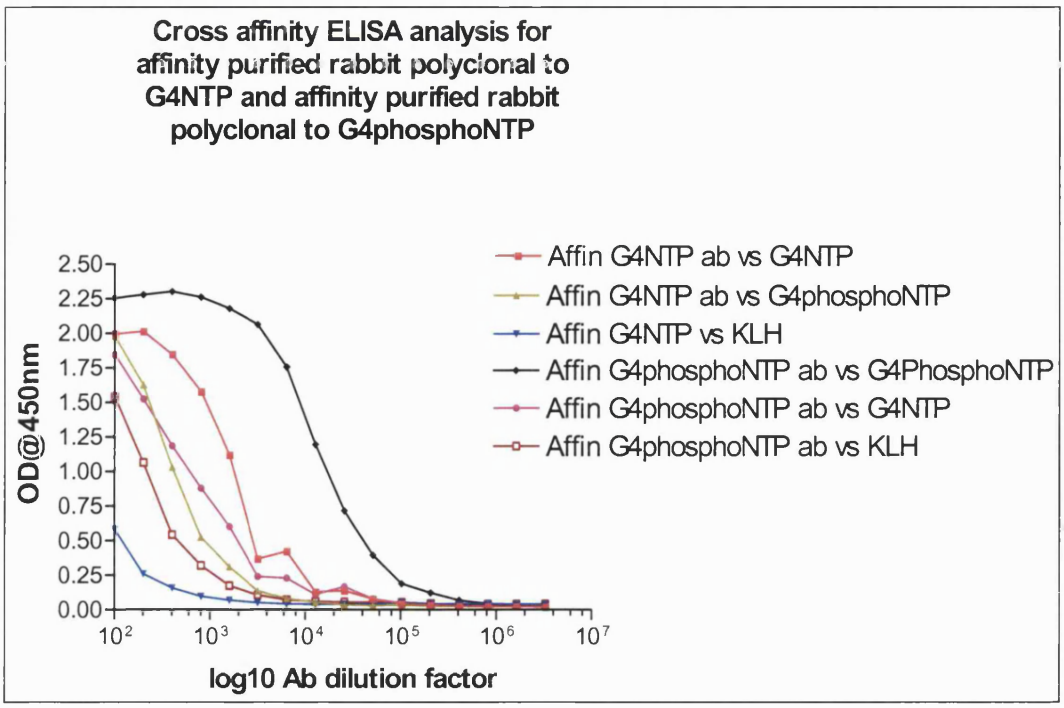

FIG4.13: **ELISA analysis of affinity purified antibodies to G4NTP and G4phosphoNTP.** The second bleed from rabbit 255 was affinity purified against the G4NTP, with the resultant purified antibody tested against the G4NTP, the carrier protein KLH and G4phosphoNTP. The second bleed from rabbit 250 was affinity purified against the G4phosphoNTP, with the resultant purified antibody tested against G4phosphoNTP, the carrier protein KLH and G4NTP. The results were displayed as optical density readings at 450 nm versus the log10 of the antibody dilution factor series used for the ELISA analysis.

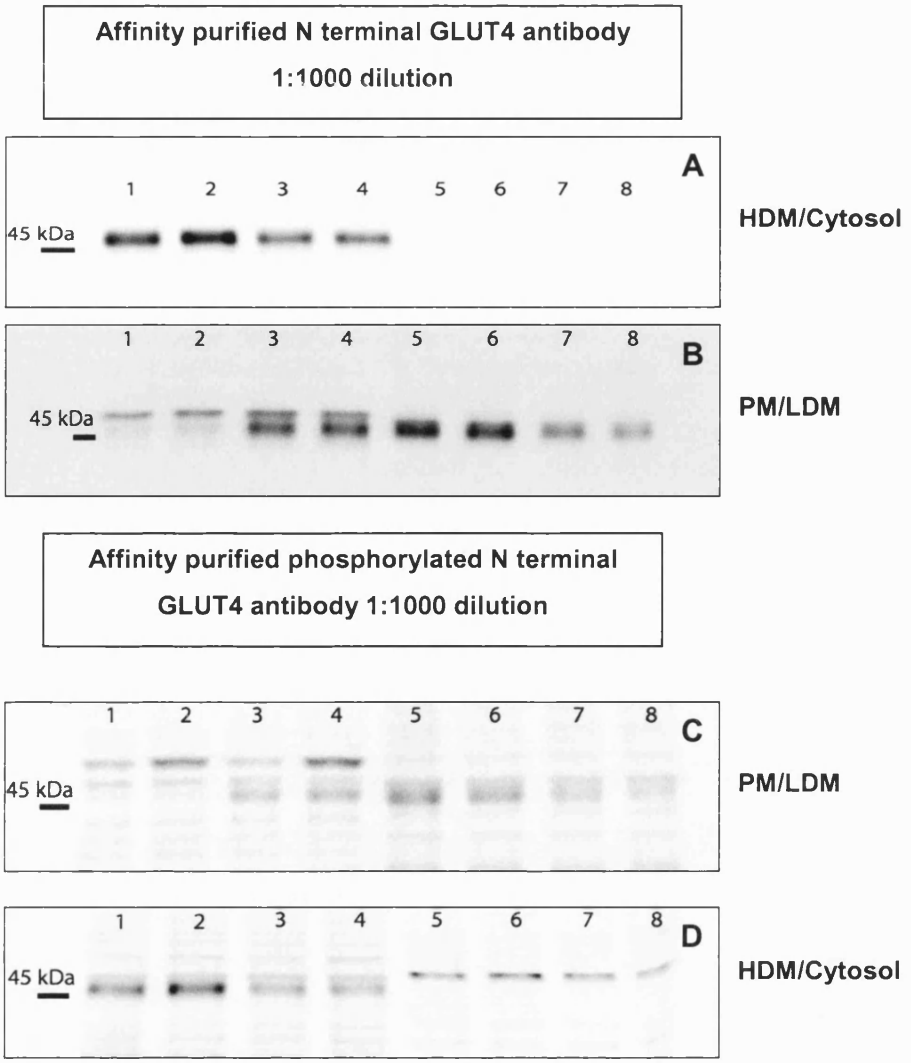

FIG 4.14: **Western blot analysis of affinity purified antibodies on the entire range of rat adipocyte sub-fractions.** The affinity-purified antibody against the G4NTP was diluted to 1:1000 for the primary antibody detection of the N terminal of GLUT4. The affinity-purified antibody against G4phosphoNTP was also diluted to 1:1000 for the potential primary antibody detection of Ser^{10} phosphorylated N terminal of GLUT4. 20 μg protein loading of the following fractions were loaded onto SDS PAGE gels for subsequent transfer and western blot detection. **Blots A and C**: Lanes 1 and 2: BHDM; Lanes 3 and 4: IHDM; Lanes 5 and 6 B cytosol; Lanes 7 and 8: I cytosol. **Blots B and D**: Lanes 1 and 2: BPM; Lanes 3 and 4: IPM; Lanes 5 and 6: BLDM; Lanes 7 and 8: ILDM.

The results from the ELISA analysis of the affinity-purified antibodies were very encouraging. Both antibodies' responses to the KLH carrier were dramatically reduced from those observed from the sera analysis, showing that an effective affinity purification of both antibodies had been achieved. The cross-affinity analysis of the antibodies also highlighted that the affinity purified G4phosphoNTP directed antibody was highly specific towards its respective peptide immunogen, with a relatively low response towards the G4NTP. The same was also true for the G4NTP directed antibody, although the difference in cross peptide specificity was not as high as that seen for the G4phosphoNTP directed antibody. Although the dilution series for both antibodies were the same, the initial antibody concentrations were different, precluding direct comparison between them.

Overall the ELISA results indicated that the G4NTP directed antibody might still detect phosphorylated N terminal GLUT4 protein, however the G4phosphoNTP directed antibody should produce a very weak signal towards the non-phosphorylated form of the N terminal of GLUT4. Any significant differences from the N and C terminal antibodies seen with this antibody were consequently considered to be due to the detection of phosphorylated N terminal GLUT4.

The results from the western blot analysis of the affinity purified antibodies provided some interesting insights into the specificity of these antibodies towards the GLUT4 protein.

The G4NTP directed affinity-purified antibody showed high specificity towards the GLUT4 protein with basal/insulin GLUT4 distribution patterns seen for PM, LDM and HDM fractions and no detection in the cytosolic fractions, which mirrors the detection of GLUT4 seen with the affinity purified C terminal antibody (results not shown). One point to note from the PM western blot analysis was the appearance of a secondary band, which showed no basal/insulin difference. This band may be non-specific or represent the detection of a sub population of GLUT4, which may be lost with C-terminal GLUT4 antibody detection, if the C-terminal of GLUT4 is masked by some process such as phosphorylation.

The G4phosphoNTP directed affinity-purified antibody produced a much weaker signal than that seen for the G4NTP directed antibody, with exposure times increased to a level where some background bands

became visible. However noticeable detection of protein bands that may correspond to GLUT4 were observed in HDM and LDM fractions with basal/insulin differences mirroring those seen with other GLUT4 antibodies. These bands could be due to the small population of G4NTP directed antibodies still present in the affinity purified antibody, but could also represent a smaller population of phosphorylated Ser^{10} N terminal GLUT4. Interestingly there was little recognition of GLUT4 like bands in the PM fractions, however the secondary band seen with the G4NTP directed antibody western blots was visible with the G4phosphoNTP antibody and also appeared in the cytosolic samples. Again this could represent a novel population of small GLUT4 containing vesicles that partition in the cytosol during subfractionation, or the bands may be non-specific. Further experimentation by colleagues in the laboratory has sought to clarify the situation. Their studies used digested basal and insulin stimulated rat adipocytes that were either homogenised as usual (see Methods 2.2.2) or homogenised in HES buffer supplemented with phosphatase inhibitors (10 mM Na-pyrophosphate, 100 mM NaF, 1mM Na-molibdate, 1mM Na-vanadate) + the usual protease inhibitor cocktail. The homogenates were then sub-fractionated, as standard, with the HES supplemented buffer used for all subsequent re-suspensions in the treated sample pool. The results from one of two separate studies are shown in Fig 4.15, provided with the kind permission of Dr. Francoise Koumanov.

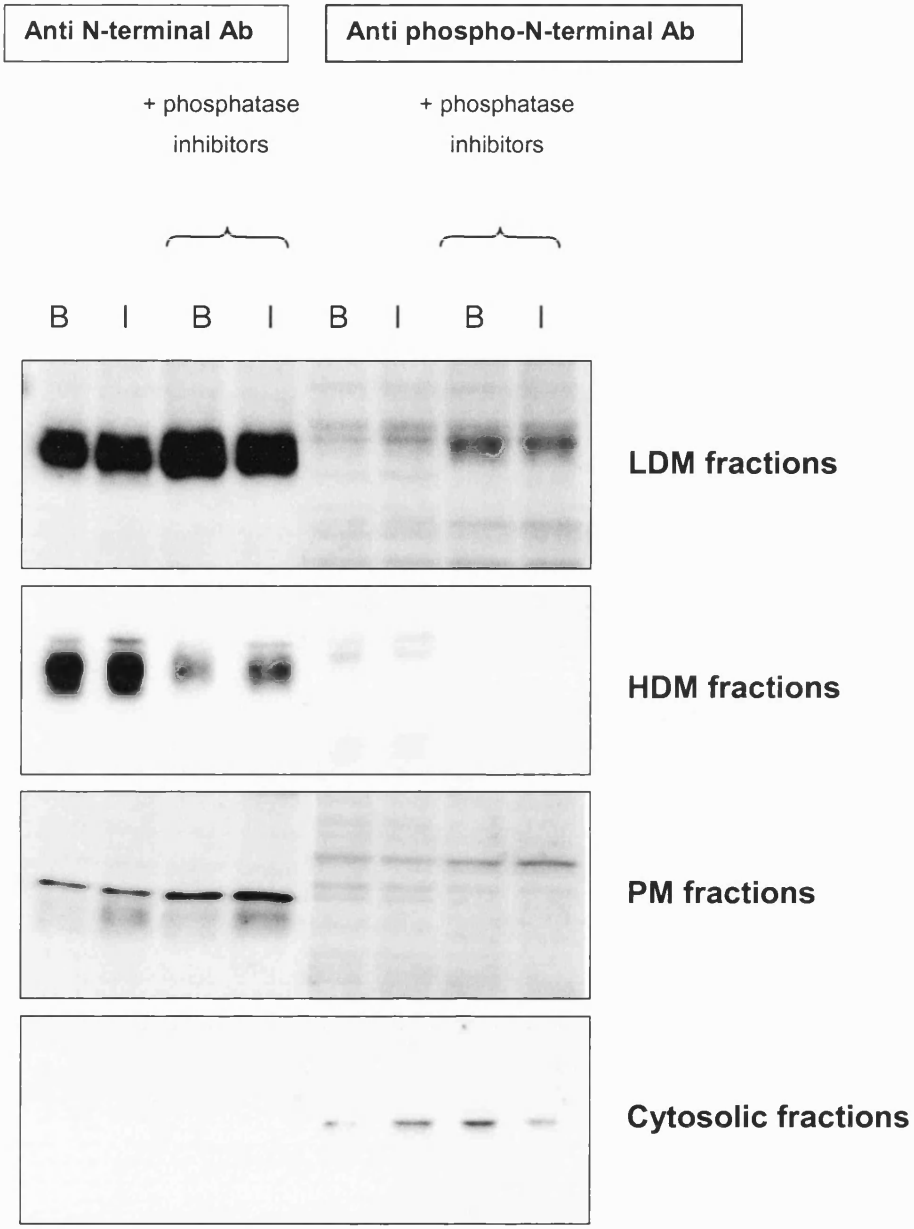

FIG 4.15: **Western blot analysis of the effects of phosphatase treatments on the effective recognition of GLUT4 by the affinity purified anti N-terminal GLUT4 antibody at 1:1000 dilution and the affinity purified anti phospho-N-terminal GLUT4 antibody at 1:500 dilution.** The results shown are representative of two independent studies performed by Dr. Francoise Koumanov, a colleague from my laboratory.

The results for the LDM fractions were very interesting with the phospho-N-terminal affinity purified GLUT4 antibody apparently recognising a stronger GLUT4 like band in the LDM fractions treated with phosphatase inhibitors, something not observed using the affinity purified C terminal GLUT4 antibody (results not shown). These results indicated the phospho-N-terminal affinity purified GLUT4 antibody was detecting phosphorylated GLUT4 that was highly sensitive to phosphatases. The balance between the phosphorylation of Ser^{10} by the G4NTP directed kinase and dephosphorylation by phosphatases may result in only a small population of phosphorylated GLUT4 existing at any one time, hence the low level of detection in the LDM fractions, without phosphatase inhibitors present.

The results for the PM fractions did not identify any bands resembling GLUT4 when blotting with the phospho N-terminal affinity purified GLUT4 antibody, even after lengthy expose times. The N-terminal affinity purified GLUT4 antibody appeared to function as before with the secondary band appearing on all PM fractions, with no basal/insulin difference but some enhancement with phosphatase inhibitor treatment.

The results for the HDM fractions showed some recognition of GLUT4 using the phospho-N-terminal affinity purified GLUT4 antibody. However good detection of GLUT4 was observed with the N-terminal affinity purified GLUT4 antibody. Interestingly the level of GLUT4 detection appeared to be significantly higher in HDM fractions not treated with phosphatase inhibitors, although the reasons for this were unclear

The cytosolic fractions showed that the N-terminal affinity purified GLUT4 antibody detected no non-specific band in the cytosol. However the phospho-N-terminal affinity purified GLUT4 antibody did detect the secondary band witnessed in previous western blots (see Fig 4.14).

Overall these results indicated that modulation of N-terminal GLUT4 phosphorylation occurs most prevalently in the LDM fractions. This coincides with the predominance of the G4NTP directed kinase in the LDM fractions, as observed by the "In Gel" kinase assays, lending overall support to the functionality of the kinase on GLUT4 *in vivo*.

4.4.3 Immunocytochemistry results on isolated rat adipocytes using affinity purified GLUT4 antibodies

Further to the western blot analysis using the affinity purified GLUT4 antibodies the antibodies were used for immunocytochemical analysis of isolated rat adipocyte fractions (see methods 4.2.4) with results shown in Fig 4.16.

The results from this study are shown merely as an initial indication of the antibodies' functionality against native GLUT4. The GLUT4 C terminal and N terminal antibodies appeared to show the same differential GLUT4 distribution in the cells observed. In the basal state the detected GLUT4 appeared to be dispersed just beneath the PM, with a predominant perinuclear distribution. Note that the large lipid droplet present in isolated adipocytes tends to alter the appearance of the adipocyte, pushing most intracellular structures to the periphery of the cell.

In the insulin stimulated adipocytes there was a noticeable redistribution of detected GLUT4 to the cell surface, with defined cell surface labelling of GLUT4 visibly encapsulating the nucleus (shown in red).

Interestingly the apparent distribution pattern of GLUT4 observed when using the affinity purified phospho-N-terminal antibody differed from that seen with the N and C terminal antibodies. The insulin stimulated adipocytes did not show a defined cell surface labelling of GLUT4, rather the detected protein appeared to still be located in a perinuclear location, possibly less dispersed than that observed in the basal adipocytes. The bands observed could represent a small pool of phosphorylated GLUT4 resident in intracellular compartments that are not re-directed towards the PM, upon insulin stimulation. However the image could also conceivably be the non-specific detection of the cytosolic protein found in the western blot analysis, using this antibody.

Due to my limited expertise with this type of procedure these results cannot be quantifiably interpreted and further work is required to confirm the speculations drawn from these findings

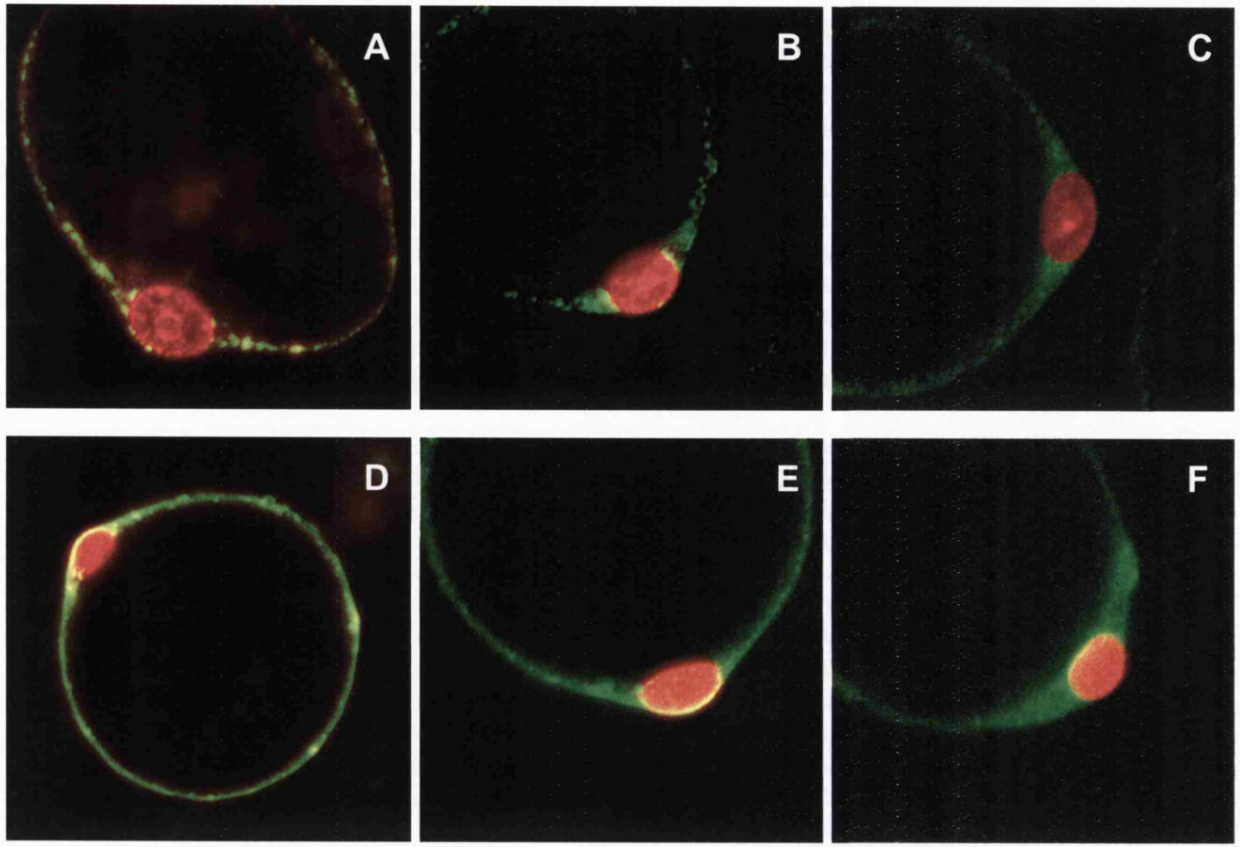

FIG 4.16: **Confocal images of Basal (A-C) and Insulin stimulated (D-F) isolated rat adipocytes using affinity purified C, N and phosphorylated N-terminal GLUT4.Antibodies** Dual channel images highlighting the nucleus in red and potential GLUT4 in green. Image A and Image D were exposed to 1:500 dilution of affinity purified C terminal GLUT4 antibody. Image B and Image E were exposed to 1:200 dilution of affinity purified N terminal GLUT4 antibody. Image C and Image F were exposed to 1:100 dilution of affinity purified phosphorylated N terminal GLUT4 antibody. Pinhole 1 was used for channels 1 and 2 and each image is representative of at least 3 separate images taken.

4.4.4 Conclusions

The studies highlighted in this section have focussed on evaluating the nature of the membrane association of the G4NTP directed kinase. The kinase seems to be predominantly found in LDM/HSP rat adipocyte fractions where it appears to be ionically associated with membranous bodies. However the results suggest that the kinase may also be dynamically associated with lipid raft elements. This may stabilise the association of the kinase with other signalling proteins, potentially enhancing its activity or merely juxtaposing it close to GLUT4, to facilitate controlled phosphorylation.

There does appear to be a population of the kinase ionically associated with the PM, however the association of this kinase population with lipid rafts has not been satisfactorily proved, due to problems encountered with lipid raft flotation analysis.

Confirmation of the existence of Ser^{10} phosphorylated GLUT4 would strongly support the notion that the G4NTP directed kinase served an *in vivo* function. To this end antibodies were generated against the N terminal of GLUT4, one against the non-phosphorylated Ser10 and the other against a sequence containing $^{P}Ser^{10}$. Both antibodies appeared to be functional, through ELISA analysis, and also worked well against GLUT4 through western blot analysis.

Evidence from phosphatase inhibitor treatment of LDM fractions showed that detection of a population of GLUT4, via the phospho-N-terminal antibody, appeared to be significantly enhanced when phosphatase action was perturbed. These results suggested that phosphorylation of the N terminal of GLUT4 might occur, but may be a delicately balanced process with only a small population of intracellular GLUT4 phosphorylated at any one time. Although the specificity of the phospho-N-terminal GLUT4 antibody needs to be fully established, through cross-affinity purification, the localisation of a pool of potentially phosphorylated GLUT4, coupled with the predominance of the G4NTP directed kinase in this fraction, provides an appealing new dimension in GLUT4 trafficking studies.

5 Attempts to isolate the G4NTP directed kinase and determine its identity.

5.1 Introduction and experimental aims

A completely divergent methodology for G4NTP directed kinase isolation, and potential isolation of G4NTP interacting proteins, involved the use of Phage Display screening. The system works on the premise that immobilised baits will specifically interact with peptides and proteins displayed on the surface of T7 phage that have been derived from the entire cDNA library of a particular tissue extract. The T7 Phage were extremely robust and were resistant to SDS, alkali, salt, reducing agents and EDTA, allowing specific elution of Phage from the immobilised bait using 1% SDS. The procedure had been successfully used to pull out adapter protein Grb2 and Tyrosine kinase Fyn, using EGFR peptide as the immobilised bait (Zozulya *et al.*, 1999). Also Phage display had identified thioredoxin and superoxide dismutase as novel protein kinase C-interacting proteins (Watson *et al.*, 1999). Consequently isolation of the G4NTP directed kinase, using G4NTP as the immobilised bait was considered a viable course of study. Only a brief overview of the procedures and results for this investigation will be shown here, as the findings from this particular isolation procedure were hampered by background contamination artefacts. The possible failings of this system will be highlighted.

All of the isolation techniques used provided further insights towards the functionality of the G4NTP directed kinase and these results will be presented with references to complementary findings presented in the two previous sections.

5.2 Experimental methods

5.2.1 Phage Display

Target sequences were fused (C terminal) with the T7 gene 10 major capsid protein so that expressed peptides and proteins were displayed on the surface of the virus (T7 bacteriophage). The copy number display on each phage can be controlled depending upon the application required. For the purposes of this investigation a medium copy number display vector was obtained from Novagen Inc (USA), termed T7 select 10-3b. This vector typically displays approximately 10 peptides per phage with a peptide size capacity of up to 1200 amino acids. The host strain used for this vector was also obtained from Novagen and was termed BLT5615.

5.2.1.1 Generation of adipocyte cDNA library in T7-Select 10-3 phage

1. Total RNA isolation. A total of six fat pads were taken from three male Wister rats (approximately 5 g of material) wrapped in aluminium foil and placed into liquid nitrogen. The tissue was ground, using a pestle and mortar, after the liquid nitrogen had evaporated. The tissue was then transferred into 10 ml of Trizol® and homogenised with six strokes then a further 10 ml of Trizol was added and the homogenate further homogenised with an additional 15 strokes. The final homogenate was transferred to two 10 ml Corex tubes and left to stand for 5 min. The homogenates were then centrifuged in a Beckman SS34 rotor for 10 min at 10000 rpm at 4°C with the resulting supernatants removed, leaving the crude pellet debris and fat behind. The supernatants were mixed with 2 ml of chloroform and gently vortexed for around 15 sec. The samples were allowed to stand at room temperature for 10 min and then centrifuged for 15 min at 10000 rpm in the SS34 rotor at 4°C. The aqueous phase (containing RNA) was removed and transferred to clean

Corex tubes. To these 5 ml of isopropanol was added and the samples were incubated at room temperature for 10 min. The samples were centrifuged at 10000 rpm for 10 min at 4°C in the SS34 rotor and the isopropanol was removed. The remaining pellets were washed in 10 ml of 75% (v/v) ethanol and air-dried. The total RNA pellets were each resuspended in 500 μl DEPC treated H_2O giving a total amount of 950 μg/ml extracted RNA as determined by spectrophotometry analysis at 260 and 280 nm.

2. Purification of mRNA. The mRNA was isolated from total RNA using the poly A tract system IV (Promega), as detailed in the product literature. Briefly the system used biotinylated oligo dT to select polyadenylated RNA (mRNA) using streptavidin coated magnetic particles. This system greatly reduced rRNA contamination that was crucial for the random priming cDNA synthesis used later in the procedure. Note that random primers initiate cDNA synthesis from all RNA species and resulting libraries will contain non-informative cDNA clones corresponding to the proportion of rRNA in the sample. Using 475 μg of total RNA this procedure isolated 30 μg of mRNA.
3. cDNA synthesis Hind III random primers and reverse transcriptase were used for the first strand synthesis, as detailed in the Novagen OrientExpress™ cDNA manual. Second strand synthesis was subsequently performed using DNA polymerase after RNAse H digestion, with the resultant cDNA precipitated using chloroform extraction as detailed in the Novagen OrientExpress™ cDNA Manual.
4. The following steps are all as detailed in the aforementioned Promega manual. The ends of the isolated cDNA were blunted using T4 DNA polymerase and then directional EcoR I/ Hind III sites were ligated onto the resultant cDNA, with subsequent digestion of the modified cDNA using EcoR I and Hind III restriction enzymes. The design of the random primers together with the directional linker design results in an EcoR I site at the 5' end of the cDNA and a Hind III site at the 3' end, facilitating directional cloning into the T7 bacteriophage vector arms.
5. The digested cDNA was size fractionated using gel filtration to remove small cDNA fragments (< 300 bp) and non-ligated directional linkers.

6. 1.5 μl of the remaining digested cDNA was then ligated into the EcoR I and Hind III T7 phage vector arms and the ligation reaction packaged into phage particles using the T7 Select 10-3 packaging extract, as detailed in the Novagen T7Select™ System Manual.
7. The packaged phage were transfected into the BLT5615 bacterial strain and the titre determined at 1.8 x 10^6 phage, using the plaque assay protocol detailed in the Novagen T7Select™ System Manual.
8. The primary library was then amplified, as detailed in the aforementioned manual, to a concentration of 1.2 x 10^{11} phage/ml lysate. The amplified library was stored and used for the bio-panning procedure.

5.2.1.2 Phage Display selection procedure (Bio-panning)

A single round of bio-panning involved the selection of phage that bound to the immobilised G4NTP bait. The G4NTP was immobilised to three different solid supports:

1. The reactive cysteine residue on the G4NTP was utilised to attach the peptide to SulphoLink beads in the same manner as used for affinity purification (see Methods 2.5.6.1).
2. The G4NTP was attached to magnetic coated Dynabeads (Dynal ASA, Norway). The tosyl groups on the beads were converted to amines through reaction with diaminopentane (Sigma). These amines were then linked to sulpho-SMCC that facilitated interaction with the free sulfhydryl groups on the G4NTP as detailed in Methods 2.5.3. This immobilisation procedure ensured that the peptide was presented in the correct orientation and also provided enhanced washing capacity as the beads were quickly attracted to magnetic fields when placed in a special holder, reducing the frequency of non-specific trapping of phage through centrifugation separation schemes.
3. The terminal cysteine residue of the G4NTP was biotinylated using biotin maleimide (Sigma). The biotinylated G4NTP was then immobilised on Neutravidin beads. By using Neutravidin beads in a pre-clearing step

the non-specific phage could be eliminated from the subsequent round of panning using the G4NTP coated Neutravidin beads.

Using one of the immobilised G4NTP baits the beads were equilibrated in PBS containing 0.5% (v/v) Tween 20 (PBST). The beads were then blocked using a 1/10 dilution of Panning blocking buffer (5% Tween 20, 10% Marvel, 10 mM EGTA, 250 μg/ml Heparin, 250 μg/ml boiled Herring sperm DNA, 0.05% (w/v) Na Azide) in PBS. Varying dilutions of the amplified phage library, in Panning blocking buffer, were incubated for 1 h at room temperature. Non specific phage were removed by twelve washes in PBST containing 25 μg/ml Heparin and the specifically bound phage were eluted using 1% SDS (w/v) in PBST.

The extremely robust nature of the eluted phage means that they can be subjected to plaque assay and phage amplification as used for the original packaged phage library (see Novagen T7Select™ System Manual). After each round of bio-panning the ratio of specific to non-specific phage binders should increase. Typically three rounds of successive bio-panning produced an acceptable level of specific phage.

5.2.1.3 Deriving sequence data from selected phage plaques

After three rounds of bio-panning, plaques containing multiple identical phage were picked from the plate as small gel plugs. These plugs were transferred into 100 μl of 10 mM EDTA pH 8.0 and heated to 65°C for 10 min. Un-dissolved agar was then removed by pelleting, with 2 μl of the supernatant, containing the released phage, added to 47 μl of PCR Master Mix (10 times PCR buffer, 10 mM dNTPs, T7 Select UP and DOWN primers, sterile water). The mixture was then overlaid with 50 μl of oil and heated to 80°C, at which point 1 μl (2.5 units) of Taq Supreme polymerase was added to the bottom layer. The samples were then run through 35 cycles of the following PCR programme: 94°C for 50 sec followed by 50°C for 50 sec and 68°C for 90 sec. At the end of the cycles the samples were maintained at 68°C for a further 6 min and then cooled to 4°C. 10 μl of the

PCR amplified sample was combined with 3 μl loading buffer and the sample run on a 1% TAE gel, alongside 1kb markers.
The resultant DNA bands were then observed with the criteria for further selection involving identifying multiple samples that appeared to contain the same insert size. The remaining PCR product of the selected samples were gel purified using the Clontech DNA extraction kit (Clontech UK) and the resulting DNA eluted into 30 μl of sterile H_2O. 5 μl of the purified DNA was then mixed with 1 μl UP primer and sent for sequence determination.

5.2.2 2-Dimensional Electrophoresis

5.2.2.1 PM solubilisation using Na Cholate

300 μg of PM fraction was pelleted by centrifugation at 37 000 rpm for 9 min using the Beckman TL-100 benchtop ultracentrifuge at 4°C, with a TLA-100.3 fixed angle rotor. The pellet was resuspended in 200 μl of 20 mM Na Cholate in 20 mM Hepes buffer (pH 7.0) and incubated on ice for 10 min. The sample was sonicated for 5 sec and then frozen overnight at -70°C. The sample was thawed at room temperature while 125 mg of Sephadex G50 (Sigma) was swelled in 15 ml 20 mM Hepes buffer (pH 7.0) for 30 min at room temperature. The swelled Sephadex G50 was then placed into a Talon disposable gravity column (Clontech) and washed with Hepes buffer. The thawed, solubilised, PM fraction was loaded onto the gel and eluted using Hepes buffer, with 100 μl fractions collected. The fractions were subjected to BCA protein assay, with fractions containing the highest level of protein (usually fractions 4 and 5) pooled and used for sample loading on IPG strips, IEF sample wicks or "In Gel" kinase assay.

5.2.2.2 2-Dimensional Electrophoresis general procedure

The procedures used for 2-dimensional electrophoresis were essentially derived from "2-D Electrophoresis using immobilised pH gradients: Principles & Methods Manual" (Amersham Pharmacia biotech). The system used for the eletrophoretic separations, in both dimensions, was the Multiphor® II Electrophoresis System (Amersham).

The first dimension gel used was the 18 cm pre-cast pH 3-10 linear IPG (immobilised pH gradient) immobiline drystrip (Amersham). These strips require rehydration using Rehydration stock solution (2% (w/v) CHAPS, 8 M Urea, Bromophenol blue (trace), ddH_20), with 2.8 mg of DTT and 20 µl IPG Buffer (Amersham) added per 1 ml of stock solution. 15 – 30 µg of the protein sample was included in the rehyradtion solution, with a total volume of 350 µl used to rehydrate one strip. The solution and the strip were placed in a reswelling tray (Amersham), overlaid with 2 ml of IPG Cover Fluid (Amersham) and rehydrated overnight at room temperature.

The rehydrated strip containing the protein sample was placed onto the Multiphor II unit, cooled to 20°C, as detailed in the 2-D Electrophoresis Manual (Amersham). The first dimension gel was focussed over a period of 20.5 h, building up to a final voltage of 3500 volts and 1 mA.

Once the proteins were focussed within the carrier ampholyte established pH gradient the strip was equilibrated in two 15 min phases using SDS equilibration buffer (Tris HCl solution (pH 8.8) containing 6 M Urea, 30% (w/v) glycerol, 2% (w/v) SDS). In the first equilibration phase, 10 ml of the SDS equilibration buffer was supplemented with 100 mg DTT to ensure that the focussed proteins were preserved in a fully reduced state. In the second phase 10 ml of the SDS equilibration buffer was supplemented with 250 mg iodoacetamide and a trace of bromophenol blue. The iodoacetamide acts to alkylate thiol groups on proteins preventing their reoxidation during electrophoresis, limiting streaking and silver staining artefact detection of proteins after second dimensional separation. The bromophenol blue was used purely to visually monitor the progression of protein separation in the second dimension.

While the strips were equilibrating a 10% polyacrylamide gel was prepared using the Large Scale SDS and Native PAGE kit for the Multiphor II Electrophoresis system (Amersham). The gel composition was the same as that detailed in Methods 2.4.2, however the dimensions were 200 x 260 x 0.5 mm (h/w/d). The 0.5 mm gel was supported with a Gelbond PAG backing film (Amersham) that facilitated manipulation of the gel after casting. In some instances 10 μM G4NTP, conjugated to poly Lysine, was incorporated into the 10% polyacrylamide gel for "In Gel" kinase assay analysis of the second dimension gel, after focussing.

The Multiphor II unit was cooled to a constant 15°C. A thin layer of Drystrip cover fluid applied to the contact surface to provide efficient contact with the gel film and ensure homogenous cooling of the gel during electrophoresis. The gel was positioned on the unit and the surface left to dry for 10 min. A pre-made anodic gel buffer strip was placed at the anodic side of the gel at a position corresponding to the 1 cm horizontal grid mark on the unit surface, which could be seen through the gel. The-pre made cathodic gel buffer strip was placed at the cathodic side of the gel at a position corresponding to the 16 cm grid mark on the unit surface.

The equilibrated IPG strip was drained on to damp blotting paper and positioned, gel face down, next to the cathodic buffer strip. The acidic end of the strip was aligned with the 3.5 cm vertical grid reference and the squared basic end at 22.5 cm. All of these grid references were kept constant for all second dimension gel runs to facilitate reproducible results.

Application strips were placed above and below the strip. 5 μl samples of HMW markers (Sigma) were resolved, to generate molecular weight reference points.

Second dimension gel electrophoresis was initiated at 1000 V, 20 mA for 45 min, at which point the sample was observed to have transferred from the IPG strip onto the 10% polyacrylamide gel (as observed by dye-front analysis). The IPG strip and application strips were removed and the focussing continued for a further 5 min at 1000 V, 40 mA. The cathodic buffer strip was then moved forward to cover the area previously occupied by the IPG strip, with the position of the cathodic electrode adjusted accordingly. The focussing was then continued for 160 min at 1000 V, 40

mA, until the dye front had reached the anodic buffer strip, at which point the second dimensional focussing was complete.

5.2.2.3 Silver Stain visualisation of 2-Dimensional electrophoresis gels

Although conventional Coomassie staining of developed 2-D gels was performed the enhanced detection sensitivity of the silver staining procedure was required for more in-depth protein distribution analysis.
After the gel focussing was complete the gel was fixed in 50% (v/v) methanol, 10% (v/v) acetic acid for 30 min at room temperature with gentle shaking. The gel was then incubated in 5% (v/v) methanol, 1% (v/v) acetic acid for a further 15 min and quickly rinsed in 50% (v/v) methanol. The gel was washed in ddH_2O and then incubated in 0.2 g/l sodium thiosulphate for 90 sec with gentle shaking. The gel was washed in ddH_2O and incubated in 0.2 g/l silver nitrate solution for 25 min with gentle shaking. The gel was washed in ddH_2O and the silver stain developed in Developing buffer (Na_2CO_3 6 g/100 ml, formaldehyde 50 µl/100 ml and 2 ml/100 ml of the pre made 0.2 g/l sodium thiosulphate solution) for up to 10 min. When an appreciable level of staining had developed the procedure was stopped with the addition of 9.6% (v/v) acetic acid for 30 min. The gel was then rinsed in ddH_2O and the image scanned or digitally photographed.

5.2.3 Alternative 2-Dimensional electrophoresis: Combining IEF and the conventional "In Gel" kinase assay

5.2.3.1 Sample preparation

Many treatments were utilised to facilitate the entry of the G4NTP directed kinase into the IEF gel, ranging from detergent solubilisation using SDS, TX100, Na-cholate or CHAPS, to urea and high pH treatment of the samples. The problems encountered with some of these applications are discussed in the results section of this chapter.

The most successful strategy appeared to derive from high salt treatment of the samples (see Chapter 2). Between 1-2 mg of LDM fraction was mixed with 2.5 ml of HES buffer + protease inhibitors (see Buffers 2.1.2) containing 1M NaCl. The sample was homogenised with ten strokes using a 25 gauge needle linked to a 5 ml syringe and the sample then incubated on ice for 45 min. The treated sample was centrifuged at 70 000 rpm for 75 min using the Beckman TL-100 benchtop ultracentrifuge at 4°C, with a TLA-100.3 fixed angle rotor. The supernatant was removed and transferred into a 3 ml Slidealyzer (Pierce) for dialysis overnight in 5 L of 10 mM Hepes buffer (pH 7.2), at 4°C. The sample was concentrated down to ~0.5 ml, using PEG 20 000, BCA protein assayed to determine the resultant protein sample concentration and used directly for Isoelectric focussing.

5.2.3.2 Isoelectric focussing (IEF) general procedure

The IEF gels were prepared using the SDS and Native PAGE, IEF Kit for the Multiphor II Electrophoresis System. The gel dimensions were 125 x 260 x 2 mm (h/w/d) and were cast onto Gelbond PAG backing film, as for the second dimension gels. The gels contained the following components: 5% T, 3% C Acrylamide/Bis solution, 10% (v/v) Glycerol, 13 mg Glutamic acid, 2.5% (v/v) Ampholines pH range 3-10 (Amersham). The gel mixture was de-gassed and then polymerised for 3 h using 1% ammonium persulphate, TEMED and 1% (w/v) Riboflavin. Riboflavin generates free

radicals, when exposed to light, facilitating acrylamide polymerisation. The lower concentrations of ammonium persulphate used reduces band spiking and the glycerol and glutamic acid act to mechanically stabilise the gel, reduce pH gradient drift and reduce band skewing.

The MultiTemp II thermostatic circulator was set to 10°C, 15 min before starting the experiment. After this cooling period the polymerised gel was applied to the cooling plate and left to dry for 10 min. Electrode strips were then soaked in the appropriate electrode solutions (Anode buffer 1M H_3PO_4; Cathode buffer 1M NaOH), drained and then positioned on the gel as detailed in the 2117 Multiphor II Electrophoresis System Manual. Sample wicks or sample application strips (Amersham) were then placed at pre-determined sites within the gel (see results for more detail). 5 µl of IEF broad range standards (pI 4.45 – 9.6) (Bio-Rad) were loaded onto one of the application points with up to 20 µl of sample loaded per sample wicks/strips. The gel was focussed for 30 min at 2500 V, 150 mA, 25 W then the sample application wicks/strips were removed and the gel run for a further 55 min at the same power settings. The gel was run at 3500 V for a further 10 min to produce sharp band focussing. In the developmental phase of this procedure the whole gel was Coomassie or silver stained and visualised. In later experiments the sample loading was duplicated on one gel with half the gel used for staining and the other half used for "In Gel" kinase assay analysis as detailed in 5.2.3.3.

5.2.3.3 Transferring 1st dimensionally focussed proteins onto the "In Gel" kinase assay for 2nd dimensional separation.

The focussed protein samples in one half of the IEF gel were excised as a series of sixteen identical gel segments corresponding to 1.5 sample lane width. Segment 1 corresponded to the level where the pI 4.6 marker focussed and segment 16 encompassed the region in which the pI 9.6 marker was found to focus. The gel segments were transferred into labelled eppendorfs containing 30 µl 3 x sample buffer containing 5 µl β-mercaptoethanol. The samples were heated to 95°C for 20 min with the sample buffer and gel segments transferred into the loading wells of a 10%

polyacrylamide large slab gel containing 10 μM G4NTP conjugated to poly Lysine (see Methods 2.4.2). The gel was resolved at 25 mA, constant current, overnight and processed as detailed for the "In Gel" kinase assay system (see Methods 3.3.2). In some instances the gel was transferred and used for western blot analysis. In these cases the G4NTP conjugated peptide was omitted from the gel and the gel transferred as detailed in Methods 2.4.3.

5.3 Results and Discussion

5.3.1 Phage display Results: A brief summary

The phage display screening methodology was developed with three different methods for bait immobilisation investigated and extensive modifications made to the blocking, washing and elution steps. Unfortunately the results from this study did not identify any potential GLUT4 N-terminal kinases, with background contamination of non- specific phage being the major obstacle. The tubes were siliconised in a last attempt to reduce the level of non-specific phage retention and although the background levels were reduced there were still no strong protein targets identified. A results table showing a sample of the cDNA clones identified, the solid support used, the frequency of their detection and a brief overview of their significance is shown in Fig 5.1.

cDNA clone/ Protein	Accession Number	Solid support	Frequency of detection	Information and significance
β-2-Microglobulin	AA68498.1	SulphoLink	5	Sequence corresponded to invariant β chain of MHC Class I, an extracellular protein, so not significant.
Sex regulated protein Janus A precursor	P20348	SulphoLink	2	Sequence found had 90% identity to the protein mentioned. Significance low.
Glutathione peroxidase 5	NM010343.1	Dynabeads	1	The cDNA sequence found in the isolated phage corresponded to the 3' non-translated region. Not significant.
Non-muscle myosin alkali light chain	S77858.1	Dynabeads	1	Potentially interesting but could not find more than one phage population.
VE-cadherin gene (lambda 5 clone)	MMVECADH5	Dynabeads	1	Did not appear to be significant and only one population detected
Rat ribosomal protein S6	M29358.1	Dynabeads	4	Would not expect this to have a role in GLUT4 binding. Probably non-specific binding
Phospholipid transfer protein (Pltp)	NM011125.1	Neutravidin	1	Only one population and so significance cannot be established
Cyclin-dependent kinase inhibitor (p57kip2)	U20553.1	Neutravidin	1	Potentially interesting but could not find more than one phage population.
Alpha-tubulin	V01227.1	Neutravidin	2	Did not translate into correct reading frame

FIG 5.1: **Tabular display of selected sequence data obtained from PCR analysis of isolated phage after 3 rounds of bio panning against immobilised G4NTP.**

The level of sequence data generated from selected phage plaques was poor, with problems encountered with the PCR amplification of the selected phage, to obtain appreciable levels of DNA for sequencing. Primer storage and compatibility were found to be the main factors involved in poor PCR, with certain UP and DOWN PCR primers not functioning when used together, the reasons for which were unclear.

There was no significant detection of a kinase that could be considered to act on GLUT4. This could be a result of background non-specific phage that may replicate more proficiently in the phage amplification procedures carried out between successive rounds of bio panning. This would result in plaques containing the specific interacting phage occurring at a low frequency that could be missed during the sampling stage. Alternatively the kinase interaction with the G4NTP may not be strong enough for the interacting phage to be retained during the washing procedures. The interaction may well be transient with lipid raft structures required to stabilise the association between the G4NTP directed kinase and GLUT4, as previously discussed in section 4.

Using yeast two-hybrid analysis Cushman and colleagues identified the phenylalanine targeting signal in GLUT4 that constituted a binding site for the medium chain adaptins μ1, μ3A and μ2 in order of preference (Al Hasani *et al.*, 2002). These findings were in line with the described *in vivo* association of GLUT4 with the adapter complexes containing these subunits (Gillingham *et al.*, 1999). Unfortunately no phage were isolated that expressed adapter μ subunit proteins on the capsid surface. Again this could be due to masking by non-specific phage contamination, or the initial cDNA phage library was not extensive enough and consequently some of the proteins found in adipocyte tissue could have been lost. Further development of the phage display screening process is required before any confidence can be placed on the results obtained from this procedure.

5.3.2 2-Dimensional Electrophoresis Results

2-Dimensional Electrophoresis proved to be technically demanding, with many experimental gel runs performed before a reasonable resolution of focussed protein spots was achieved. Many of the difficulties centred around the production of satisfactory second dimension polyacrylamide gels and their subsequent positioning on the Multiphor electrophoresis unit. It was found that a very fine layer of cover fluid was required between the cooling unit surface and the PAG gel backing film. All air bubbles had to be removed between the film and the cooling unit surface as this affected the homogenous cooling of the gel and consequently affected protein resolution. Also care had to be taken to remove any excess fluid from the surface of the gel, as this caused protein streaking. Another interesting observation revealed that the level of protein sample incorporated into the IPG immobiline drystrips, in the rehydration step, was critical to the latter resolution of the proteins, with increasing protein loading directly decreasing protein spot resolution.

A major factor that affected protein resolution was the insolubility of the membrane fractions that contained the G4NTP directed kinase. The PM fractions obtained from rat adipocyte tissue would not resolve satisfactorily using the 2-D electrophoresis system. Early gels attempted to increase the membrane fraction solubility through pre-treatment of PM samples with a 3% (w/v) SDS solubilisation buffer, with subsequent dilution into the rehydrating solution. Unfortunately the resolution of these samples was very poor (data not shown). However pre-treatment of the PM samples with Na Cholate and the subsequent removal of lipids by filtration through a Sephadex G50 column appeared to significantly enhance the resolving capacity of the solubilised proteins (see methods 5.2.2.1). The results from one of the 2-Dimensional electrophoresis gels, using this methodology, can be seen in Fig 5.2.

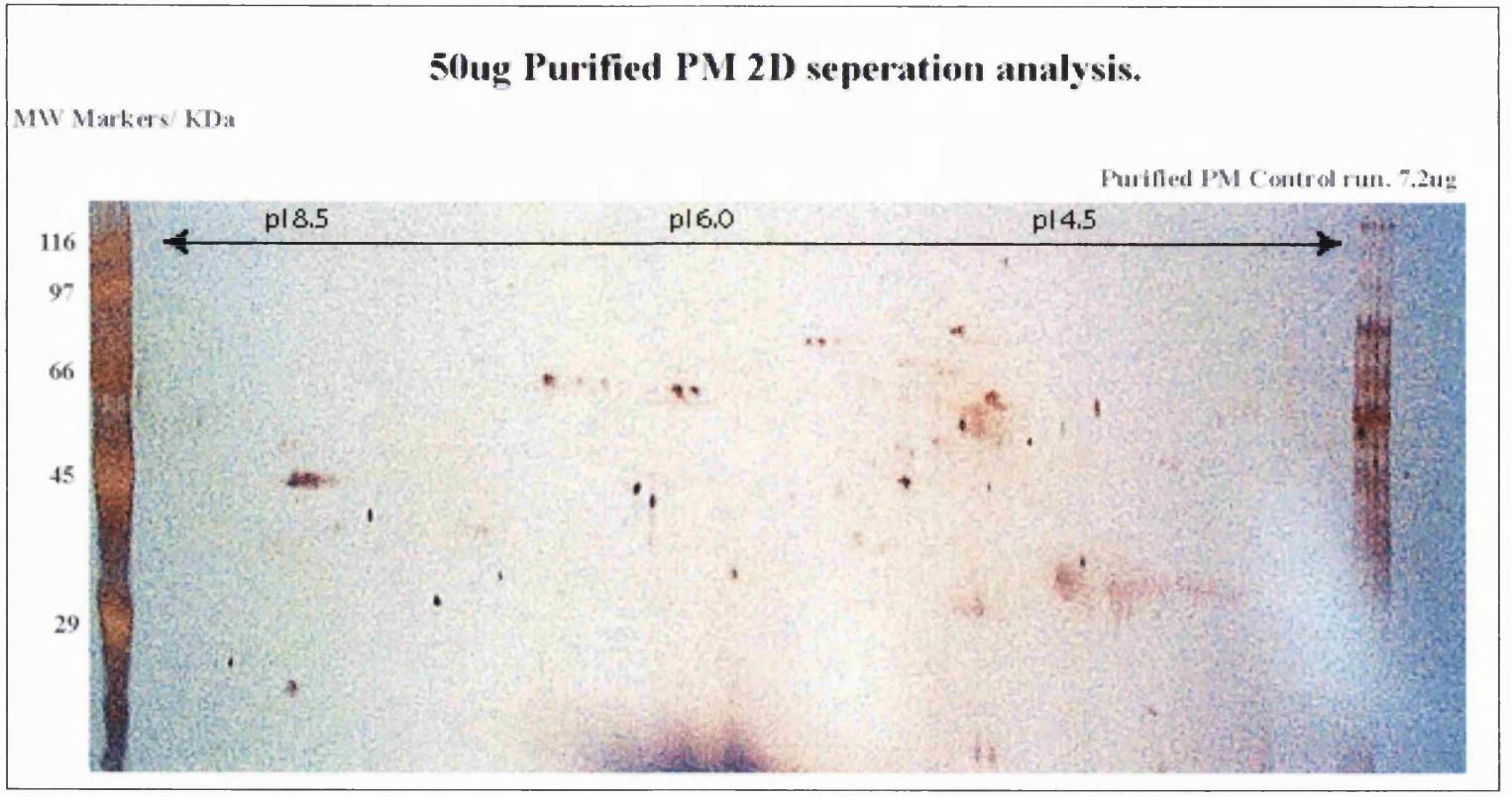

FIG 5.2: **Digital image analysis of silver stained 2-Dimensional Electrophoresis separation of Na Cholate purified PM proteins.** 50 μg of purified PM protein sample was used in the rehydration buffer for the pI 3-10 linear IPG drystrip. The developed gel shows molecular weight standards along with 7.2 μg of purified PM that were focussed in the second dimension only. The pI marker range shown on the gel was determined by overlaying a pI template developed from an identically processed 2-Dimensional Electrophoresis gel using pI markers (BioRad). The gel shown is representative of two separate studies.

The results from the purified PM fractions were encouraging with defined protein separation, reduced protein streaking, probably due to the removal of lipid components, and also good reproducibility between two separately processed gels. Only a few proteins above 90 kDa were visualised using this methodology, however many more proteins could be present that were at a low concentration and consequently were not detected by silver staining at the exposure time used.

The success of the resolution profiles seen with this methodology spurred the progression of this procedure towards a 2-Dimensional "In Gel" kinase assay. 10 μM G4NTP conjugate was incorporated into the second dimension 10% polyacrylamide gel in much the same manner as utilised for the "In Gel" kinase assay (see Chapter 1). The incorporation of the peptide conjugate into the gel precluded the visualisation of proteins by silver staining and the only protein analysis possible was through autoradiograph visualisation after the focussed second dimension gel had undergone "In Gel" kinase assay development. Unfortunately no significant specific [γ^{32}P] labelling of focussed proteins was detected using this procedure even after 48 h exposure times (results not shown). The only spots detected on the autoradiographs were caused by static, as they were not reproduced between successive exposures of the same processed gel. The reasons for this procedure not identifying the G4NTP directed kinase might include the following:

1. Incorporation of the G4NTP conjugate prevented the effective resolution of proteins in the second dimension, however this could not be confirmed due to the impracticalities of silver staining conjugate containing gels.
2. The high voltages used for the focussing of the gel may affect the homogenous distribution of the G4NTP conjugate, removing the substrate for the G4NTP directed kinase in the area where it focussed.
3. The level of G4NTP directed kinase loaded into the gel after Na Cholate purification may have been so low that it wasn't detected using the "In Gel" kinase assay.

4. The development of the "In Gel" kinase assay may require modified denaturation / renaturation periods, using the larger second dimension gel, compared with the small gels normally used for this procedure.

A G4NTP conjugate containing second dimension gel where no protein was loaded onto the gel was focussed, with the resultant silver stain showing an even distribution of the conjugate throughout the gel (results not shown). This discounted the possibility of non-homogenous distribution of the peptide as possible reason for the assay failure. Modifying the incubation times for the "In Gel" kinase assay failed to detect the G4NTP directed kinase (results not shown).

The next course of action involved going back to the drawing board and attempting to optimise the loading and resolution of LDM fractions, which contained the highest proportion of the G4NTP directed kinase. The results from the separation of the LDM fractions were initially promising (see Fig 5.3), with a greater diversity of clearly resolved proteins evident on the second dimension gel. Unfortunately when this format was progressed towards the "In Gel" kinase assay format, as previously attempted with the purified PM samples, there was no clear resolution of proteins that corresponded to the G4NTP directed kinase (results not shown). This was disappointing but suggested that the problem did not rely on the level of protein loaded onto the gel. The ineffectiveness of this system in the isolation of the G4NTP directed kinase was considered to be as a result of the G4NTP conjugate, in the second dimension gel, affecting protein resolution in this system. If the proteins had resolved then some [γ^{32}P] incorporation would be expected in protein spots where autophosphorylation had occurred, as previously identified in the "In Gel" kinase assay results discussed in Chapter 1. Clearly this method needed to be adapted in order to regain "In Gel" kinase functionality whilst still separating the G4NTP directed kinase away from other contaminating proteins of the same apparent molecular weight.

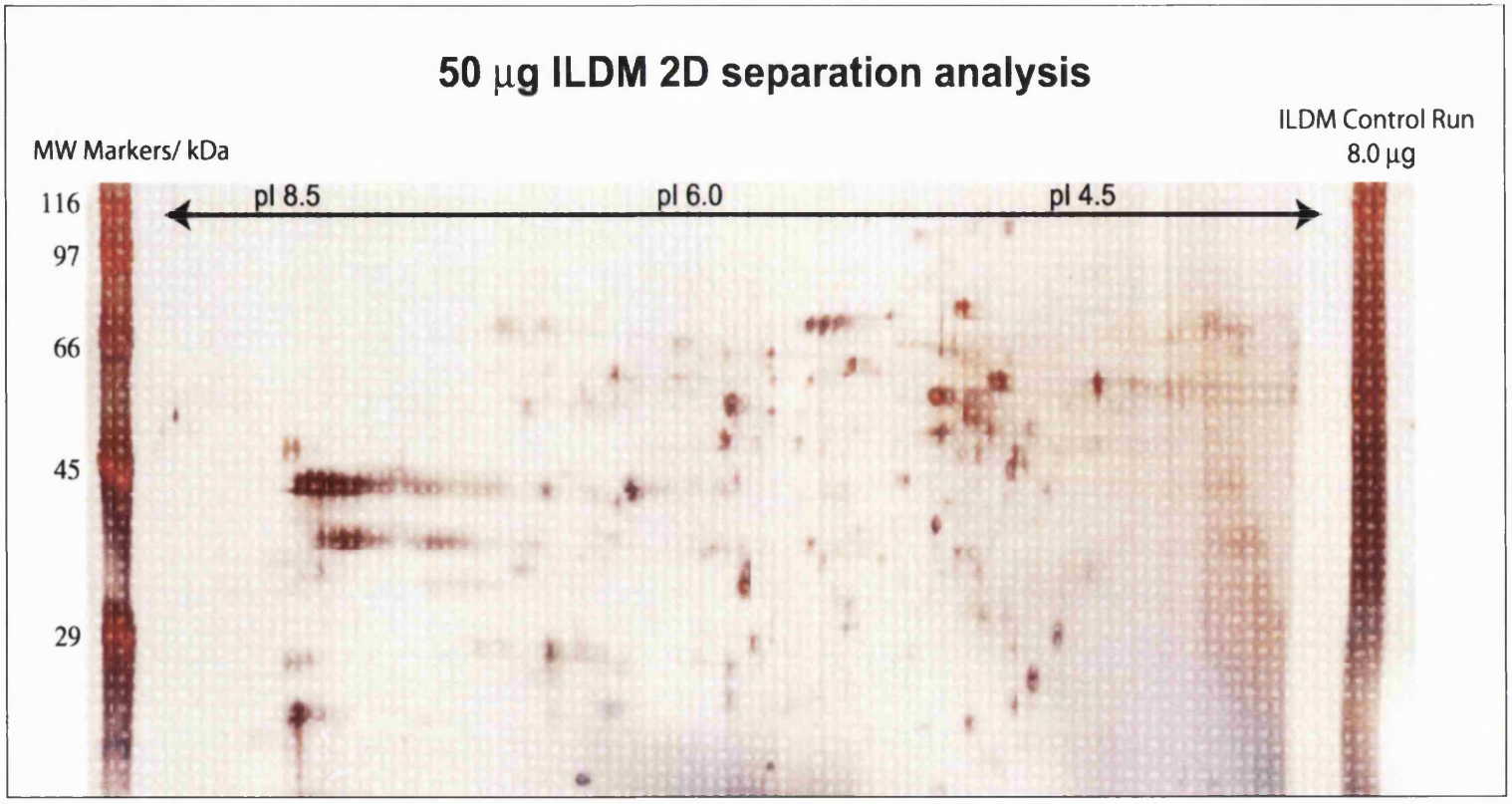

FIG 5.3: **Digital image analysis of silver stained 2-Dimensional Electrophoresis separation of ILDM proteins.** 50 µg of ILDM protein sample was used in the rehydration buffer for the pI 3-10 linear IPG drystrip. The developed gel shows molecular weight standards along with 8.0 µg of ILDM that were focussed in the second dimension only. The pI marker range shown on the gel was determined by overlaying a pI template developed from an identically processed 2-Dimensional Electrophoresis gel using pI markers (BioRad). The gel shown is representative of two separate studies however some slight variation in protein resolution was observed in the replica gel.

5.3.3 Alternative 2-Dimensional Electrophoresis Results

5.3.3.1 Development of IEF gel loading and sample transfer to the "In Gel" kinase assay

2-Dimensional Electrophoresis involves separating proteins in one dimension based upon their pI values (the pH at which the protein possess no overall charge), followed by separation of these proteins in the second dimension, based upon their molecular weight characteristics. The failing of the "In Gel" kinase assay, when incorporated into the conventional 2-Dimensional Electrophoresis system, meant that an alternative method was required. The method selected incorporated the benefits of 2-Dimensional protein focussing along with utilisation of the previously established "In Gel" kinase assay format. The new methodology meant that proteins in the second dimension would be resolved as bands rather than focussed spots and the resolution of these proteins should not be affected by incorporation of the G4NTP conjugate.

A great deal of developmental work was required to implement this alternative 2-Dimensional Electrophoresis / "In Gel" kinase assay system. Firstly the Isoelectric focussing (IEF) stage could not use the pI 3-10 linear IPG drystrip technology. Instead gels containing a mixture of ampholytes that electrophoretically focussed, within the gel, generating a pH gradient to allow IEF focussing of the protein samples were required.

Once satisfactory IEF gels could be produced the next stage required optimisation of protein loading and focussing. This stage coincided with work carried out to define the membrane association of the G4NTP directed kinase (see Chapter 2), focussing on the separation of LDM samples that appeared to contain the highest proportion of the G4NTP directed kinase. It was found that up to 50 μg of LDM sample could be loaded onto the IEF gel format, with optimal resolution obtained when the sample wicks were applied at the cathodic end of the gel. The gel stain development shown in Fig 5.4 highlights the reproducible focussing of the ILDM sample using the developed IEF methodology and displays the grid reference used for the subsequent second dimension "In Gel" kinase assay (see Fig 5.5).

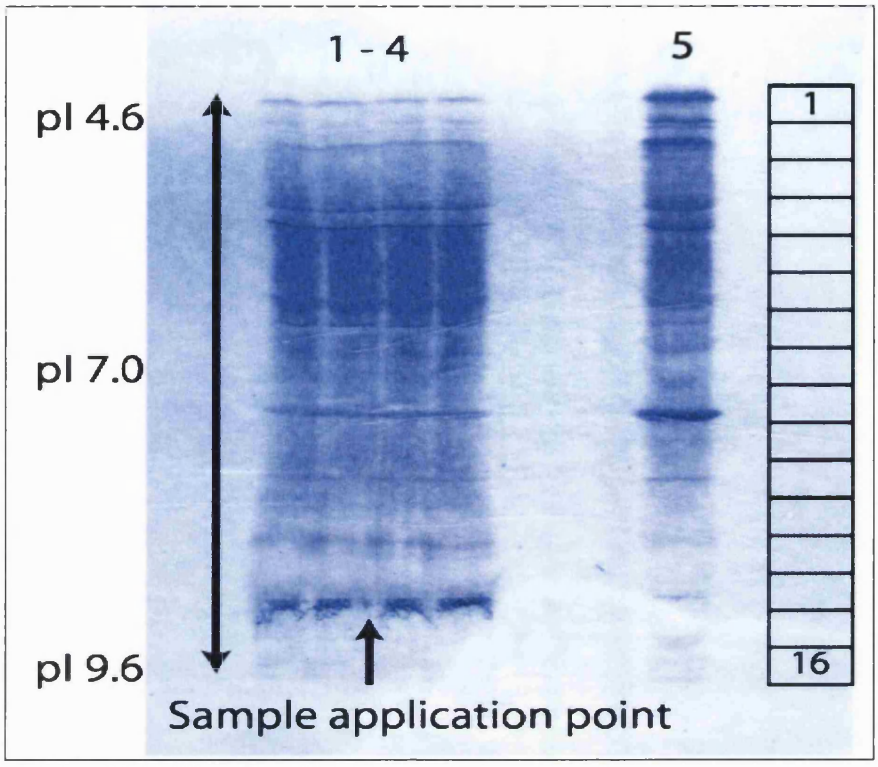

FIG 5.4: **IEF separation of ILDM samples showing tight band focussing and high lane to lane reproducibility.** Lanes 1-4 represent four identical cathodic wick applications of 50 μg ILDM samples, resolved by IEF (see methods 5.2.3.2) and visualised by Coomassie staining. The pI ranges shown were determined from IEF standards that were focussed alongside the ILDM samples (not shown on this image). Note the high degree of band resolution identity between the four ILDM samples. Sample 5 was from 50 μg of cathodic wick applied Basal Cytosol sample and was used as a solubility control. The grid reference shown next to the image highlights the size of the gel segments extracted from a replicate gel, which was not stained for visualisation. The gel segments comprised around 1 and a half ILDM sample lanes, equivalent to 75 μg total loading over all 16 gel segments. The image shown was typical of the resolution obtained using this method of application with 50 μg of LDM sample.

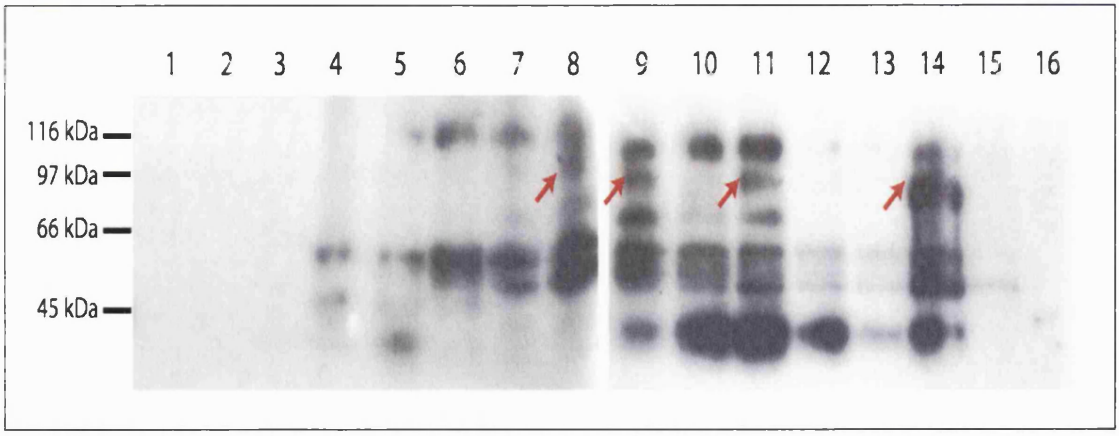

FIG 5.5: **Autoradiograph development of an Alternative 2-Dimensional Electrophoresis "In Gel" kinase assay.** Sixteen gel segments were taken from an identical IEF gel to that shown in Fig 5.4, according to the grid reference shown in Fig 5.4. The segments were heated for 20 min with sample buffer and β-mercaptoethanol and then loaded onto 10 μM G4NTP conjugate containing 10 % polyacrylamide gels. The gels were processed in the conventional manner for "In Gel" kinase assay, with [γ32P] incorporation detected through autoradiography. The image shown represents a three day autoradiograph exposure. The red arrows indicate potential areas of G4NTP directed kinase detection, with the strongest detection observed in gel segment 14, which corresponds to the area of sample application (see Fig 5.4).

The results shown in Fig 5.4 and 5.5 were initially promising as they showed protein resolution in the first dimension and second dimension gels. Also autophosphorylation of proteins within the second dimension "In Gel" kinase assay gel was detected, something which was not achievable in the conventional 2-Dimensional Electrophoresis system initially employed. The resuts did however highlight the fact that recovery of the G4NTP directed kinase was limited using crude LDM samples.

The length of autoradiograph exposure required to obtain protein bands that corresponded to the apparent molecular weight of the G4NTP directed kinase was considerably longer than for conventional "In Gel" kinase assays. This may be due to a restricted amount of the kinase transfering from the sample wick into the IEF gel. Indeed the highest detection of a

band that could represent the G4NTP directed kinase was found in gel segment 14, corresponding to the area where the sample wick was placed on the IEF gel.

In an attempt to improve protein solubilty denaturing IEF gels were utilised, containing 8 M Urea and 2% (v/v) NP40. Although this was an accepted methodology (See 2117 Multiphor II Electrophoresis System Handbook (Amersham)) a major problem encountered with this system involved re-crystalisation of urea during the focussing steps. To overcome this problem the temperature of the cooling plate was increased, however this detrimentally affected protein resolution to a degree where this system could not be further utilised for second dimensional focusing.

Potential reasons for poor protein solubilty were investigated with the following factors found to be significant to this process:

1. Particulate matter can severely restrict the level of protein transfer from the sample wick to the IEF gel.
2. The protein may focus at the site of application and so does not easily transfer from the wick into the Gel
3. The protein may be associated with a large protein complex or lipid arrangement and is thus too large to enter into the native IEF gel.

The findings detailed in Chapter 2 identified that a large proportion of the G4NTP directed kinase appeared to be associated ionically either to membranous elements or cytoskeletal complexes in the LDM and treatment with 1 M NaCl significantly increased the solubility of the kinase.

As a consequence of these studies a new methodology was developed in which the LDM fractions were treated with 1 M NaCl. The insoluble material was pelleted and the soluble material dialysed against 10 mM Hepes buffer (pH 7.2) and then concentrated down to an appreciable volume for IEF gel application. This procedure not only removed large protein complex solubility problems but also eliminated any particulate contamination.

An initial IEF gel tested the affects of protein solubility and resolution when treated samples were applied at various positions on the gel (see Fig 5.6) The use of sample application strips, as opposed to the conventional application wicks, was also analysed to ascertain if this had appreciable affects on protein solubility.

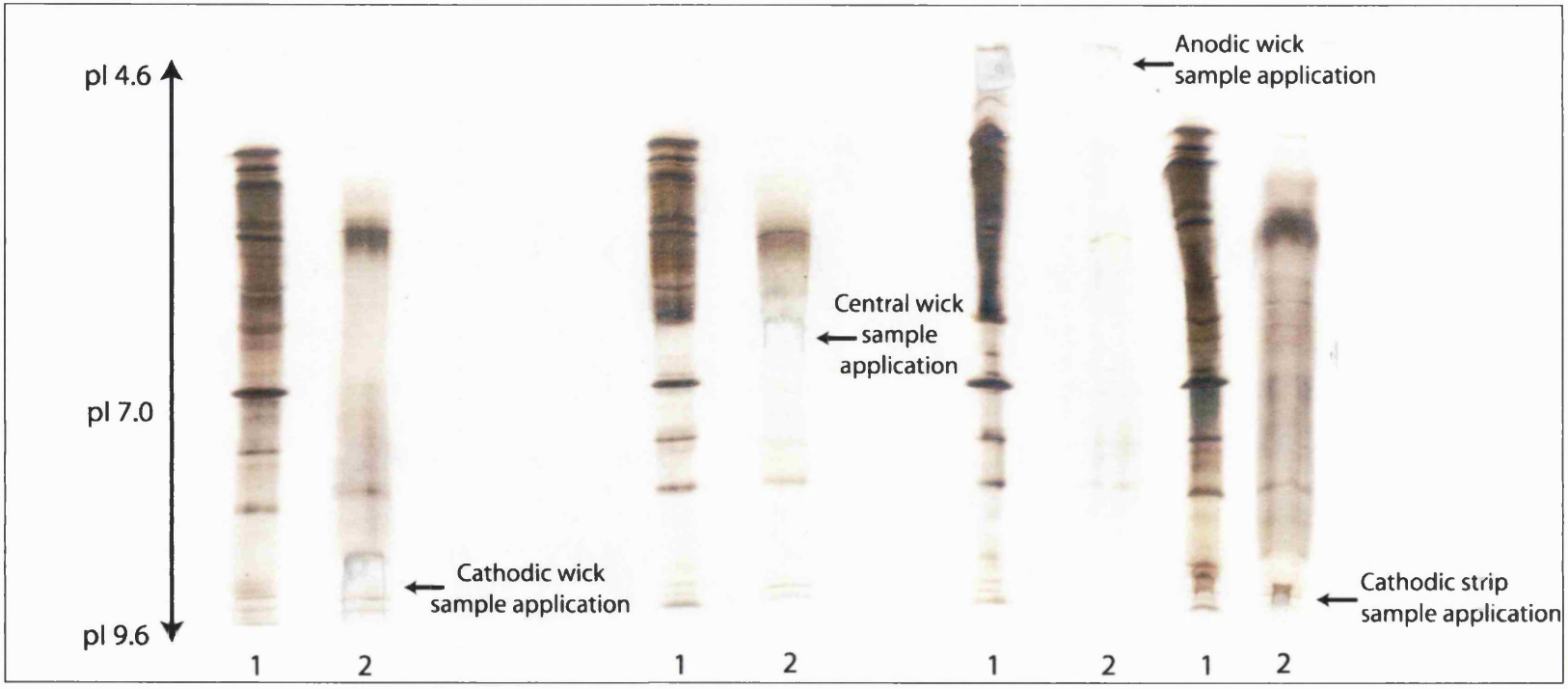

FIG 5.6: **Silver stain development of an IEF gel, highlighting protein focussing of cytosolic and 1 M NaCl solubilised protein samples using varying sample application sites and application media.** 20 μg Basal Cytosol (1) or 8 μg of dialysed 1 M NaCl solubilised ILDM sample (2) were applied onto a IEF gel using traditional application wicks or using a sample application strip that allowed direct contact of the sample with the gel. The samples were applied in one of three positions, Cathodic, Central or Anodic, and the IEF gel focussed as detailed in methods 5.2.3.2. The focused gel was visualised using the silver staining protocol with the pI range determined from IEF protein standards (Bio-Rad) which have been removed from this image for ease of interpretation.

.

The results showed that the level of protein detected at the point of application was dramatically reduced from that seen using crude LDM fractions (see Fig 5.4), showing that protein solubility and retention were reduced using the treated LDM samples.

Interestingly anodic sample application produced poor focussing of both the treated ILDM and basal cytosolic samples, highlighting the importance of correct sample placement to achieve optimal protein recovery on the IEF gel. Cathodic sample application appeared to produce the optimal focussing range for the majority of the detected proteins. Also the image showed that applying the ILDM treated sample directly to the gel, using the sample application strips, increased the level of protein entering the IEF gel compared to that seen using the conventional sample wicks. Increasing the level of protein entering the IEF gel, whilst still retaining protein resolution, was vital for the second dimension "In Gel" kinase assay and consequently sample application strips were used for all further IEF focussing experiments

5.3.3.2 Characterisation of proteins in the treated LDM samples to determine functionality of the Alternative 2-Dimensional Electrophoresis system.

5.3.3.2.1 IEF characterisation

Although the high salt treatment and subsequent dialysis of LDM protein samples did not adversely affect the resolution of proteins on the IEF gel it was considered prudent to check that the G4NTP directed kinase was still detectable by "In gel" kinase assay, before the Alternative 2-Dimensional Electrophoresis procedure was pursued. To this end samples from the high salt insoluble pellet and the dialysed high salt supernatant were subjected to western blot analysis using antibodies directed against GLUT4 and the p85 subunit of PI3K. These proteins differentially partition into one of the two phases under high salt treatment and were used to confirm that the procedure was functioning correctly (see Image A Fig 5.7). The samples were also tested in the "In Gel" kinase assay using 10 μM G4NTP conjugate containing gels to ascertain the degree of kinase activity detected after ILDM sample treatments (see Image B Fig 5.7).

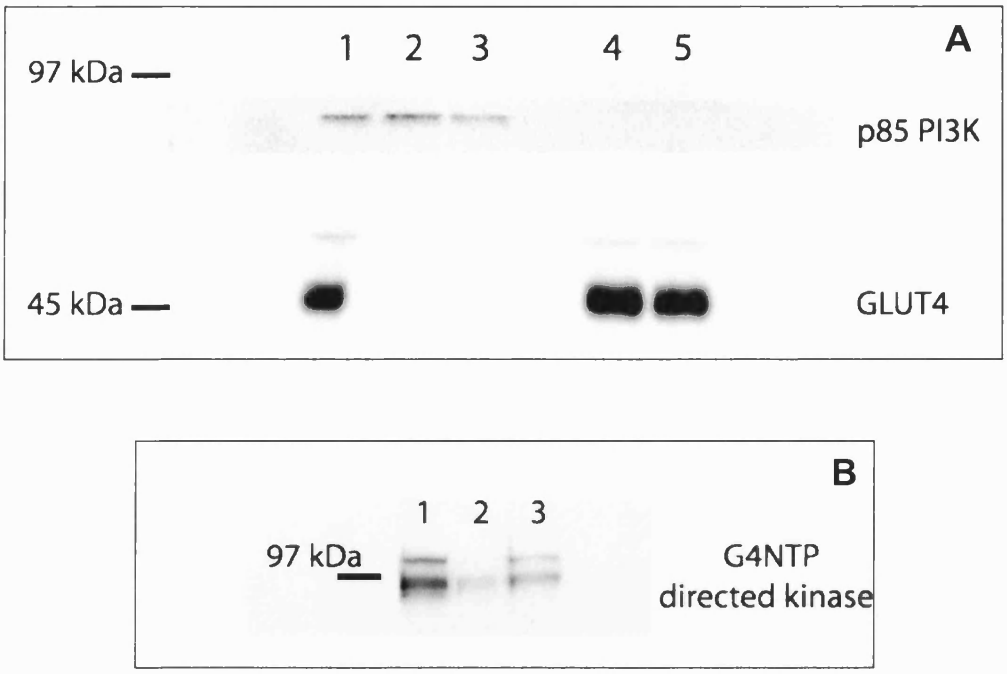

FIG 5.7: **Recovery of LDM proteins after treatment with 1 M NaCl and dialysis into 10 mM Hepes (pH 7.2).** Image **A** western blot analysis; Lane 1: 20 μg ILDM loading control; Lanes 2-3: 8 μg of dialysed ILDM high salt supernatant sample; Lanes 4-5: 20 μg of ILDM pellet after high salt treatment. GLUT4 was detected using the C-Terminal GLUT4 affinity purified antibody at 1:4000 dilution and p85 PI3K using the monoclonal antibody at 1:1000 dilution. Image **B** "In Gel" kinase assay analysis of 90 min autoradiograph exposure. Lane 1: 30 μg of ILDM loading control; Lane 2: 40 μg of high salt pellet; Lane 3: 16 μg of dialysed high salt ILDM supernatant sample. The results show that PI3K and the majority of G4NTP directed kinase partitioned into the high salt solubilised fraction. Subsequent dialysis did not adversely affect PI3K protein recovery, however the level of kinase activity was reduced.

The western blot analysis of the high salt treated fractions concurred with earlier findings (See Chapter 2 Section 4.3.1), highlighting integral membrane proteins, like GLUT4, remained insoluble under 1 M NaCl treatment, whereas ionically associated proteins such as PI3K partition into the soluble fraction under the same conditions. Thus it appeared that the dialysis step did not adversely affect protein recovery.

The findings from the "In Gel" kinase assay were encouraging in that G4NTP directed kinase activity was detectable in the dialysed, high salt treated, ILDM soluble sample. However the level of kinase activity was slightly lower than expected, with some of this attributed to retention of a fraction of the kinase in the insoluble pellet. Although only 16 μg of ILDM treated supernatant was loaded this would be expected to consist of a higher proportion of the G4NTP directed kinase compared with 16 μg ILDM, however quantification of the level of this expected increase was not possible. Nevertheless the results supported the progression of the ILDM treated sample through IEF and onto second dimensional focussing and "In Gel" kinase assay analysis.

5.3.3.2.2 Second Dimensional focussing / "In Gel" kinase assay characterisation

The resolution of the ILDM treated sample on the second dimension gel, after primary focussing on the IEF gel, was investigated by generating an IEF gel containing two identical series of four sample application strip loaded dialysed ILDM samples. After IEF the two areas containing pI resolved samples were dissected into twelve equal gel segments, which were then treated and loaded onto 10% polyacrylamide large slab gels as detailed in methods 5.2.2.3. In addition to the gel segments the remaining solution from the application strips was mixed with sample buffer and was loaded onto the gels alongside 40 μg of ILDM loading control. One series of gel segments were used for "In Gel" kinase assay to detect isolated G4NTP directed kinase whilst the other series of gel fragments were used for western blot analysis of Akt 2 to ascertain if ionically associated proteins could be isolated using this system, (See Fig 5.8).

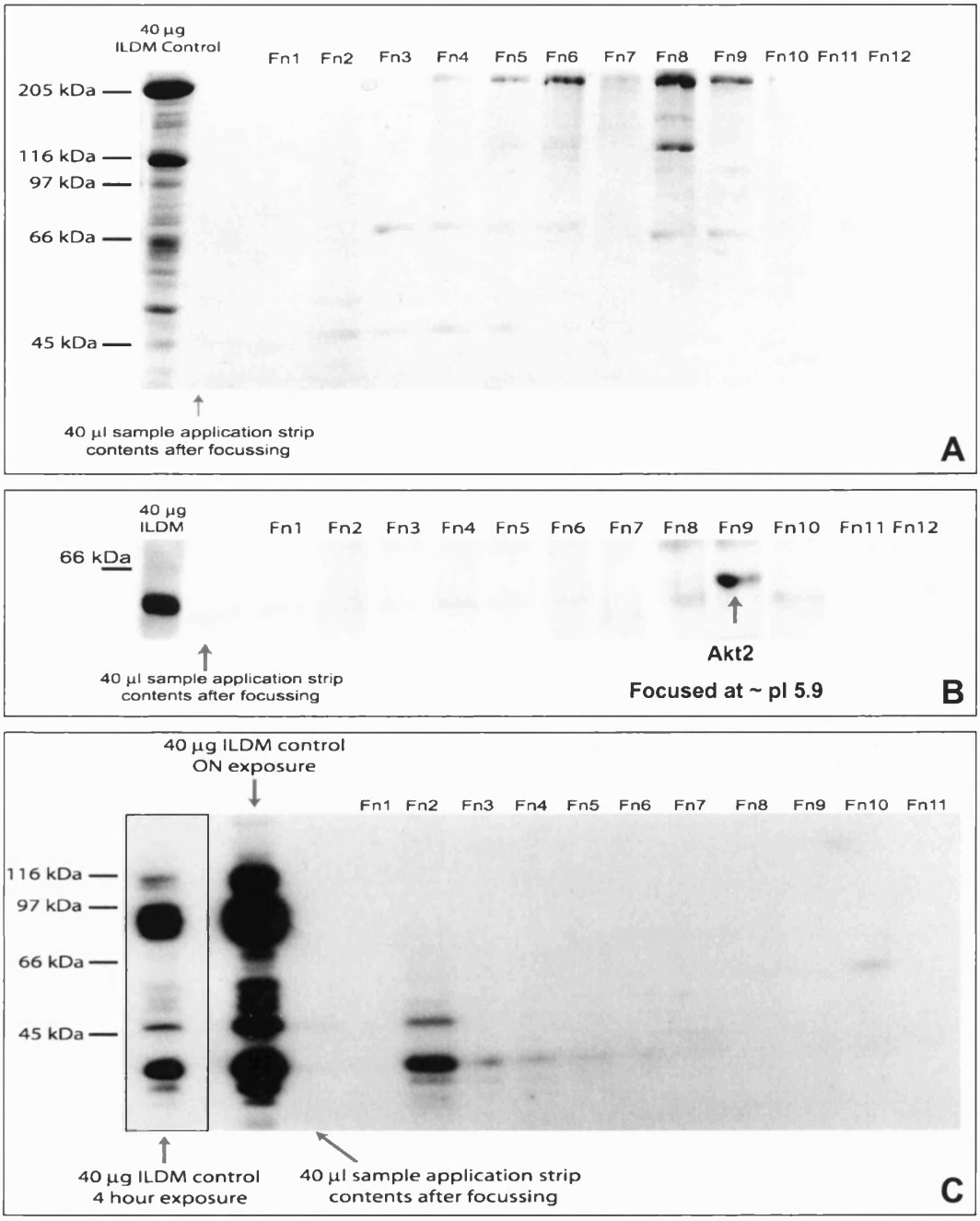

FIG 5.8: **Analysis of the Alternative 2-Dimensional Electrophoresis system.** Dialysed, high salt treated, ILDM samples were applied to an IEF gel at a cathodic position using sample application strips in two lots of four samples and processed as detailed. Two lots of 12 gel fractions were disected from the IEF gel and treated as detailed. The fractions were then transferred to two large 10% polyacrylamide slab gels. One was used for western blotting for Akt 2 (Image B) with the post transfer gel Coomassie stained (Image A). The other gel contained 10 µM G4NTP conjugate and was used for "In Gel" kinase assay analysis (Image C).

The Akt 2 western blot analysis, from one series of gel segments, provided the first tangible evidence that the alternative 2-Dimensional Electrophoresis system could isolate ionically associated proteins, derived from LDM samples. The gel segment in which Akt 2 was detected appeared fractionally higher than that observed in the ILDM control lane. However this should be expected, as there would be some lag time in the transfer of proteins out of the IEF gel segment into the stacking gel. This would not occur with the control sample that was directly loaded into the stacking gel wells. By correlating the gel segment against the IEF markers on the original IEF gel the pI of this segment was determined to lie in the range of pI 5.9 – 6.0. Interestingly the theoretical pI for rat Akt 2 (Swiss-Prot Accession number P47197) was pI 5.98, lending support to the authentication of the Akt 2 detected on the western blot and also providing evidence that satisfactory resolution of proteins was achieved both in terms of Isoelectric and molecular weight determinates.

The results from the "In Gel" kinase assay, using large slab gels, showed that gel size did not adversely affect the functionality of the assay. This was highlighted with the 40 μg ILDM control that revealed a distinctive band at around 95 kDa, corresponding to the G4NTP directed kinase. However the control was loaded directly onto the second dimension gel and did not confirm that recovery of kinase activity was possible after the protein was isoelectrically focussed. Unfortunately the "In Gel" kinase assay results obtained from the IEF gel segments did not identify any protein bands corresponding to the G4NTP directed kinase. This did not appear to be a result of solubility problems as the contents from the sample application strips, after IEF, did not reveal any detectable levels of the kinase, even after 3 day autoradiograph exposures (data not shown).

5.3.4 Conclusions

The lack of kinase detection using the alternative 2-Dimensional Electrophoresis system was perplexing, especially as the procedure was validated with Akt 2 isolation and analysis. It appeared that something in the IEF procedure dramatically reduced the activity of the G4NTP directed kinase, preventing its subsequent detection in the "In Gel" kinase assay.
One possible explanation was that the pH at which the kinase develops a neutral charge (the proteins pI) was high or low enough that it adversely affected the recovery of kinase activity in the "In gel" kinase assay. To test this theory LDM samples were incubated in high pH solution (0.1 M Na_2CO_3 (pH 11.4) for 30 min, on ice. The insoluble material was pelleted as for the 1 M NaCl treatments. The pellet and the chloroform / methanol precipitated soluble proteins were resuspended in sample buffer and analysed by "In Gel" kinase assay (see Fig 5.9).

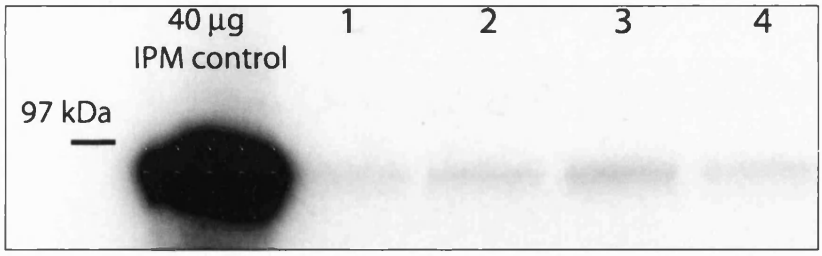

FIG 5.9: **High pH treatment dramatically reduces G4NTP directed protein kinase activity detection using the "In Gel" kinase assay.** 100 µg BLDM and ILDM samples were treated with 0.1 M Na_2CO_3 (pH 11.4) with half of the resultant insoluble and soluble proteins (50 µg equivalent) isolated and resuspended in sample buffer with 10% (v/v) β-Mercaptoethanol. The autoradiograph image shown was from a 3 h exposure with 40 µg IPM loading control for kinase activity comparison. Lane 1: ILDM high pH soluble protein fraction (chloroform / methanol precipitated); Lane 2 ILDM high pH insoluble protein fraction; Lane 3: BLDM high pH soluble protein fraction (chloroform / methanol precipitated); Lane 4: BLDM high pH insoluble protein fraction. The "In Gel" kinase assay used 10 µM G4NTP conjugate and 50 µCi [γ^{32}P] ATP.

The results from this initial study were compelling with a dramatic reduction in the level of kinase activity apparent in the high pH treated LDM samples. These results indicated that pH appeared to modulate the recovery of G4NTP directed kinase activity and the IEF step could indeed render a large proportion of the kinase inactive.

Bischoff and colleagues described that retention of some remnant of secondary or higher structure appeared to be crucial for recovery of kinase activity following SDS-PAGE (Bischoff *et al.*, 1998). They postulated that small islands of higher-order structure were retained within denatured polypeptide chains. These areas serve as nucleation sites for the subsequent refolding of the protein into a catalytically competent conformation and provided what was termed "molecular memory" that pre-disposed proteins to fold into their native confirmation under suitable conditions.

It is conceivable that extremes of pH may be deleterious to the conservation of these islands of higher order structure and consequently limit the level of renaturation of the G4NTP directed kinase. Effective renaturation of the kinase is the foundation for "In Gel" kinase assay function and a significant reduction in this could account for the apparent lack of active kinase observed in the second dimension gels observed.

GAD65 kinase activity appears to be directly modulated by alterations in the pH of its surroundings (see Introduction 1.5.5.2) with conformational modifications in either or both GAD65 and GAD65 kinase potentially accounting for these observations. Differential pH environments could modify charge characteristics of certain residues, within these proteins, that intrinsically modulate the level of kinase activity.

The G4NTP directed kinase appears to share many of the same traits as the GAD65 kinase and also seems to be particularly sensitive to pH with IEF abolishing the recovery of G4NTP directed kinase activity. Clearly this severely hampers the isolation of the G4NTP directed kinase using kinase activity as the means of detection.

Future work may need to reassess the isolation procedure and try to overcome these inactivation issues. Ion exchange chromatography could be used instead of the IEF gel step to assess if kinase activity was recoverable in this format. There is also the option of running multiple "In Gel" kinase

assays and attempting to perform autoradiograph analysis without drying the gels down. The autoradiographs could then be used as templates from which gel bands corresponding to the G4NTP directed kinase could be removed. The proteins within the gel segment could be further separated on an 8% polyacrylamide gel, removing the G4NTP conjugate and further separating proteins within the 90 kDa region. The phosphorylated proteins could then be re-detected using autoradiography and excised for protein sequence analysis.

6 Overall Conclusions

When GAD65 is reversibly anchored to membranes of synaptic vesicles it appears to be phosphorylated on multiple sites by an uncharacterised membrane associated kinase. Interestingly an area within this multiple phosphorylation site (GSEDGE) bears high sequence identity to an area downstream of the FQQI motif found in the cytoplasmic amino terminal of GLUT4. The aims of the research presented were to ascertain if this region of GLUT4 was phosphorylated and to identify the kinase responsible.

Phosphorylation of the cytoplasmic carboxyl terminal of GLUT4 has been demonstrated (see Introduction 1.5.2.5). Although no conclusive evidence of cytoplasmic amino terminal GLUT4 phosphorylation was documented in previous literature the methods for studying this phenomenon were restricted to *in vitro* phosphorylation assays, which analysed tryptic digested GLUT4 fragments. High background readings coupled with the lack of a GLUT4 amino terminal antibody, to specifically distinguish between the digested cytoplasmic domains of GLUT4, meant that small levels of phosphorylation in the amino terminal of GLUT4 were not detected in previous studies.

The generation of antibodies to phosphorylated G4NTP described here has provided some indication that phosphorylation of the N terminal of GLUT4 might occur *in vivo*. Supplementary studies by colleagues in the laboratory have provided preliminary data supporting the specificity of this detection in isolated adipocytes and cardiomyocytes (personal communication with Dr. Francoise Koumanov and Dr. Jing Yang).

Immobilisation of a peptide corresponding to the postulated phosphorylation site (G4NTP), within a gel matrix, provided a highly sensitive detection system to establish if any kinases phosphorylated this region of GLUT4. The procedure was termed the "In Gel" kinase assay and a kinase was found in the assay that appeared to display enhanced autophosphorylation and specifically phosphorylated the G4NTP. The kinase appeared as a doublet of around 90 kDa, which was considered to represent two post-translational modified versions of the same kinase. The doublet was considered to be as a result of differing phosphorylation states of the

protein. Further study will be required to confirm this theory, with the isolation of the kinase providing many of the answers.

The sensitivity of kinase detection was enhanced through peptide conjugation to poly-$_L$-lysine. This not only increased retention of the peptide within the gel matrix but also appeared to enhance specific directed phosphorylation of the peptide. The charged local environment, provided by poly-$_L$-Lysine potentially increases specific kinase interaction with the peptide, resulting in its increased phosphorylation.

Further characterisation of the kinase revealed that it was predominantly associated with intracellular membrane compartments, although significant levels of G4NTP directed kinase were detected in the PM fractions derived from rat adipocyte cell preparations. The nature of the membrane association appeared to be ionic, however a population of the kinase appeared to be involved with dynamic lipid raft complexes.

GLUT4 trafficking modulation through the interaction of a series of GLUT4 motifs with adapter complex proteins and cytoskeletal-associated proteins have been described in the literature, although the nature of these interactions remain to be established (see Introduction 1.5). If we consider GLUT4 in the three dimensional context of the proteins architecture then this creates the possibility that different structural presentations, of combinations of motifs, may determine the trafficking fate of GLUT4 in differing cellular locations.

The structural recognition theory would fit with the experimental evidence presented here, with the putative G4NTP directed kinase acting at the PM and intracellular compartments such as the PR-GSC. The GSEDGE motif, which appears to be phosphorylated by the kinase detected in the "In Gel" kinase assay, may be an extension of the upstream FQQI motif or a separate motif recognised by GGAs or adapter complexes (see Introduction 1.5.3). Phosphorylation of the GSEDGE motif may modify the predicted β turn at the adjacent glycine residue, altering the recognition of this motif by one set of adapter proteins, GGA's or cytoskeletal associated proteins to one-another. A similar scenario has been documented within the acidic cluster (AC) motif of furin. The TGN localisation of furin is thought to be achieved through its retrieval from the post-TGN endosomal compartment by binding of the novel cytosolic sorting protein phosphofurin acidic cluster

sorting protein1 (PACS-1) (Wan *et al.*, 1998). The action of AP1 and PACS-1 together generates a situation where furin is in a bi-cycling loop between the TGN and the post-TGN endosomal compartment. The phosphorylation of the AC motif, by CKII, is thought to mediate its interaction with PACS-1 and the balance between AC dephosphorylation by PP2A and its phosphorylation by CKII determines the predominance of furin's localisation (Jones *et al.,* 1995; Molloy *et al.*, 1998).

The bi-cycling of GLUT4 between multiple sites under the control of differential protein interactions is an appealing idea, however the nature of the G4NTP directed kinase in this postulated trafficking mechanism remains to be established.

The kinase may be in a large protein complex associated with the cytoskeleton, with populations of the kinase dynamically associated with lipid raft structures. Lipid rafts are not only found in the PM but also in many intracellular compartments, including the TGN and recycling endosomes. They have been implicated in promoting curvature of membranes to facilitate vesicle docking and recognition of motifs in secretory granule biogenesis (Tooze *et al.*, 2001). Lipid raft association may mimic the stabilised microenvironment seen in the "In Gel" kinase assay, whereby the kinase activity is optimised and GLUT4 can be brought into close juxtaposition. The putative perinuclear detection of N terminal phosphorylated GLUT4, through phosphorylated G4NTP directed antibody analysis, may therefore implicate N terminal GLUT4 phosphorylation in the directed sorting of GLUT4 between the TGN, PR-GSC and DV-GSC (see introduction 1.5.1), via modulated interaction with adapter proteins and GGAs.

The G4NTP directed kinase, like the GAD65 kinase, appeared to be highly regulated by pH, with almost complete activity loss at high pH. The activity of GAD65 kinase is directly modulated by v-ATPase and this may provide another interesting level of control for the GLUT4 trafficking model. Insulin stimulation leads to a signalling cascade that may inactivate certain v-ATPases, resulting in the alkalisation of certain intracellular compartments. The increase in intracellular pH may result in the inactivation of the G4NTP directed kinase and consequently decrease the level of N terminal GLUT4 phosphorylation. By inference this would alter the bi-cycling mechanism and

consequently shift the balance of GLUT4 trafficking, or cellular sorting, between the PR-GSC and the DV-GSC or the TGN/recycling endosomes and the PR-GSC. The population of the kinase detected in the PM may also be involved in an internalisation process. Further studies using the phosphorylated N terminal GLUT4 directed antibody should address these specific questions. The effects may be restricted to the intracellular compartments, with little influence on the direct translocation of GLUT4 to the PM. Also only a small population of GLUT4 may be N terminally phosphorylated at any one time and therefore gross changes in GLUT4 trafficking are unlikely.

Future studies need to establish an isolation procedure to overcome the inactivation issues encountered to date, with some potential areas for development discussed in Chapter 3. The results obtained with the phosphorylated N terminal GLUT4 directed antibody are forming the foundation for future research and should ensure that future investigation of this area of GLUT4 trafficking is pursued.

7 References

Ahmed, Z, Smith, BJ, and Pillay, TS. (2000). The APS adapter protein couples the insulin receptor to the phosphorylation of c-Cbl and facilitates ligand-stimulated ubiquitination of the insulin receptor. *FEBS Lett.* **475** (1), 31-34.

Al Hasani, H, Kunamneni, RK, Dawson,K, Hinck,CS, Muller-Wieland,D, and Cushman,SW. (2002). Roles of the N- and C-termini of GLUT4 in endocytosis. *J Cell Sci.* **115** 131-140.

Allende, JE and Allende, CC. (1995). Protein kinases. 4. Protein kinase CK2: an enzyme with multiple substrates and a puzzling regulation. *FASEB J.* **9** (5), 313-323.

Anai,M, Ono,H, Funaki,M, Fukushima,Y, Inukai,K, Ogihara,T, Sakoda,H, Onishi,Y, Yazaki,Y, Kikuchi,M, Oka,Y, and Asano,T. (1998). Different subcellular distribution and regulation of expression of insulin receptor substrate (IRS)-3 from those of IRS-1 and IRS-2. *J Biol.Chem.* **273** (45), 29686-29692.

Anderson, RG, Brown, MS, and Goldstein,JL. (1977). Role of the coated endocytic vesicle in the uptake of receptor-bound low density lipoprotein in human fibroblasts. *Cell* **10** (3), 351-364.

Araki, E, Lipes, MA, Patti, ME, Bruning, JC, Haag, B, III, Johnson, RS, and Kahn, CR (1994). Alternative pathway of insulin signalling in mice with targeted disruption of the IRS-1 gene. *Nature* **372** (6502), 186-190.

Araki, S, Yang, J, Hashiramoto, M, Tamori, Y, Kasuga, M, and Holman, GD. (1996). Subcellular trafficking kinetics of GLU4 mutated at t. *Biochem.J.* **315 (Pt 1)** 153-159.

Arcaro, A, Volinia, S, Zvelebil, MJ, Stein, R, Watton, SJ, Layton, MJ, Gout, I, Ahmadi, K, Downward, J, and Waterfield, MD. (1998). Human phosphoinositide 3-kinase C2beta, the role of calcium and the C2 domain in enzyme activity. *J.Biol.Chem.* **273** (49), 33082-33090.

Arsenis, G. (1995). Activation of the Na+/H+ exchanger by cellular pH and extracellular Na+ in rat adipocytes; inhibition by isoproterenol. *Endocrinology* **136** (7), 3128-3136.

Babitt, J, Trigatti, B, Rigotti, A, Smart, EJ, Anderson, RG, Xu, S, and Krieger, M. (1997). Murine SR-BI, a high density lipoprotein receptor that mediates selective lipid uptake, is N-glycosylated and fatty acylated and colocalizes with plasma membrane caveolae. *J Biol.Chem.* **272** (20), 13242-13249.

Backer, JM, Myers, MG, Jr., Sun, XJ, Chin, DJ, Shoelson, SE, Miralpeix, M, and White, MF. (1993). Association of IRS-1 with the insulin receptor and the phosphatidylinositol 3'-kinase. Formation of binary and ternary signaling complexes in intact cells. *J.Biol.Chem.* **268** (11), 8204-8212.

Baird, B, Sheets, ED, and Holowka, D. (1999). How does the plasma membrane participate in cellular signaling by receptors for immunoglobulin E? *Biophys Chem.* **82** (2-3), 109-119.

Ball, CL, Hunt, SP, and Robinson, MS. (1995). Expression and localization of alpha-adaptin isoforms. *J Cell Sci.* **108 (Pt 8)** 2865-2875.

Bandyopadhyay, G, Standaert, ML, Kikkawa, U, Ono, Y, Moscat, J, and Farese, RV. (1999). Effects of transiently expressed atypical (zeta, lambda), conventional (alpha, beta) and novel (delta, epsilon) protein kinase C isoforms on insulin-stimulated translocation of epitope-tagged GLUT4 glucose transporters in rat adipocytes: specific interchangeable effects of protein kinases C-zeta and C-lambda. *Biochem.J.* **337 (Pt 3)** 461-470.

Baumann, CA, Brady, MJ, and Saltiel, AR. (2001). Activation of glycogen synthase by insulin in 3T3-L1 adipocytes involves c-Cbl-associating protein (CAP)-dependent and CAP-independent signaling pathways. *J.Biol.Chem.* **276** (9), 6065-6068.

Baumann, CA, Ribon, V, Kanzaki, M, Thurmond, DC, Mora, S, Shigematsu, S, Bickel, PE, Pessin, JE, and Saltiel, AR. (2000). CAP defines a second signalling pathway required for insulin-stimulated glucose transport. *Nature* **407** (6801), 202-207.

Beck, KA and Keen, JH. (1991). Interaction of phosphoinositide cycle intermediates with the plasma membrane-associated clathrin assembly protein AP-2. *J Biol.Chem.* **266** (7), 4442-4447.

Begum, N, Leitner, W, Reusch, JE, Sussman, KE, and Draznin, B. (1993). GLUT-4 phosphorylation and its intrinsic activity. Mechanism of Ca(2+)-induced inhibition of insulin-stimulated glucose transport. *J.Biol.Chem.* **268** (5), 3352-3356.

Beltzer, JP and Spiess, M. (1991). In vitro binding of the asialoglycoprotein receptor to the beta adaptin of plasma membrane coated vesicles. *EMBO J* **10** (12), 3735-3742.

Benitez, MJ, Mier, G, Briones, F, Moreno, FJ, and Jimenez, JS. (1997). A surface-plasmon-resonance analysis of polylysine interactions with a peptide substrate of protein kinase CK2 and with the enzyme. *Biochem.J.* **324 (Pt 3)** 987-994.

Bereziat, V, Kasus-Jacobi, A, Perdereau, D, Cariou, B, Girard, J, and Burnol, AF. (2002). Inhibition of insulin receptor catalytic activity by the molecular adapter grb14. *J Biol.Chem.* **277** (7), 4845-4852.

Bickel, PE, Scherer, PE, Schnitzer, JE, Oh, P, Lisanti, MP, and Lodish, HF. (1997). Flotillin and epidermal surface antigen define a new family of caveolae- associated integral membrane proteins. *J.Biol.Chem.* **272** (21), 13793-13802.

Bischoff, KM, Shi, L, and Kennelly, PJ. (1998). The detection of enzyme activity following sodium dodecyl sulfate- polyacrylamide gel electrophoresis. *Anal.Biochem.* **260** (1), 1-17.

Bonadonna, RC, Del Prato, S, Saccomani, MP, Bonora, E, Gulli, G, Ferrannini, E, Bier, D, Cobelli, C, and DeFronzo, RA. (1993). Transmembrane glucose transport in skeletal muscle of patients with non-insulin-dependent diabetes. *J.Clin.Invest* **92** (1), 486-494.

Brown, DA and London, E. (1998). Functions of lipid rafts in biological membranes. *Annu.Rev.Cell Dev.Biol.* **14** 111-136.

Brown, DA and London, E. (2000). Structure and function of sphingolipid- and Cholesterol-rich Membrane Rafts. *J.Biol.Chem.* **275** (23), 17221-17224.

Brown, DA and Rose, JK. (1992). Sorting of GPI-anchored proteins to glycolipid-enriched membrane subdomains during transport to the apical cell surface. *Cell* **68** (3), 533-544.

Brown, RA, Domin, J, Arcaro, A, Waterfield, MD, and Shepherd, PR. (1999). Insulin activates the alpha isoform of class II phosphoinositide 3-kinase. *J Biol.Chem.* **274** (21), 14529-14532.

Bruckner, K, Pablo, LJ, Scheiffele, P, Herb, A, Seeburg, PH, and Klein, R. (1999). EphrinB ligands recruit GRIP family PDZ adaptor proteins into raft membrane microdomains. *Neuron* **22** (3), 511-524.

Bucci, C, Lutcke, A, Steele-Mortimer, O, Olkkonen, VM, Dupree, P, Chiariello, M, Bruni, CB, Simons, K, and Zerial, M. (1995). Co-operative regulation of endocytosis by three Rab5 isoforms. *FEBS Lett.* **366** (1), 65-71.

Burks, DJ, Wang, J, Towery, H, Ishibashi, O, Lowe, D, Riedel, H, and White, MF. (1998). IRS pleckstrin homology domains bind to acidic motifs in proteins. *J.Biol.Chem.* **273** (47), 31061-31067.

Ceresa, BP, Kao, AW, Santeler, SR, and Pessin, JE. (1998). Inhibition of clathrin-mediated endocytosis selectively attenuates specific insulin receptor signal transduction pathways. *Mol.Cell Biol.* **18** (7), 3862-3870.

Cerneus, DP, Ueffing, E, Posthuma, G, Strous, GJ, and van der, EA. (1993). Detergent insolubility of alkaline phosphatase during biosynthetic transport and endocytosis. Role of cholesterol. *J Biol.Chem.* **268** (5), 3150-3155.

Chamberlain, LH, Burgoyne, RD, and Gould, GW. (2001). SNARE proteins are highly enriched in lipid rafts in PC12 cells: implications for the spatial control of exocytosis. *Proc.Natl.Acad.Sci.U.S.A* **98** (10), 5619-5624.

Chang, WJ, Ying, YS, Rothberg, KG, Hooper, NM, Turner, AJ, Gambliel, HA, De Gunzburg, J, Mumby, SM, Gilman, AG, and Anderson, RG. (1994). Purification and characterization of smooth muscle cell caveolae. *J.Cell Biol.* **126** (1), 127-138.

Cheatham, B, Vlahos, CJ, Cheatham, L, Wang, L, Blenis, J, and Kahn, CR. (1994). Phosphatidylinositol 3-kinase activation is required for insulin stimulation of pp70 S6 kinase, DNA synthesis, and glucose transporter translocation. *Mol.Cell Biol.* **14** (7), 4902-4911.

Chiang, SH, Baumann, CA, Kanzaki, M, Thurmond, DC, Watson, RT, Neudauer, CL, Macara, IG, Pessin, JE, and Saltiel, AR. (2001). Insulin-stimulated GLUT4 translocation requires the CAP-dependent activation of TC10. *Nature* **410** (6831), 944-948.

Chinni, SR and Shisheva, A. (1999). Arrest of endosome acidification by bafilomycin A1 mimics insulin action on GLUT4 translocation in 3T3-L1 adipocytes. *Biochem J* **339 (Pt 3)** 599-606.

Cinek, T and Horejsi, V. (1992). The nature of large noncovalent complexes containing glycosyl- phosphatidylinositol-anchored membrane glycoproteins and protein tyrosine kinases. *J.Immunol.* **149** (7), 2262-2270.

Clark, SF, Martin, S, Carozzi, AJ, Hill, MM, and James, DE. (1998). Intracellular localization of phosphatidylinositide 3-kinase and insulin receptor substrate-1 in adipocytes: potential involvement of a membrane skeleton. *J.Cell Biol.* **140** (5), 1211-1225.

Clark, SF, Molero, JC, and James, DE. (2000). Release of insulin receptor substrate proteins from an intracellular complex coincides with the development of insulin resistance. *J.Biol.Chem.* **275** (6), 3819-3826.

Clarke, JF, Young, PW, Yonezawa, K, Kasuga, M, and Holman, GD. (1994). Inhibition of the translocation of GLUT1 and GLUT4 in 3T3-L1 cells by the phosphatidylinositol 3-kinase inhibitor, wortmannin. *Biochem.J.* **300 (Pt 3)** 631-635.

Collawn, JF, Stangel, M, Kuhn, LA, Esekogwu, V, Jing, SQ, Trowbridge, IS, and Tainer, JA. (1990). Transferrin receptor internalization sequence YXRF implicates a tight turn as the structural recognition motif for endocytosis. *Cell* **63** (5), 1061-1072.

Cope, DL, Lee, S, Melvin, DR, and Gould, GW. (2000). Identification of further important residues within the Glut4 carboxy- terminal tail which regulate subcellular trafficking. *FEBS Lett.* **481** (3), 261-265.

Cortright, RN and Dohm, GL. (1997). Mechanisms by which insulin and muscle contraction stimulate glucose transport. *Can.J.Appl.Physiol* **22** (6), 519-530.

Couet, J, Li, S, Okamoto, T, Ikezu, T, and Lisanti, MP. (1997). Identification of peptide and protein ligands for the caveolin- scaffolding domain. Implications for the interaction of caveolin with caveolae-associated proteins. *J Biol.Chem.* **272** (10), 6525-6533.

Crump, CM, Xiang, Y, Thomas, L, Gu, F, Austin, C, Tooze, SA, and Thomas, G. (2001). PACS-1 binding to adaptors is required for acidic cluster motif- mediated protein traffic. *EMBO J.* **20** (9), 2191-2201.

Cushman, SW, Goodyear, LJ, Pilch, PF, Ralston, E, Galbo, H, Ploug, T, Kristiansen, S, and Klip, A. (1998). Molecular mechanisms involved in GLUT4 translocation in muscle during insulin and contraction stimulation. *Adv.Exp.Med.Biol.* **441** 63-71.

Cushman, SW and Wardzala, LJ. (1980). Potential mechanism of insulin action on glucose transport in the isolated rat adipose cell. Apparent translocation of intracellular transport systems to the plasma membrane. *J.Biol.Chem.* **255** (10), 4758-4762.

Czech, MP, Chawla, A, Woon, CW, Buxton, J, Armoni, M, Tang, W, Joly, M, and Corvera, S. (1993). Exofacial epitope-tagged glucose transporter chimeras reveal COOH- terminal sequences governing cellular localization. *J.Cell Biol.* **123** (1), 127-135.

Davies, SP, Reddy, H, Caivano, M, and Cohen, P. (2000). Specificity and mechanism of action of some commonly used protein kinase inhibitors. *Biochem.J.* **351** (Pt 1), 95-105.

DeFronzo, RA, Bonadonna, RC, and Ferrannini, E. (1992). Pathogenesis of NIDDM. A balanced overview. *Diabetes Care* **15** (3), 318-368.

Dell'Angelica, EC, Klumperman, J, Stoorvogel, W, and Bonifacino, JS. (1998). Association of the AP-3 adaptor complex with clathrin. *Science* **280** (5362), 431-434.

Desnos, C, Clift-O'Grady, L, and Kelly, RB. (1995). Biogenesis of synaptic vesicles in vitro. *J Cell Biol.* **130** (5), 1041-1049.

Dietzen, DJ, Hastings, WR, and Lublin, DM. (1995). Caveolin is palmitoylated on multiple cysteine residues. Palmitoylation is not necessary for localization of caveolin to caveolae. *J Biol.Chem.* **270** (12), 6838-6842.

Dittie, AS, Thomas, L, Thomas, G, and Tooze, SA. (1997). Interaction of furin in immature secretory granules from neuroendocrine cells with the AP-1 adaptor complex is modulated by casein kinase II phosphorylation. *EMBO J* **16** (16), 4859-4870.

Doege, H, Schurmann, A, Ohnimus, H, Monser, V, Holman, GD, and Joost, HG. (1998). Serine-294 and threonine-295 in the exofacial loop domain between helices 7 and 8 of glucose transporters (GLUT) are involved in the conformational alterations during the transport process. *Biochem.J.* **329 (Pt 2)** 289-293.

Domin, J, Gaidarov, I, Smith, ME, Keen, JH, and Waterfield, MD. (2000). The class II phosphoinositide 3-kinase PI3K-C2alpha is concentrated in the trans-Golgi network and present in clathrin-coated vesicles. *J.Biol.Chem.* **275** (16), 11943-11950.

Drivas, GT, Shih, A, Coutavas, E, Rush, MG, and D'Eustachio, P. (1990). Characterization of four novel ras-like genes expressed in a human teratocarcinoma cell line. *Mol.Cell Biol.* **10** (4), 1793-1798.

Drose, S, Bindseil, KU, Bowman, EJ, Siebers, A, Zeeck, A, and Altendorf, K. (1993). Inhibitory effect of modified bafilomycins and concanamycins. *Biochemistry* **32** (15), 3902-3906.

Dupree, P, Parton, RG, Raposo, G, Kurzchalia, TV, and Simons, K. (1993). Caveolae and sorting in the trans-Golgi network of epithelial cells. *EMBO J* **12** (4), 1597-1605.

el Jack, AK, Kandror, KV, and Pilch, PF. (1999). The formation of an insulin-responsive vesicular cargo compartment is an early event in 3T3-L1 adipocyte differentiation. *Mol.Biol.Cell* **10** (5), 1581-1594.

Elmendorf, JS, Boeglin, DJ, and Pessin, JE. (1999). Temporal separation of insulin-stimulated GLUT4/IRAP vesicle plasma membrane docking and fusion in 3T3L1 adipocytes. *J.Biol.Chem.* **274** (52), 37357-37361.

Emoto, M, Langille, SE, and Czech, MP. (2001). A role for kinesin in insulin-stimulated GLUT4 glucose transporter translocation in 3t3-L1 adipocytes. *J.Biol.Chem.* **276** (14), 10677-10682.

Etgen, GJ, Valasek, KM, Broderick, CL, and Miller, AR. (1999). In vivo adenoviral delivery of recombinant human protein kinase C-zeta stimulates glucose transport activity in rat skeletal muscle. *J.Biol.Chem.* **274** (32), 22139-22142.

Farah, S, Agazie, Y, Ohan, N, Ngsee, JK, and Liu, XJ. (1998). A rho-associated protein kinase, ROKalpha, binds insulin receptor substrate-1 and modulates insulin signaling. *J.Biol.Chem.* **273** (8), 4740-4746.

Fasshauer, M, Klein, J, Ueki, K, Kriauciunas, KM, Benito, M, White, MF, and Kahn, CR. (2000). Essential role of insulin receptor substrate-2 in insulin stimulation of Glut4 translocation and glucose uptake in brown adipocytes. *J.Biol.Chem.* **275** (33), 25494-25501.

Faundez, V, Horng, JT, and Kelly, RB. (1998). A function for the AP3 coat complex in synaptic vesicle formation from endosomes. *Cell* **93** (3), 423-432.

Field, KA, Holowka, D, and Baird, B. (1995). Fc epsilon RI-mediated recruitment of p53/56lyn to detergent-resistant membrane domains accompanies cellular signaling. *Proc.Natl.Acad.Sci.U.S.A* **92** (20), 9201-9205.

Fielding, CJ and Fielding, PE. (2001b). Caveolae and intracellular trafficking of cholesterol. *Adv.Drug Deliv.Rev.* **49** (3), 251-264.

Fielding, CJ and Fielding, PE. (2001a). Cellular cholesterol efflux. *Biochim.Biophys Acta* **1533** (3), 175-189.

Fletcher, LM, Welsh, GI, Oatey, PB, and Tavare, JM. (2000). Role for the microtubule cytoskeleton in GLUT4 vesicle trafficking and in the regulation of insulin-stimulated glucose uptake. *Biochem.J.* **352 Pt 2** 267-276.

Folsch, H, Pypaert, M, Schu, P, and Mellman, I. (2001). Distribution and function of AP-1 clathrin adaptor complexes in polarized epithelial cells. *J Cell Biol.* **152** (3), 595-606.

Foran, PG, Fletcher, LM, Oatey, PB, Mohammed, N, Dolly, JO, and Tavare, JM. (1999). Protein kinase B stimulates the translocation of GLUT4 but not GLUT1 or transferrin receptors in 3T3-L1 adipocytes by a pathway involving SNAP- 23, synaptobrevin-2, and/or cellubrevin. *J Biol.Chem.* **274** (40), 28087-28095.

Friedrichson, T and Kurzchalia, TV. (1998). Microdomains of GPI-anchored proteins in living cells revealed by crosslinking. *Nature* **394** (6695), 802-805.

Fukuda, M, Moreira, JE, Lewis, FM, Sugimori, M, Niinobe, M, Mikoshiba, K, and Llinas, R. (1995). Role of the C2B domain of synaptotagmin in vesicular release and recycling as determined by specific antibody injection into the squid giant synapse preterminal. *Proc.Natl.Acad.Sci.U.S.A* **92** (23), 10708-10712.

Gagescu, R, Demaurex, N, Parton, RG, Hunziker, W, Huber, LA, and Gruenberg, J. (2000). The recycling endosome of Madin-Darby canine kidney cells is a mildly acidic compartment rich in raft components. *Mol.Biol.Cell* **11** (8), 2775-2791.

Gaidarov, I, Smith, ME, Domin, J, and Keen, JH. (2001). The class II phosphoinositide 3-kinase C2alpha is activated by clathrin and regulates clathrin-mediated membrane trafficking. *Mol.Cell* **7** (2), 443-449.

Garcia, JC, Strube, M, Leingang, K, Keller, K, and Mueckler, MM. (1992). Amino acid substitutions at tryptophan 388 and tryptophan 412 of the HepG2 (Glut1) glucose transporter inhibit transport activity and targeting to the plasma membrane in Xenopus oocytes. *J.Biol.Chem.* **267** (11), 7770-7776.

Garippa, RJ, Judge, TW, James, DE, and McGraw, TE. (1994). The amino terminus of GLUT4 functions as an internalization motif but not an intracellular retention signal when substituted for the transferrin receptor cytoplasmic domain. *J.Cell Biol.* **124** (5), 705-715.

Garza, LA and Birnbaum, MJ. (2000). Insulin-responsive aminopeptidase trafficking in 3T3-L1 adipocytes. *J.Biol.Chem.* **275** (4), 2560-2567.

Gatica, M. (1993). Effect of metal ions on the activity of casein kinase II from Xenopus laevis. *FEBS Lett.* **315** (2), 1730-1737.

Geahlen, RL, Anostario, M, Jr., Low, PS, and Harrison, ML. (1986). Detection of protein kinase activity in sodium dodecyl sulfate-polyacrylamide gels. *Anal.Biochem.* **153** (1), 151-158.

Gherzi, R, Russell, DS, Taylor, SI, and Rosen, OM. (1987). Re-evaluation of the evidence that an antibody to the insulin receptor is insulinmimetic without activating the protein tyrosine kinase activity of the receptor. *J.Biol.Chem.* **262** (35), 16900-16905.

Gibbs, EM, Calderhead, DM, Holman, GD, and Gould, GW. (1991). Phorbol ester only partially mimics the effects of insulin on glucose transport and glucose-transporter distribution in 3T3-L1 adipocytes. *Biochem J* **275 (Pt 1)** 145-150.

Gibbs, EM, Lienhard, GE, and Gould, GW. (1988). Insulin-induced translocation of glucose transporters to the plasma membrane precedes full stimulation of hexose transport. *Biochemistry* **27** (18), 6681-6685.

Gillingham, AK, Koumanov, F, Pryor, PR, Reaves, BJ, and Holman, GD. (1999). Association of AP1 adaptor complexes with GLUT4 vesicles. *J.Cell Sci.* **112 (Pt 24)** 4793-4800.

Glenney, JR, Jr. (1989). Tyrosine phosphorylation of a 22-kDa protein is correlated with transformation by Rous sarcoma virus. *J Biol.Chem.* **264** (34), 20163-20166.

Glenney, JR, Jr. (1992). The sequence of human caveolin reveals identity with VIP21, a component of transport vesicles. *FEBS Lett.* **314** (1), 45-48.

Gould, GW and Holman, GD. (1993). The glucose transporter family: structure, function and tissue-specific expression. *Biochem.J.* **295 (Pt 2)** 329-341.

Gould, GW and Seatter, MJ. (1997). Introduction to the Facilitative Glucose Transporter family. (1), 3-

Gruenberg, J. (2001). The endocytic pathway: a mosaic of domains. *Nat.Rev.Mol.Cell Biol.* **2** (10), 721-730.

Guilherme, A and Czech, MP. (1998). Stimulation of IRS-1-associated phosphatidylinositol 3-kinase and Akt/protein kinase B but not glucose transport by beta1-integrin signaling in rat adipocytes. *J.Biol.Chem.* **273** (50), 33119-33122.

Gustavsson, J, Parpal, S, Karlsson, M, Ramsing, C, Thorn, H, Borg, M, Lindroth, M, Peterson, KH, Magnusson, KE, and Stralfors, P. (1999). Localization of the insulin receptor in caveolae of adipocyte plasma membrane. *FASEB J.* **13** (14), 1961-1971.

Haney, PM, Levy, MA, Strube, MS, and Mueckler, M. (1995). Insulin-sensitive targeting of the GLUT4 glucose transporter in L6 myoblasts is conferred by its COOH-terminal cytoplasmic tail. *J Cell Biol.* **129** (3), 641-658.

Haney, PM, Slot, JW, Piper, RC, James, DE, and Mueckler, M. (1991). Intracellular targeting of the insulin-regulatable glucose transporter (GLUT4) is isoform specific and independent of cell type. *J.Cell Biol.* **114** (4), 689-699.

Harder, T, Scheiffele, P, Verkade, P, and Simons, K. (1998). Lipid domain structure of the plasma membrane revealed by patching of membrane components. *J Cell Biol.* **141** (4), 929-942.

Hashiramoto, M and James, DE. (2000). Characterization of insulin-responsive GLUT4 storage vesicles isolated from 3T3-L1 adipocytes. *Mol.Cell Biol.* **20** (1), 416-427.

Haucke, V and De Camilli, P. (1999). AP-2 recruitment to synaptotagmin stimulated by tyrosine-based endocytic motifs. *Science* **285** (5431), 1268-1271.

Haucke, V, Wenk, MR, Chapman, ER, Farsad, K, and De Camilli, P. (2000). Dual interaction of synaptotagmin with mu2- and alpha-adaptin facilitates clathrin-coated pit nucleation. *EMBO J* **19** (22), 6011-6019.

Heller-Harrison, RA, Morin, M, and Czech, MP. (1995). Insulin regulation of membrane-associated insulin receptor substrate 1. *J.Biol.Chem.* **270** (41), 24442-24450.

Herman, PK, Stack, JH, DeModena, JA, and Emr, SD. (1991). A novel protein kinase homolog essential for protein sorting to the yeast lysosome-like vacuole. *Cell* **64** (2), 425-437.

Hill, MM, Clark, SF, Tucker, DF, Birnbaum, MJ, James, DE, and Macaulay, SL. (1999). A role for protein kinase Bbeta/Akt2 in insulin-stimulated GLUT4 translocation in adipocytes. *Mol.Cell Biol.* **19** (11), 7771-7781.

Hirokawa, N, Noda, Y, and Okada, Y. (1998). Kinesin and dynein superfamily proteins in organelle transport and cell division. *Curr.Opin.Cell Biol.* **10** (1), 60-73.

Hirst, J and Robinson, MS. (1998). Clathrin and adaptors. *Biochim.Biophys Acta* **1404** (1-2), 173-193.

Hodel, A, An, SJ, Hansen, NJ, Lawrence, J, Wasle, B, Schrader, M, and Edwardson, JM. (2001). Cholesterol-dependent interaction of syncollin with the membrane of the pancreatic zymogen granule. *Biochem.J.* **356** (Pt 3), 843-850.

Hoessli, DC, Ilangumaran, S, Soltermann, A, Robinson, PJ, Borisch, B, and Nasir, UD. (2000). Signaling through sphingolipid microdomains of the plasma membrane: the concept of signaling platform. *Glycoconj.J.* **17** (3 -4), 191-197.

Hofmann, MW, Honing, S, Rodionov, D, Dobberstein, B, von Figura, K, and Bakke, O. (1999). The leucine-based sorting motifs in the cytoplasmic domain of the invariant chain are recognized by the clathrin adaptors AP1 and AP2 and their medium chains. *J.Biol.Chem.* **274** (51), 36153-36158.

Holman, GD and Kasuga, M. (1997). From receptor to transporter: insulin signalling to glucose transport. *Diabetologia* **40** (9), 991-1003.

Holman, GD, Kozka, IJ, Clark, AE, Flower, CJ, Saltis, J, Habberfield, AD, Simpson, IA, and Cushman, SW. (1990). Cell surface labeling of glucose transporter isoform GLUT4 by bis- mannose photolabel. Correlation with stimulation of glucose transport in rat adipose cells by insulin and phorbol ester. *J.Biol.Chem.* **265** (30), 18172-18179.

Holman, GD, Lo, LL, and Cushman, SW. (1994). Insulin-stimulated GLUT4 glucose transporter recycling. A problem in membrane protein subcellular trafficking through multiple pools. *J.Biol.Chem.* **269** (26), 17516-17524.

Holman, GD and Sandoval, IV. (2001). Moving the insulin-regulated glucose transporter GLUT4 into and out of storage. *Trends Cell Biol.* **11** (4), 173-179.

Holowka, D and Baird, B. (2001). Fc(epsilon)RI as a paradigm for a lipid raft-dependent receptor in hematopoietic cells. *Semin.Immunol.* **13** (2), 99-105.

Hosaka, M, Toda, K, Takatsu, H, Torii, S, Murakami, K, and Nakayama, K. (1996). Structure and intracellular localization of mouse ADP-ribosylation factors type 1 to type 6 (ARF1-ARF6). *J Biochem (Tokyo)* **120** (4), 813-819.

Hsu, CC, Davis, KM, Jin, H, Foos, T, Floor, E, Chen, W, Tyburski, JB, Yang, CY, Schloss, JV, and Wu, JY. (2000). Association of L-glutamic acid decarboxylase to the 70-kDa heat shock protein as a potential anchoring mechanism to synaptic vesicles. *J.Biol.Chem.* **275** (27), 20822-20828.

Hsu, CC, Thomas, C, Chen, W, Davis, KM, Foos, T, Chen, JL, Wu, E, Floor, E, Schloss, JV, and Wu, JY. (1999). Role of synaptic vesicle proton gradient and protein phosphorylation on ATP-mediated activation of membrane-associated brain glutamate decarboxylase. *J.Biol.Chem.* **274** (34), 24366-24371.

Huang, J, Imamura, T, and Olefsky, JM. (2001). Insulin can regulate GLUT4 internalization by signaling to Rab5 and the motor protein dynein. *Proc.Natl.Acad.Sci.U.S.A* **98** (23), 13084-13089.

Huang, JD, Brady, ST, Richards, BW, Stenolen, D, Resau, JH, Copeland, NG, and Jenkins, NA. (1999). Direct interaction of microtu. *Nature* **397** (6716), 267-270.

Hutchcroft, JE, Anostario, M, Jr., Harrison, ML, and Geahlen, RL. (1991). Renaturation and assay of protein kinases after electrophoresis in sodium dodecyl sulfate-polyacrylamide gels. *Methods Enzymol.* **200** 417-423.

Ikonen, E. (2001). Roles of lipid rafts in membrane transport. *Curr.Opin.Cell Biol.* **13** (4), 470-477.

Isakoff, SJ, Taha, C, Rose, E, Marcusohn, J, Klip, A, and Skolnik, EY. (1995). The inability of phosphatidylinositol 3-kinase activation to stimulate GLUT4 translocation indicates additional signaling pathways are required for insulin-stimulated glucose uptake. *Proc.Natl.Acad.Sci.U.S.A* **92** (22), 10247-10251.

Jackson, CL and Casanova, JE. (2000). Turning on ARF: the Sec7 family of guanine-nucleotide-exchange factors. *Trends Cell Biol.* **10** (2), 60-67.

James, DE, Hiken, J, and Lawrence, JC, Jr. (1989). Isoproterenol stimulates phosphorylation of the insulin-regulatable glucose transporter in rat adipocytes. *Proc.Natl.Acad.Sci.U.S.A* **86** (21), 8368-8372.

James, DE and Piper, RC. (1994). Insulin resistance, diabetes, and the insulin-regulated trafficking of GLUT-4. *J.Cell Biol.* **126** (5), 1123-1126.

Janes, PW, Ley, SC, and Magee, AI. (1999). Aggregation of lipid rafts accompanies signaling via the T cell antigen receptor. *J Cell Biol.* **147** (2), 447-461.

Janes, PW, Ley, SC, Magee, AI, and Kabouridis, PS. (2000). The role of lipid rafts in T cell antigen receptor (TCR) signalling. *Semin.Immunol.* **12** (1), 23-34.

Jiang, T, Sweeney, G, Rudolf, MT, Klip, A, Traynor-Kaplan, A, and Tsien, RY. (1998). Membrane-permeant esters of phosphatidylinositol 3,4,5-trisphosphate. *J.Biol.Chem.* **273** (18), 11017-11024.

Joazeiro, CA, Wing, SS, Huang, H, Leverson, JD, Hunter, T, and Liu, YC. (1999). The tyrosine kinase negative regulator c-Cbl as a RING-type, E2-dependent ubiquitin-protein ligase. *Science* **286** (5438), 309-312.

Johnson, AO, Lampson, MA, and McGraw, TE. (2001). A di-leucine sequence and a cluster of acidic amino acids are required for dynamic retention in the endosomal recycling compartment of fibroblasts. *Mol.Biol.Cell* **12** (2), 367-381.

Johnson, LS, Dunn, KW, Pytowski, B, and McGraw, TE. (1993). Endosome acidification and receptor trafficking: bafilomycin A1 slows receptor externalization by a mechanism involving the receptor's internalization motif. *Mol.Biol.Cell* **4** (12), 1251-1266.

Jones, BG, Thomas, L, Molloy, SS, Thulin, CD, Fry, MD, Walsh, KA, and Thomas, G. (1995). Intracellular trafficking of furin is modulated by the phosphorylation state of a casein kinase II site in its cytoplasmic tail. *EMBO J.* **14** (23), 5869-5883.

Joost, HG and Thorens, B. (2001). The Extended GLUT-family of Sugar/Polyol Transport Facilitators- Nomenckature, Sequence Characteristics, and Potential Function of its Novel Members. *Molecular Membrane Biology*

Joost, HG, Weber, TM, Cushman, SW, and Simpson, IA. (1987). Activity and phosphorylation state of glucose transporters in plasma membranes from insulin-, isoproterenol-, and phorbol ester-treated rat adipose cells. *J.Biol.Chem.* **262** (23), 11261-11267.

Kaburagi, Y, Satoh, S, Tamemoto, H, Yamamoto-Honda, R, Tobe, K, Veki, K, Yamauchi, T, Kono-Sugita, E, Sekihara, H, Aizawa, S, Cushman, SW, Akanuma, Y, Yazaki, Y, and Kadowaki, T. (1997). Role of insulin receptor substrate-1 and pp60 in the regulation of insulin-induced glucose transport and GLUT4 translocation in primary adipocytes. *J.Biol.Chem.* **272** (41), 25839-25844.

Kadota, K and Kaneseki, T. (1969). Isolation of a synaptic vesicle fraction from guinea pig brain with the use of DEAE-sephadex column chromatography and some of its properties. *J Biochem (Tokyo)* **65** (5), 839-842.

Kamal, A and Goldstein, LS. (2000). Connecting vesicle transport to the cytoskeleton. *Curr.Opin.Cell Biol.* **12** (4), 503-508.

Kameshita, I and Fujisawa, H. (1989). A sensitive method for detection of calmodulin-dependent protein kinase II activity in sodium dodecyl sulfate-polyacrylamide gel. *Anal.Biochem.* **183** (1), 139-143.

Kameshita, I and Fujisawa, H. (1996). Detection of protein kinase activities toward oligopeptides in sodium dodecyl sulfate-polyacrylamide gel. *Anal.Biochem.* **237** (2), 198-203.

Kanzaki, M and Pessin, JE. (2001). Insulin-stimulated GLUT4 translocation in adipocytes is dependent upon cortical actin remodeling. *J.Biol.Chem.* **276** (45), 42436-42444.

Kao, AW, Noda, Y, Johnson, JH, Pessin, JE, and Saltiel, AR. (1999). Aldolase mediates the association of F-actin with the insulin- responsive glucose transporter GLUT4. *J Biol.Chem.* **274** (25), 17742-17747.

Kasuga, M, Karlsson, FA, and Kahn, CR. (1982). Insulin stimulates the phosphorylation of the 95,000-dalton subunit of its own receptor. *Science* **215** (4529), 185-187.

Keeling, DJ, Herslof, M, Ryberg, B, Sjogren, S, and Solvell, L. (1997). Vacuolar H(+)-ATPases. Targets for drug discovery? *Ann.N.Y.Acad.Sci.* **834** 600-608.

Kenworthy, AK, Petranova, N, and Edidin, M. (2000). High-resolution FRET microscopy of cholera toxin B-subunit and GPI- anchored proteins in cell plasma membranes. *Mol.Biol.Cell* **11** (5), 1645-1655.

Kirchhausen, T. (1999). Adaptors for clathrin-mediated traffic. *Annu.Rev.Cell Dev.Biol.* **15** 705-732.

Klip, A, Ramlal, T, and Cragoe, EJ, Jr. (1986). Insulin-induced cytoplasmic alkalinization and glucose transport in muscle cells. *Am.J Physiol* **250** (5 Pt 1), C720-C728.

Klumperman, J, Hille, A, Veenendaal, T, Oorschot, V, Stoorvogel, W, von Figura, K, and Geuze, HJ. (1993). Differences in the endosomal distributions of the two mannose 6- phosphate receptors. *J Cell Biol.* **121** (5), 997-1010.

Knudsen, BS, Feller, SM, and Hanafusa, H. (1994). Four proline-rich sequences of the guanine-nucleotide exchange factor C3G bind with unique specificity to the first Src homology 3 domain of Crk. *J.Biol.Chem.* **269** (52), 32781-32787.

Kobayashi, T, Gu, F, and Gruenberg, J. (1998a). Lipids, lipid domains and lipid-protein interactions in endocytic membrane traffic. *Semin.Cell Dev.Biol.* **9** (5), 517-526.

Kobayashi, T, Stang, E, Fang, KS, de Moerloose, P, Parton, RG, and Gruenberg, J. (1998b). A lipid associated with the antiphospholipid syndrome regulates endosome structure and function. *Nature* **392** (6672), 193-197.

Kohn, AD, Summers, SA, Birnbaum, MJ, and Roth, RA. (1996). Expression of a constitutively active Akt Ser/Thr kinase in 3T3-L1 adipocytes stimulates glucose uptake and glucose transporter 4 translocation. *J.Biol.Chem.* **271** (49), 31372-31378.

Kotani, K, Carozzi, AJ, Sakaue, H, Hara, K, Robinson, LJ, Clark, SF, Yonezawa, K, James, DE, and Kasuga, M. (1995). Requirement for phosphoinositide 3-kinase in insulin-stimulated GLUT4 translocation in 3T3-L1 adipocytes. *Biochem.Biophys.Res.Commun.* **209** (1), 343-348.

Kublaoui, B, Lee, J, and Pilch, PF. (1995). Dynamics of signaling during insulin-stimulated endocytosis of its receptor in adipocytes. *J.Biol.Chem.* **270** (1), 59-65.

Kuhne, MR, Pawson, T, Lienhard, GE, and Feng, GS. (1993). The insulin receptor substrate 1 associates with the SH2-containing phosphotyrosine phosphatase Syp. *J.Biol.Chem.* **268** (16), 11479-11481.

Kurzchalia, TV, Dupree, P, Parton, RG, Kellner, R, Virta, H, Lehnert, M, and Simons, K. (1992). VIP21, a 21-kD membrane protein is an integral component of trans-Golgi- network-derived transport vesicles. *J Cell Biol.* **118** (5), 1003-1014.

Kurzchalia, TV and Parton, RG. (1999). Membrane microdomains and caveolae. *Curr.Opin.Cell Biol.* **11** (4), 424-431.

Kyriakis, JM and Avruch, J. (1990). pp54 microtubule-associated protein 2 kinase. A novel serine/threonine protein kinase regulated by phosphorylation and stimulated by poly-L- lysine. *J Biol.Chem.* **265** (28), 17355-17363.

Lang, T, Bruns, D, Wenzel, D, Riedel, D, Holroyd, P, Thiele, C, and Jahn, R. (2001). SNAREs are concentrated in cholesterol-dependent clusters that define docking and fusion sites for exocytosis. *EMBO J.* **20** (9), 2202-2213.

Langlet, C, Bernard, AM, Drevot, P, and He, HT. (2000). Membrane rafts and signaling by the multichain immune recognition receptors. *Curr.Opin.Immunol.* **12** (3), 250-255.

Lawrence, JC, Jr., Hiken, JF, and James, DE. (1990b). Phosphorylation of the glucose transporter in rat adipocytes. Identification of the intracellular domain at the carboxyl terminus as a target for phosphorylation in intact-cells and in vitro. *J.Biol.Chem.* **265** (4), 2324-2332.

Lawrence, JC, Jr., Hiken, JF, and James, DE. (1990a). Stimulation of glucose transport and glucose transporter phosphorylation by okadaic acid in rat adipocytes. *J.Biol.Chem.* **265** (32), 19768-19776.

Le Good, JA, Ziegler, WH, Parekh, DB, Alessi, DR, Cohen, P, and Parker, PJ. (1998). Protein kinase C isotypes controlled by phosphoinositide 3-kinase through the protein kinase PDK1. *Science* **281** (5385), 2042-2045.

Lee, H, Volonte, D, Galbiati, F, Iyengar, P, Lublin, DM, Bregman, DB, Wilson, MT, Campos-Gonzalez, R, Bouzahzah, B, Pestell, RG, Scherer, PE, and Lisanti, MP. (2000). Constitutive and growth factor-regulated phosphorylation of caveolin-1 occurs at the same site (Tyr-14) in vivo: identification of a c-Src/Cav- 1/Grb7 signaling cassette. *Mol.Endocrinol.* **14** (11), 1750-1775.

Lee, W and Jung, CY. (1997). A synthetic peptide corresponding to the GLUT4 C-terminal cytoplasmic domain causes insulin-like glucose transport stimulation and GLUT4 recruitment in rat adipocytes. *J.Biol.Chem.* **272** (34), 21427-21431.

Lee, W, Samuel, J, Zhang, W, Rampal, AL, Lachaal, M, and Jung, CY. (1997). A myosin-derived peptide C109 binds to GLUT4-vesicles and inhibits the insulin-induced glucose transport stimulation and GLUT4 recruitment in rat adipocytes [published erratum appears in Biochem Biophys Res Commun 1998 Feb 13;243(2):639]. *Biochem.Biophys.Res.Commun.* **240** (2), 409-414.

Leung, T, Manser, E, Tan, L, and Lim, L. (1995). A novel serine/threonine kinase binding the Ras-related RhoA GTPase which translocates the kinase to peripheral membranes. *J.Biol.Chem.* **270** (49), 29051-29054.

Lewin, DA, Sheff, D, Ooi, CE, Whitney, JA, Yamamoto, E, Chicione, LM, Webster, P, Bonifacino, JS, and Mellman,I . (1998). Cloning, expression, and localization of a novel gamma-adaptin-like molecule. *FEBS Lett.* **435** (2-3), 263-268.

Li, J, DeFea, K, and Roth, RA. (1999). Modulation of insulin receptor substrate-1 tyrosine phosphorylation by an Akt/phosphatidylinositol 3-kinase pathway. *J.Biol.Chem.* **274** (14), 9351-9356.

Li, S, Couet, J, and Lisanti, MP. (1996a). Src tyrosine kinases, Galpha subunits, and H-Ras share a common membrane-anchored scaffolding protein, caveolin. Caveolin binding negatively regulates the auto-activation of Src tyrosine kinases. *J Biol.Chem.* **271** (46), 29182-29190.

Li, S, Galbiati, F, Volonte, D, Sargiacomo, M, Engelman, JA, Das, K, Scherer, PE, and Lisanti, MP. (1998). Mutational analysis of caveolin-induced vesicle formation. Expression of caveolin-1 recruits caveolin-2 to caveolae membranes. *FEBS Lett.* **434** (1-2), 127-134.

Li, S, Seitz, R, and Lisanti, MP. (1996c). Phosphorylation of caveolin by src tyrosine kinases. The alpha-isoform of caveolin is selectively phosphorylated by v-Src in vivo. *J Biol.Chem.* **271** (7), 3863-3868.

Li, S, Song, KS, Koh, SS, Kikuchi, A, and Lisanti, MP. (1996b). Baculovirus-based expression of mammalian caveolin in Sf21 insect cells. A model system for the biochemical and morphological study of caveolae biogenesis. *J Biol.Chem.* **271** (45), 28647-28654.

Li, S, Song, KS, and Lisanti, MP. (1996d). Expression and characterization of recombinant caveolin. Purification by polyhistidine tagging and cholesterol-dependent incorporation into defined lipid membranes. *J Biol.Chem.* **271** (1), 568-573.

Lippincott-Schwartz, J, Yuan, L, Tipper, C, Amherdt, M, Orci, L, and Klausner, RD. (1991). Brefeldin A's effects on endosomes, lysosomes, and the TGN suggest a general mechanism for regulating organelle structure and membrane traffic. *Cell* **67** (3), 601-616.

Liu, ML, Gibbs, EM, McCoid, SC, Milici, AJ, Stukenbrok, HA, McPherson, RK, Treadway, JL, and Pessin, JE. (1993). Transgenic mice expressing the human GLUT4/muscle-fat facilitative glucose transporter protein exhibit efficient glycemic control. *Proc.Natl.Acad.Sci.U.S.A* **90** (23), 11346-11350.

Liu, SC, Wang, Q, Lienhard, GE, and Keller, SR. (1999). Insulin receptor substrate 3 is not essential for growth or glucose homeostasis. *J.Biol.Chem.* **274** (25), 18093-18099.

Liu, YF, Paz, K, Herschkovitz, A, Alt, A, Tennenbaum, T, Sampson, SR, Ohba, M, Kuroki, T, LeRoith, D, and Zick, Y. (2001). Insulin stimulates PKCzeta -mediated phosphorylation of insulin receptor substrate-1 (IRS-1). A self-attenuated mechanism to negatively regulate the function of IRS proteins. *J.Biol.Chem.* **276** (17), 14459-14465.

Livingstone, C, James, DE, Rice, JE, Hanpeter, D, and Gould, GW. (1996). Compartment ablation analysis of the insulin-responsive glucose transporter (GLUT4) in 3T3-L1 adipocytes. *Biochem J* **315 (Pt 2)** 487-495.

Luetterforst, R, Stang, E, Zorzi, N, Carozzi, A, Way, M, and Parton, RG. (1999). Molecular characterization of caveolin association with the Golgi complex: identification of a cis-Golgi targeting domain in the caveolin molecule. *J Cell Biol.* **145** (7), 1443-1459.

Machleidt, T, Li, WP, Liu, P, and Anderson, RG. (2000). Multiple domains in caveolin-1 control its intracellular traffic. *J.Cell Biol.* **148** (1), 17-28.

Madoff, DH, Martensen, TM, and Lane, MD. (1988). Insulin and insulin-like growth factor 1 stimulate the phosphorylation on tyrosine of a 160 kDa cytosolic protein in 3T3-L1 adipocytes. *Biochem.J.* **252** (1), 7-15.

Madore, N, Smith, KL, Graham, CH, Jen, A, Brady, K, Hall, S, and Morris, R. (1999). Functionally different GPI proteins are organized in different domains on the neuronal surface. *EMBO J* **18** (24), 6917-6926.

Malide, D, Ramm, G, Cushman, SW, and Slot, JW. (2000). Immunoelectron microscopic evidence that GLUT4 translocation explains the stimulation of glucose transport in isolated rat white adipose cells. *J.Cell Sci.* **113 Pt 23** 4203-4210.

Marsh, BJ, Alm, RA, McIntosh, SR, and James, DE. (1995). Molecular regulation of GLUT-4 targeting in 3T3-L1 adipocytes. *J.Cell Biol.* **130** (5), 1081-1091.

Marsh, BJ, Martin, S, Melvin, DR, Martin, LB, Alm, RA, Gould, GW, and James,DE. (1998). Mutational analysis of the carboxy-terminal phosphorylation site of GLUT-4 in 3T3-L1 adipocytes. *Am.J.Physiol* **275** (3 Pt 1), E412-E422.

Martin, BC, Warram, JH, Krolewski, AS, Bergman, RN, Soeldner, JS, and Kahn, CR. (1992). Role of glucose and insulin resistance in development of type 2 diabetes mellitus: results of a 25-year follow-up study [see comments]. *Lancet* **340** (8825), 925-929.

Martin, LB, Shewan, A, Millar, CA, Gould, GW, and James, DE. (1998). Vesicle-associated membrane protein 2 plays a specific role in the insulin-dependent trafficking of the facilitative glucose transporter GLUT4 in 3T3-L1 adipocytes. *J Biol.Chem.* **273** (3), 1444-1452.

Martin, S, Millar, CA, Lyttle, CT, Meerloo, T, Marsh, BJ, Gould, GW, and James, DE. (2000). Effects of insulin on intracellular GLUT4 vesicles in adipocytes: evidence for a secretory mode of regulation. *J.Cell Sci.* **113 Pt 19** 3427-3438.

Martin, S, Reaves, B, Banting, G, and Gould, GW. (1994). Analysis of the co-localization of the insulin-responsive glucose transporter (GLUT4) and the trans Golgi network marker TGN38 within 3T3- L1 adipocytes. *Biochem J* **300 (Pt 3)** 743-749.

Martin, S, Tellam, J, Livingstone, C, Slot, JW, Gould, GW, and James, DE. (1996). The glucose transporter (GLUT-4) and vesicle-associated membrane protein-2 (VAMP-2) are segregated from recycling endosomes in insulin-sensitive cells. *J Cell Biol.* **134** (3), 625-635.

Martinez-Arca, S, Lalioti, VS, and Sandoval, IV. (2000). Intracellular targeting and retention of the glucose transporter GLUT4 by the perinuclear storage compartment involves distinct carboxyl-tail motifs. *J.Cell Sci.* **113 (Pt 10)** 1705-1715.

Mastick, CC and Saltiel, AR. (1997). Insulin-stimulated tyrosine phosphorylation of caveolin is specific for the differentiated adipocyte phenotype in 3T3-L1 cells. *J.Biol.Chem.* **272** (33), 20706-20714.

Mattsson, JP and Keeling, DJ. (1996). [3H]Bafilomycin as a probe for the transmembrane proton channel of the osteoclast vacuolar H(+)-ATPase. *Biochim.Biophys Acta* **1280** (1), 98-106.

Mauxion, F, Le Borgne, R, Munier-Lehmann, H, and Hoflack, B. (1996). A casein kinase II phosphorylation site in the cytoplasmic domain of the cation-dependent mannose 6-phosphate receptor determines the high affinity interaction of the AP-1 Golgi assembly proteins with membranes. *J Biol.Chem.* **271** (4), 2171-2178.

Maxfield, FR and Mayor, S. (1997). Cell surface dynamics of GPI-anchored proteins. *Adv.Exp.Med.Biol.* **419** 355-364.

Meggio, F, Boldyreff, B, Marin, O, Marchiori, F, Perich, JW, Issinger, OG, and Pinna, LA. (1992). The effect of polylysine on casein-kinase-2 activity is influenced by both the structure of the protein/peptide substrates and the subunit composition of the enzyme. *Eur.J Biochem.* **205** (3), 939-945.

Melkonian, KA, Ostermeyer, AG, Chen, JZ, Roth, MG, and Brown, DA. (1999). Role of lipid modifications in targeting proteins to detergent-resistant membrane rafts. Many raft proteins are acylated, while few are prenylated. *J.Biol.Chem.* **274** (6), 3910-3917.

Mellman, I. (1992). The importance of being acid: the role of acidification in intracellular membrane traffic. *J Exp.Biol.* **172** 39-45.

Mellman, I, Fuchs, R, and Helenius, A. (1986). Acidification of the endocytic and exocytic pathways. *Annu.Rev.Biochem* **55** 663-700.

Melvin, DR, Marsh, BJ, Walmsley, AR, James, DE, and Gould, GW. (1999). Analysis of amino and carboxy terminal GLUT-4 targeting motifs in 3T3- L1 adipocytes using an endosomal ablation technique. *Biochemistry* **38** (5), 1456-1462.

Meresse, S and Hoflack, B. (1993). Phosphorylation of the cation-independent mannose 6-phosphate receptor is closely associated with its exit from the trans-Golgi network. *J Cell Biol.* **120** (1), 67-75.

Merzendorfer, H, Graf, R, Huss, M, Harvey, WR, and Wieczorek, H. (1997). Regulation of proton-translocating V-ATPases. *J Exp.Biol.* **200 (Pt 2)** 225-235.

Millar, CA, Powell, KA, Hickson, GR, Bader, MF, and Gould, GW. (1999b). Evidence for a role for ADP-ribosylation factor 6 in insulin-stimulated glucose transporter-4 (GLUT4) trafficking in 3T3-L1 adipocytes. *J Biol.Chem.* **274** (25), 17619-17625.

Millar, CA, Shewan, A, Hickson, GR, James, DE, and Gould, GW. (1999a). Differential regulation of secretory compartments containing the insulin-responsive glucose transporter 4 in 3T3-L1 adipocytes. *Mol.Biol.Cell* **10** (11), 3675-3688.

Min, J, Okada, S, Kanzaki, M, Elmendorf, JS, Coker, KJ, Ceresa, BP, Syu, LJ, Noda, Y, Saltiel, AR, and Pessin, JE. (1999). Synip: a novel insulin-regulated syntaxin 4-binding protein mediating GLUT4 translocation in adipocytes. *Mol.Cell* **3** (6), 751-760.

Molloy, SS, Thomas, L, Kamibayashi, C, Mumby, MC, and Thomas, G. (1998). Regulation of endosome sorting by a specific PP2A isoform. *J Cell Biol.* **142** (6), 1399-1411.

Moodie, SA, Alleman-Sposeto, J, and Gustafson, TA. (1999). Identification of the APS protein as a novel insulin receptor substrate. *J Biol.Chem.* **274** (16), 11186-11193.

Morgan, JR, Prasad, K, Hao, W, Augustine, GJ, and Lafer, EM. (2000). A conserved clathrin assembly motif essential for synaptic vesicle endocytosis. *J Neurosci.* **20** (23), 8667-8676.

Mueckler, M, Caruso, C, Baldwin, SA, Panico, M, Blench, I, Morris, HR, Allard, WJ, Lienhard, GE, and Lodish, HF. (1985). Sequence and structure of a human glucose transporter. *Science* **229** (4717), 941-945.

Mueckler, M, Weng, W, and Kruse, M. (1994). Glutamine 161 of Glut1 glucose transporter is critical for transport activity and exofacial ligand binding. *J.Biol.Chem.* **269** (32), 20533-20538.

Murata, M, Peranen, J, Schreiner, R, Wieland, F, Kurzchalia, TV, and Simons, K. (1995). VIP21/caveolin is a cholesterol-binding protein. *Proc.Natl.Acad.Sci.U.S.A* **92** (22), 10339-10343.

Namchuk, M, Lindsay, L, Turck, CW, Kanaani, J, and Baekkeskov, S. (1997). Phosphorylation of serine residues 3, 6, 10, and 13 distinguishes membrane anchored from soluble glutamic acid decarboxylase 65 and is restricted to glutamic acid decarboxylase 65alpha [published erratum appears in J Biol Chem 1997 Jul 4;272(27):17246]. *J.Biol.Chem.* **272** (3), 1548-1557.

Nichols, BJ, Kenworthy, AK, Polishchuk, RS, Lodge, R, Roberts, TH, Hirschberg, K, Phair, RD, and Lippincott-Schwartz, J. (2001). Rapid cycling of lipid raft markers between the cell surface and Golgi complex. *J.Cell Biol.* **153** (3), 529-541.

Nishimura, H, Saltis, J, Habberfield, AD, Garty, NB, Greenberg, AS, Cushman, SW, Londos, C, and Simpson, IA. (1991). Phosphorylation state of the GLUT4 isoform of the glucose transporter in subfractions of the rat adipose cell: effects of insulin, adenosine, and isoproterenol. *Proc.Natl.Acad.Sci.U.S.A* **88** (24), 11500-11504.

Norman, JC, Price, LS, Ridley, AJ, and Koffer, A. (1996). The small GTP-binding proteins, Rac and Rho, regulate cytoskeletal organization and exocytosis in mast cells by parallel pathways. *Mol.Biol.Cell* **7** (9), 1429-1442.

Odorizzi, G, Babst, M, and Emr, SD. (2000). Phosphoinositide signaling and the regulation of membrane trafficking in yeast. *Trends Biochem.Sci.* **25** (5), 229-235.

Ogawa, W, Matozaki, T, and Kasuga, M. (1998). Role of binding proteins to IRS-1 in insulin signalling. *Mol.Cell Biochem.* **182** (1-2), 13-22.

Ohno, H, Fournier, MC, Poy, G, and Bonifacino, JS. (1996). Structural determinants of interaction of tyrosine-based sorting signals with the adaptor medium chains. *J Biol.Chem.* **271** (46), 29009-29015.

Okamoto, T, Schlegel, A, Scherer, PE, and Lisanti, MP. (1998). Caveolins, a family of scaffolding proteins for organizing "preassembled signaling complexes" at the plasma membrane. *J.Biol.Chem.* **273** (10), 5419-5422.

Olefsky, JM. (1999). Insulin-stimulated glucose transport minireview series. *J Biol.Chem.* **274** (4), 1863-

Olson, AL, Trumbly, AR, and Gibson, GV. (2001). Insulin-mediated GLUT4 translocation is dependent on the microtubule network. *J.Biol.Chem.* **276** (14), 10706-10714.

Omata, W, Shibata, H, Li, L, Takata, K, and Kojima, I. (2000). Actin filaments play a critical role in insulin-induced exocytotic recruitment but not in endocytosis of GLUT4 in isolated rat adipocytes. *Biochem.J.* **346 Pt 2** 321-328.

Orci, L, Ravazzola, M, Storch, MJ, Anderson, RG, Vassalli, JD, and Perrelet, A. (1987). Proteolytic maturation of insulin is a post-Golgi event which occurs in acidifying clathrin-coated secretory vesicles. *Cell* **49** (6), 865-868.

Owen, DJ and Evans, PR. (1998). A structural explanation for the recognition of tyrosine-based endocytotic signals. *Science* **282** (5392), 1327-1332.

Owen, DJ, Setiadi, H, Evans, PR, McEver, RP, and Green, SA. (2001). A third specificity-determining site in mu 2 adaptin for sequences upstream of Yxx phi sorting motifs. *Traffic.* **2** (2), 105-110.

Owen, DJ, Vallis, Y, Noble, ME, Hunter, JB, Dafforn, TR, Evans, PR, and McMahon, HT. (1999). A structural explanation for the binding of multiple ligands by the alpha-adaptin appendage domain. *Cell* **97** (6), 805-815.

Owen, DJ, Vallis, Y, Pearse, BM, McMahon, HT, and Evans, PR. (2000). The structure and function of the beta 2-adaptin appendage domain. *EMBO J* **19** (16), 4216-4227.

Palacios, S, Lalioti, V, Martinez-Arca, S, Chattopadhyay, S, and Sandoval, IV. (2001). Recycling of the insulin-sensitive glucose transporter GLUT4. Access of surface internalized GLUT4 molecules to the perinuclear storage compartment is mediated by the Phe5-Gln6-Gln7-Ile8 motif. *J.Biol.Chem.* **276** (5), 3371-3383.

Palade, G.E. (1953). Fine structure of blood capillaries. *J Appl Physics* **24** 1424-1432.

Panaretou, C, Domin, J, Cockcroft, S, and Waterfield, MD. (1997). Characterization of p150, an adaptor protein for the human phosphatidylinositol (PtdIns) 3-kinase. Substrate presentation by phosphatidylinositol transfer protein to the p150.Ptdins 3-kinase complex. *J.Biol.Chem.* **272** (4), 2477-2485.

Parpal, S, Karlsson, M, Thorn, H, and Stralfors, P. (2001). Cholesterol depletion disrupts caveolae and insulin receptor signaling for metabolic control via insulin receptor substrate-1, but not for mitogen-activated protein kinase control. *J.Biol.Chem.* **276** (13), 9670-9678.

Patki, V, Buxton, J, Chawla, A, Lifshitz, L, Fogarty, K, Carrington, W, Tuft, R, and Corvera, S. (2001). Insulin action on GLUT4 traffic visualized in single 3T3-l1 adipocytes by using ultra-fast microscopy. *Mol.Biol.Cell* **12** (1), 129-141.

Patti, ME, Sun, XJ, Bruening, JC, Araki, E, Lipes, MA, White, MF, and Kahn, CR. (1995). 4PS/insulin receptor substrate (IRS)-2 is the alternative substrate of the insulin receptor in IRS-1-deficient mice. *J.Biol.Chem.* **270** (42), 24670-24673.

Pearse, BM. (1976). Clathrin: a unique protein associated with intracellular transfer of membrane by coated vesicles. *Proc.Natl.Acad.Sci.U.S.A* **73** (4), 1255-1259.

Pearse, BM and Robinson, MS. (1990). Clathrin, adaptors, and sorting. *Annu.Rev.Cell Biol.* **6** 151-171.

Pearse, BM, Smith, CJ, and Owen, DJ. (2000). Clathrin coat construction in endocytosis. *Curr.Opin.Struct.Biol.* **10** (2), 220-228.

Perschl, A, Lesley, J, English, N, Hyman, R, and Trowbridge, IS. (1995). Transmembrane domain of CD44 is required for its detergent insolubility in fibroblasts. *J.Cell Sci.* **108 (Pt 3)** 1033-1041.

Pfeffer, SR. (2001). Caveolae on the move. *Nat.Cell Biol.* **3** (5), E108-E110.

Phelan, P and Gordan-Weeks, P. (1997). Isolation of synaptosomes, growth cones and their subcellular components. 1-38.

Piper, RC, James, DE, Slot, JW, Puri, C, and Lawrence, JC, Jr. (1993b). GLUT4 phosphorylation and inhibition of glucose transport by dibutyryl cAMP. *J.Biol.Chem.* **268** (22), 16557-16563.

Piper, RC, Tai, C, Kulesza, P, Pang, S, Warnock, D, Baenziger, J, Slot, JW, Geuze, HJ, Puri, C, and James, DE. (1993a). GLUT-4 NH2 terminus contains a phenylalanine-based targeting motif that regulates intracellular sequestration. *J.Cell Biol.* **121** (6), 1221-1232.

Piper, RC, Tai, C, Slot, JW, Hahn, CS, Rice, CM, Huang, H, and James, DE. (1992). The efficient intracellular sequestration of the insulin-regulatable glucose transporter (GLUT-4) is conferred by the NH2 terminus. *J.Cell Biol.* **117** (4), 729-743.

Ploug, T, van Deurs, B, Ai, H, Cushman, SW, and Ralston, E. (1998). Analysis of GLUT4 distribution in whole skeletal muscle fibers: identification of distinct storage compartments that are recruited by insulin and muscle contractions. *J Cell Biol.* **142** (6), 1429-1446.

Pralle, A, Keller, P, Florin, EL, Simons, K, and Horber, JK. (2000). Sphingolipid-cholesterol rafts diffuse as small entities in the plasma membrane of mammalian cells. *J Cell Biol.* **148** (5), 997-1008.

Puertollano, R and Alonso, MA. (1998). A short peptide motif at the carboxyl terminus is required for incorporation of the integral membrane MAL protein to glycolipid- enriched membranes. *J.Biol.Chem.* **273** (21), 12740-12745.

Pytowski, B, Judge, TW, and McGraw, TE. (1995). An internalization motif is created in the cytoplasmic domain of the transferrin receptor by substitution of a tyrosine at the first position of a predicted tight turn. *J Biol.Chem.* **270** (16), 9067-9073.

Ramm, G, Slot, JW, James, DE, and Stoorvogel, W. (2000). Insulin recruits GLUT4 from specialized VAMP2-carrying vesicles as well as from the dynamic endosomal/trans-Golgi network in rat adipocytes. *Mol.Biol.Cell* **11** (12), 4079-4091.

Rapoport, I, Chen, YC, Cupers, P, Shoelson, SE, and Kirchhausen, T. (1998). Dileucine-based sorting signals bind to the beta chain of AP-1 at a site distinct and regulated differently from the tyrosine-based motif- binding site. *EMBO J* **17** (8), 2148-2155.

Rapoport, I, Miyazaki, M, Boll, W, Duckworth, B, Cantley, LC, Shoelson, S, and Kirchhausen, T. (1997). Regulatory interactions in the recognition of endocytic sorting signals by AP-2 complexes. *EMBO J* **16** (9), 2240-2250.

Razani, B, Schlegel, A, and Lisanti, MP. (2000). Caveolin proteins in signaling, oncogenic transformation and muscular dystrophy. *J Cell Sci.* **113 (Pt 12)** 2103-2109.

Rea, S and James, DE. (1997). Moving GLUT4: the biogenesis and trafficking of GLUT4 storage vesicles. *Diabetes* **46** (11), 1667-1677.

Resh, MD. (1999). Fatty acylation of proteins: new insights into membrane targeting of myristoylated and palmitoylated proteins. *Biochim.Biophys.Acta* **1451** (1), 1-16.

Reusch, JE, Begum, N, Sussman, KE, and Draznin, B. (1991). Regulation of GLUT-4 phosphorylation by intracellular calcium in adipocytes. *Endocrinology* **129** (6), 3269-3273.

Reusch, JE, Sussman, KE, and Draznin, B. (1993). Inverse relationship between GLUT-4 phosphorylation and its intrinsic activity. *J.Biol.Chem.* **268** (5), 3348-3351.

Ribon, V, Printen, JA, Hoffman, NG, Kay, BK, and Saltiel, AR. (1998). A novel, multifuntional c-Cbl binding protein in insulin receptor signaling in 3T3-L1 adipocytes. *Mol.Cell Biol.* **18** (2), 872-879.

Ribon, V and Saltiel, AR. (1997). Insulin stimulates tyrosine phosphorylation of the proto-oncogene product of c-Cbl in 3T3-L1 adipocytes. *Biochem.J.* **324 (Pt 3)** 839-845.

Ricort, JM, Tanti, JF, Van Obberghen, E, and Marchand-Brustel, Y. (1996). Different effects of insulin and platelet-derived growth factor on phosphatidylinositol 3-kinase at the subcellular level in 3T3-L1 adipocytes. A possible explanation for their specific effects on glucose transport. *Eur.J.Biochem.* **239** (1), 17-22.

Rietveld, A, Neutz, S, Simons, K, and Eaton, S. (1999). Association of sterol and glycosylphosphatidylinositol-linked proteins with Drosophila lipid microdomains. *J.Biol.Chem.* **274** (17), 12049-12054.

Robinson, MS and Bonifacino, JS. (2001). Adaptor-related proteins. *Curr.Opin.Cell Biol.* **13** (4), 444-453.

Robinson, MS and Kreis, TE. (1992). Recruitment of coat proteins onto Golgi membranes in intact and permeabilized cells: effects of brefeldin A and G protein activators. *Cell* **69** (1), 129-138.

Rogers, SL and Gelfand, VI. (2000). Membrane trafficking, organelle transport, and the cytoskeleton. *Curr.Opin.Cell Biol.* **12** (1), 57-62.

Roper, K, Corbeil, D, and Huttner, WB. (2000). Retention of prominin in microvilli reveals distinct cholesterol-based lipid micro-domains in the apical plasma membrane. *Nat.Cell Biol.* **2** (9), 582-592.

Ross, SA, Keller, SR, and Lienhard, GE. (1998). Increased intracellular sequestration of the insulin-regulated aminopeptidase upon differentiation of 3T3-L1 cells. *Biochem J* **330 (Pt 2)** 1003-1008.

Roth, MG. (1999). Lipid regulators of membrane traffic through the Golgi complex. *Trends Cell Biol.* **9** (5), 174-179.

Roy, S, Luetterforst, R, Harding, A, Apolloni, A, Etheridge, M, Stang, E, Rolls, B, Hancock, JF, and Parton, RG. (1999). Dominant-negative caveolin inhibits H-Ras function by disrupting cholesterol-rich plasma membrane domains. *Nat.Cell Biol.* **1** (2), 98-105.

Saltis, J, Habberfield, AD, Egan, JJ, Londos, C, Simpson, IA, and Cushman, SW. (1991). Role of protein kinase C in the regulation of glucose transport in the rat adipose cell. Translocation of glucose transporters without stimulation of glucose transport activity. *J Biol.Chem.* **266** (1), 261-267.

Sargiacomo, M, Scherer, PE, Tang, Z, Kubler, E, Song, KS, Sanders, MC, and Lisanti, MP. (1995). Oligomeric structure of caveolin: implications for caveolae membrane organization. *Proc.Natl.Acad.Sci.U.S.A* **92** (20), 9407-9411.

Sargiacomo, M, Sudol, M, Tang, Z, and Lisanti, MP. (1993). Signal transducing molecules and glycosyl-phosphatidylinositol-linked proteins form a caveolin-rich insoluble complex in MDCK cells. *J.Cell Biol.* **122** (4), 789-807.

Sariola, M, Saraste, J, and Kuismanen, E. (1995). Communication of post-Golgi elements with early endocytic pathway: regulation of endoproteolytic cleavage of Semliki Forest virus p62 precursor. *J Cell Sci.* **108 (Pt 6)** 2465-2475.

Sato-Yoshitake, R, Yorifuji, H, Inagaki, M, and Hirokawa, N. (1992). The phosphorylation of kinesin regulates its binding to synaptic vesicles. *J Biol.Chem.* **267** (33), 23930-23936.

Scheiffele, P, Roth, MG, and Simons, K. (1997). Interaction of influenza virus haemagglutinin with sphingolipid- cholesterol membrane domains via its transmembrane domain. *EMBO J.* **16** (18), 5501-5508.

Scherer, PE, Lisanti, MP, Baldini, G, Sargiacomo, M, Mastick, CC, and Lodish, HF. (1994). Induction of caveolin during adipogenesis and association of GLUT4 with caveolin-rich vesicles. *J Cell Biol.* **127** (5), 1233-1243.

Scherer, PE, Okamoto, T, Chun, M, Nishimoto, I, Lodish, HF, and Lisanti, MP. (1996). Identification, sequence, and expression of caveolin-2 defines a caveolin gene family. *Proc.Natl.Acad.Sci.U.S.A* **93** (1), 131-135.

Schlegel, A and Lisanti, MP. (2000). A molecular dissection of caveolin-1 membrane attachment and oligomerization. Two separate regions of the caveolin-1 C-terminal domain mediate membrane binding and oligomer/oligomer interactions in vivo. *J Biol.Chem.* **275** (28), 21605-21617.

Schlegel, A and Lisanti, MP. (2001). Caveolae and their coat proteins, the caveolins: from electron microscopic novelty to biological launching pad. *J.Cell Physiol* **186** (3), 329-337.

Schlegel, A, Volonte, D, Engelman, JA, Galbiati, F, Mehta, P, Zhang, XL, Scherer, PE, and Lisanti, MP. (1998). Crowded little caves: structure and function of caveolae. *Cell Signal.* **10** (7), 457-463.

Schnitzer, JE, Oh, P, Pinney, E, and Allard, J. (1994). Filipin-sensitive caveolae-mediated transport in endothelium: reduced transcytosis, scavenger endocytosis, and capillary permeability of select macromolecules. *J Cell Biol.* **127** (5), 1217-1232.

Schoonderwoert, VT, Holthuis, JC, Tanaka, S, Tooze, SA, and Martens, GJ. (2000). Inhibition of the vacuolar H+-ATPase perturbs the transport, sorting, processing and release of regulated secretory proteins. *Eur.J Biochem* **267** (17), 5646-5654.

Schroeder, R, London, E, and Brown, D. (1994). Interactions between saturated acyl chains confer detergent resistance on lipids and glycosylphosphatidylinositol (GPI)-anchored proteins: GPI- anchored proteins in liposomes and cells show similar behavior. *Proc.Natl.Acad.Sci.U.S.A* **91** (25), 12130-12134.

Schroeder, RJ, Ahmed, SN, Zhu, Y, London, E, and Brown, DA. (1998). Cholesterol and sphingolipid enhance the Triton X-100 insolubility of glycosylphosphatidylinositol-anchored proteins by promoting the formation of detergent-insoluble ordered membrane domains. *J.Biol.Chem.* **273** (2), 1150-1157.

Schurmann, A, Doege, H, Ohnimus, H, Monser, V, Buchs, A, and Joost, HG. (1997). Role of conserved arginine and glutamate residues on the cytosolic surface of glucose transporters for transporter function. *Biochemistry* **36** (42), 12897-12902.

Schurmann, A, Keller, K, Monden, I, Brown, FM, Wandel, S, Shanahan, MF, and Joost, HG. (1993). Glucose transport activity and photolabelling with 3-[125I]iodo-4- azidophenethylamido-7-O-succinyldeacetyl (IAPS)-forskolin of two mutants at tryptophan-388 and -412 of the glucose transporter GLUT1: dissociation of the binding domains of forskolin and glucose. *Biochem.J.* **290 (Pt 2)** 497-501.

Schurmann, A, Mieskes, G, and Joost, HG. (1992). Phosphorylation of the adipose/muscle-type glucose transporter (GLUT4) and its relationship to glucose transport activity. *Biochem.J.* **285 (Pt 1)** 223-228.

Schutz, GJ, Kada, G, Pastushenko, VP, and Schindler, H. (2000). Properties of lipid microdomains in a muscle cell membrane visualized by single molecule microscopy. *EMBO J* **19** (5), 892-901.

Seatter, MJ, De la Rue, SA, Porter, LM, and Gould, GW. (1998). QLS motif in transmembrane helix VII of the glucose transporter family interacts with the C-1 position of D-glucose and is involved in substrate selection at the exofacial binding site. *Biochemistry* **37** (5), 1322-1326.

Sevinsky, JR, Rao, LV, and Ruf, W. (1996). Ligand-induced protease receptor translocation into caveolae: a mechanism for regulating cell surface proteolysis of the tissue factor- dependent coagulation pathway. *J.Cell Biol.* **133** (2), 293-304.

Sharma, PM, Egawa, K, Gustafson, TA, Martin, JL, and Olefsky, JM. (1997). Adenovirus-mediated overexpression of IRS-1 interacting domains abolishes insulin-stimulated mitogenesis without affecting glucose transport in 3T3-L1 adipocytes. *Mol.Cell Biol.* **17** (12), 7386-7397.

Shenoy-Scaria, AM, Gauen, LK, Kwong, J, Shaw, AS, and Lublin, DM. (1993). Palmitylation of an amino-terminal cysteine motif of protein tyrosine kinases p56lck and p59fyn mediates interaction with glycosyl-phosphatidylinositol-anchored proteins. *Mol.Cell Biol.* **13** (10), 6385-6392.

Shepherd, PR, Withers, DJ, and Siddle, K. (1998). Phosphoinositide 3-kinase: the key switch mechanism in insulin signalling [published erratum appears in Biochem J 1998 Nov 1;335(Pt 3):711]. *Biochem.J* **333 (Pt 3)** 471-490.

Shewan, AM, Marsh, BJ, Melvin, DR, Martin, S, Gould, GW, and James, DE. (2000). The cytosolic C-terminus of the glucose transporter GLUT4 contains an acidic cluster endosomal targeting motif distal to the dileucine signal. *Biochem.J.* **350 Pt 1** 99-107.

Shi, Y, Samuel, SJ, Lee, W, Yu, C, Zhang, W, Lachaal, M, and Jung, CY. (1999). Cloning of an L-3-hydroxyacyl-CoA dehydrogenase that interacts with the GLUT4 C-terminus. *Arch.Biochem.Biophys.* **363** (2), 323-332.

Shih, W, Gallusser, A, and Kirchhausen, T. (1995). A clathrin-binding site in the hinge of the beta 2 chain of mammalian AP-2 complexes. *J Biol.Chem.* **270** (52), 31083-31090.

Simons, K and Ikonen, E. (1997). Functional rafts in cell membranes. *Nature* **387** (6633), 569-572.

Simons, K and Toomre, D. (2000). LIPID RAFTS AND SIGNAL TRANSDUCTION. *Nat.Rev.Mol.Cell Biol.* **1** (1), 31-39.

Simson, R, Yang, B, Moore, SE, Doherty, P, Walsh, FS, and Jacobson, KA. (1998). Structural mosaicism on the submicron scale in the plasma membrane. *Biophys.J.* **74** (1), 297-308.

Singer, SJ and Nicolson, GL. (1972). The fluid mosaic model of the structure of cell membranes. *Science* **175** (23), 720-731.

Slot, JW, Garruti, G, Martin, S, Oorschot, V, Posthuma, G, Kraegen, EW, Laybutt, R, Thibault, G, and James, DE. (1997). Glucose transporter (GLUT-4) is targeted to secretory granules in rat atrial cardiomyocytes. *J Cell Biol.* **137** (6), 1243-1254.

Slot, JW, Geuze, HJ, Gigengack, S, James, DE, and Lienhard, GE. (1991a). Translocation of the glucose transporter GLUT4 in cardiac myocytes of the rat. *Proc.Natl.Acad.Sci.U.S.A* **88** (17), 7815-7819.

Slot, JW, Geuze, HJ, Gigengack, S, Lienhard, GE, and James, DE. (1991b). Immuno-localization of the insulin regulatable glucose transporter in brown adipose tissue of the rat. *J Cell Biol.* **113** (1), 123-135.

Smaby, JM, Momsen, M, Kulkarni, VS, and Brown, RE. (1996). Cholesterol-induced interfacial area condensations of galactosylceramides and sphingomyelins with identical acyl chains. *Biochemistry* **35** (18), 5696-5704.

Smart, EJ, Ying, YS, Mineo, C, and Anderson, RG. (1995). A detergent-free method for purifying caveolae membrane from tissue culture cells. *Proc.Natl.Acad.Sci.U.S.A* **92** (22), 10104-10108.

Smith, RM, Charron, MJ, Shah, N, Lodish, HF, and Jarett, L. (1991). Immunoelectron microscopic demonstration of insulin-stimulated translocation of glucose transporters to the plasma membrane of isolated rat adipocytes and masking of the carboxyl-terminal epitope of intracellular GLUT4. *Proc.Natl.Acad.Sci.U.S.A* **88** (15), 6893-6897.

Somwar, R, Kim, DY, Sweeney, G, Huang, C, Niu, W, Lador, C, Ramlal, T, and Klip, A. (2001). GLUT4 translocation precedes the stimulation of glucose uptake by insulin in muscle cells: potential activation of GLUT4 via p38 mitogen-activated protein kinase. *Biochem.J.* **359** (Pt 3), 639-649.

Standaert, ML, Bandyopadhyay, G, Sajan, MP, Cong, L, Quon, MJ, and Farese, RV. (1999). Okadaic acid activates atypical protein kinase C (zeta/lambda) in rat and 3T3/L1 adipocytes. An apparent requirement for activation of Glut4 translocation and glucose transport. *J.Biol.Chem.* **274** (20), 14074-14078.

Standaert, ML, Galloway, L, Karnam, P, Bandyopadhyay, G, Moscat, J, and Farese, RV. (1997). Protein kinase C-zeta as a downstream effector of phosphatidylinositol 3-kinase during insulin stimulation in rat adipocytes. Potential role in glucose transport. *J Biol.Chem.* **272** (48), 30075-30082.

Staubs, PA, Nelson, JG, Reichart, DR, and Olefsky, JM. (1998). Platelet-derived growth factor inhibits insulin stimulation of insulin receptor substrate-1-associated phosphatidylinositol 3-kinase in 3T3-L1 adipocytes without affecting glucose transport. *J.Biol.Chem.* **273** (39), 25139-25147.

Stephens, L, Smrcka, A, Cooke, FT, Jackson, TR, Sternweis, PC, and Hawkins, PT. (1994). A novel phosphoinositide 3 kinase activity in myeloid-derived cells is activated by G protein beta gamma subunits. *Cell* **77** (1), 83-93.

Sun, XJ, Rothenberg, P, Kahn, CR, Backer, JM, Araki, E, Wilden, PA, Cahill, DA, Goldstein, BJ, and White, MF. (1991). Structure of the insulin receptor substrate IRS-1 defines a unique signal transduction protein. *Nature* **352** (6330), 73-77.

Suzuki, K and Kono, T. (1980). Evidence that insulin causes translocation of glucose transport activity to the plasma membrane from an intracellular storage site. *Proc.Natl.Acad.Sci.U.S.A* **77** (5), 2542-2545.

Takatsu, H, Sakurai, M, Shin, HW, Murakami, K, and Nakayama, K. (1998). Identification and characterization of novel clathrin adaptor-related proteins. *J Biol.Chem.* **273** (38), 24693-24700.

Takei, K and Haucke, V. (2001). Clathrin-mediated endocytosis: membrane factors pull the trigger. *Trends Cell Biol.* **11** (9), 385-391.

Takeuchi, H, Matsuda, M, Yamamoto, T, Kanematsu, T, Kikkawa, U, Yagisawa, H, Watanabe, Y, and Hirata, M. (1998). PTB domain of insulin receptor substrate-1 binds inositol compounds. *Biochem.J.* **334 (Pt 1)** 211-218.

Tamemoto, H, Kadowaki, T, Tobe, K, Yagi, T, Sakura, H, Hayakawa, T, Terauchi, Y, Ueki, K, Kaburagi, Y, Satoh, S. (1994). Insulin resistance and growth retardation in mice lacking insulin receptor substrate-1. *Nature* **372** (6502), 182-186.

Tang, X and Downes, CP. (1997). Purification and characterization of Gbetagamma-responsive phosphoinositide 3-kinases from pig platelet cytosol. *J.Biol.Chem.* **272** (22), 14193-14199.

Tanti, JF, Gremeaux, T, Van Obberghen, E, and Marchand-Brustel, Y. (1994). Serine/threonine phosphorylation of insulin receptor substrate 1 modulates insulin receptor signaling. *J Biol.Chem.* **269** (8), 6051-6057.

Todaka, M, Hayashi, H, Imanaka, T, Mitani, Y, Kamohara, S, Kishi, K, Tamaoka, K, Kanai, F, Shichiri, M, Morii, N, Narumiya, S, and Ebina, Y. (1996). Roles of insulin, guanosine 5'-[gamma-thio]triphosphate and phorbol 12- myristate 13-acetate in signalling pathways of GLUT4 translocation. *Biochem J* **315 (Pt 3)** 875-882.

Tooze, SA. (1998). Biogenesis of secretory granules in the trans-Golgi network of neuroendocrine and endocrine cells. *Biochim.Biophys Acta* **1404** (1-2), 231-244.

Tooze, SA, Martens, GJ, and Huttner, WB. (2001). Secretory granule biogenesis: rafting to the SNARE. *Trends Cell Biol.* **11** (3), 116-122.

Traub, LM, Ostrom, JA, and Kornfeld, S. (1993). Biochemical dissection of AP-1 recruitment onto Golgi membranes. *J Cell Biol.* **123** (3), 561-573.

Trowbridge, IS, Collawn, JF, and Hopkins, CR. (1993). Signal-dependent membrane protein trafficking in the endocytic pathway. *Annu.Rev.Cell Biol.* **9** 129-161.

Ueki, K, Yamamoto-Honda, R, Kaburagi, Y, Yamauchi, T, Tobe, K, Burgering, BM, Coffer, PJ, Komuro, I, Akanuma, Y, Yazaki, Y, and Kadowaki, T. (1998). Potential role of protein kinase B in insulin-induced glucose transport, glycogen synthesis, and protein synthesis. *J Biol.Chem.* **273** (9), 5315-5322.

Uittenbogaard, A and Smart, EJ. (2000). Palmitoylation of caveolin-1 is required for cholesterol binding, chaperone complex formation, and rapid transport of cholesterol to caveolae. *J Biol.Chem.* **275** (33), 25595-25599.

Uittenbogaard, A, Ying, Y, and Smart, EJ. (1998). Characterization of a cytosolic heat-shock protein-caveolin chaperone complex. Involvement in cholesterol trafficking. *J Biol.Chem.* **273** (11), 6525-6532.

Urso, B, Brown, RA, O'Rahilly,S, Shepherd, PR, and Siddle, K. (1999). The alpha-isoform of class II phosphoinositide 3-kinase is more effectively activated by insulin receptors than IGF receptors, and activation requires receptor NPEY motifs. *FEBS Lett.* **460** (3), 423-426.

Vainio, S, Heino, S, Mansson, JE, Fredman, P, Kuismanen, E, Vaarala, O, and Ikonen, E. (2002). Dynamic association of human insulin receptor with lipid rafts in cells lacking caveolae. *EMBO Rep.* **3** (1), 95-100.

Valverde, AM, Kahn, CR, and Benito, M. (1999). Insulin signaling in insulin receptor substrate (IRS)-1-deficient brown adipocytes: requirement of IRS-1 for lipid synthesis. *Diabetes* **48** (11), 2122-2131.

Van Meer, G and Simons, K. (1988). Lipid polarity and sorting in epithelial cells. *J.Cell Biochem.* **36** (1), 51-58.

van Weert, AW, Dunn, KW, Gueze, HJ, Maxfield, FR, and Stoorvogel, W. (1995). Transport from late endosomes to lysosomes, but not sorting of integral membrane proteins in endosomes, depends on the vacuolar proton pump. *J Cell Biol.* **130** (4), 821-834.

Vanhaesebroeck, B and Alessi, DR. (2000). The PI3K-PDK1 connection: more than just a road to PKB. *Biochem.J.* **346 Pt 3** 561-576.

Vanhaesebroeck, B, Higashi, K, Raven, C, Welham, M, Anderson, S, Brennan, P, Ward, SG, and Waterfield, MD. (1999). Autophosphorylation of p110delta phosphoinositide 3-kinase: a new paradigm for the regulation of lipid kinases in vitro and in vivo. *EMBO J* **18** (5), 1292-1302.

Vanhaesebroeck, B, Leevers, SJ, Ahmadi, K, Timms, J, Katso, R, Driscoll, PC, Woscholski, R, Parker, PJ, and Waterfield, MD. (2001). SYNTHESIS AND FUNCTION OF 3-PHOSPHORYLATED INOSITOL LIPIDS. *Annu.Rev.Biochem.* **70** 535-602.

Vannucci, SJ, Nishimura, H, Satoh, S, Cushman, SW, Holman, GD, and Simpson, IA. (1992). Cell surface accessibility of GLUT4 glucose transporters in insulin- stimulated rat adipose cells. Modulation by isoprenaline and adenosine. *Biochem J* **288 (Pt 1)** 325-330.

VanRenterghem, B, Morin, M, Czech, MP, and Heller-Harrison, RA. (1998). Interaction of insulin receptor substrate-1 with the sigma3A subunit of the adaptor protein complex-3 in cultured adipocytes. *J.Biol.Chem.* **273** (45), 29942-29949.

Varma, R and Mayor, S. (1998). GPI-anchored proteins are organized in submicron domains at the cell surface. *Nature* **394** (6695), 798-801.

Verhey, KJ and Birnbaum, MJ. (1994). A Leu-Leu sequence is essential for COOH-terminal targeting signal of GLUT4 glucose transporter in fibroblasts. *J.Biol.Chem.* **269** (4), 2353-2356.

Verhey, KJ, Hausdorff, SF, and Birnbaum, MJ. (1993). Identification of the carboxy terminus as important for the isoform- specific subcellular targeting of glucose transporter proteins. *J.Cell Biol.* **123** (1), 137-147.

Verhey, KJ, Yeh, JI, and Birnbaum, MJ. (1995). Distinct signals in the GLUT4 glucose transporter for internalization and for targeting to an insulin-responsive compartment. *J.Cell Biol.* **130** (5), 1071-1079.

Vigers, GP, Crowther, RA, and Pearse, BM. (1986). Location of the 100 kd-50 kd accessory proteins in clathrin coats. *EMBO J* **5** (9), 2079-2085.

Vik, SB and Antonio, BJ. (1994). A mechanism of proton translocation by F1F0 ATP synthases suggested by double mutants of the a subunit. *J Biol.Chem.* **269** (48), 30364-30369.

Viola, A, Schroeder, S, Sakakibara, Y, and Lanzavecchia, A. (1999). T lymphocyte costimulation mediated by reorganization of membrane microdomains. *Science* **283** (5402), 680-682.

Vitale, ML, Seward, EP, and Trifaro, JM. (1995). Chromaffin cell cortical actin network dynamics control the size of the release-ready vesicle pool and the initial rate of exocytosis. *Neuron* **14** (2), 353-363.

Waheed, AA, Shimada, Y, Heijnen, HF, Nakamura, M, Inomata, M, Hayashi, M, Iwashita, S, Slot, JW, and Ohno-Iwashita, Y. (2001). Selective binding of perfringolysin O derivative to cholesterol-rich membrane microdomains (rafts). *Proc.Natl.Acad.Sci.U.S.A* **98** (9), 4926-4931.

Wakabayashi, S, Shigekawa, M, and Pouyssegur, J. (1997). Molecular physiology of vertebrate Na+/H+ exchangers. *Physiol Rev.* **77** (1), 51-74.

Walter, J, Schnolzer, M, Pyerin, W, Kinzel, V, and Kubler, D. (1996). Induced release of cell surface protein kinase yields CK1- and CK2-like enzymes in tandem. *J.Biol.Chem.* **271** (1), 111-119.

Wan, L, Molloy, SS, Thomas, L, Liu, G, Xiang, Y, Rybak, SL, and Thomas, G. (1998). PACS-1 defines a novel gene family of cytosolic sorting proteins required for trans-Golgi network localization. *Cell* **94** (2), 205-216.

Watson, JA, Rumsby, MG, and Wolowacz, RG. (1999). Phage display identifies thioredoxin and superoxide dismutase as novel protein kinase C-interacting proteins: thioredoxin inhibits protein kinase C-mediated phosphorylation of histone. *Biochem.J.* **343 Pt 2** 301-305.

Webb, Y, Hermida-Matsumoto, L, and Resh, MD. (2000). Inhibition of protein palmitoylation, raft localization, and T cell signaling by 2-bromopalmitate and polyunsaturated fatty acids. *J Biol.Chem.* **275** (1), 261-270.

Weber, T, Zemelman, BV, McNew, JA, Westermann, B, Gmachl, M, Parlati, F, Sollner, TH, and Rothman, JE. (1998). SNAREpins: minimal machinery for membrane fusion. *Cell* **92** (6), 759-772.

Wei, ML, Bonzelius, F, Scully, RM, Kelly, RB, and Herman, GA. (1998). GLUT4 and transferrin receptor are differentially sorted along the endocytic pathway in CHO cells. *J Cell Biol.* **140** (3), 565-575.

Werner, G, Hagenmaier, H, Drautz, H, Baumgartner, A, and Zahner, H. (1984). Metabolic products of microorganisms. 224. Bafilomycins, a new group of macrolide antibiotics. Production, isolation, chemical structure and biological activity. *J Antibiot.(Tokyo)* **37** (2), 110-117.

West, MA, Bright, NA, and Robinson, MS. (1997). The role of ADP-ribosylation factor and phospholipase D in adaptor recruitment. *J Cell Biol.* **138** (6), 1239-1254.

White, MF. (1998). The IRS-signalling system: a network of docking proteins that mediate insulin action. *Mol.Cell Biochem.* **182** (1-2), 3-11.

Whitehead, JP, Clark, SF, Urso, B, and James, DE. (2000). Signalling through the insulin receptor. *Curr.Opin.Cell Biol.* **12** (2), 222-228.

Whitman, M, Downes, CP, Keeler, M, Keller, T, and Cantley, L. (1988). Type I phosphatidylinositol kinase makes a novel inositol phospholipid, phosphatidylinositol-3-phosphate. *Nature* **332** (6165), 644-646.

Wilson, BS, Pfeiffer, JR, and Oliver, JM. (2000). Observing FcepsilonRI signaling from the inside of the mast cell membrane. *J Cell Biol.* **149** (5), 1131-1142.

Wong, DH and Brodsky, FM. (1992). 100-kD proteins of G. *J Cell Biol.* **117** (6), 1171-1179.

Wu, X, Jung, G, and Hammer, JA, III. (2000). Functions of unconventional myosins. *Curr.Opin.Cell Biol.* **12** (1), 42-51.

Xu, T, Vasilyeva, E, and Forgac, M. (1999). Subunit interactions in the clathrin-coated vesicle vacuolar (H(+))-ATPase complex. *J Biol.Chem.* **274** (41), 28909-28915.

Yamada, E. (1955). The fine structure of the gall bladder epithelium of the mouse. *J.Biophys Biochem Cytol* **1** 445-458.

Yang, J, Clark, AE, Kozka ,IJ, Cushman, SW, and Holman, GD. (1992). Development of an intracellular pool of glucose transporters in 3T3-L1 cells. *J Biol.Chem.* **267** (15), 10393-10399.

Yang, J, Clarke, JF, Ester, CJ, Young, PW, Kasuga, M, and Holman, GD. (1996). Phosphatidylinositol 3-kinase acts at an intracellular membrane site to enhance GLUT4 exocytosis in 3T3-L1 cells. *Biochem.J.* **313 (Pt 1)** 125-131.

Yang, J, Hodel, A, and Holman, GD. (2002). Insulin and Isoproterenol Have Opposing Roles in the Maintenance of Cytosol pH and Optimal Fusion of GLUT4 Vesicles with the Plasma Membrane. *J Biol.Chem.* **277** (8), 6559-6566.

Yang, J and Holman, GD. (1993). Comparison of GLUT4 and GLUT1 subcellular trafficking in basal and insulin-stimulated 3T3-L1 cells. *J.Biol.Chem.* **268** (7), 4600-4603.

Yenush, L, Makati, KJ, Smith-Hall, J, Ishibashi, O, Myers, MG, Jr., and White, MF. (1996). The pleckstrin homology domain is the principal link between the insulin receptor and IRS-1. *J.Biol.Chem.* **271** (39), 24300-24306.

Yin, Y, Terauchi, Y, Solomon, GG, Aizawa, S, Rangarajan, PN, Yazaki, Y, Kadowaki, T, and Barrett, JC. (1998). Involvement of p85 in p53-dependent apoptotic response to oxidative stress. *Nature* **391** (6668), 707-710.

Yoshimori, T, Yamamoto, A, Moriyama, Y, Futai, M, and Tashiro, Y. (1991). Bafilomycin A1, a specific inhibitor of vacuolar-type H(+)-ATPase, inhibits acidification and protein degradation in lysosomes of cultured cells. *J Biol.Chem.* **266** (26), 17707-17712.

Zeuzem, S, Feick, P, Zimmermann, P, Haase, W, Kahn, RA, and Schulz, I. (1992). Intravesicular acidification correlates with binding of ADP-ribosylation factor to microsomal membranes. *Proc.Natl.Acad.Sci.U.S.A* **89** (14), 6619-6623.

Ziehm, D, Schurmann, A, Weiland, M, and Joost, HG. (1993). Biphasic alteration of glucose transport in 3T3-L1 cells during differentiation to the adipocyte-like phenotype. *Horm.Metab Res.* **25** (2), 71-76.

Zozulya, S, Lioubin, M, Hill, RJ, Abram, C, and Gishizky, ML. (1999). Mapping signal transduction pathways by phage display. *Nat.Biotechnol.* **17** (12), 1193-1198.